Package Design Safety Report for package design DN30

0023-BSH-2016-001-Rev0

TABLE OF CONTENTS

LIST OF ABBREVIATIONS

ACT ..... *Accident Conditions of Transport*
BAM ..... *German Federal Institute for Material Research and Testing*
CSI ..... *Criticality Safety Index*
FEM ..... *Finite Element Method*
IMS ..... *Integrated Management System*
MNOP ..... *Maximum Normal Operating Pressure*
MTSP ..... *Manufacturing and Test Sequence Plan*
NCT ..... *Normal Conditions of Transport*
PDSR ..... *Package Design Safety Report*
PIR ..... *Polyisocyanurate foam*
RCT ..... *Routine Conditions of Transport*

LIST OF TABLES

LIST OF FIGURES

LITERATURE

[ADN 2015] Accord européen relatif au transport international des marchandises dangereuses par voie de navigation intérieure (ADN) as applicable from 1 January 2015

[ADR 2015] European Agreement of 30 September 1957 concerning International Transports of Dangerous Goods on the Road, ADR, Attachment A and B of ADR, 2015 Edition

[ANSI N14.1] Uranium Hexafluoride – Packaging for Transport, ANSI N14.1- 2001

[ANSYS] ANSYS®, Release 17.0, Help System, ANSYS, Inc

[ANSYS WB] ANSYS®, Release 17.0, Help System, Workbench, User's Guide, ANSYS, Inc.

[ANSYS HS] ANSYS®, Release 17.0, Help System, Mechanical APDL, ANSYS LS-DYNA User's Guide, ANSYS, Inc.

[ANSYS DM] ANSYS®, Release 17.0, Help System, Design Modeler, User's Guide, ANSYS, Inc.

[ASTM C996] Standard Specification for Uranium Hexafluoride enriched to less than 5 wt. % 235U

[BEGUE 2013] Begue L., Milin M., Caplin G., Evo S., Nuclear Criticality Safety of Enriched UF6 cylinders, PATRAM 2013

[CONNOR 2013] O'Connor G., Regulatory Criticality safety Review of Uranium Hexafluoride Transport Package Applications, PATRAM 2013

[DIN EN 10028-3] Flat products made of steels for pressure purposes - Part 3: Weldable fine grain steels, normalized, edition 2009

[DIN 18230] DIN 18230.3: 2002: Constructive fire protection in industry construction – part 3: calculation values

[DIN 25478] DIN 25478: Use of calculation systems for the proof of criticality safety, edition 1994-07. Beuth Verlag

[EN 10088-1] Stainless steels, Part 1: List of stainless steels, September 2005

[EN 10088-2] Stainless steels, Part 2: Technical delivery conditions for sheet/plate and strip of corrosion resisting steels for general purposes, September 2005

[FKM 2003] Rechnerischer Festigkeitsnachweis für Maschinenbauteile aus Stahl, Eisenguss- und Aluminiumwerkstoffen (Translation: Proof of strength by calculation for machine parts made of steel, cast iron and aluminum materials), FKM-Richtline (Guideline), VDAM Verlag, 2003

[HEATING 7.2] Heating 7.2: User's Manual, NUREG/CR-0200, Revision 6, Volume 2, Section F10, ORNL/NUREG/CSD-2/V2/R6, Oak Ridge, 2000

[IAEA 608] IAEA - TECDOC - 608, Interim Guidance on the Safe Transport of Uranium Hexafluoride, June 1991

[IAEA 2012] Regulations for the Safe Transport of Radioactive Material, 2009 Edition, SS-R-6, IAEA, Vienna

[IMDG 2014] International Maritime Code for Dangerous Goods (IMDG-Code) as applicable from 1 January 2014

[ISO 12807] Safe transport of radioactive materials – Leakage testing on packages, ISO 12807, 1996

[ISO 7195] ISO 7195, Nuclear Energy – Packaging of uranium hexafluoride (UF6) for transport, Second edition, 2005-09-01

[LS-DYNA 2015] LS-DYNA. Keyword User's Manual – Volume I, LS-DYNA R8.0, 2015

[LS-DYNA 2006] LS-DYNA. Theory Manual, 2006.

[LS-PREPOST] http://www.lstc.com/lspp (25.11.2016)

[MILIN 2016] Milin M., Rannou J., Viaulle L., Caplin G., Evo S., Hydration of uranium residues contained in enriched UF6 cylinders, PATRAM 2016

[NEA 2008] International Handbook of Evaluated Criticality Safety Benchmark Experiments, NEA Nuclear Science Committee, September 2008 Edition, NEA/NSC/DOC(95)03

[PATRAM92] G. Wieser, B. Droste: Thermal test requirements and their verification by different test methods, PATRAM 1992

[REZGUI 2013] Rezgui S., Hilbert F., Criticality Analyses of Enriched Uranium-Hexafluoride Containing Impurities, PATRAM 2013

[RID 2015] Règlement concernant le transport international ferroviaire de marchandises Dangereuses (RID) as applicable from 1 January 2015

[SCALE 2009] SCALE 6, A Modular Code System for Performing Standardized Computer Analyses, ORNL/TM-2005/39, Version 6, Oak Ridge National Laboratory, 2009

[SCALE 2011] SCALE 6.1, Comprehensive Modeling and Simulation Suite for Nuclear Safety Analysis and Design ORNL/TM-2005/39, Version 6.1, Oak Ridge National Laboratory, 2011

[SSG-26] Advisory Material for the IAEA Regulations for the Safe Transport of Radioactive Material (2012 Edition), Specific Safety Guide No. SSG-26, IAEA, Vienna, 2012

[SWIFT 1952] H.W. Swift: Plastic instability under plane stress, Journal of Mechanics and Physics of Solids, Volume 1, Issue 1, October 1952

[USEC 651] The UF6 Manual – Good Handling Practices for Uranium Hexafluoride, Rev. 9, USEC, 2006

[VDI 2230] Systematic calculation of highly stressed bolted joints - Joints with one cylindrical bolt, edition 2015

[YOUNG 1998] Warren C. Young, Roark's Formulas for Stress and Strain, Sixth Edition, Mc.Graw Hill, 1998

PART 1

1.1 LIST AND STATUS OF DOCUMENTS PERTAINING TO THIS PDSR

The list of applicable documents and their status pertaining to this PDSR is included in Appendix 1.1 (List of Applicable Documents).

1.2 ADMINISTRATIVE INFORMATION

1.2.1 NAME OF PACKAGE

The package is designated: **DN30**

1.2.2 IDENTIFICATION OF PACKAGE DESIGNER

The DN30 package designer and license holder is:

DAHER NUCLEAR TECHNOLOGIES GmbH

In this report, DAHER NUCLEAR TECHNOLOGIES GmbH will be designated as “DAHER NT”.

1.2.3 TYPE OF PACKAGE DESIGN

The DN30 packaging loaded with the allowable content as described in section 1.3 fulfils the requirements according to [ADR 2015] and [IAEA 2012] for a package of:

- Type IF for UF_6 containing commercial grade or reprocessed uranium complying with the requirements for LSA–II, and an enrichment of not more than 5 wt.% U-235 in uranium
- Type AF for UF_6 containing commercial grade uranium or reprocessed uranium in less or equal to A_2 quantities, and an enrichment of not more than 5 wt.% U-235 in uranium
- Type B(U)F for UF_6 containing commercial grade uranium or reprocessed uranium with an enrichment of not more than 5 wt.% U-235 in uranium

1.2.4 PACKAGE DESIGN IDENTIFICATION AND RESTRICTIONS

A unique manufacturing serial number is assigned to each DN30 packaging valid for the whole usage lifetime. This number is stamped on the nameplate under the entry “manufacturers serial no.”.

The serial number is in this form:

XX-YYYY-ZZZZ

Where:

XX = designation of the fabricator (abbreviation assigned by DAHER NT)

YYYY = year of manufacturing

ZZZZ = sequential number

The list of all serial numbers is managed and filed by DAHER NT. All users of the DN30 packaging will be requested to update the status of the individual packaging after completion of the regular periodical inspections. Packagings with overdue periodical inspections (more than 1 year overdue) will be marked in that list as “not in use”.

Each individual package may be marked with an owner serial number different from the manufacturer serial number. This owner serial number may be marked on the nameplate under the entry “owners serial no.” or on an additional nameplate attached to the DN30 PSP. The owner serial number may change whenever required by the owner.

1.2.5 MODES OF TRANSPORT FOR WHICH THE PACKAGE IS DESIGNED

1) The DN30 package is designed for transport by road, rail, sea and inland waterways.
2) Transport by air is not permitted.

1.2.6 LOWEST TRANSPORT TEMPERATURE FOR WHICH THE PACKAGE IS DESIGNED

The lowest temperature allowed for the transport of the DN30 package is -40°C.

1.2.7 MAXIMUM NORMAL OPERATING PRESSURE

The maximum normal operating pressure for the DN30 package is defined as the pressure at the triple point of UF_6 (see Table 7):

MNOP = 152 kPa

Remark: the MNOP of the 30B cylinder is specified in [ISO 7195] and [ANSI N14.1] with 1.38 MPa. This definition applies to the use of the 30B cylinder in the enrichment and fuel fabrication process and not for its use as part of the DN30 packaging.

1.2.8 REFERENCE TO APPLICABLE REGULATIONS AND STANDARDS

The safety proof of the DN30 PSP is based on following regulations and standards:

- [IAEA 2012] Regulations for the Safe Transport of Radioactive Material, 2012 Edition, SS-R-6, IAEA, Vienna, 2009
- [ADN 2015] Accord européen relatif au transport international des marchandises dangereuses par voie de navigation intérieure (ADN) as applicable from 1 January 2015

- [ADR 2015] European Agreement of September 30, 1957 concerning the international carriage of dangerous goods by road (ADR) as applicable from 1 January 2015
- [ANSI N14.1] American National Standard, For Nuclear Materials – Uranium Hexafluoride – Packagings for Transport, ANSI N14.1-2012
- [ASTM C996] Standard Specification for uranium Hexafluoride Enriched to Less than 5 % ^{235}U
- [IMDG 2014] International Maritime Code for Dangerous Goods (IMDG-Code) as applicable from 1 January 2014
- [ISO 7195] ISO 7195, Nuclear Energy – Packaging of uranium hexafluoride (UF_6) for transport, Second edition, 2005-09-01
- [RID 2015] Règlement concernant le transport international ferroviaire de marchandises Dangereuses (RID) as applicable from 1 January 2015

The safety proof is based on [IAEA 2012] and [ADR 2015]. The other applicable regulations [ADN 2015], [IMDG 2014] and [RID 2015] are covered by this proof and are only mentioned in case of additional requirements not specified in [ADR 2015].

1.3 SPECIFICATION OF THE RADIOACTIVE CONTENTS

The UF_6 is contained in the primary packaging 30B cylinder according to [ISO 7195] and [ANSI N14.1]. The DN30 PSP accommodates the 30B cylinder and provides mechanical and thermal protection during RCT, NCT and ACT.

1.3.1 GENERAL SPECIFICATION

The 30B cylinders are filled with uranium in the chemical composition Uranium Hexafluoride (UF_6).

1.3.1.1 Permissible mass of UF_6

- The permissible mass of UF_6 in all types of packages specified below containing UF_6 other than heels is between 0 kg and 2277 kg.
- The permissible mass of UF_6 including all other chemical compositions in all types of packages specified below containing heels is between 0 kg and 11.4 kg.

1.3.1.2 Purity of UF_6

- The UF_6 concentration shall not be less than 99.5 g UF_6 per 100 g. This is corresponding to an atomic number ratio H/U of not more than 0.088.

1.3.1.3 Permissible conditions for repeated use

Cylinders complying with [ISO 7195] and [ANSI N14.1] and within the valid recertification period specified in these standards may be refilled under following conditions:

- For uranium complying with [ASTM C996] enriched commercial grade refilling of cylinders containing heels is permissible[1].
- For reprocessed uranium refilling of cylinders containing heels is not permitted. Refilling of any clean and washed-out cylinders with reprocessed uranium is permissible.

1.3.1.4 Non-fissile and fissile material

The uranium is classified as fissile material.

- Enriched uranium with a max. enrichment of 5.0 wt. % U-235 from uranium with natural isotopic composition
- Reprocessed enriched uranium with a max. enrichment of 5.0 wt. % U-235 in uranium

[1] commercial natural UF_6, or depleted natural UF_6 are included

1.3.1.5 Total and specific radioactivity

The uranium is classified according to its total or specific radioactivity:

Total activity less or equal to A_2:

- Uranium with natural isotopic composition;
- Reprocessed uranium with a total radioactivity less than A_2 of the mixture of nuclides present in the uranium

Specific activity less or equal to 10^{-4} A_2/g:

- Reprocessed uranium with a specific activity less or equal to 10^{-4} A_2/g

Total activity greater than A_2 and a specific activity greater than 10^{-4} A_2/g:

- Heels of reprocessed uranium with a specific activity greater than 10^{-4} A_2/g

1.3.1.6 Basis compositions for the definition of the permissible contents

The permissible contents are based on:

- The composition of commercial grade uranium as given in [ASTM C996] and listed in Table 1
- The composition of reprocessed uranium as given in [ASTM C996] and listed in Table 2
- The compositions of reprocessed uranium as listed in Table 4 and Table 6. These compositions are outside the scope of [ASTM C996]

1.3.1.6.1 Compositions of UF_6 based on [ASTM C996]

The following definitions are strictly based on the specifications given in [ASTM C996].

Table 1: Content of enriched commercial grade UF_6 complying with [ASTM C996]1)2)

Radionuclides	Weight percent max. (wt. %)	Gamma radiation max. (MeVBq/kgU)	Alpha activity max. (Bq/kgU)	Remark
U-232	1.0×10^{-8}			
U-234	5.5×10^{-2}			
U-235	5.0×10^{0}			See restrictions for fissile excepted
U-236	2.5×10^{-2}			
U-238	rest			
Tc-99	1.0×10^{-6}			

1) commercial natural UF_6, or depleted natural UF_6 are included
2) impurities from multiple refilling of a cylinder containing heels of UF_6 complying with Table 1 are permissible

Table 2: Permissible content of enriched reprocessed UF6 complying with [ASTM C996]1)

Radionuclides	Weight percent max. (wt. %)	Gamma radiation max. (MeVBq/kgU)	Alpha activity max. (Bq/kgU)	Remark
U-232				See Table 3
U-234	2.0×10^{-1}			
U-235	5.0×10^{0}			See restrictions for fissile excepted
U-236	3.0×10^{0}			
U-238	rest			
Fission products		4.4×10^{5}		
Tc-99	5.0×10^{-4}			
Neptunium and plutonium			3.3×10^{3}	

1) not enriched reprocessed UF_6, or depleted reprocessed UF_6 are included

Table 3: Permissible concentration of U-232 as function of the time period between processing / analysis and beginning of transport for enriched reprocessed UF_6 complying with [ASTM C996]

Time period between processing and beginning of transport	Concentration (µg/gU)
Within 1 month	5.0×10^{-2}
Within 1 year	4.0×10^{-2}
Within 2 years	3.0×10^{-2}
No time restraint	2.0×10^{-2}

1.3.1.6.2 Compositions of UF_6 exceeding [ASTM C996]

The following definition exceeds [ASTM C996].

Table 4: Permissible content of enriched reprocessed UF_6 to be transported in a type IF or B(U)F package[2)]

Radionuclides	Weight percent max. (wt. %)	Gamma radiation max. (MeVBq/kgU)	Alpha activity max. (Bq/kgU)	Remark
U-232				See Table 5
U-234	1.0×10^0			
U-235	5.0×10^0			See restrictions for fissile excepted
U-236	5.0×10^0			
U-238	rest			
Fission products[1)]		2.4×10^6		
Tc-99	1.0×10^0			
Neptunium and plutonium			1.0×10^7	

[1)] includes max. 1.2×10^6 MeVBq/kgU Co-60

[2)] not enriched reprocessed UF_6, or depleted reprocessed UF_6 are included

Table 5: Permissible concentration of U-232 as function of the time period between processing / analysis and beginning of transport for enriched reprocessed UF6 to be transported in a type IF or B(U)F package

Time period between processing and begin of transport	Concentration (µg/gU)
Within 1 month	6.0×10^{-2}
Within 1 year	4.0×10^{-2}
Within 2 years	3.0×10^{-2}
No time restraint	2.0×10^{-2}

1.3.1.6.3 Compositions of reprocessed UF_6 with restricted nuclide contents to satisfy type A limits

In the following definition nuclides are restricted so that transport in a type AF package is allowed.

Table 6: Permissible content of enriched reprocessed UF6 to be transported in a type AF package[2)]

Radionuclides	Weight percent max. wt. %	Gamma radiation max. MeVBq/kgU	Alpha activity max. Bq/kgU	Remark
U-232	6.0×10^{-8}			
U-234	3.0×10^{-4}			
U-235	5.0×10^{0}			See restrictions for fissile excepted
U-236	2.5×10^{-2}			
U-238	rest			
Fission products[1)]		4.4×10^{5}		
Tc-99	5.0×10^{-4}			
Neptunium and plutonium			3.3×10^{3}	

[1)] including Co-60

[2)] not enriched reprocessed UF_6, or depleted reprocessed UF_6 is included

1.3.2 DEFINITION OF THE PERMISSIBLE CONTENTS FOR EACH PACKAGE TYPE

The permissible content for the DN30 package is described below for each different package type in detail. Depending on the package type different restrictions apply. Following general classification is used:

- UF_6 containing commercial grade uranium with natural composition including heels can be transported in all types of packages[2];
- UF_6 containing reprocessed uranium excluding heels can be transported in type IF or B(U)F packages depending on the specific activity[3]; a type AF package is only possible under rather restricted conditions (see Table 6);
- UF_6 containing heels of reprocessed uranium needs to be transported in type B(U)F packages; furthermore the dose rate constraint as defined in section 1.3.2.4 must be met; type AF packages and immediate transport after emptying are only possible under rather restrictive conditions (see Table 6).

[2] Generally, for this material a type AF package would be used
[3] In some countries, type IP-2 packages for fissile material are not allowed

1.3.2.1 ***Permissible content in a type IF package***

The radioactive material complies with one of the following specifications a) to c):

a) UF_6 with a composition complying with Table 1
b) UF_6 with a composition complying with Table 2
c) UF_6 with a composition complying with Table 4

Total permissible radioactivity: 227 A_2

1.3.2.2 ***Permissible content in a type AF package***

The radioactive material complies with one of the following specifications a) to d):

a) UF_6 with a composition complying with Table 1
b) UF_6 with a composition complying with Table 6
c) Heels of UF_6 with a composition complying with Table 1
d) Heels of UF_6 with a composition complying with Table 6

Total permissible radioactivity: 1 A_2

1.3.2.3 ***Permissible contents in a type B(U)F package***

The radioactive material complies with one of the following specifications a) to e):

a) UF_6 with a composition complying with Table 1
b) UF_6 with a composition complying with Table 4
c) Heels of UF_6 with a composition complying with Table 1, and complying with the dose rate constraint in section 1.3.2.4
d) Heels of UF_6 with a composition complying with Table 6, and complying with the dose rate constraint in section 1.3.2.4
e) Heels of UF_6 with a composition complying with Table 4, and complying with the dose rate constraint in section 1.3.2.4

Total permissible radioactivity: 227 A_2

1.3.2.4 ***Dose rate constraints for cylinders containing heels of reprocessed UF_6 to be transported in DN30 packagings as type B(U)F packages***

The dose rates at the surface of 30B cylinders containing heels of reprocessed uranium are depending on the initial concentration of U-232 in the UF_6, on the time period the 30B cylinders have been filled with UF_6, the time period the cylinder was stored in empty (heels) condition before transport, and the arrangement of the heels quantity of material inside the cylinder. A tabular specification of permissible transport conditions is impracticable and error prone.

Hence a simplified dose rate related condition is defined in test procedure 0023-PA-2015-019.

1. Measure and record the dose rate at the surface of the bare cylinder as specified in Figure 1
2. Determine the maximum dose rate
3. The maximum dose rate must be less than 5000 µSv/h to allow shipment under exclusive use conditions and less than 2000 µSv/h to allow shipment under non-exclusive use conditions

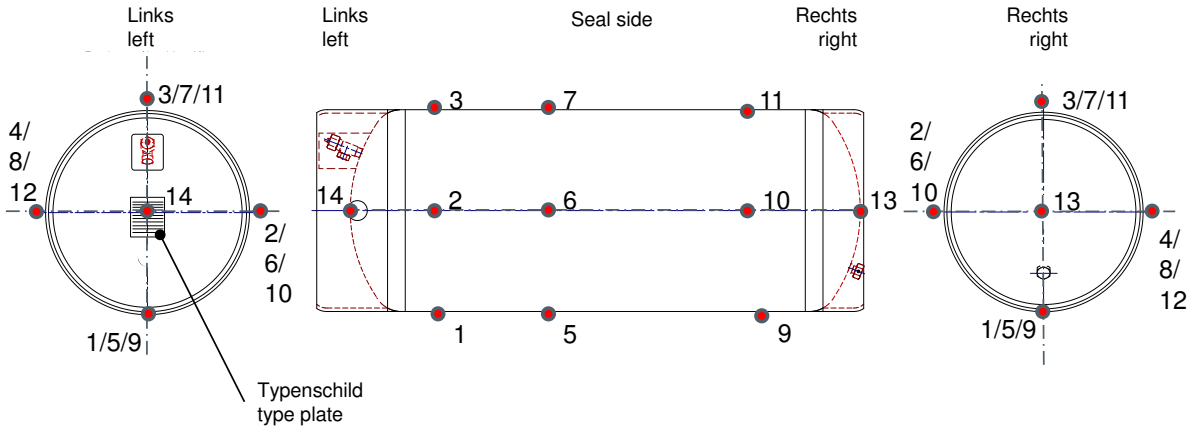

Figure 1:..Definition of the dose rate measurement points on bare cylinders containing heels of reprocessed uranium

1.3.3 PHYSICAL AND CHEMICAL STATE

During transport, the UF_6 contained in the DN30 package is in solid form. Table 7 shows some properties of UF_6.

Table 7: UF_6 properties (extract from [USEC 651])

Property	Value
Density in solid state (20°C)	5.1 g/cm³
Density in liquid state (64.1°C)	3.6 g/cm³
Density in liquid state (121°C)	3.3 g/cm³
Sublimation point	56.6°C (101 kPa)
Triple point	64.1°C (152 kPa)
Heat of sublimation (64.1°C)	135 kJ/Kg
Heat of fusion (64.1°C)	56 kJ/Kg
Heat if vaporization (64.1°C)	81 kJ/Kg
Critical pressure	4.61 MPa
Critical temperature	230.2°C
Specific heat, solid (27°C)	477 J/Kg/°K
Specific heat, liquid (72°C)	544 J/Kg/°K

Concerning the chemical properties, UF_6 reacts slightly with most of metals (Nickel, Monel, Copper, and Aluminum) to create a fluoride of the metal and other uranium compounds. It reacts heavily with hydrocarbons, hence the absence of hydrocarbons in empty cylinders before filling with UF_6 is essential.

UF_6 does not react with Nitrogen, Oxygen, Carbon Dioxide or dry air. However, UF_6 reacts strongly with water and water vapor in the air producing HF-H_2O fog. This fog is highly harmful if inhaled.

$UF_6 + 2H_2O \rightarrow UO_2F_2 + 4HF$

The UF_6 could contain some impurities due to chemical reactions. These impurities, like HF or UO_2F_2*5.5H_2O, are also taken into account in the safety criticality analysis, see section 2.2.5.

1.3.4 SPECIAL FORM OR LOW DISPERSIBLE RADIOACTIVE MATERIAL

The radioactive content in the DN30 package is not in special or low dispersible form.

1.3.5 NATURE AND CHARACTERISTICS OF THE RADIATION EMITTED

The radiation emitted by the content of the DN30 package is mainly gamma radiation with a very small contribution of neutron radiation.

1.3.6 LIMITATION OF THE HEAT GENERATION RATE OF THE CONTENT

Table 8 shows the heat generation rate of 2277 kg of UF_6 complying with the composition given in Table 2 [ASTM C996]. The most significant contribution is from U-234 with a concentration of 0.2 wt% in U. Taking into account the higher value for U-234 of 1.0 wt% in U specified in Table 4, the enveloping heat generation rate for UF_6 as defined in this report is 3 W. The contribution of the traces of fission products and other actinides to the thermal power are negligible.

Table 8: Heat generation rate of 2277 kg UF_6 complying with the composition given in Table 2

Nuclide	Composition g/gU	Heat generation rate (W)
Tl-208		1.32E-02
Pb-212		2.91E-03
Bi-212		2.61E-02
Po-212		5.30E-02
Po-216		6.38E-02
Rn-220		5.92E-02
Ra-224		5.35E-02
Th-228		5.09E-02
Th-231		1.63E-04
Th-234		1.87E-04
Pa-234m		2.33E-03
Pa-234		8.61E-06
U-232	5.00E-08	5.00E-02
U-234	2.00E-03	5.52E-01
U-235	5.00E-02	4.56E-03
U-236	3.00E-02	8.08E-02
U-238	9.18E-01	1.20E-02
Total	1.00E+00	1.02E+00

1.3.7 MASS OF FISSILE MATERIAL AND NUCLIDES

The maximum mass of the fissile material is calculated from

Maximum total mass of UF_6 = 2277 kg

Maximum enrichment in U-235 = 5 wt.%

m_{fiss} = 2277 x 0.05 x 238/ (238 + 6 x 19) = 77 kg U-235

There are traces of fissile plutonium nuclides in reprocessed uranium (see Table 2, Table 4, and Table 6).

1.3.8 OTHER DANGEROUS PROPERTIES

According to [ADR 2015] UF_6 is also classified as Class 8 “Corrosive”.

1.3.9 CONTENTS NOT PERMITTED

All contents not complying with the definitions in this chapter 1.3 are not permitted.

1.4 SPECIFICATION OF THE PACKAGING

1.4.1 LIST OF ALL PACKAGING COMPONENTS AND COMPLETE DESIGN DRAWINGS

The DN30 packaging consists of the DN30 Protective Structural Packaging (PSP) and the 30B cylinder specified in [ISO 7195] and [ANSI N14.1]. The DN30 PSP provides both mechanical and thermal protection for the 30B cylinder and its radioactive content and is designed to meet RCT, NCT, and ACT as required by [ADR 2015] and [IAEA 2012].

The main packaging components are:

- 30B cylinder specified in [ISO 7195] and [ANSI N14.1] with installed valve and plug,
- Bottom half with two feet welded to the outer structure for tie-down during transport incorporating four handling attachment points to be used for the loaded package and two fork-lifter pockets for handling the empty and loaded packaging,
- Top half with two handling attachment points for handling of the top half,
- Valve protecting device attached to the bottom half by means of hinges,
- Plug protecting device mounted in the bottom half,
- Rotation preventing devices consisting of two pins mounted in the bottom half,
- Closure system consisting of in total six steel blocks welded to the top half and six steel blocks welded to the bottom half forming mortise-and-tenon style joints connected by steel pins,
- Steel blocks welded to the top and bottom half for sealing the package.

The complete parts list and drawings of the 30B cylinder are specified in [ISO 7195] and [ANSI N14.1]. The complete parts list and drawings of the DN30 PSP are given in Appendix 1.4.1 (Drawings).

1.4.2 LIST OF MATERIALS

1.4.2.1 30B cylinder

The 30B cylinder is specified [ISO 7195] and [ANSI N14.1]. The following specifications for the pressure envelope and the valve are an extract from [ISO 7195].

1.4.2.1.1 Pressure envelope

The materials of the pressure envelope are specified in Table 9.

Table 9: Materials of the pressure envelope of the 30B cylinder (extract from [ISO 7195])

Item	Applicable standards
Shells	The following are acceptable materials: a) normalized steel conforming to ASTM A516/A516M:2004, grade 55, 60, 65 or 70, meeting heat treatment and supplementary requirements S5 b) coil steel meeting all requirements of ASTM A516/A516M material, c) steel conforming to [DIN EN 10028-3], grade P275NL1 or P355NL1
Heads and skirts	The following are acceptable materials: a) normalized steel conforming to ASTM A516/A516M:2004, grade 55, 60, 65 or 70, meeting heat treatment and supplementary requirements S5 b) steel conforming to [DIN EN 10028-3], grade P275NL1 or P355NL1
Seal loops	Steel conforming to ASTM A36/A36M or from steel conforming to EN 10025:1990, grade S235 JRG2/11
Valve and plug couplings	forged steel conforming to ASTM A105/A105M:2003 or ASTM A106-A:2004b, grade C
Pipe plugs	upset forged or extruded, or extruded and drawn, aluminium bronze UNS C61300 conforming to ASTM B150:1998

1.4.2.1.2 Valve

The materials of the valve are specified in Table 10.

Table 10: Materials of the valve of the 30B cylinder (extract from [ISO 7195])

Item	Applicable standards
Valve body	Forging, aluminium bronze alloy UNS C63600 (CDA alloy 636)
Port cap	The following are acceptable materials: a) bar aluminium bronze alloy UNS C63600 (CDA alloy 636) b) nickel-copper alloy conforming to ASTM B164:2003 N04400, c) bar aluminium bronze UNS C61300
Packing nut	The following are acceptable materials: a) nickel-copper alloy conforming to ASTM B164:2003 N04400, b) bar aluminium bronze UNS C61300
Packing follower and packing ring	The following are acceptable materials: a) bar aluminium bronze alloy UNS C63600 (CDA alloy 636) b) bar aluminium bronze UNS C61300

Item	Applicable standards
Stem	Nickel-copper alloy bar conforming to ASTM B164:2003, class A or B
Packing and port cap gasket	Teflon, 100 % virgin TFE unfilled
Fluorinated lubricant	Occidental-Hooker HO-125 or valve-buyer approved equivalent
Solder	Tin-lead conforming to ASTM B32 or to ISO 9453 and having a minimum tin content of 45 %, such as alloy ASTM B32 SN50.

1.4.2.2 DN30 PSP

The materials of the DN30 PSP are specified in Table 11. The material properties of the PIR foam used as shock absorbing and thermal insulating material were determined by testing. The summary report of these tests as well as the results is given in Appendix 1.4.2 (Material Data PIR Foam).

Table 11: Material specification of the DN30 PSP

Item	Applicable standards
Inner and outer steel shells	DIN EN 10088-2, 1.4301
Inner structure	DIN EN 10088-2, 1.4301
Feet	DIN EN 10088-2, 1.4301
Steel structure of valve protecting device	DIN EN 10088-2, 1.4301
Rotation preventing device	DIN EN 10088-2, 1.4301
Plug protection device	DIN EN 10088-2, 1.4301
Closure device	DIN EN 10088-2, 1.4541
Pin of closure device	DIN EN 10088-2, 1.4542
Gaskets	EPDM
Foam	Polyisocyanurate rigid foam (PIR foam) conforming to the specifications RTS120 and RTS320 (details see Table 12)
Thermal insulation (intumescent material)	Promaseal-PL®

Table 12: Foam properties

Item	Standards	Units	Foam type	
			RTS120	RTS320
Density	EN 1602 / ASTM D1622	kg/m³	120±10	>320
Compression strength – parallel	EN 826 / ASTM D1621	MPa	1.68 ± 0.16	7.20 ± 0.20
Compression strength - perpendicular	EN 826 / ASTM D1621	MPa	1.50 ± 0.20	7.20 ± 0.20
Tensile strength - parallel - (Method A)	EN 1607 / ASTM D1623	MPa	1.90 ± 0.20	6.20 ± 0.20
Tensile strength - perpendicular - (Method A)	EN 1607 / ASTM D1623	MPa	1.70 ± 0.20	6.00 ± 0.20
Shear strength - perpendicular	EN 12090 / ASTM C273	kPa	6.70 ± 0.10	1,20 ± 0,1
Thermal conductivity	EN 12667 / ASTM C518	mW/mK	35.0	54.0
Operating temperature		℃	-180/+120	-196/+120
Closed cells	EN ISO 4590/ASTM D6226	%min	92	95
Fire reaction (maximum extent of the burnt area)	EN ISO 3582	mm	<30	<60
Fire reaction (extinguishing time)	EN ISO 3582	sec	<60	<120

1.4.2.2.1 Static and dynamic mechanical tests with samples of the technical foam

The static and dynamic tests with samples of the technical foam used for the DN30 PSP are documented in Appendix 1.4.2 (Material Data PIR Foam). Table 13 gives a summary of the mechanical tests carried out with foam samples.

Table 13: Summary of the mechanical tests with PIR foam samples

Temperature ℃	Orientation with respect to foaming	Test condition	Impact velocity m/s
-40℃	parallel	quasi-static	
-40℃	perpendicular	quasi-static	
-20℃	parallel	quasi-static	
-20℃	perpendicular	quasi-static	
+20℃	parallel	quasi-static	
+20℃	perpendicular	quasi-static	
+50℃	parallel	quasi-static	
+50℃	perpendicular	quasi-static	
+80℃	parallel	quasi-static	
+80℃	perpendicular	quasi-static	
-40℃	parallel	dynamic	13
-40℃	perpendicular	dynamic	13
-20℃	parallel	dynamic	13
-20℃	perpendicular	dynamic	13
+20℃	parallel	dynamic	13
+20℃	perpendicular	dynamic	13
+50℃	parallel	dynamic	13
+50℃	perpendicular	dynamic	13
+80℃	parallel	dynamic	13
+80℃	perpendicular	dynamic	13

The summary of the results is shown in Figure 2 for RTS120 foam and Figure 3 for RTS320 foam. These figures show:

- The deformation force is depending on the temperature; deformation force and temperature are linearly correlated;
- The deformation force is depending on the test conditions; for dynamic test conditions the deformation force is higher than for quasi-static tests conditions;
- There is almost no dependency on the foaming orientation.

The results of these tests with samples were used for the FE-analyses of the DN30 packaging under NCT and ACT.

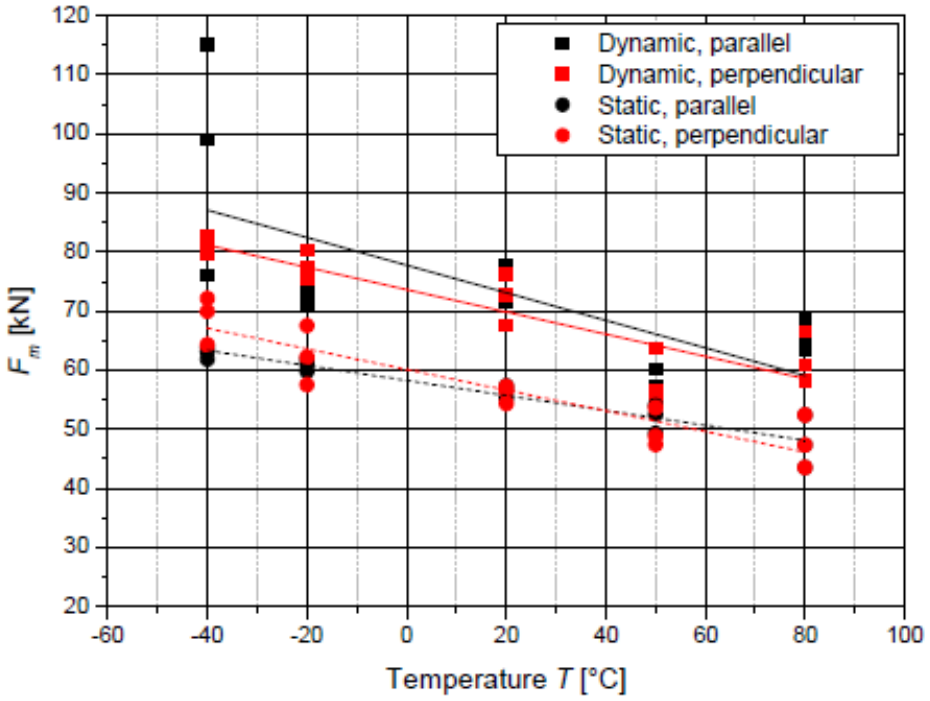

Figure 2: Deformation force as function of the temperature with parameters orientation and test condition for RTS120 foam

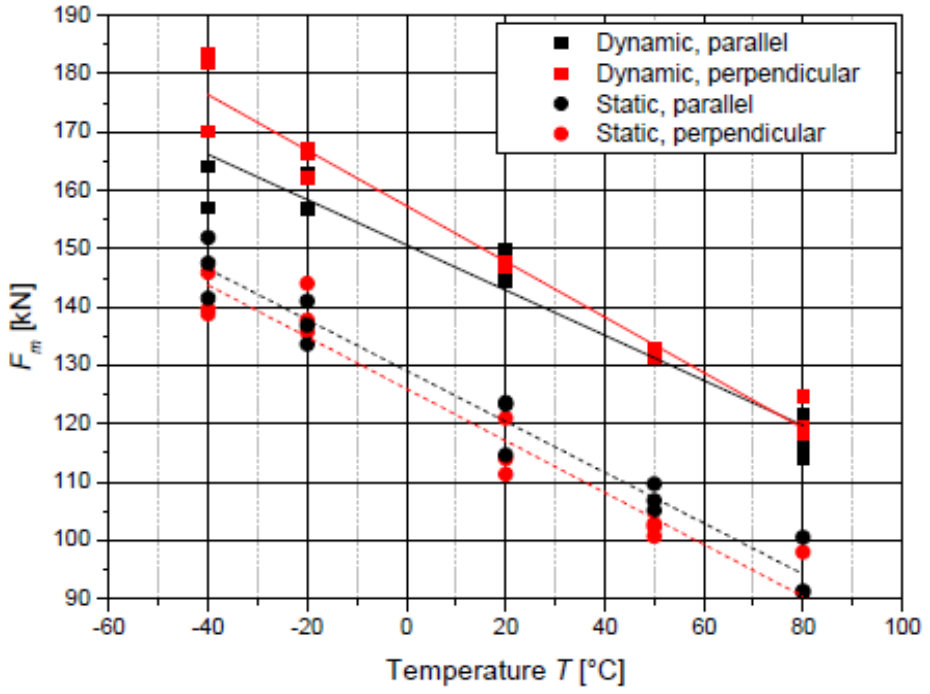

Figure 3: Deformation force as function of the temperature with parameters orientation and test condition for RTS320 foam

1.4.2.2.2 Thermal tests with samples of the technical foam

The thermal tests with samples of the technical foam used for the DN30 PSP are documented in Appendix 1.4.2 (Material Data PIR Foam).

The tests carried out were:

- A thermo gravimetric analysis by heating samples up to 800°C
- Measurement of thermal diffusivity, thermal expansion, heat capacity and density up to about 300°C
- Gas analysis of the gases produced when the foam disintegrates at higher temperatures

The summary of the results is:

- Thermal properties of the foam can be determined up to approx. 20-250°C; beyond that temperature the foam disintegrates
- During disintegration no dangerous gases are produced

The results of these tests with samples were used for the thermal analyses of the DN30 packaging under RCT, NCT and ACT.

1.4.3 DESCRIPTION OF THE DN30 PACKAGING

The DN30 packaging consists of

- the 30B cylinder specified in [ISO 7195] and [ANSI N14.1],
- the DN30 protective structural packaging (PSP).

1.4.3.1 30B cylinder

The 30B cylinder is described in [ISO 7195] and [ANSI N14.1]. The main data are extracted from there and listed in Table 14.

Table 14: Main data of the 30B cylinder

Item	Value
Nominal diameter:	760 mm
Nominal length:	2060 mm
Wall thickness:	13 mm
Nominal tare weight:	635 kg
Max net weight:	2277 kg
Minimum volume:	0.736 m^3

1.4.3.2 DN30 PSP

The DN30 PSP consists of

- The top half with integrated feet, handling attachment points suitable for the loaded package, valve protecting device, plug protecting device, rotation preventing device and bottom half of the closure device
- The top half with integrated handling attachment points suitable for the top half and the top half of the closure device.

The main data are listed in Table 15.

Table 15: Main data of the DN30 PSP

Item	Value
Nominal diameter	1216 mm
Nominal height	1329 mm
Nominal length:	2437 mm
Nominal tare weight:	1080 kg
Nominal gross weight:	4100 kg
Minimum volume:	0.736 m^3

1.4.3.2.1 Bottom half of the DN30 PSP

The body of the bottom half is made of an inner and outer shell of stainless steel both, in the form of a tub, which are connected at the top by a flange. The cavity between inner and outer shell and flange is filled with PIR foam. At the side the thickness of the inner shell is 2 mm and of the outer shell 3 mm. At the ends the thickness of the inner shell is 10 mm and of the outer shell 4 mm.

At the bottom side there are two feet of stainless steel welded to the outer shell at each end of the PSP. The feet have a base plate made of 2 x 10 mm thick stainless steel which contains at each side two holes for tie-down to an adapted flat-rack (the arrangement and size of these holes is compatible with existing PSP designs).

At the side of each of the feet there is an eyelet welded to the side plate of the foot. These eyelets are designed to be used for lifting the loaded DN30 package.

At the top side of the bottom half of the DN30 PSP there are the lower halves of the mortise-and-tenon closure system welded to the outer shell three per side. Adjacent to one of these parts of the closure device the sealing block is welded to the outer shell.

At the inside of the bottom half there is the valve protecting device attached by hinges to the flange at one end. The valve protecting device consists of a casing of stainless steel filled with PIR foam and a protecting housing, with its inner walls covered with intumescent material.

On the other end there is the plug protecting device in the form of a pot welded into the inner shell and with its walls covered with intumescent material.

At the inner sides of the flange there are two rotation preventing devices welded to the flange. These devices consist of a pin, which is withdrawn into the flange during loading and inserted during transport into the two holes in the skirt of the 30B cylinder.

All the surfaces of the inner shell of the bottom half are covered with intumescent material.

1.4.3.2.2 Top half of the DN30 PSP

The body of the top half is similar to the bottom half. It is made of an inner and outer shell of stainless steel both in the form of a tub which are connected at the bottom by a flange. The cavity between inner and outer shell and flange is filled with PIR foam. At the side the thickness of the inner shell is 2 mm and of the outer shell 3 mm. At the ends the thickness of the inner shell is 10 mm and of the outer shell 4 mm.

At the top there are two eyelets welded to the outer shell one on each side. These eyelets are designed to be used for lifting the top half only.

At the bottom side of the top half of the DN30 PSP there are the upper halves of the mortise-and-tenon closure system welded to the outer shell three per side. Adjacent to one of these parts of the closure device the sealing block is welded to the outer shell.

At the inside of the top half there is a recess to accommodate the valve protecting device.

In the flange of the top half there is an elastomeric gasket to prevent inleakage of water during routine conditions of transport.

All the surfaces of the inner shell of the top half are covered with intumescent material.

1.4.3.3 Design safety features of the DN30 packaging

1.4.3.3.1 Mechanical protection system

The mechanical protection system consists of the stainless steel/foam structure of the bottom and top half of the DN30 PSP. It prevents excessive mechanical impacts onto the 30B cylinder during RCT, NCT and ACT.

1.4.3.3.2 Thermal protection system

The thermal protection system consists of the stainless steel/foam structure of the bottom and top half of the DN30 PSP and the intumescent material at the inner surfaces of the DN30 PSP. It prevents excessive thermal impacts onto the 30B cylinder during RCT, NCT and ACT.

1.4.3.3.3 Closure system

The two halves of the DN30 PSP are connected by the closure system consisting of 6 robust mortise-and-tenon like devices and the flange.

The two parts of each mortise-and-tenon system have four teeth each with a hole in the center. When closed, the two halves are connected by a pin inserted into these holes. This pin is secured by a bolt. The design of the the mortise-and-tenon system is such that neither the connecting pin nor the securing bolt are exposed to mechanical impacts but protected by the massive body of the system. The system prevents excessive relative movements of top and bottom half in vertical direction in RCT, NCT and ACT.

The flange is shaped like an upside down U. It prevents excessive relative movements of top and bottom half in all horizontal directions in RCT, NCT and ACT. Furthermore, in flat drop orientations the flange will be deformed in such a way that top and bottom half are clamped together.

1.4.3.3.4 Valve protecting device

The valve protecting device consists of a stainless steel housing filled with PIR foam. It is shaped like a U and encloses the valve of the 30B cylinder during transport. It is connected to the bottom half of the DN30 PSP by two hinges. In open condition it is turned to horizontal position to allow loading and unloading of the cylinder. When the filled cylinder is loaded into the PSP, the device is turned by 90° to vertical orientation so that it is in contact with the cylinder head. The valve protection device prevents contact of the valve with any part of the PSP or any other part the 30B cylinder except its original point of contact (thread) during RCT, NCT and ACT.

A protecting housing is placed inside the U-shape of the valve protecting device. This housing is made of a thin stainless steel sheet and the inside is covered with intumescent material.

1.4.3.3.5 Plug protecting device

The plug protecting device consists of a pot made of stainless steel welded to the inner shell of the bottom half of the PSP. This device allows the plug to move in axial direction without making contact with any part of the PSP during RCT, NCT and ACT. The inside of the pot is covered with intumescent material.

1.4.3.3.6 Rotation preventing system

The rotation preventing system consists of two rotation preventing devices installed at the sides of the inner flange of the bottom half of the PSP. The device consists of a stainless steel pin

accommodated in two sleeves, an internal sleeve in contact with the pin and an external sleeve which is welded to the flange. A handlebar is welded onto the steel pin to allow turning and lateral movements. In open condition the steel pin is withdrawn into the flange so that the cylinder can be loaded and unloaded. In this condition the top half of the PSP cannot be put onto the bottom half as the position of the handle-bar prevents the placement of the top flange onto the bottom flange. The connection of top and bottom half is only possible when the rotation preventing system is properly engaged.

1.4.3.3.7 Sealing system

For sealing of the DN30 package there are two sealing blocks welded to the top and bottom half adjacent to a closure device. These blocks allow the use of high security seals compliant with ISO 17712:2010 / C-TPAT.

1.4.3.4 Handling features of the DN30 packaging

1.4.3.4.1 Lifting of the loaded DN30 package and empty DN30 PSP

The DN30 package can be lifted:

- By using the 4 lifting lugs welded to the upper part of the feet,
- By using a fork-lifter,
- By using handling slings.

The handling of the empty PSP should be carried out in the same manner as for the loaded package.

1.4.3.4.1.1 Lifting by using the 4 lifting lugs

For lifting of the DN30 package by using the 4 lifting lugs welded to the upper part of the feet shackles must be used and fixed to the lifting lugs. It is preferable to use lifting slings made from Polyester or Nylon.

The angle between the vertical axis of the lifting lugs and the slings/chains must not be greater than 30° (see Figure 4)

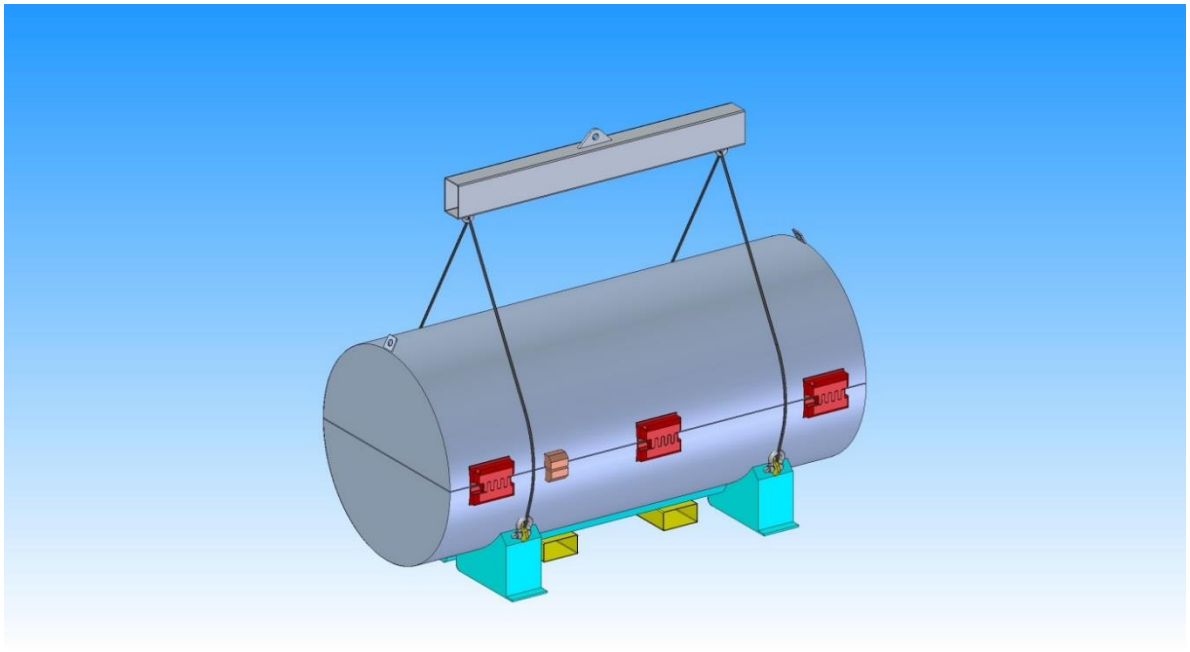

Figure 4: Lifting of the DN30 package by using the 4 lifting lugs

1.4.3.4.1.2 Lifting by using a fork-lifter

The loaded DN30 package may be handled and lifted by using a fork-lifter. For this purpose there are two fork-lifter pockets welded to the bottom half of the DN30 PSP (see Figure 5).

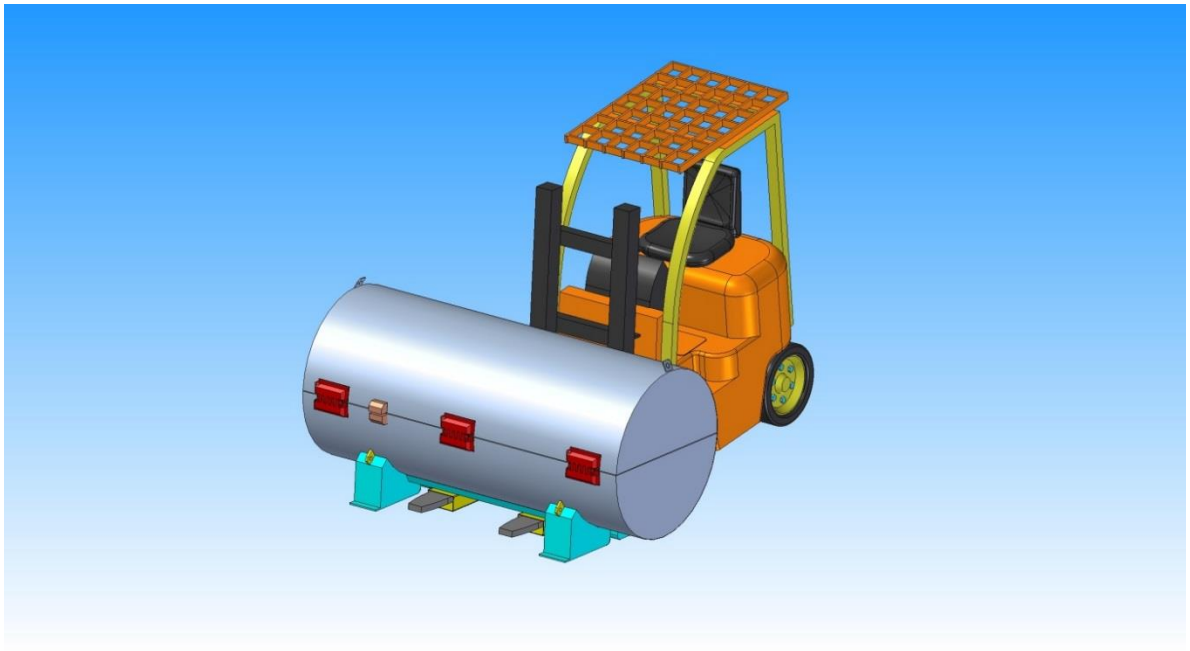

Figure 5: Lifting of the DN30 package by using a fork-lifter

1.4.3.4.1.3 Lifting by using slings (only for empty PSP)

The empty DN30 packaging may be handled by slings attached to the bottom half of the DN30 package according to Figure 6.

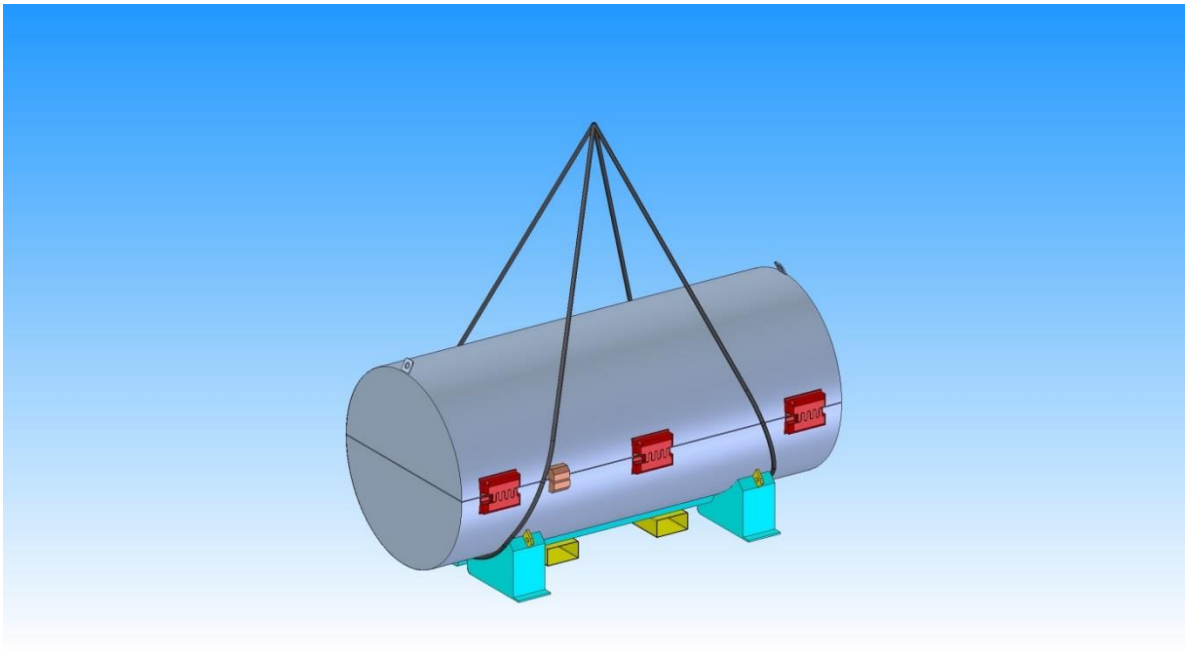

Figure 6: Lifting of the empty DN30 PSP by using slings

1.4.3.4.2 Lifting of the top half of the DN30 packaging

In general, the loaded DN30 package or the empty DN30 PSP is mounted with its feet to dedicated flatracks when transported. At the destination, only the top half needs to be removed for loading and unloading of the 30B cylinders from the DN30 PSPs.

For handling, see Figure 7, of the top half there are two lifting lugs, one at each end, welded to the outer shell of the PSP. These lifting lugs are only designed for the handling of the top half of the DN30 PSP. They must be blocked during transport to avoid inadvertent use of these attachment points for lifting of the loaded package, e.g. by inserting bolts.

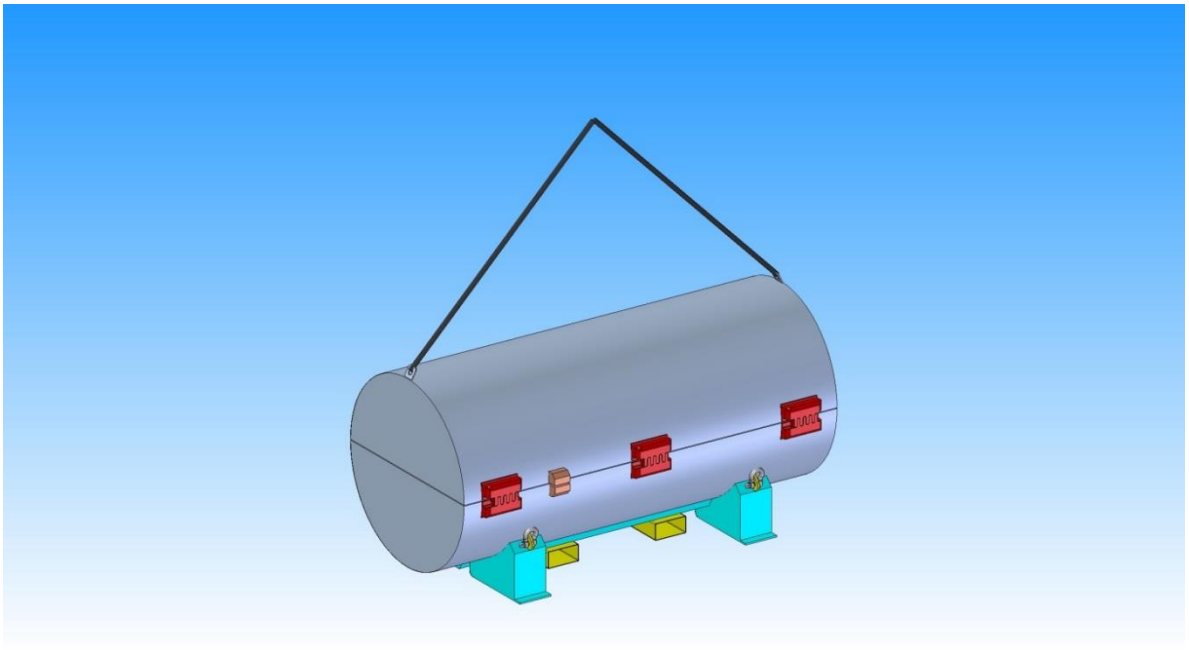

Figure 7: Lifting of the top half of the DN30 packaging

1.4.3.5 Tie-down features of the DN30 packaging

For tie-down, the DN30 PSP is equipped with two feet. The base plates of the feet consist of 2 x 10 mm thick stainless steel sheets which contain two holes at each end. The dimension and placement of these holes is compatible with PSPs currently in use. During transport, the DN30 PSP is bolted to a dedicated flat-rack (see Figure 8).

Only for the transport of DN30 PSP not loaded with a 30B cylinder or loaded with a cylinder containing heels quantities of UF_6 and in case a dedicated flat-rack cannot be made available, tie-down by using straps according to Figure 9 is allowed. In that case, a tie-down plan has to be drawn up based on a tie-down calculation.

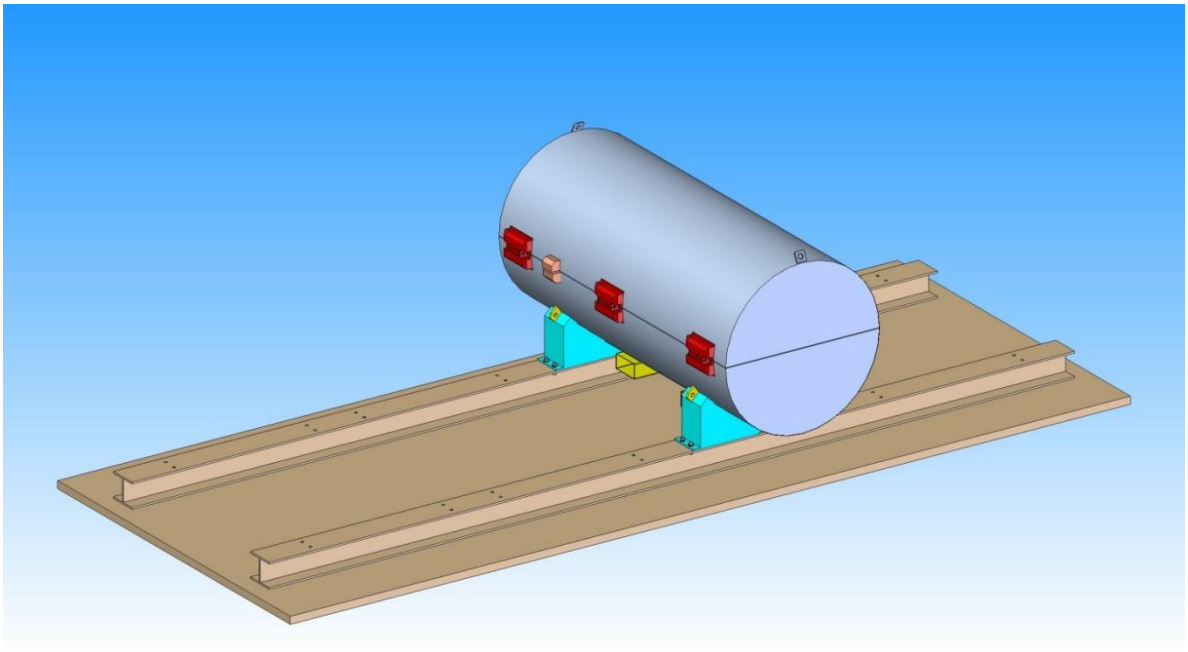

Figure 8: General tie-down method for the DN30 package / DN30 PSP

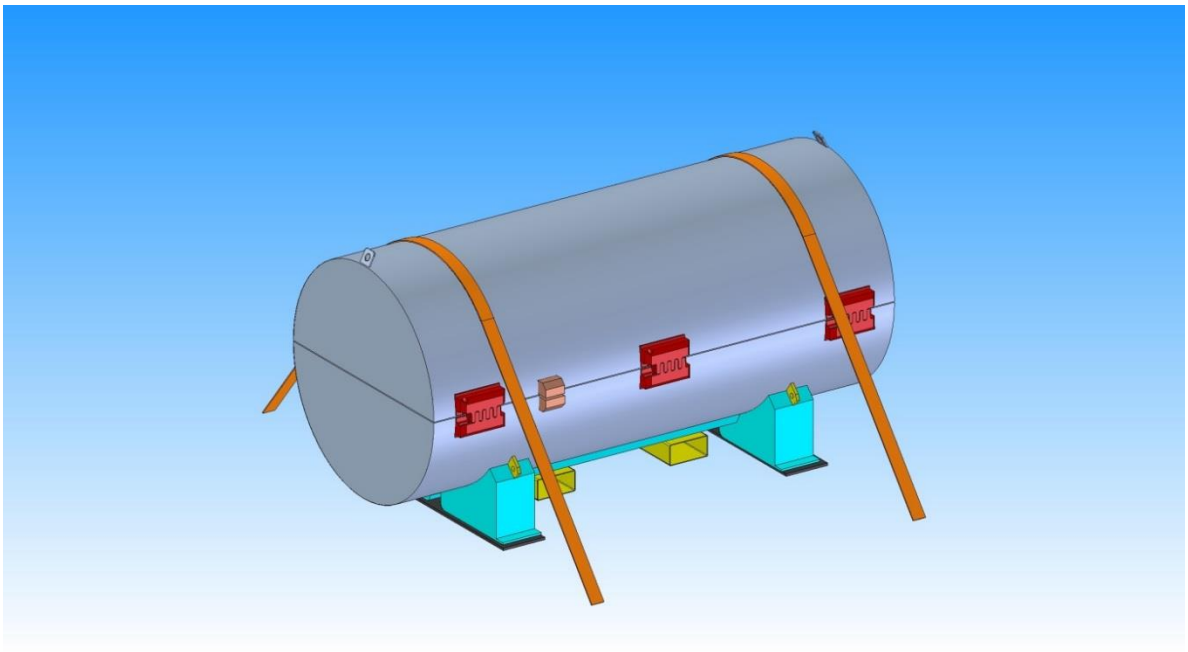

Figure 9: Tie-down of the DN30 package loaded with a cylinder containing heels quantities of UF6 or a DN30 PSP without a cylinder using straps

1.4.4 THE COMPONENTS OF THE PACKAGING RELEVANT FOR THE CONTAINMENT SYSTEM

The containment system consists of

- The 30B cylinder shell and heads together with the welding seams connecting the pressure envelope,
- The valve body and the stem, including the threaded connection between valve and cylinder body,
- The plug including the threaded connection between plug and cylinder body.

This containment system complies with the requirements defined in [ISO 7195] and [ANSI N14.1].

1.4.5 THE COMPONENTS OF THE PACKAGING RELEVANT FOR SHIELDING

The DN30 packaging has no components with shielding as the primary purpose. However, some level of shielding is provided by the shell of the 30B cylinder as well as the inner and outer shells of the DN30 PSP.

1.4.6 THE COMPONENTS OF THE PACKAGING RELEVANT FOR THE CONFINEMENT SYSTEM

The confinement system consists of

- The components of the containment system.

Only for 30B cylinders with a wall thickness of less than 11 mm, the inner and outer shell of the DN30 PSP would have to be added to the confinement system.

1.4.7 THE COMPONENTS OF THE PACKAGING RELEVANT FOR THERMAL PROTECTION

The complete DN30 PSP is relevant for thermal protection.

1.4.8 THE COMPONENTS OF THE PACKAGING RELEVANT FOR HEAT DISSIPATION

Due to the very low level of thermal power there is no dedicated component for heat dissipation.

1.4.9 THE PROTECTION AGAINST CORROSION

All outer and inner surfaces of the DN30 PSP are made of austenitic stainless steel and are hence resistant to corrosion.

The 30B cylinder is generally coated with high quality paint preventing excessive corrosion.

Corrosion at the inside of the 30B cylinder is negligible. The long term and world-wide experience with this cylinder design proves that there is no excessive corrosion within the 5 year recertification period or when stored with UF_6 or heels which could impair the safety functions of the cylinder.

1.4.10 THE PROTECTION AGAINST CONTAMINATION

All outer and inner surfaces of the DN30 PSP are made of austenitic stainless steel and hence are easy to decontaminate.

The intumescent material is protected by an easy to decontaminate coating.

The 30B cylinder is generally coated with paint which can be easily decontaminated. In transport configuration, the surface of the 30B cylinder is not accessible from the outside.

1.4.11 THE SHOCK ABSORBING COMPONENTS OF THE PACKAGING

The complete DN30 PSP is relevant for shock absorption.

1.4.12 THE TRANSPORT CONCEPT

Generally, the DN30 package is transported on dedicated flat-racks. A maximum of four DN30 packages can be mounted onto a 20' flat-rack by bolting them down via the holes in the feet. Alternatively, due to their low gross weight, for packages containing heels quantities individual transport is feasible by lashing the packages with straps to the transport means.

- The components of the packaging relevant for lifting are described in section 1.4.3.4.
- The components of the packaging relevant for tie-down are described in section 1.4.3.5.

1.5 PACKAGE PERFORMANCE CHARACTERISTICS

1.5.1 MAIN DESIGN PRINCIPLES

The packaging DN30 consists of the DN30 PSP which accommodates the 30B cylinder. The DN30 PSP is designed by DAHER NT whereas the design of the 30B cylinder is fixed and specified in [ISO 7195] and [ANSI N14.1].

The 30B cylinder is primarily designed to be used as a pressure vessel in enrichment and fuel manufacturing plants to accept enriched UF_6 from the enrichment process and to feed enriched UF_6 into the process at the fuel manufacturer's site. It acts as well as primary packaging for internal transports and as buffer storage on these sites. Hence, the 30B cylinder design provides the containment and the confinement function of the DN30 package.

For public transportation the 30B cylinder is protected by the DN30 PSP against mechanical and thermal impacts as defined in [ADR 2015] and [IAEA 2015] so that the containment and confinement function of the 30B cylinder are maintained under NCT and ACT.

1.5.2 PERFORMANCE CHARACTERISTICS

1.5.2.1 Performance characteristics under RCT

Under RCT, the main performance characteristics are:

- Safe handling of the DN30 package,
- Safe tie-down of the DN30 package,
- Adequate design for accelerations and vibrations to be routinely expected,
- Easy handling operations under the environmental conditions to be routinely expected,
- Resistance to corrosion,
- Long term usability by taking into account temperatures and ambient conditions to be routinely expected.

1.5.2.2 Performance characteristics under NCT

Under NCT, the main performance characteristics are:

- Protection of the 30B cylinder against the mechanical conditions to be expected under NCT,
- Limitations of deformations to fulfill the requirement concerning dose rate increase.

1.5.2.3 Performance characteristics under ACT

Under ACT, the main performance characteristics are:

- Protection of the 30B cylinder against mechanical conditions to be expected under ACT,
- Protection of the 30B cylinder against the thermal conditions to be expected under ACT.

1.5.3 ASSUMPTIONS USED FOR THE SAFETY ANALYSIS

1.5.3.1 Containment function

The containment function is provided by the 30B cylinder and its installations valve and plug. With reference to [ADR 2015] Nr. 6.4.11.8 or [IAEA 2012] para. 680 (b) it is assumed that the containment function is preserved if

- Following the tests prescribed in [ADR 2015] Nr. 6.4.11.13 b) or [IAEA 2012] para. 685 (b) there is no physical contact between the valve or plug and any other component of the packaging other than their original points of attachment,

  And where, in addition

- Following the test prescribed in [ADR 2015] Nr. 6.4.17.3 or [IAEA 2012] para. 728 the valve and the plug remain leak tight.

1.5.3.2 Dose rates

The shielding function is provided by the shell of the 30B cylinder and the inner and outer shells of the DN30 PSP. For RCT and NCT the foam between inner and outer shell of the DN30 PSP is taken into account as well. For ACT the shielding properties of the foam are completely neglected.

For the proof that the increase of the dose rate after the mechanical tests simulating NCT does not exceed the limits specified in the regulations, the reduction of the wall thickness of the DN30 PSP due to deformation is taken into account.

1.5.3.3 Criticality safety

The proof of criticality safety is based on the 30B cylinder. There are no requirements on the content, neither on its arrangement within the 30B cylinder nor regarding the distribution of impurities.

The containment function of the cylinder must be preserved according to section 1.5.3.1.

Only in the case that the wall thickness of a cylinder is less than 11 mm, the stainless steel shells of the DN30 PSP are part of the confinement system. Neither the foam nor the distance between inner and outer shell must be preserved as these parameters are not relevant for criticality safety. In this case, the closure system must assure that the top and bottom half of the DN30 PSP remain connected during RCT, NCT and ACT.

1.6 COMPLIANCE WITH REGULATORY REQUIREMENTS

In this section, the compliance of the package design DN30 with the international regulations [IAEA 2012], [ADR 2015], [RID 2015], [IMDG 2014] and [ADN 2015] is shown in the Table 16.

Table 16: Compliance with regulatory requirements

[IAEA 2012]	[ADR 2015] [RID 2015] [IMDG 2014] [ADN 2015]	IP-2	A	B(U)	Fissile	UF_6	Remarks [1)]
222	2.2.7.1.3				X		There is only the fissile nuclide U-235 present in the content; Plutonium nuclides are only present in traces in reprocessed Uranium.
226	2.2.7.1.3	X					The content permissible in a type IF package is specified in section 1.3.2.1; this definition complies with the requirements for LSA-II.
306	1.7.3	X	X	X	X	X	The management system of DAHER NT is audited and certified by the German competent authority (see chapter 1.9).
408	2.2.7.2.4.2	X					See paras 226, 409, 411 and 517-519, 521 and 522
409	2.2.7.2.3.1.2	X					The activity in UF_6 is homogeneously distributed and the specific activity is specified in section 0.
411	2.2.7.2.4.2	X					See paras 517 and 522.
417	2.2.7.2.3.5	X	X	X	X	X	See specification of contents in section 1.3.1.4; there are no exceptions by one of the provisions specified in this para.
418	4.1.9.3				X		The certificates of package approval are applied for based on this PDSR (certificates of package approval for a type AF, a type IF and a type B(U)F package are applied for).
419	2.2.7.2.4.5.1				X	X	For the DN30 package the UN numbers UN2977 shall be assigned.
420	2.2.7.2.4.5.2					X	The mass of UF_6 contained in the DN30 PSP complies with the mass specified for the 30B cylinder in [ISO 7195] or [ANSI N14.1], see section 1.3.1.
428	-		X				See paras 429 and 430.
429	2.2.7.2.4.4		X				The activity in a DN30 package licensed as type AF package is restricted to A_2, see section 1.3.2.2.

[1)] For cross references in this matrix the paras of [IAEA 2012] are used

[IAEA 2012]	[ADR 2015] [RID 2015] [IMDG 2014] [ADN 2015]	IP-2	A	B(U)	Fissile	UF_6	Remarks [1)]
430	2.2.7.2.4.4		X				For mixtures of radionuclides the respective formula is applied, see section 1.3.2.2.
431	2.2.7.2.4.6			X			See paras 432 and 433.
432	2.2.7.2.4.6.1			X			For the type B(U)F package design a certificate of package approval is applied for based on this PDSR.
433	2.2.7.2.4.6.2			X			For the type B(U)F package design a certificate of package approval is applied for based on this PDSR.
501	4.1.9.1.6	X	X	X	X	X	The 30B cylinder as containment system is manufactured and tested before its first use to comply with [ISO 7195] and [ANSI N14.1]; before the first use of a type B(U) or a packaging designed to contain fissile material an inspection is carried out and recorded, see section 1.7.1.
502	4.1.9.1.7	X	X	X	X	X	Administrative controls ensure that only the contents as specified in the certificate of package approval are loaded into the DN30 PSP, see section 1.7.2.
503	4.1.9.1.8	X	X	X			The handling instructions defined in sections 1.7.3, 1.7.4, 1.7.5 take into account the respective measures.
507	1.7.5 2.1.3.5.3(a)	X	X	X		X	Other dangerous properties of UF_6 are taken into account, see section 1.7.7.
508	4.1.9.1.2	X	X	X		X	Contamination checks defined in section 1.7.2 take the specified limits into account
517	4.1.9.2.1	X					The radiation level at 3 m distance from the unshielded material is below 10 mSv/h, see section 2.2.4.8.2.
518	4.1.9.2.2	X					See paras 568 and 569.
519	4.1.9.2.3	X					See para. 673.
520	4.1.9.2.4	X					UF_6 is LSA-II and not LSA-I
521	4.1.9.1.5	X					UF_6 complying with LSA is packed in an IP-2 package, see section 1.3.2.1.
522	7.5.11 CV33 1.1 (2)	X					The activity limit for UF_6 (LSA-II, non-combustible solid) for conveyances other than inland waterway craft is unlimited. According to [IAEA 2012] the activity limit for LSA-II for any inland waterway craft is $100A_2$; however, in [ADN 2015] this limit is not specified and instead the unlimited value applies.

[1)] For cross references in this matrix the paras of [IAEA 2012] are used

[IAEA 2012]	[ADR 2015] [RID 2015] [IMDG 2014] [ADN 2015]	IP-2	A	B(U)	Fissile	UF_6	Remarks [1)]
526	4.1.9.1.10	X	X	X			The TI of each package types considered here except packagings containing heels of reprocessed UF_6 is below 10, see section 2.2.4.8.3.
527	4.1.9.1.11	X	X	X			The radiation level at the surface of each package types considered here is below 2 mSv/h, see section 2.2.4.8.4.
533	5.2.1.7.3	X	X	X			The package mass is marked on the name plate, see section 1.4.3.
566 (b)	7.5.11 CV33, 3.3b)	X	X	X			The radiation level of a conveyance of each package type considered here is below 2 mSv/h at any point of the external surface and below 0.1 mSv/h at 2 m distance from the external surface, see section 2.2.4.
568	7.5.11 CV33 4.1	X	X	X	X		The CSI of the DN30 package is in all cases 0; hence also for groups of DN30 packages the sum of the CSIs is 0.
569	7.5.11 CV33 4.2	X	X	X	X		Not applicable, see para. 568.
570	7.5.11 CV33 4.3	X	X	X	X		Not applicable, as the material defined in section 1.3.2 does not meet any of the provisions (a)-(f) in para. 417.
575	[IMDG 2014] 5.1.5.3.4.3	X	X	X			The radiation level at the surface of each package type considered here is below 2 mSv/h, see section 2.2.4.8.4.
607	6.4.2.1	X	X	X			The package can be easily and safely transported and properly secured during transport, see section 1.4.3.4 and 1.4.3.5.
608	6.4.2.2	X	X	X			The lifting attachments on the package are designed for their intended purpose, see section 2.2.1.2.
609	6.4.2.3	X	X	X			The attachments on the package which could be used for lifting are designed to support its mass, see section 1.4.3.4.1 and section 2.2.1.2.3.1; any other feature which could be used for lifting is rendered incapable, see section 1.4.3.4.2.
610	6.4.2.4	X	X	X			The outer surfaces of the packaging consist of stainless steel and can be easily decontaminated, see section 1.4.3.
611	6.4.2.5	X	X	X			The outer layer of the package prevents the collection and retention of water, see section 1.4.3.
612	6.4.2.6	X	X	X			There are no features added to the package at the time of transport that could reduce its safety, see section 1.4.3.5.

[1)] For cross references in this matrix the paras of [IAEA 2012] are used

[IAEA 2012]	[ADR 2015] [RID 2015] [IMDG 2014] [ADN 2015]	IP-2	A	B(U)	Fissile	UF_6	Remarks [1)]
613	6.4.2.7	X	X	X			The package is designed to withstand effects of any acceleration, vibration or vibration resonance that may arise under RCT, see section 2.2.1.3.
614	6.4.2.8	X	X	X			The materials of the packaging, mainly steel and technical foam, are physically and chemically compatible with each other; any part in contact with the radioactive content has been designed for such purpose, see section 1.4.3.
615	6.4.2.9	X	X	X			The valve and the plug of the 30B cylinder are protected by the DN30 PSP during transport and cannot be operated unauthorized, see section 1.4.3.
616	6.4.2.10	X	X	X			The package is designed to comply with the requirements for type B(U) packages; it takes into account ambient temperatures and pressures that are likely to be encountered during RCT.
617	6.4.2.11	X	X	X			Proof of shielding is contained in section 2.2.4.
618	6.4.2.12	X	X	X			The other dangerous properties of UF_6 are taken into account, see section 1.3.8.
-	6.4.2.13	X	X	X	X	X	The documentation for the package to be provided to the user is assembled in the packaging documentation book, see section 1.7.
623	6.4.5.2	X					The package is designed to fulfill the requirements for an IP-1 package, see paras 607-618 and [ADR 2015] no. 6.4.2.13 and 636.
624	6.4.5.2	X					The package fulfills the requirements of para. 623 and prevents the loss of or dispersal of the radioactive content (see section 2.2.3) and the increase of the dose rate of more than 20% (see section 2.2.4.8.6) when subjected to the free drop test simulating NCT and the stacking test.
631	6.4.6.1					X	The content of the DN30 PSP, UF_6, is packed and transported according to [ISO 7195] and in compliance with the requirements of para. 632 and 633.
632	6.4.6.2					X	(a) The 30B cylinder compliant with [ISO 7195] and [ANSI N14.1] withstands the hydraulic test with a test

[1)] For cross references in this matrix the paras of [IAEA 2012] are used

[IAEA 2012]	[ADR 2015] [RID 2015] [IMDG 2014] [ADN 2015]	IP-2	A	B(U)	Fissile	UF_6	Remarks [1)]
							pressure of 2.76 MPa (the DN30 PSP is not affected by this test). (b) The DN30 package withstands, without loss or dispersal of the UF_6, the free drop test simulating NCT, see section 2.2.3. (c) The DN30 package withstands without rupture of the containment system the thermal test simulating ACT, see section 2.2.1.5.3.
633	6.4.6.3					X	The DN30 package has no pressure relief valves
635	6.4.7.1		X	X			The DN30 package is designed to meet the requirements of paras 607-618 and [ADR 2015] no. 6.4.2.13 and paras 636-651.
636	6.4.7.2		X	X			The smallest overall dimension is not less than 10 cm, see section 1.4.
637	6.4.7.3		X	X			There is a sealing system at the outside of the package, see section 1.4.3.3.7.
638	6.4.7.4		X	X			The tie-down attachment on the package is so designed that under NCT and ACT the forces of the tie-down do not impair the ability of the package to meet the requirements of the Regulations, see section 2.2.1.3.3.
639	6.4.7.5		X	X			The design of the packaging takes into account temperatures ranging from -40°C to +70°C, see section 1.4.2.
640	6.4.7.6		X	X			The design and manufacturing techniques are in accordance with ISO and EN standards.
641	6.4.7.7		X	X			The containment system is defined in section 1.4.4; unintentional opening is not possible as the containment system is enclosed in the DN30 PSP during transport; and the containment system withstands a test pressure of 2.76 MPa, which is much higher than the internal pressure during RCT and NCT.
642	6.4.7.8		X	X			Not applicable
643	6.4.7.9		X	X			The valve and plug are positive fastening devices, see section 1.4.4 and [ISO 7195] resp. [ANSI N14.1].

[1)] For cross references in this matrix the paras of [IAEA 2012] are used

[IAEA 2012]	[ADR 2015] [RID 2015] [IMDG 2014] [ADN 2015]	IP-2	A	B(U)	Fissile	UF_6	Remarks [1)]
644	6.4.7.10		X	X			The design of the 30B cylinder is standardized in [ISO 7195] and [ANSI N14.1]; this design is world-wide in use since decades.
645	6.4.7.11		X	X			The pressure in the 30B cylinder during transport is below atmospheric pressure. As the 30B cylinder withstands a test pressure of 2.76 MPa, the containment is not affected by a reduction of the ambient pressure of 60 kPa.
646	6.4.7.12		X	X			The 30B cylinder with its valve is enclosed by the DN30 PSP during transport.
647	6.4.7.13		X	X			The 30B cylinder is enclosed in the DN30 PSP which is securely closed by a positive fastening device, see section 1.4.3.
648	6.4.7.14		X	X			The DN30 package is so designed that if it were subjected to the tests simulating NCT it would prevent (a) loss or dispersal of the UF_6, see section 2.2.3 (b) more than 20% increase in the maximum radiation level at any external surface of the package, see section 2.2.4.8.6
649	6.4.7.15		X	X			During transport the physical state of UF_6 is solid; however, to make provisions for filling effects the 30B cylinder is filled to about 60% to take care of the expansion of UF_6 during the phase change of solid to liquid in case the UF_6 is liquefied during filling/emptying.
650	6.4.7.16		X	X			Not applicable as during transport the physical state of UF_6 is solid.
651	6.4.7.17		X	X			Not applicable as during transport the physical state of UF_6 is solid.
652	6.4.8.1			X			The DN30 package is designed to meet the requirements of paras 607-618 and [ADR 2015] no. 6.4.2.13 and paras 636-649, except as specified in para. 648 (a) and additionally the requirements of paras 653-666.

[1)] For cross references in this matrix the paras of [IAEA 2012] are used

[IAEA 2012]	[ADR 2015] [RID 2015] [IMDG 2014] [ADN 2015]	IP-2	A	B(U)	Fissile	UF_6	Remarks [1)]
653	6.4.8.2			X			The heat generation rate of the content of the DN30 package is negligible, see section1.3.6; any influence on the safety functions of the package can be excluded, see section 2.2.2.3.4.
654	6.4.8.3			X			Due to the very low heat generation rate of the content and in absence of insolation the temperature on the accessible surface of the package will practically not exceed the ambient temperature of 38°C and is hence lower than 50°C, see section 2.2.2.3.4.1.
655	6.4.8.4			X			Due to the very low heat generation rate of the content and in absence of insolation the temperature on the accessible surface of the package will practically not exceed the ambient temperature of 38°C and is hence lower than 50°C, see section 2.2.2.3.4.1.
656	6.4.8.5			X			For the thermal analysis a reference temperature of 38°C is assumed, see section 2.2.2.3.2.4.
657	6.4.8.6			X			For the thermal analysis the solar insolation conditions as specified are used, see section 2.2.2.3.2.4.
658	6.4.8.7			X			The DN30 PSP is the thermal protection for the 30B cylinder and its content. In calculations and real tests with prototypes it is shown that the thermal protection remains effective after the tests to demonstrate its ability to withstand NCS and ACT, see sections 2.1.3.1.2, 0, 2.2.1 and 2.2.2. The thermal protection feature foam is protected on the outside by a shell of stainless steel of 2 mm thickness which prevents effectively deterioration by ripping, cutting, skipping, abrading or rough handling. The thermal protection feature intumescent material is protected by the shell of the DN30 PSP as it is applied on the inner side of the top and bottom half.

[1)] For cross references in this matrix the paras of [IAEA 2012] are used

[IAEA 2012]	[ADR 2015] [RID 2015] [IMDG 2014] [ADN 2015]	IP-2	A	B(U)	Fissile	UF_6	Remarks [1)]
659	6.4.8.8			X			The DN30 package is so designed that if it were subjected to: (a) The tests simulating NCT it would restrict the loss of radioactive contents to not more than 10^{-6} A_2 per hour, see section 2.2.3.6.1. (b) The tests simulating ACT i. It would retain sufficient shielding to ensure that the external radiation level at 1 m distance from the package would not exceed 10 mSv/h, see section 2.2.4.8.7. ii. It would restrict the loss of radioactive contents to not more than A_2 per week, see section 2.2.3.6.2.
660	6.4.8.9			X			The activity of the radioactive contents is less than 10^5 A_2, see section 1.3.2.3.
661	6.4.8.10			X			Neither filters nor a mechanical cooling system are part of the design of the DN30 package, see section 1.4.3.
662	6.4.8.11			X			A pressure relief system is no part of the design of the DN30 package, see section 1.4.3.
663	6.4.8.12			X			The pressure envelope of the 30B cylinder is designed to withstand a test pressure of 2.76 MPa. The MNOP of the DN30 package as defined in section 1.2.7 has no influence on the results of the tests simulating NCT and ACT.
664	6.4.8.13			X			The maximum normal operation pressure of the DN30 packaging is less than 700 kPa, see section 1.2.7.
665	6.4.8.14			X			UF_6 is not LDM
666	6.4.8.15			X			The package is designed for a temperature range of -40°C (see section 1.2.5) and +38°C (see section 2.2.1).
673	6.4.11.1				X		Subcriticality of the DN30 package is proven in section 2.2.5 under RCT, NCT and ACT taking into account: i. Leakage of water into the packages from operation and the water immersion test to the extent as restricted by para. 680 (b). ii. There are no built-in neutron absorbers or moderators.

[1)] For cross references in this matrix the paras of [IAEA 2012] are used

[IAEA 2012]	[ADR 2015] [RID 2015] [IMDG 2014] [ADN 2015]	IP-2	A	B(U)	Fissile	UF_6	Remarks [1)]
							iii. Rearrangement of the contents within the package (inside the 30B cylinder); a loss from the package has not to be considered. iv. Reduction of spaces within or between the packages. v. Packages becoming immersed in water or buried in snow (surrounded by water of varying density). vi. Temperature changes (affecting the density of the UF_6). Following requirements are met: i. The smallest overall dimension is not less than 10 cm, see section 1.4. ii. The requirements prescribed elsewhere in this compliance matrix. iii. There is a sealing system at the outside of the package, see section 1.4.3.3.7. iv. See paras 676-686.
674	6.4.11.2				X		The exceptions specified do not apply to the DN30 package.
675	6.4.11.3				X		The content specification of the DN30 package comprises only contents with traces of Plutonium, see section 1.3.2.
676	6.4.11.4				X		The chemical form of UF_6 is well known. For the isotopic compositions maximal values of the fissile nuclide U-235 are assumed. Physical form, mass, concentration of impurities, moderation ratio or density and geometrical configuration are varied to determine the maximum neutron multiplication factor. The variation calculations are documented in section 2.2.5.5 respectively Appendix 2.2.5 (Criticality Safety Analysis).
677	6.4.11.5				X		UF_6 is not considered irradiated nuclear fuel.
678	6.4.11.6				X		The DN30 package after the tests simulating NCT: (a) Preserves minimum overall outside dimension of at least 10 cm, see section 2.2.1. (b) Prevents the entry of a 10 cm cube, see section 2.2.1.
679	6.4.11.7				X		The package is designed for a temperature range of -40°C (see section 1.2.5) and +38°C (see section 2.2.1).

[1)] For cross references in this matrix the paras of [IAEA 2012] are used

[IAEA 2012]	[ADR 2015] [RID 2015] [IMDG 2014] [ADN 2015]	IP-2	A	B(U)	Fissile	UF_6	Remarks [1)]
680	6.4.11.8				X		For the individual DN30 package in isolation, containing uranium hexafluoride only, with a maximum uranium enrichment of 5 wt. % in U-235, it is assumed, that • Following the tests prescribed in [ADR 2015] no. 6.4.11.13 b) or [IAEA 2012] para. 685 (b) there is no physical contact between the valve or plug and any other component of the packaging other than their original points of attachment, And where, in addition • Following the test prescribed in [ADR 2015] no. 6.4.17.3 or [IAEA 2012] para. 728 the valve and the plug remain leak tight. These conditions are verified in section 2.2.1. In section 1.9 the high degree of quality management and control for manufacturing, maintenance (section 1.8) and repair of packagings as well as operations (section 1.7) is specified.
681	6.4.11.9				X		The analysis for an individual package in isolation assumes at least a layer of 20 cm water surrounding the DN30 package, see section 2.2.5.5.1.
682	6.4.11.10				X		The DN30 package is analyzed consistent with (a) RCT (b) NCT (c) ACT See section 2.2.5.
683	6.4.11.11				X		The DN30 package shall not be transported by air.
684	6.4.11.12				X		The number N derived for the DN30 package is infinite. The proof of subcriticality for NCT is contained in section 2.2.5.
685	6.4.11.13				X		The number N derived for the DN30 package is infinite. The proof of subcriticality for ACT is contained in section 2.2.5.
686	6.4.11.14				X		For the DN30 package the following applies: CSI = 0.

[1)] For cross references in this matrix the paras of [IAEA 2012] are used

[IAEA 2012]	[ADR 2015] [RID 2015] [IMDG 2014] [ADN 2015]	IP-2	A	B(U)	Fissile	UF_6	Remarks [1)]
701	6.4.12.1	X	X	X	X	X	For the demonstration of compliance the following methods are used: • Performance of tests, see section 2.2.1.5, Appendix 2.2.1.2 (Drop Test Reports), section Appendix 2.2.2.2 (Thermal Test Report). • Analysis and calculations, see sections 2.1.3 and 2.2.
702	6.4.12.2	X	X	X	X	X	The prototypes used for the tests are assessed before and after the tests according to written procedures, see Appendix 2.2.1.2 (Drop Test Reports), Appendix 2.2.2.2 (Thermal Test Report).
713	6.4.12.3	X	X	X	X	X	The specimens are inspected before each test according to a written procedure. The results of the inspection are documented. The inspection comprises at least: (a) Divergence from the design (b) Defects in manufacture (c) Corrosion and deterioration (d) Distortion of features The inspection procedures are specified in Appendix 2.2.1.2 (Drop Test Reports), Appendix 2.2.2.2 (Thermal Test Report).
714	6.4.12.3	X	X	X	X	X	The 30B cylinder with its valve and plug is the containment system.
715	6.4.12.3	X	X	X	X	X	The prototypes are marked with a serial no. and can be easily referenced, see Appendix 2.2.1.2 (Drop Test Reports), Appendix 2.2.2.2 (Thermal Test Report).
716	6.4.13	X	X	X	X	X	The results of the tests are recorded, documented and assesse with respect to influence on the integrity of the containment and confinement system, Appendix 2.2.1.2 (Drop Test Reports), Appendix 2.2.2.2 (Thermal Test Report).
717	6.4.14	X	X	X	X	X	The target for drop tests complies with the requirements of [SG-26], para. 718.2, see Appendix 2.2.1.2 (Drop Test Reports).
718	6.4.21.5					X	The 30B cylinder complies with [ISO 7195] and [ANSI N14.1] and is tested hydraulically with a test pressure of 2.76 MPa.
719	6.4.15.1	X	X	X	X	X	See paras 722-724.

[1)] For cross references in this matrix the paras of [IAEA 2012] are used

[IAEA 2012]	[ADR 2015] [RID 2015] [IMDG 2014] [ADN 2015]	IP-2	A	B(U)	Fissile	UF_6	Remarks [1)]
720	6.4.15.2	X	X	X	X	X	The time interval between the water spray test and the subsequent tests is not relevant, see para. 721.
721	6.4.15.3		X	X	X		The DN30 PSP is a fully closed and welded structure of stainless steel. Any influence of the water spray test on the properties of the DN30 package can be excluded.
722	6.4.15.4	X	X	X	X	X	The free drop test is analyzed in section 2.2.1 and carried out on prototypes as documented in Appendix 2.2.1.2 (Drop Test Reports).
723	6.4.15.5	X	X	X	X		The shape of the packaging prevents stacking; hence the stacking test is omitted.
724	6.4.15.6		X	X	X		The DN30 package is tested to withstand accident conditions of transport. The drop test onto the bar required under ACT is much more severe than the penetration test defined in para. 724.
725	6.4.16		X				Not applicable as during transport the physical state of UF_6 is solid.
726	6.4.17.1			X	X		A prototype used for testing was subject to the cumulative effects of twice the mechanical tests specified in para. 722 and followed by twice the tests specified in para. 727 and finally followed by the thermal test specified in para. 728, see section 2.2.2.3.2.2 and Appendix 2.2.2.2 (Thermal Test Report).
727 (a)	6.4.17.2 (a)			X	X		As the mass of the DN30 package exceeds a mass of 500 kg, the 9 m drop test is carried out. The test results are documented and analyzed in 2.2.1 and Appendix 2.2.1.2 (Drop Test Reports).
727 (b)	6.4.17.2 (b)			X	X		It was determined in analyses, that the most damaging drop tests sequence is the 9 m drop followed by the drop onto the bar. The test results are documented and analyzed in 2.2.1 and Appendix 2.2.1.2 (Drop Test Reports).
727 (c)	6.4.17.2 (c)			X	X		As the mass of the DN30 package exceeds a mass of 500 kg, the dynamic crush test is not applicable.

[1)] For cross references in this matrix the paras of [IAEA 2012] are used

[IAEA 2012]	[ADR 2015] [RID 2015] [IMDG 2014] [ADN 2015]	IP-2	A	B(U)	Fissile	UF_6	Remarks [1)]
728	6.4.17.3			X	X	X	The thermal test is carried out using a specimen which the cumulative effects of twice the mechanical tests specified in para. 722 and followed by twice the tests specified in para. 727.
729	6.4.17.4			X	X		The water immersion test is analyzed in section 2.2.1.5.2; inleakage of water during this test is taken into account for the criticality safety analysis, see section 2.2.5.5.
730	6.4.18			X			As the total activity in a DN30 package is less than 10^5 A_2 (see section1.3.2), the enhanced water immersion test is not applicable.
731	6.4.19.1				X		Under the provisions of para. 680 (b) water inleakage into the 30B cylinder has been excluded.
732	6.4.19.2				X		The test conditions before the water inleakage test comply with the test conditions required by para. 659 and 685.
733	6.4.19.3				X		The test conditions of the water inleakage test defined here are less stringent than the test conditions defined in para. 729.

[1)] For cross references in this matrix the paras of [IAEA 2012] are used

1.7 OPERATION

Operation is subdivided into four lifetime phases of the DN30 packaging:

1. Testing and controls before its first use,
2. Regular usage and testing and controls before each transport,
3. Periodical inspection in defined intervals,
4. Repairs to return the DN30 packaging to service.

All these phases are regulated in manufacturing specifications, handling and test instructions specified below. At the time of application of these specifications and instructions the user must make sure that he has the valid revision of the respective specifications and instructions available.

1.7.1 TESTING REQUIREMENTS AND CONTROLS BEFORE FIRST USE

The testing requirements and controls before the first use of the packaging are specified in

- [ISO 7195] and [ANSI N14.1] for the 30B cylinder.
- Specification no. 0023-SPZ-2016-001 for the DN30 PSP (see Appendix 1.9.2 (Manufacturing Specification)).

1.7.2 TESTING REQUIREMENTS AND CONTROLS BEFORE EACH TRANSPORT

The testing requirements and controls before each transport are described in

- Handling instruction no. 0023-HA-2015-001 (see Appendix 1.7.1 (Handling Instruction)).

For maintenance and treatment of non-conformances and deviations, see section 1.8.1.

1.7.3 HANDLING AND TIE DOWN REQUIREMENTS

Handling of the DN30 package and packaging and its parts is described in section 1.4.3.4. For the handling operations adequate means as described in the handling instruction no. 0023-HA-2015-001 have to be used.

Tie-down of the DN30 package and packaging is described in section 1.4.3.5. The procedures to be applied to ensure proper tie-down are specified in the handling instruction no. 0023-HA-2015-001.

1.7.4 LOADING AND UNLOADING OF THE PACKAGE CONTENTS.

The DN30 PSP can only be loaded with a 30B cylinder. The respective handling procedure is described in the handling instruction no. 0023-HA-2015-001.

Filling of the 30B cylinder with UF_6 is described in the site specific operating handbooks, which are not part of this PDSR. It must be assured that before transport the 30B cylinder was given ample time for cooling down such that the UF_6 is in solid state.

1.7.5 ASSEMBLY OF THE PACKAGING COMPONENTS

During usage of the DN30 PSP only the top half needs to be separated from and installed on the bottom half of the DN30 PSP and the 30B cylinder loaded into or unloaded from the DN30 PSP.

1.7.5.1 Loading of the 30B cylinder into the DN30 PSP

An overview of the safety related loading steps during loading of a 30B cylinder into the DN30 PSP are listed in the following. Details of the handling steps are specified in handling instruction no. 0023-HA-2015-001.

1) The rotation preventing devices are in position “open”.
2) The valve protecting device and its housing are in position “open”.
3) Lower the 30B cylinder in horizontal orientation with the valve in 12°o’clock position into the bottom half of the DN30 PSP.
4) When the lower rim of the cylinder skirt has passed the valve protecting device, rotate this valve protecting device towards the cylinder head by approx. 90° until it is in contact with the cylinder head. Then lower the cylinder until it rests on the inner shell of the bottom half of the DN30 PSP. Then push the housing in position “closed”.
5) Move the rotation preventing devices to position “closed”.
6) Lower the top half of the DN30 PSP onto the bottom half.
7) Insert the pins into the six mortise-and-tenon closure devices and fix the pins with the securing bolts.
8) Install the seals.

1.7.5.2 Unloading of the 30B cylinder from the DN30 PSP

In order to prevent damage of any safety related feature during unloading, the following general steps are required. Details are given in handling instruction no. 0023-HA-2015-001.

1) Check and remove the seals.
2) Loosen the securing bolts and remove the pins of the six mortise-and-tenon closure devices.
3) Lift off the top half of the DN30 PSP.
4) Move the rotation preventing devices to position “open”.
5) Pull the housing from the valve protecting device.
6) Lift the 30B cylinder and rotate the valve protecting device by about 90° until it rests on the flange of the bottom half.
7) Lift the 30B cylinder out of the bottom half of the DN30 PSP.

1.7.6 SUPPLEMENTARY EQUIPMENT AND OPERATIONAL CONTROLS

No supplementary equipment except means for tie-down are used during transport of the DN30 package in any transport modes.

1.7.7 PRECAUTIONS AND MEASURES DUE TO THE OTHER DANGEROUS PROPERTIES OF THE CONTENT

No precautions and measures due to the other dangerous properties of the content are required except the correct labeling according to the respective transport modes.

1.8 MAINTENANCE

1.8.1 MAINTENANCE AND INSPECTION REQUIREMENTS BEFORE EACH SHIPMENT

The maintenance of the DN30 packaging and checks before each use are described in handling instruction no. 0023-HA-2015-001 (see Appendix 1.7.1 (Handling Instruction)). This handling instruction references test instruction no. 0023-PA-2015-016 (see Appendix 1.8.2 (Inspection Criteria)) in which the criteria for the checks are defined and measures in case of non-conformances or deviations are specified.

In the case that non-conformances or deviations might affect the safety of the DN30 packaging the user of the packaging has to inform the owner of the certificate of package approval in writing about the non-conformance or deviation. It is then the decision of the owner of the certificate of package approval to undertake suitable measures to return the packaging to service in full compliance with the PDSR and the certificate of package approval.

1.8.2 MAINTENANCE AND INSPECTION REQUIREMENTS AT PERIODIC INTERVALS FOR THE LIFETIME

The periodical inspections of the DN30 packaging are subdivided into the periodical recertification of the 30B cylinder and the periodical inspection of the DN30 PSP.

The recertification of the 30B cylinder is regulated in [ISO 7195] and [ANSI N14.1]. There are no additional requirements for the use of the 30B cylinder as part of the DN30 packaging.

The periodical inspections of the DN30 PSP are described in test instruction no. 0023-PA-2015-015 (see Appendix 1.8.1 (Periodical Inspections)) and test instruction no. 0023-PA-2015-016 (see Appendix 1.8.2 (Inspection Criteria)), in which the criteria for the checks are defined and measures in case of non-conformances or deviations are specified.

In case non-conformances or deviations might affect the safety of the DN30 packaging the user of the packaging has to inform the owner of the certificate of package approval in writing about the non-conformance or deviation. It is then the decision of the owner of the certificate of package approval to undertake suitable measures to return the packaging to service in full compliance with the PDSR and the certificate of package approval.

1.9 MANAGEMENT SYSTEM

The management system of company DAHER NUCLEAR TECHNOLOGIES GmbH (DAHER NT) is laid down in the Integrated Management Handbook (see Appendix 1.9.1 (IMS)).

The management system is certified according to

- DIN EN ISO 9001
- DIN EN ISO 14001
- OSHAS 18001
- KTA 1401
- BAM GGR 011

covering design and development, manufacturing and operation of packagings for packages requiring approval by the competent authorities for the transport of radioactive material.

1.9.1 DESIGN, PDSR, DOCUMENTATION AND RECORDS

1.9.1.1 General

The 30B cylinder is specified in [ISO 7195] and [ANSI N14.1]. These standards define the design, manufacturing, inspection and controls before first use and operation including maintenance and periodical recertification of the cylinder. No additional documents are provided by DAHER NT for this component of the DN30 package design.

DAHER NT is responsible for the design, development, safety analyses, manufacturer planning and surveillance, inspection and controls before first use and operation including maintenance and periodical recertification of the DN30 PSP.

All documents like drawings, calculations, specifications etc. are written, checked and released in accordance with the IMS of DAHER NT. The author and the examiner must be experienced in the respective field of technology whereas the person releasing the document must be authorized according to the organizational structure of DAHER NT. For each field of technology the different roles of the employees of DAHER NT are described in the IMS.

Any design modifications including any revisions of specifications, drawings and instructions are carried out according to the processes laid down in the IMS and documented accordingly.

In case there are documents from suppliers, DAHER NT will check these documents according to the process laid down in the IMS.

1.9.1.2 Design

DAHER NT is responsible for the whole design process from establishing the requirements based on the applicable regulations and standards up to the completion of the drawings, safety analyses and the manufacturing specification. All individual steps necessary for the design process are stipulated in the IMS of DAHER NT.

Design modifications required due to the progress in carrying out the safety analyses or resulting from the outcome of physical tests with specimens or prototypes are introduced into the design process in compliance with the respective process described in the IMS of DAHER NT.

1.9.1.3 Documents and Records

Traceability of each document and record relevant during the design process is assured by the requirements of the IMS of DAHER NT with respect to a unique numbering and filing system.

For each document written and released by DAHER NT, the original workable document is stored together with the signed document as image. For documents and records of suppliers only the image of the document might be made available and stored.

During the design process the documents listed in section 1.1 are produced and filed.

1.9.2 MANUFACTURING AND TESTING

1.9.2.1 Manufacturing of 30B cylinders

Manufacturing of 30B cylinders is specified in [ISO 7195] and [ANSI N14.1].

1.9.2.2 Manufacturing of serial DN30 PSPs

Qualification and selection of the manufacturer as well as the requirements towards QA during material procurement, manufacturing and final inspection before first use are specified in manufacturing specification no. 0023-SPZ-2016-001 (see Appendix 1.9.2 (Manufacturing Specification)). This specification details among others the following requirements:

- Qualification of manufacturer,
- Scope of services and responsibilities of manufacturer,
- Responsibilities of DAHER NT,
- Requirements for materials including certification,
- Requirements concerning fabrication including welding,
- Requirements concerning final acceptance test,
- Treatment of non-conformances,
- Manufacturing test sequence plan (MTSP).

1.9.2.3 Testing of samples and prototypes

Manufacturing and testing of samples and prototypes is managed comparably to the standards specified for the serial DN30 PSPs.

Samples for mechanical and thermal testing of the foam used as shock absorbing material and thermal insulation are manufactured, certified and documented identicaly to the foam used in the prototypes and serial DN30 PSPs.

The tests to determine the properties of the foam are documented in the summary report contained in Appendix 1.4. For these tests qualified institutes were involved:

- The Material Testing Institute, University of Stuttgart (MPA), for the mechanical tests.

- The institute for combustion and gas dynamics, University of Duisburg-Essen, for the analysis of the chemical composition of the foam under different thermal conditions.

- Company Influtherm, an independent society specialized in thermal measurements and services, for the measurement of the thermal properties of the foam and the intumescent material.

Tests with prototypes were carried out by the BAM. For package approvals originating in Germany, BAM is one of two competent authorities.

1.9.3 OPERATION

The quality management requirements for operation are specified in the handling instruction no. 0023-HA-2015-001 (see Appendix 1.7.1 (Handling Instruction)).

In the case that the DN30 PSP is leased out for transports to a customer, the handling instruction will be provided to the respective customer and he has to confirm in writing that he will comply with the requirements stipulated there.

In case the DN30 PSP is sold to a customer, the handling instruction and the test instruction regulating maintenance and periodical retesting will be provided to the respective customer and he has to confirm in writing that he will comply with the requirements stipulated there.

1.9.4 MAINTENANCE AND REPAIR

The quality management requirements for periodical inspections of the DN30 PSP are described in test instruction no. 0023-PA-2015-015 (see Appendix 1.8.1 (Periodical Inspections)).

Both of these instructions refer to test instruction no. 0023-PA-2015-016 (see Appendix 1.8.2 (Inspection Criteria)) in which the non-conformances and deviations are described for which repair is required. In all cases where repair is required DAHER NT must be involved in the planning, authorization and execution of the repair measures.

For repair other than replacement of parts, the specification no. 0023-SPZ-2016-001 (see Appendix 1.9.2 (Manufacturing Specification)) must be complied with.

1.9.5 COMPLIANCE OF ANY ACTIVITY WITH THE PDSR

Specification no. 0023-SPZ-2016-001 (see Appendix 1.9.2 (Manufacturing Specification)) ensures that during manufacturing and final acceptance test before first use the requirements of the PDSR towards the design are met. In detail the following requirements are considered:

- Specification of the material properties in material data sheets to comply with the properties used throughout this PDSR.

- Requirements for welders and welding to ensure the structural properties of the DN30 PSP as defined in this PDSR.

- Specification of tests and documentation during manufacturing and before first use to ensure that the design of the DN30 PSP complies with the drawings.

Handling instruction no. 0023-HA-2015-001 (see Appendix 1.7.1 (Handling Instruction)) and test instruction no. 0023-PA-2015-015 (see Appendix 1.8.1 (Periodical Inspections)) together with the applicable secondary document test instruction no. 0023-PA-2015-016 (see Appendix

1.8.2 (Inspection Criteria)) ensure that during operation the DN30 is always kept in compliance with the PDSR.

1.10 PACKAGE ILLUSTRATION

Figure 10 and Figure 11 show an illustration of the DN3 package. Appendix 1.4.1 (Drawings) contains the set of drawings for the DN30 PSP. The 30B cylinder is specified and shown in [ISO 7195] and [ANSI N14.1].

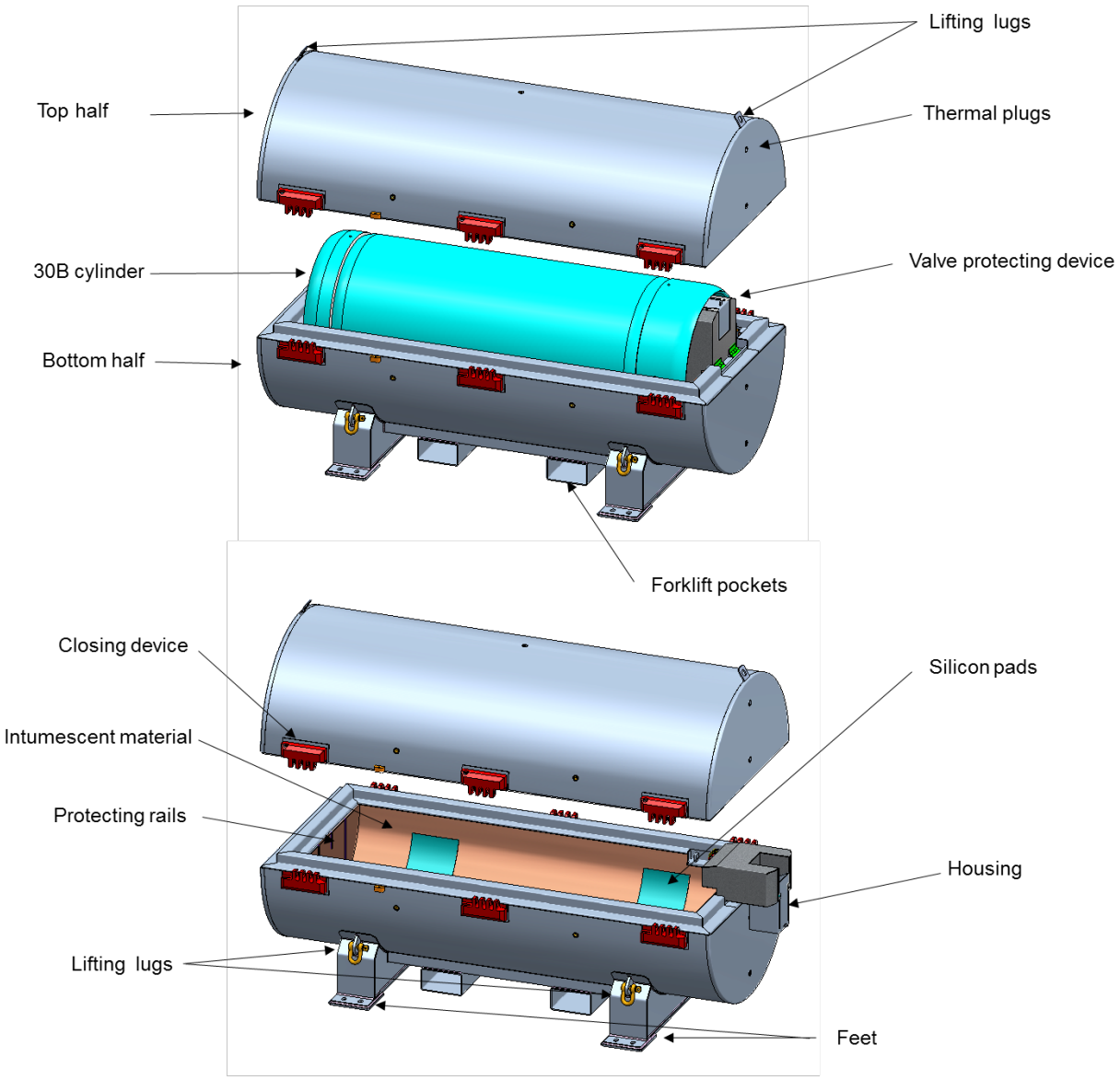

Figure 10: DN30 PSP overview

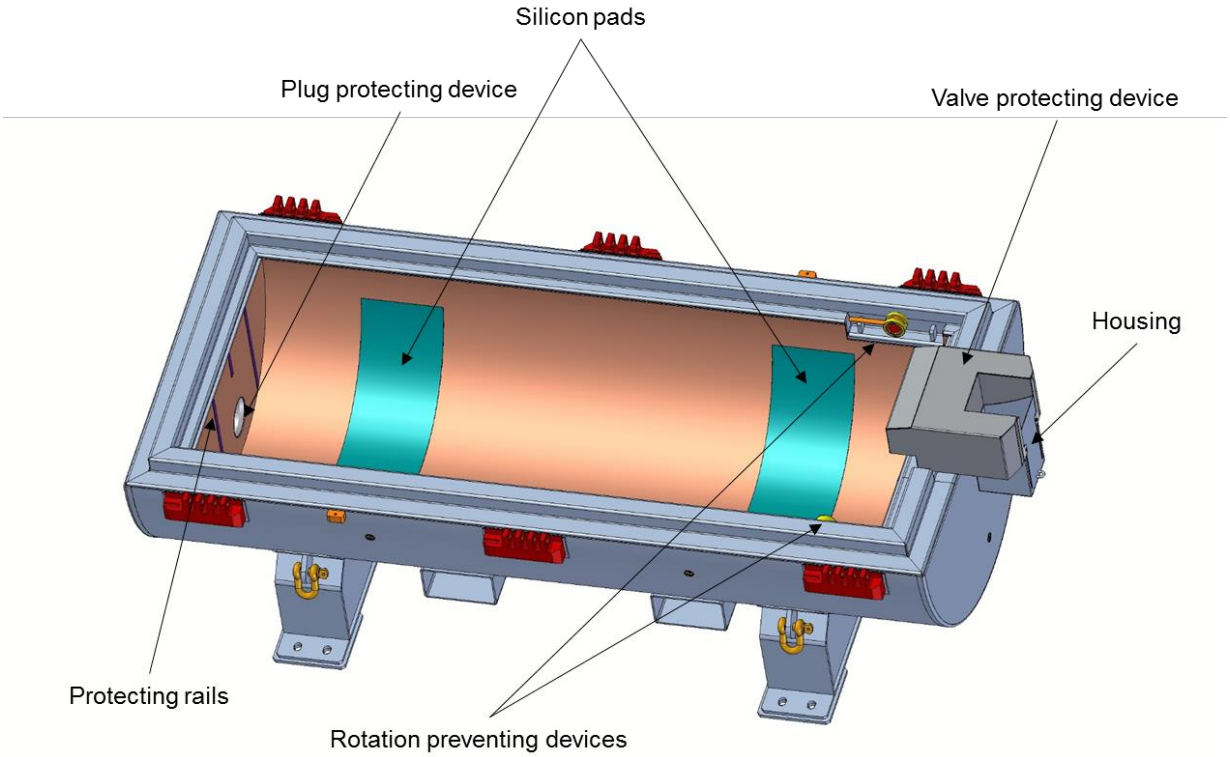

Figure 11: DN30 PSP bottom half

PART 2

2.1 COMMON PROVISIONS FOR ALL TECHNICAL ANALYSES

In this section the common provisions valid for all technical analysis are described. For a better overview also the provisions of the respective technical analysis which might have an influence on other analyses are summarized as an extract from the detailed technical analysis.

2.1.1 PACKAGE DESIGN

The analyzed package design is described in section 1.3 (content) and in section 1.4 (30B cylinder and DN30 PSP).

2.1.1.1 Content

The content for all analyses is UF_6. However, for the different analyses only few properties of the material are relevant and taken into account:

- For the structural analysis the density is the only important physical property of the content. As the mechanical properties of solid UF_6 are not well known, a content simulated by a solid block of material (iron concrete) is analyzed. The solid concrete has the same density as solid UF_6.

  For the solid block it is assumed that the material fills approx. 60% of the lower part of the cylinder (standard transport configuration).

  There is no distinction between commercial grade and reprocessed UF_6 in the structural analysis.

- For the thermal analysis the important physical properties are the density, the thermal conductivity and the specific heat capacity. For the thermal analysis it is assumed that the UF_6 completely fills the cavity of the 30B cylinder. The density is adjusted accordingly so that the full cylinder contains 2277 kg of UF_6.

  There is no distinction between commercial grade and reprocessed UF_6 in the thermal analysis.

- For the containment analysis the important physical property is the viscosity of the gaseous UF_6. For this analysis the content configuration has no influence on results.

  The source terms for the radioactive contents for commercial grade and reprocessed UF_6 are treated separately according to the specification given in section 1.3. The physical properties are assumed to be identical for commercial grade and reprocessed UF_6.

- For the external dose rate analysis the important physical properties are the density and the shielding properties of the UF_6. Here, conservatively different filling ratios of the cylinder are considered up to an only theoreticaly possible completely filled cylinder.

  For cylinders containing heels different configurations of the small amount of residues are analyzed. The configurations are heels forming a puddle at the lower side of the cylinder or the homogeneous contamination of parts or the whole inner surface of the cylinder shell with UF_6.

  The source terms for the radioactive contents for commercial grade and reprocessed UF_6 are treated separately according to the specification given in section 1.3. The physical properties are assumed to be identical for commercial grade and reprocessed UF_6.

- For the criticality safety analysis the important physical properties are the density, the purity (hydrogen impurities) and the nuclear physical properties of the nuclides present in the UF_6. For this analysis a variety of configurations is analyzed comprising a full cylinder, partially filled cylinders, UF_6 forming a layer at the inner surface the cylinder, grained structures and local concentrations of impurities.

  There is no distinction between commercial grade and reprocessed UF_6 in the criticality safety analyses.

2.1.1.2 30B cylinder

The 30B cylinder design is standardized and defined in [ISO 7195] and [ANSI N14.1].

- For the structural analysis the standard dimensions are assumed.
- For the thermal analysis a simplified model of the 30B cylinder is used. The round ends of the cylinder are replaced by flat ends. The wall thickness, diameter, length and the cylinder volume are preserved. For the material standard physical properties are assumed.
- For the containment analysis neither the dimensions nor the physical properties of the cylinder are relevant.

  However, the free volume in the cylinder is part of the analysis and for the evaluation of this parameter the standard volume of the cylinder reduced by the respective filling ratios is assumed. Furthermore, the design of the valve, especially the connection to the cylinder and the seat of the valve are taken into account based on the standards.
- For the external dose rate analysis a simplified cylinder with flat ends is assumed.
- For the criticality safety analysis a simplified model with flat ends as well as a model with round ends are analyzed. Furthermore, dimensions and wall thickness are varied to assess the most reactive cases.

2.1.1.3 DN30 PSP

The design of the DN30 PSP is defined in the drawings specified in section 1.4.

- For the structural analysis the standard dimensions are assumed. The influence of temperatures of the components evaluated in the thermal analysis on the mechanical behavior is analyzed in variation calculations.
- For the thermal analysis under RCT and NCT the standard dimensions and standard physical properties are assumed.

  For the thermal analysis under ACT the standard dimensions and deteriorated physical properties are assumed. Furthermore, incineration of the foam as experienced in the thermal test is modelled.
- For the containment analysis the DN30 PSP is completely neglected.
- For the external dose rate analysis the standard dimensions and standard physical properties are assumed. For the analysis of the external dose rate under ACT the foam as well as the distance between inner and outer shell of the DN30 PSP are neglected.
- For the criticality safety analysis, the DN30 PSP is generally completely neglected. Only in the case of a wall thickness of the 30B cylinder of less than 11 mm (standard

wall thickness 13 mm) the stainless steel shell of the DN30 PSP has to be taken into account to prove criticality safety.

2.1.2 ACCEPTANCE CRITERIA AND DESIGN ASSUMPTIONS

2.1.2.1 Mechanical design

The acceptance criteria and design assumptions for the mechanical design are:

- No physical contact of the 30B cylinder valve with any other packaging component except for the initial point of connection (thread).
- No physical contact of the 30B cylinder plug with any other packaging component except for the initial point of connection (thread).
- No failure of the 30B cylinder containment system.
- No failure of the DN30 closing system.

2.1.2.2 Thermal design

The acceptance criteria and design assumptions for the thermal design are:

- The temperatures at the thread connection between 30B cylinder valve and cylinder should not lead to a leakage rate in excess of 1.0E-4 Pa m^3 / s during the thermal test simulating ACT for a package in the condition after the mechanical tests simulating NCT and ACT.
- The temperatures at the thread connection between 30B cylinder plug and cylinder should not lead to a leakage rate in excess of 1.0E-4 Pa m^3 / s during the thermal test simulating ACT for a package in the condition after the mechanical tests simulating NCT and ACT.
- No failure of the 30B cylinder containment system.

The thermal design takes into account different filling ratios between a full cylinder containing 2277 kg UF_6 and an emptied cylinder containing heels.

2.1.2.3 Containment system design

The acceptance criteria and design assumptions for the containment system design are:

- The activity release rate for NCT and ACT as defined in [ADR 2015] and [IAEA 2012] must not be exceeded.
- The containment is the 30B cylinder with its valve and plug.
- The DN30 PSP has no containment function.

2.1.2.4 External dose rate assessment

The acceptance criteria and design assumptions for the containment system design are:

- The external dose rate limits for ACT, NCT and ACT as defined in [ADR 2015] and [IAEA2012] must not be exceeded.
- For the assessment of the dose rates, conservative assumptions with respect to the cylinder filling ratio and the shape of the 30B cylinder are used.
- For the assessment of the dose rate at the vehicle, two respectively four packages loaded side by side are considered.
- For the assessment of the dose rate increase after the tests simulating NCT, a permissible deformation is evaluated (with respect to the limit of 20% dose rate increase) and compared with the deformations calculated for NCT.

2.1.2.5 Criticality safety assessment

The acceptance criteria and design assumptions for the criticality safety assessment are:

- Criticality safety is assured by the 30B cylinder whenever the wall thickness of the cylinder is not less than 11 mm. The DN30 PSP is in this case not relevant for criticality safety.
- Only in case of a reduction of the wall thickness of the 30B cylinder below 11 mm (as specified in [ISO 7195] or [ANSI N14.1]) the stainless steel shells of the DN30 PSP have to be taken into account to assure criticality safety.
- The foam is not a part of the confinement system.
- For RCT, NCT and ACT the criticality safety criterion is $k_{eff} + 3\sigma + \Delta k < 0.95$ (see section 2.2.5.1 for details).

2.1.3 DESCRIPTION AND JUSTIFICATION OF ANALYSIS METHODS

2.1.3.1 Structural analysis

2.1.3.1.1 Mechanical analysis of RCT

The mechanical analysis of RCT comprises

- Analysis of the lifting attachment points.
- Analysis of the features of the packaging used for tie-down.

These analyses are carried out by hand calculations using well established formulas for stress and strain.

2.1.3.1.2 Mechanical analysis of NCT and ACT

The mechanical analysis of NCT and ACT comprises the analysis of a sequence of the following tests:

Test 1: 1.2 m free drop test

Test 2: 9 m drop

Test 3: 1 m drop onto a bar

The mechanical analysis of NCT and ACT was carried out in three major steps:

- Pre-analysis of the behavior of the package by using proven FEM tools and selection of benchmarks for the real drop tests with prototypes.
- Real testing of prototypes by applying the selected benchmark test sequences.
- Refinement of the FEM-model based on the results of the test results and complete analysis of the behavior of the package DN30 under NCT and ACT for the operating temperature range of -40°C to +60°C.

2.1.3.1.2.1 Pre-analysis

In the analysis the following sequences were considered:

- Test 1 – Test 2 – Test 3
- Test 1 – Test 3 – Test 2

The analyses were carried out for all considerable orientations of the package before the tests:

- Flat onto the valve side.
- Flat onto the plug side.
- Flat onto the closure system.
- Flat onto the top side.
- Inclined onto the valve side so that the line between center of gravity and point of impact is perpendicular to the target surface.

- Inclined onto the plug side so that the line between center of gravity and point of impact is perpendicular to the target surface.
- Inclined onto the closure system so that the line between center of gravity and point of impact is perpendicular to the target surface.
- Inclined onto the feet (slap-down).

The analyses were carried out by using the FEM tool LS-DYNA. The results of the pre-analysis were used to set up the drop test sequences. The documentation of the pre-analysis is not part of the PDSR.

2.1.3.1.2.2 Real tests

For the real tests 5 sequences were selected:

- Flat onto the valve side.
- Inclined onto the valve side so that the line between center of gravity and point of impact is perpendicular to the target surface.
- Inclined onto the plug side so that the line between center of gravity and point of impact is perpendicular to the target surface.
- Inclined onto the closure system so that the line between center of gravity and point of impact is perpendicular to the target surface.
- Inclined onto the feet (slap-down).

These tests were carried out at the drop test facility of BAM.

2.1.3.1.2.3 Refinement of the calculation model and complete analysis for NCT and ACT

In this step the real tests results are used to refine the calculation model so that agrees with the results of the real drop tests. This “benchmarked” calculation model is then used to perform a comprehensive analysis of the DN30 package under NCT and ACT taking into account the operating temperature range of -40°C to +60°C.

The calculations are documented in Appendix 2.2.1.3 (Structural Analysis of the DN30 Package under NCT and ACT).

2.1.3.1.3 Description of the used calculation programs

The results of the drop test simulations in this report are obtained by the numerical solving of differential equations, which are based on the finite element method (FEM). Due to the highly dynamic nature of this kind of simulations, the FEM solver LS-DYNA (MPP S R8.0.0) [LS-DYNA 2015] of the software developer LSTC is used, which is integrated in ANSYS®, Release 17.0 [ANSYS]. LS-DYNA is widely used for crash simulations by the automobile industry. Other applications include sheet metal forming and cutting in the manufacturing industry as well as bird strike, jet engine blade containment and structural failure in the aerospace industry.

As a pure FEM solver, LS-DYNA lacks any modeling features. Therefore, most of the modelling is performed in ANSYS Workbench [ANSYS WB], which provides several tools for geometry modifications and FEM modeliing. The built-in software ANSYS DesignModeler [ANSYS DM] is used for the geometry modifications while the FEM model itself is developed in ANSYS Mechanical with the plugin “Explicit Dynamics (LS-DYNA Export)” [ANSYS HS]. An input file for LS-DYNA is exported that is further modified with the pre- and postprocessor LS-PrePost

(V4.2) [LS-PREPOST] because the LS-DYNA plugin for ANSYS Mechanical only provides very basic features of LS-DYNA, especially concerning contact and material modelling. After the results are calculated, they are analyzed in LS-PrePost.

2.1.3.2 Thermal analysis

2.1.3.2.1 Thermal analysis of RCT and NCT

The thermal analysis of RCT and NCT comprises:

- Analysis of the DN30 package under an ambient temperature of 38°C without solar insolation.
- Analysis of the DN30 package under an ambient temperature of 38°C taking into account solar insolation.

These analyses are carried out by using the finite-difference code HEATING 7.2 [HEATING 7.2].

2.1.3.2.2 Thermal analysis of ACT

The thermal analysis of ACT comprises:

- Analysis of the DN30 package under the conditions of the thermal test with an ambient temperature of 800°C and an exposure time of 30 min.

2.1.3.2.2.1 Pre-analysis

In the pre-analysis the following conditions of the DN30 package specimen were considered:

- Condition of the DN30 PSP after an accumulation of a full drop test sequence inclined onto the valve side and a full drop test sequence inclined onto the plug side.
- Completely empty 30B cylinder to minimize the thermal capacity of the 30B cylinder and content and hence maximize the temperature increase of the cylinder and its components.

The results of the pre-analysis were used to set up the thermal test conditions. The documentation of the pre-analysis is not part of the PDSR.

2.1.3.2.2.2 Real tests

The real test was carried out with a DN30 package specimen which was

- Pre-damaged by a full drop test sequence inclined onto the valve side followed by a full drop test sequence inclined onto the plug side.
- Contained an empty 30B cylinder.
- Heated up to a temperature of approx. 64°C to take into account the initial conditions due to an ambient temperature of 38°C and solar insolation.

2.1.3.2.2.3 Refinement of the calculation model and analysis for RCT, NCT and ACT

In this step the real tests results are used to refine the calculation model so that it agrees with the results of the real thermal tests. This “benchmarked” calculation model is then used to perform a comprehensive analysis of the DN30 package under RCT, NCT and ACT.

2.1.3.2.3 Description of the used calculation programs

The thermal analysis is carried out with the computer code HEATING 7.2 [HEATING 7.2].

HEATING is a general-purpose conduction heat transfer program written in FORTRAN 77. HEATING can solve steady-state and/or transient heat conduction problems in one-, two-, or three-dimensional Cartesian, cylindrical, or spherical coordinates. A model may include multiple materials, and the thermal conductivity, density, and specific heat of each material may be both time- and temperature-dependent. The thermal conductivity may also be anisotropic. Materials may undergo change of phase. Thermal properties of materials may be entered as data or may be extracted from a material properties library. Heat-generation rates may be dependent on time, temperature, and position, and boundary temperatures may be time- and position dependent. The boundary conditions, which may be surface-to-environment or surface-to-surface, may be specified temperatures or any combination of prescribed heat flux, forced convection, natural convection, and radiation. The boundary condition parameters may be time- and/or temperature-dependent. General gray body radiation problems may be modeled with user-defined factors for radiant exchange. The mesh spacing may be variable along each axis. HEATING uses a run-time memory allocation scheme to avoid having to recompile to match memory requirements for each specific problem. HEATING utilizes free-form input.

Three steady-state solution techniques are available: point-successive-overrelaxation iterative method with extrapolation, direct-solution (for one-dimensional or two-dimensional problems), and conjugate gradient. Transient problems may be solved using any one of several finite-difference schemes: Crank-Nicolson implicit, Classical Implicit Procedure (CIP), Classical Explicit Procedure (CEP), or Levy explicit method (which for some circumstances allows a time step greater than the CEP stability criterion). The solution of the system of equations arising from the implicit techniques is accomplished by point-successive-overrelaxation iteration and includes procedures to estimate the optimum acceleration parameter.

The program code HEATING was selected for the analysis of the DN30 package based on following advantages in important features:

- The formulation of the program allows easy simulation of phase change of the materials; in other codes the formulation of such material behavior is difficult.
- As will be shown later, the insulation material of the DN30 PSP incinerates during and after the fire causing an additional heat source; the simulation of such material behavior is easily implemented in HEATING and difficult to simulate with other codes.
- The shortcomings of HEATING due to its limited modeling capabilities are not relevant for the DN30 package as it can be easily modeled in cylindrical coordinates.

2.1.3.3 Containment design analysis

The containment analysis is performed for RCT, NCT and ACT. For all analyses a maximal standard Helium leakage rate of 1.0E-4 Pa m^3 / s is assumed. This assumption is justified in the comprehensive drop test program.

The containment design analysis is carried out according to [ISO 12807] in the following steps:

Step 1:	Determination of the radioactive inventory (see Appendix 1.3 (Radioactivity))
Step 2:	Determination of the activity releasable rate
Step 3:	Specification of the permissible activity release rate
Step 4:	Determination of the permissible activity release rate due to leakage
Step 5:	Determination of the activity concentration
Step 6:	Determination of the maximal volume leakage rate
Step 7:	Determination of the equivalent capillary diameter
Step 8:	Evaluation of the permissible standard leakage rate

The package has no elastomeric gaskets; hence there is no permeation activity release rate to be considered.

2.1.3.4 External dose rate analysis

2.1.3.4.1 External dose rate analysis for RCT

The external dose rate analysis for RCT consists of

- The analysis of the external dose rate at the surface of the DN30 package and at a distance of 2 m from the external surface of the DN30 package.
- The analysis of the external dose rate at a distance of 1 m from the external surface of the DN30 package to provide an estimate for the TI to be expected; the TI for transport will be determined in any case by measurement before transport.
- The analysis of the external dose rate at the surface of a standard vehicle routinely used for the transport of the DN30 package and in a distance of 2 m from the external surface of the vehicle; for this analysis it is assumed that 20' flatracks are used for the transport of four DN30 packages side by side, so that the dose rates at the surface of the vehicle are identical to the dose rates at the front surfaces of the DN30 package; for the analysis of the external dose rate in 2 m distance from the vehicle the influence of all four DN30 packages is taken into account.
- For LSA-II material additionally the external dose rate at 3 m distance from the unshielded material is analyzed

2.1.3.4.2 External dose rate analysis for NCT

The external dose rate analysis for NCT consists of the calculation of the maximal dose rate for a non-damaged DN30 package complying with the manufacturing drawings and a damaged DN30 package taking into account NCT and comparison of the respective values to prove that the increase is not greater than 20%.

2.1.3.4.3 External dose rate analysis for ACT

Only for type B(U)F packages it is shown that the dose rate at a distance of 1 m from the surface is less than 10 mSv/h.

2.1.3.4.4 Description of the used calculation programs

The calculation of external dose rates at the DN30 package is carried out by means of the program system SCALE 6.1 [SCALE 2011].

In a first step, the gamma and neutron source terms are determined by means of the depletion analysis sequence ORIGEN-ARP. By considering a mass of 1 g of each nuclide individually, the decay of the involved nuclides is individually evaluated and the respective neutron and gamma source terms are determined in the v7-27n-19g energy-group structure [SCALE 2011].

In a second step, the dose rates of 1 g of each radionuclide are calculated by means of the analysis sequence MAVRIC. The results used in the safety assessment are based on radial detectors, since calculations described in Appendix 2.2.4 (Dose Rate Analysis) show that for DN30 packages containing filled 30B cylinders the dose rates for radial detectors are always higher than the dose rates for axial detectors at the same distance from the surface of the package.

In a third step, the dose rates of 1 g of each radionuclide are multiplied by the concentration of the respective nuclide concentrations based on the content description in section 1.3 and by the mass of uranium modelled in the calculation model.

The second and third step are performed for each of the required calculations: 3 m distance from the unshielded material surface, surface of the DN30 package, 1 m distance from the DN30 package and 2 m distance from the vehicle.

2.1.3.5 Criticality safety analysis

2.1.3.5.1 General assumptions for the criticality safety analysis

Criticality safety analysis is based on the following assumptions

- For the single package in isolation and for the array of packages, flood with water is excluded because of the results of analyses and drop tests described in the mechanical analysis in section 2.2.1.
- Criticality safety is not based on the effect of neutron absorbers inside the package.
- For all contents the most reactive arrangement in the packaging is determined in all cases. Any credible rearrangement of contents in the package is taken into account in the analyses. Based on the results of analyses and drop tests described in the mechanical analysis, release of contents from the package needs not be assumed.
- A possible reduction of gaps in the package is analyzed. For arrays of packages, the distance between the packages is varied.
- Water around the package is considered in different layer thicknesses in the analysis of an array of packages.
- Temperature changes are taken into account by assuming a conservatively high density for UF_6. In the analyses with theoretical maximal water density of 1 g/cm^3, the particular optimal moderation for the arrangement is calculated. A decrease of water

density caused by a temperature rise or freezing will lead to lower moderation which is less reactive.

2.1.3.5.2 Description of the used calculation programs

All criticality safety calculations in this document are performed by means of the sequence CSAS6 of the criticality safety code KENO VI. Both versions SCALE 6.0 [SCALE 2009] and SCALE 6.1.1 [SCALE 2011] are used for the analyses.

The most recent libraries, based on ENDB/BVII data, are used for the criticality safety calculations. This includes the library v7-238 being used for energy multi-group cross sections.

2.1.4 RESULTS OF PHYSICAL TESTING OF SPECIMENS AND PROTOTYPES

2.1.4.1 Overview of the physical tests

In order to support and benchmark the mechanical and thermal analyses, physical tests with specimens and prototypes were carried out:

- Static and dynamic mechanical tests with specimens of the technical foam used as shock absorbing material and thermal insulation (see Appendix 1.4.2 (Material Data PIR Foam).
- Thermal tests with specimens of the technical foam used as shock absorbing material and thermal insulation (see Appendix 1.4.2 (Material Data PIR Foam) and Appendix 1.4.3 (Material Data Intumescent Material)).
- Drop tests with prototypes of the DN30 package loaded with a 30B cylinder loaded with surrogate material simulating the maximal permissible mass of UF_6 (see Appendix 2.2.1.2 (Drop Test Reports)).
- A fire test with a prototype of the DN30 package loaded with an empty 30B cylinder; the DN30 PSP prototype had been pre-damaged by two consecutive IAEA drop test sequences loaded with a 30B cylinder containing the maximal permissible mass of UF_6 (see Appendix 2.2.2.2 (Thermal Test Report)).

The results of the tests with prototypes and the comparison with the analyses are described in detail in section 2.2.1 and section 2.2.2.

2.1.4.2 Deviations between prototype and series

The feedback of users during the drop tests and the thermal tests as well as the result of some tests gave reason to certain design improvements of the DN30 PSP. These design improvements are described in the following sections. For each design improvement, the reason is specified and the impact on the results of the physical tests is evaluated.

2.1.4.2.1 The closure device

2.1.4.2.1.1 Description of the design modification

The pin of the closure system is secured by a bolt. In the prototype design this bolt was a standard socket head screw.

In the series design the standard socket head screw is replaced by:

- A captive socket head screw.
- Placement of a special washer between head and closure system body to prevent loosening of the bolt.

2.1.4.2.1.2 Justification of the design modification

The series design of the securing bolt ensures that the bolt remains connected to the closure system at all times during handling. To remove the bolt, the user has to pull the bolt and unscrew it at the same time. Without pulling at the bolt, removal of the bolt from the closure system is not possible.

Vibrations during transport could lead to a loosening of the bolt. The use of washers to secure the bolt ensures that it remains fixed during transport.

2.1.4.2.1.3 Impact on the results of the physical testing

2.1.4.2.1.3.1 Mechanical tests

The design of teeth and pin of the closure device of prototype and series DN30 PSP is identical. The design of the bolt has no influence on the results of the mechanical tests.

2.1.4.2.1.3.2 Thermal test

The design of the bolt of the closure device has no influence on the results of the thermal test.

2.1.4.2.2 The feet

2.1.4.2.2.1 Description of the design modification

During the drop test campaign it was noticed that handling of the prototype of the DN30 package by using a fork lifter might lead to damages at the bottom of the bottom half shell as the distance between floor and bottom half was too small to allow the forks of the fork lifter to be inserted under the DN30 prototype.

Following modifications were introduced:

- The height of the feet was increased by 48 mm.
- The four individual parts of the feet are simplified to two individual parts.
- The number of subparts was reduced and the thickness of sheets adjusted to their function.
- Fork lifter pockets were added to improve safety during handling with a fork lifter.

2.1.4.2.2.2 Justification of the design modification

The design modification leads to a considerable improvement of safety during handling of the DN30 package.

2.1.4.2.2.3 Impact on the results of the physical testing

2.1.4.2.2.3.1 Mechanical tests

The modifications of the design of the feet only have an impact on drop orientations onto the feet. The impact on the slap-down drop test is discussed in detail in Appendix 2.2.1.3 (Structural Analysis of the DN30 Package under NCT and ACT). There is no or only negligible impact on other drop orientations.

2.1.4.2.2.3.2 Thermal test

The design of the feet has no influence on the results of the thermal test.

2.1.4.2.3 The rotation preventing devices

2.1.4.2.3.1 Description of the design modification

The design of the rotation preventing device as used in the prototypes is shown in Figure 12 a) and the design of the rotation preventing device as used in the series design is shown in Figure 12 b).

The prototype design is made of a pin which rests in a sleeve with a longitudinal and radial slit. The handle consists of a rectangular bar which is welded to the pin after the pin is inserted into the sleeve.

The series design is made of a pin which rests in an intermediate sleeve (the drive) which itself rests in an outer sleeve. The handle consists of a round bar which is screwed into the bolt and secured by a spot weld.

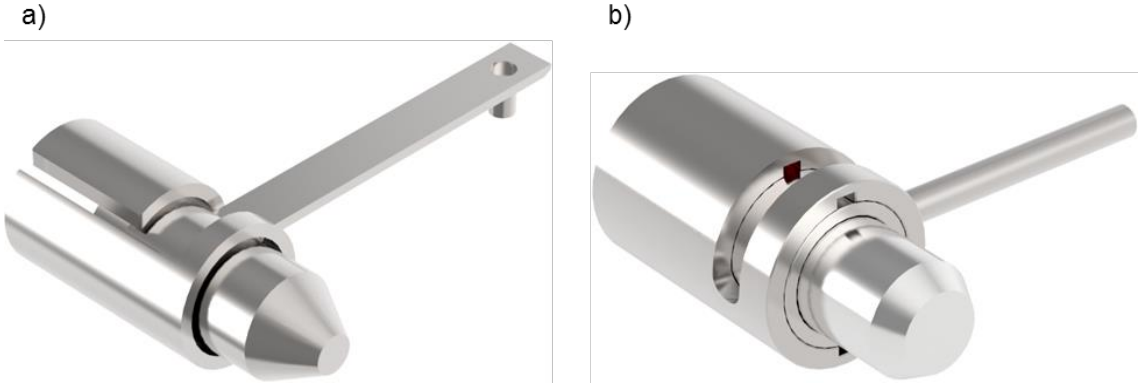

Figure 12: Rotation preventing device: a) DN30 PSP prototype b) DN30 PSP

2.1.4.2.3.2 Justification of the design modification

After the handling practice during the physical testing the prototype design of the rotation preventing device was not considered to be a suitable solution for the series design of the DN30 PSP:

- The design of the welded connection between the handle and the pin was rather weak.
- The shape of the handle was not user friendly.

- Handling of the rotation preventing device was difficult, especially when wearing gloves.
- There is a discontinuity in the sealing line of the flange of the bottom half. Hence the ingress of water into the DN30 PSP could not be excluded.

For the series design the following applies:

- The handle is connected to the pin by a robust bolted connection. This connection is secured by a spot weld. In case of a damage to the handle it can be easily exchanged by opening the spot weld and unscrewing the handle.
- The round shape of the handle is user friendly.
- Handling of the rotation preventing device, even when wearing gloves, is facilitated.
- The continuity of the sealing line of the flange of the bottom half is preserved.
- The overall design of the rotation preventing device is more robust than the prototype design.
- The series design allows lower tolerances between pin and sleeve and thus reduces the relative movement between pin and sleeve during ACT.

2.1.4.2.3.3 Impact on the results of the physical testing

2.1.4.2.3.3.1 Mechanical tests

The prototype design of the rotation preventing device was structurally weaker than the series design:

- The sleeve of the rotation preventing device connecting the device to the bottom half is stronger for the series design than for the prototype design.
- The connection between handle and pin is stronger for the series design than for the prototype design.
- The remaining design modifications only have an impact on the handling of the rotation preventing device.

Hence, a negative impact on the results of the mechanical tests can be excluded.

2.1.4.2.3.3.2 Thermal test

The rotation preventing device has no influence on the results of the thermal test.

2.1.4.2.4 The reinforcement plate at the valve side

2.1.4.2.4.1 Description of the design modification

The outer front plate at the valve side of the top half of the prototypes of the DN30 PSP is reinforced by a round steel plate positioned in the middle of the front plate as shown in Figure 13 a). In the modified design used for the series DN30 PSP the reinforcement plate is extended to a semicircle.

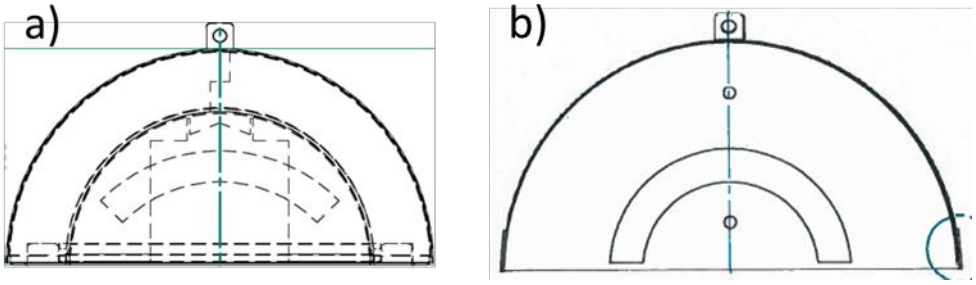

Figure 13: Reinforcement plate: a) DN30 PSP prototype b) DN30 PSP

2.1.4.2.4.2 Justification of the design modification

During manufacturing of the prototypes it was noticed that the positioning of the reinforcement plate is complicated and requires supervision. Additionally, the welding seams between front plate and reinforcement plate affect the appearance of the front plate. Hence, the reinforcement plate is extended to a semicircle so that the welding seams can be placed near the flange.

2.1.4.2.4.3 Impact on the results of the physical testing

2.1.4.2.4.3.1 Mechanical tests

The reinforcement plate was placed at the inner side of the outer shell to avoid puncture of the shell by the bar. It is shown in the drop tests that the front plate with a thickness of the shell of 4 mm is not punctured by the bar, even in areas not covered by the reinforcement plate. However, the reinforcement plate was kept as a design feature to provide additional safety in the valve area.

Neither the 1.2 m drop test simulating NCT nor the 9 m drop test simulating ACT are affected by the design change.

2.1.4.2.4.3.2 Thermal test

The design of the reinforcement plate has no influence on the results of the thermal test.

2.1.4.2.5 The flange between top and bottom half and its gasket

2.1.4.2.5.1 Description of the design modification

In the design of the prototype of the DN 30 PSP there was no barrier against water ingress in the valve protecting device area.

The design modification is as follows:

- There is a steel bar welded to the bottom half outside the hinges of the valve protecting device, providing a geometrical water barrier.
- There is a gasket attached to the top half which is pressed onto the steel bar when the DN30 PSP is closed.

2.1.4.2.5.2 Justification of the design modification

The design modification improves the ability of the DN30 PSP with an improved protection against water ingress into the cavity.

Remark: the design modification has no influence on the containment system provided by the 30B cylinder.

2.1.4.2.5.3 Impact on the results of the physical testing

2.1.4.2.5.3.1 Mechanical tests

There is no impact on the results of the mechanical tests as there were no or only minor recorded deformations in that area of the DN30 PSP.

2.1.4.2.5.3.2 Thermal test

The design of the sealing line at the valve protecting device area has no influence on the results of the thermal test.

2.1.4.2.6 Intumescent material

2.1.4.2.6.1 Description of the design modification

An additional thermal protection is positioned on the inner shell of the DN30 PSP. This additional protection is comprised of a 2.6 mm thick intumescent material.

To protect the intumescent material during the loading and unloading of the 30B cylinder protecting rails are welded to the inner shell on both front plates. These rails guide the 30B cylinder and prevent a direct contact between the skirt and the intumescent material when loading or unloading the 30B cylinder from the DN30 PSP.

2.1.4.2.6.2 Justification of the design modification

In a preliminary thermal test it was detected that hot gases from the decomposition of the PIR foam might enter through openings in the inner shell into the cavity of the DN30 PSP and lead to a considerable increase of the temperature of the 30B cylinder. This could impair the containment system provided by the 30B cylinder and its valve and plug.
The improved design prevents any inflow of decomposition gases into the cavity and suppresses any heat transfer by convection between DN30 PSP and 30B cylinder.

2.1.4.2.6.3 Impact on the results of the physical testing

2.1.4.2.6.3.1 Mechanical tests

This intumescent material does not influence the results of the mechanical test:

- The mechanical properties of the DN30 PSP are not affected.
- The thin layer of intumescent material does not significantly affect the interaction of the 30B cylinder and the DN30 PSP during the drop tests.

- The reduced gap between 30B cylinder and DN30 PSP reduces the possible impact energy of the 30B cylinder with the DN30 PSP as the possible relative movement of 30B cylinder and DN30 PSP is reduced.
- The protecting rails with a thickness of 4 mm and a width of 15 mm have no influence on the strength of the 10 mm thick front plates.

The intumescent material was part of the design of the prototype of the DN30 package used for the thermal test. This prototype was pre-damaged in two full drop test sequences consisting of a 10.2 m drop test onto the valve corner and on the plug corner and a subsequent 1 m drop test onto the bar on the valve corner and the plug corner. The deformations of the DN30 PSP after these test sequences were similar to the deformations after the drop test sequences without intumescent material.

2.1.4.2.6.3.2 Thermal test

The intumescent material was tested in the thermal test.

2.1.4.2.7 The housing of the valve protecting device

2.1.4.2.7.1 Description of the design modification

The valve protecting device used in the mechanical tests was shaped like a “U” with open upper side and front side. For the thermal test a housing made of 1 mm thick stainless steel sheet was added into the U-shape to close the upper and front side. The housing is covered on the inside with intumescent material.

The housing is moveable in the axis direction of the valve to facilitate loading and unloading of the 30B cylinder into the DN30 PSP.

2.1.4.2.7.2 Justification of the design modification

In a preliminary thermal test it was detected that hot gases from the decomposition of the PIR foam might enter through cracks resulting from mechanical tests into the cavity of the DN30 PSP and lead to a considerable increase of the temperature of the 30B cylinder. This could impair the containment system provided by the 30B cylinder and its valve and plug.
The improved design prevents any inflow of decomposition gases onto the valve as the steel sheet housing provides a mechanical barrier and the intumescent material tightly encloses the valve after expansion due to increased temperatures.

2.1.4.2.7.3 Impact on the results of the physical testing

2.1.4.2.7.3.1 Mechanical tests

The housing does not affect the results of the drop tests:

- The mechanical properties of the DN30 PSP are not affected.
- The thin steel sheet (1 mm) does not affect the mechanical strength of the valve protecting device.
- The remaining distance between valve and any part of the valve protecting device was with minimal 21 mm in RCT and with a minimal of 5 mm in ACT (see Appendix 2.2.1.3 (Structural Analysis of the DN30 Package under NCT and ACT)) much

greater than the thickness of the steel sheet (1 mm) and the thickness of the intumescent material (2.6 mm). The requirement, that there is no contact between valve and any other part of the 30B cylinder or the DN30 PSP after the mechanical tests is fulfilled.

- The housing was part of the design of the prototype of the DN30 package used for the thermal test. This prototype was pre-damaged in two full drop test sequences consisting of a 10.2 m drop test onto the valve corner and on the plug corner and a subsequent 1 m drop test onto the bar on the valve corner and the plug corner. There was no contact between valve or plug and any other part of the 30B cylinder or the DN30 prototype after the test sequences.

The impact of the design modification is analyzed in detail in Appendix 2.2.1.3 (Structural Analysis of the DN30 Package under NCT and ACT).

2.1.4.2.7.3.2 Thermal test

The housing was part of the design of the prototype of the DN30 package used for the thermal test.

2.1.4.2.8 The thermal plugs

2.1.4.2.8.1 Description of the design modification

The design, position and the number of the thermal plugs is modified. In the series design the following applies:

- The thermal plugs are screwed into a cylindrical receptacle which is welded to the outer shell. There is an EPDM gasket between thermal plug and receptacle to avoid water inleakage into the foam.
- There are nine thermal plugs in the bottom half and nine thermal plugs in the top half.
- The thermal plugs are distributed in such a way that the decomposition gases produced during the thermal test can escape from the interspace between the inner and outer shell of the DN30 PSP to the environment.

2.1.4.2.8.2 Justification of the design modification

In a preliminary thermal test it was detected that hot gases from the decomposition of the PIR foam might enter through any openings in the inner shell into the cavity of the DN30 PSP and lead to a considerable increase of the temperature of the 30B cylinder. This could impair the containment system provided by the 30B cylinder and its valve and plug.
The improved design prevents any inflow of decomposition gases through the holes of the thermal plugs positioned at the inner shell.

2.1.4.2.8.3 Impact on the results of the physical testing

2.1.4.2.8.3.1 Mechanical tests

The thermal plugs have a diameter of 21 mm. Their size is small compared to the dimensions of DN30 PSP. The holes in the outer shell of the DN30 PSP for the thermal plugs are reinforced

by a cylindrical receptacle which is welded to the shell. Hence, the outer shell is not weakened in the area of the thermal plugs and any influence on the results of the mechanical tests can be excluded.

The new design of the thermal plugs was part of the design of the prototype of the DN30 package used for the thermal test. This prototype was pre-damaged in two full drop test sequences consisting of a 10.2 m drop test onto the valve corner and on the plug corner and a subsequent 1 m drop test onto the bar on the valve corner and the plug corner. There was no rupture of the external shell initiated by the thermal plugs.

2.1.4.2.8.3.2 Thermal test

The design of the thermal plugs was tested in the thermal test.

2.1.4.2.9 Support pads

2.1.4.2.9.1 Description of the design modification

The material of the support pads for the 30B cylinder in the bottom half of the DN30 PSP are made of silicone.

2.1.4.2.9.2 Justification of the design modification

The pads used in the prototype of the DN30 package were made of NBR/SBR. Silicone has much better thermal properties. In the thermal test pads will remain intact as the decomposition temperature of silicone is not reached. Thus a possible decomposition of the pads made of other materials is avoided.

2.1.4.2.9.3 Impact on the results of the physical testing

2.1.4.2.9.3.1 Mechanical tests

The support pads have no influence on the results of the mechanical tests.

2.1.4.2.9.3.2 Thermal test

The support pads have no influence on the results of the thermal test.

2.1.4.2.10 Sealing block

2.1.4.2.10.1 Description of the design modification

The prototypes were equipped with one massive sealing block positioned on only one side of the DN30 PSP. The serial DN30 PSPs are equipped with two less massive sealing blocks positioned on both sides of the PSP.

2.1.4.2.10.2 Justification of the design modification

By using two sealing blocks on opposite sides of the DN30 PSP an opening of the DN30 PSP without breaking the seals is not possible.

2.1.4.2.10.3 Impact on the results of the physical testing

2.1.4.2.10.3.1 Mechanical tests

The design of the sealing block has no influence on the results of the mechanical tests.

2.1.4.2.10.3.2 Thermal test

The design of the sealing block has no influence on the results of the thermal test.

2.2 TECHNICAL ANALYSES

2.2.1 STRUCTURAL ANALYSIS

In this chapter the structural design of the DN30 package is analyzed and it is proven that the requirements towards a type B(U)F package are met. With that, also the requirements towards a type IF and a type AF package are met. The following proofs are carried out:

- Static structural analysis for RCT.
- Fatigue analysis for dynamically loaded components.
- Dynamic structural analysis for NCT and ACT.

Fracture analysis at -40°C is not required for components of austenitic stainless steels according to [SSG-26], para. V.9.

2.2.1.1 Basic assumptions for the calculations

Basic assumptions for the calculations are listed in the following. They include load assumptions for different load situations, the definition of calculation methods and material parameters of the materials used for the proof.

2.2.1.1.1 Load assumptions

Load assumptions are made for the following situations:

- Handling
- RCT
- NCT
- ACT

The individual load assumptions are discussed in the following sections.

2.2.1.1.1.1 Handling

Load assumptions for handling include

- Temperatures at the package corresponding to an ambient temperature of 38 °C and solar insolation.
- Hoisting coefficients which have to be considered for handling operations.
- Internal and external pressure.

Load assumptions as basis for calculations for handling the package are listed in Table 17.

Table 17: Load assumptions for handling

Load assumption	To be used for component	Value
Temperature	30B cylinder	64 °C
	Lifting lugs at feet	70 °C
	Lifting lugs at top half	100 °C
	Feet	70 °C
Hoisting coefficient	Lifting lugs	2
Pressure	30B cylinder, internal	152 kPa
	30B cylinder, external	100 kPa
Fatigue analysis	Lifting lugs	load cycle number 100000

2.2.1.1.1.2 RCT

Load assumptions for routine conditions of transport include

- Temperatures at the package corresponding to an ambient temperature of 38°C and solar insolation (see section 2.2.2).
- Maximum transport accelerations.
- Vibrations during transport.

Load assumptions as basis for calculations for routine conditions of transport are listed in Table 18.

Table 18: Load assumptions for RCT

Load assumption	To be used for component	Value
Temperature (for ambient temperature of 38°C, with insolation, see section 2.2.2)	Outer shell, feet	70°C
	30B cylinder	64°C
Temperature (for ambient temperature of -40°C, without insolation, see section 2.2.2)	Complete packaging	-40°C
Accelerations[1)] • axial • lateral • vertical	Complete packaging	 2 g 2 g +/-2 g
Vibrations	Complete packaging	0.3 g

[1)] The accelerations defined cover the accelerations specified in [ISO 7195] and [SSG-26] for the transport of packagings containing UF_6 for road, rail, sea and inland waterways)

2.2.1.1.1.3 NCT

Load assumptions for normal conditions of transport include

- Temperatures at the package corresponding to an ambient temperature of 38 °C and solar insolation (see section 2.2.2).
- Tests for demonstrating ability to withstand normal conditions of transport according to [ADR 2015], No. 6.4.15. [IAEA 2012], para. 719.
- Reduction of ambient pressure.

Load assumptions as basis for calculations for normal conditions of transport are listed in Table 19.

Table 19: Load assumptions for NCT

Load assumption	Individual test	To be used for component	Value
Temperature	Drop test, stacking test, penetration test	DN30 PSP	60 °C
		30B cylinder	64 °C
Tests according to [ADR 2015], No. 6.4.15. [IAEA 2012], para. 719	Water spray test	Packaging surface	[ADR 2015], No. 6.4.15.3, [IAEA 2012], para. 721
	Drop test	Complete package	[ADR 2015], No. 6.4.15.4, [IAEA 2012], para. 722 Free drop height 1.2 m
	Stacking test	Complete package	[ADR 2015], No. 6.4.15.5, [IAEA 2012], para. 723
	Penetration test	Packaging surface	[ADR 2015], No. 6.4.15.6, [IAEA 2012], para. 724
Ambient pressure	-	30B cylinder	[ADR 2015], No. 6.4.7.11, [IAEA 2012], para. 645 60 kPa

2.2.1.1.1.4 ACT

Load assumptions for accident conditions of transport include

- Temperatures at the package corresponding to an ambient temperature of 38 °C and solar insolation (see section 2.2.2).
- Tests for demonstrating ability to withstand accident conditions of transport according to [ADR 2015], No. 6.4.17. [IAEA 2012], para. 726.
- Internal and external pressure.

Load assumptions for accident conditions of transport are listed in Table 20.

Table 20: Load assumptions for ACT

Load assumption	Individual test	To be applied for component	Value
Temperature	Drop test I and drop test II	Packaging main body outer shell	60 °C
		30B cylinder	64 °C
Tests according to [ADR 2015], No. 6.4.17. [IAEA 2012], para. 726	Drop test I	Complete package	[ADR 2015], No. 6.4.17.2 a), [IAEA 2012], para. 727 (a) Free drop height 9 m
	Drop test II	Complete package	[ADR 2015], No. 6.4.17.2 b), [IAEA 2012], para. 727 (b) Free drop height 1 m
	Thermal test	Complete package	[ADR 2015], No. 6.4.17.3, [IAEA 2012], para. 728
	Water immersion test	30B cylinder	[ADR 2015], No. 6.4.17.4, [IAEA 2012], para. 729 150 kPa, 8 h
Water pressure	Water immersion test for packages containing fissile materials	30B cylinder	[ADR 2015], No. 6.4.19, [IAEA 2012], para. 731 9 kPa, 8 h
Pressure increase due to max. temperatures during the thermal test	Thermal test	30B cylinder	[ADR 2015], No. 6.4.17.3, [IAEA 2012], para. 728 215 kPa (see section 2.2.2)

2.2.1.1.2 Material data

Materials are specified in section 1.4.2. For the static analysis, the following data given in Table 21 to Table 23 are used. For the dynamic analysis the values are specified in Appendix 2.2.1.3 (Structural Analysis of the DN30 Package under NCT and ACT).

Table 21: Material data for material No. 1.4301

Material property	Designation	Temperature	Value	Reference
Density	ρ	20 °C	7.9 g/cm³	[DIN EN 10088-1]
0.2% yield stress	$R_{p0.2}$	20 °C	220 MPa	[DIN EN 10088-2]
		70 °C	175 MPa	[DIN EN 10088-2]
		100 °C	147 MPa	[DIN EN 10088-2]
1.0% yield stress	$R_{p1.0}$	20 °C	250 MPa	[DIN EN 10088-2]
		70 °C	207 MPa	[DIN EN 10088-2]
		100 °C	181 MPa	[DIN EN 10088-2]
Ultimate tensile strength	R_m	20 °C	520 MPa	[DIN EN 10088-2]
Elastic modulus	E	20 °C	2.00E5 MPa	[DIN EN 10088-1]
		100 °C	1.94E5 MPa	[DIN EN 10088-1]
Poisson's ratio	v		0.3	
Elongation at fracture	A		45 %	[DIN EN 10088-2]
Linear thermal expansion coefficient	α	20-100°C	16E-6 K^{-1}	[DIN EN 10088-1]

Table 22: Material data for material No. 1.4541

Material property	Designation	Temperature	Value	Reference
Density	ρ	20 °C	7.9 g/cm³	[DIN EN 10088-1]
0.2% yield stress	$R_{p0.2}$	20 °C	200 MPa	[DIN EN 10088-2]
		70 °C	185 MPa	[DIN EN 10088-2]
		100 °C	176 MPa	[DIN EN 10088-2]
1.0% yield stress	$R_{p1.0}$	20 °C	240 MPa	[DIN EN 10088-2]
		70 °C	220 MPa	[DIN EN 10088-2]
		100 °C	208 MPa	[DIN EN 10088-2]
Ultimate tensile strength	R_m	20 °C	500 MPa	[DIN EN 10088-2]
Elastic modulus	E	20 °C	2.00E5 MPa	[DIN EN 10088-1]
		100 °C	1.94E5 MPa	[DIN EN 10088-1]
Poisson's ratio	v		0.3	
Elongation at fracture	A		45 %	[DIN EN 10088-2]
Linear thermal expansion coefficient	α	20-100°C	16E-6 K^{-1}	[DIN EN 10088-1]

Table 23: Material data for material No. 1.4542

Material property	Designation	Temperature	Value	Reference
Density	ρ	20 °C	7.8 g/cm³	[DIN EN 10088-1]
0.2% yield stress	$R_{p0.2}$	20 °C	720 MPa	[DIN EN 10088-3]
		100 °C	680 MPa	[DIN EN 10088-3]
Ultimate tensile strength	R_m	20 °C	930-1100 MPa	[DIN EN 10088-3]
Elastic modulus	E	20 °C	2.00E5 MPa	[DIN EN 10088-1]
		100 °C	1.85E5 MPa	[DIN EN 10088-1]
Poisson's ratio	v		0.3	
Elongation at fracture	A		16 %	[DIN EN 10088-2]
Linear thermal expansion coefficient	α	20-100°C	10.9E-6 K^{-1}	[DIN EN 10088-1]

2.2.1.2 Handling

The packaging DN30 is designed for the transport of UF_6. Specified contents are defined in section 1.3.

Strains in the packaging may generally result from the following loads:

- internal pressure
- external pressure
- assembling loads
- handling loads
- temperature gradients in the components

2.2.1.2.1 Internal and external pressure

During handling and transport the content UF_6 is in a solid state. For the analysis of the packaging it is assumed that the UF_6 and hence the 30B cylinder have a temperature of 64°C which is equivalent to the triple point. In this condition the gas pressure above the solid UF_6 is 152 kPa. This value is used for the analytical proof of an internal pressure in the 30B cylinder. For the proof of an external pressure in the 30B cylinder a pressure difference of 100 kPa is assumed between ambient and internal pressure of the 30B cylinder.

The 30B cylinder is designed according to [ISO 7195] and [ANSI N14.1] for an external pressure of 172 kPa and an internal pressure of 1.38 MPa. Hence, the requirements concerning the internal and external pressure for the 30B cylinder and therefore also for the DN30 package are fulfilled.

2.2.1.2.2 Assembling

The components of the packaging are inserted into each other during assembling without using forces. Stresses in the components during assembling are negligibly low. For tightening the securing bolt of the closure system axis tightening torques are defined in handling instruction no. 0023-HA-2015-001.

2.2.1.2.3 Handling loads

The following handling processes are carried out with the packaging:

- Handling of the loaded and empty packaging by using the lifting lugs at the feet (see Figure 4).
- Handling of the loaded and empty package using a fork lifter (see Figure 5).
- Handling of the empty package by using slings (see Figure 6).
- Handling of the top half by using the lifting lugs (see Figure 7).

All other operations during handling and loading are carried out manually. The stresses in the respective components are negligible.

2.2.1.2.3.1 Lifting lugs at the feet

For the analysis of the stresses in the lifting lugs the model shown in Figure 14 and Figure 15 is used.

The DN30 package is lifted with a handling beam. The angle of the load attaching means to the vertical is assumed to be 30°. The load is distributed over four load attaching points of the DN30 package. For the loaded DN30 PSP a mass of 4100 kg is assumed. Hence, taking into account the hoisting coefficient of 2 the force acting on one lug is

$$F = 2 \cdot \frac{4100\,\mathrm{kg} \cdot 9.81\,\frac{\mathrm{m}}{\mathrm{s}^2}}{4 \cdot \cos 30°} = 23.2\,\mathrm{kN}$$

The cross section across the hole is (cross section A-A in Figure 15)

$$A_{\mathrm{AA}} = (64\,\mathrm{mm} - 25\,\mathrm{mm}) \cdot 15\,\mathrm{mm} = 585\,\mathrm{mm}^2$$

The nominal stress in the lifting lug is

$$\sigma = \frac{F}{A_{\mathrm{AA}}} = \frac{23.2\,\mathrm{kN}}{585\,\mathrm{mm}^2} = 39.7\,\mathrm{MPa} < R_{\mathrm{p0.2}} = 175\,\mathrm{MPa}\ (\mathrm{at}\ 70°\mathrm{C})$$

The cross section above the hole is (cross section B-B in Figure 15)

$$A_{\mathrm{BB}} = \left(35\,\mathrm{mm} - \frac{25\,\mathrm{mm}}{2}\right) \cdot 15\,\mathrm{mm} = 337\,\mathrm{mm}^2$$

The shear stress is

$$\tau = \frac{F}{A_{\mathrm{BB}}} = \frac{23.2\,\mathrm{kN}}{337\,\mathrm{mm}^2} = 68.8\,\mathrm{MPa} < \frac{R_{\mathrm{p0.2}}}{\sqrt{3}} = 101\,\mathrm{MPa}\ (\mathrm{at}\ 70°\mathrm{C})$$

For proof of the fatigue strength [FKM 2003] is used. The required minimal number of load cycles is assumed to be

$$\bar{N} = 100000$$

This number is higher than the expected number, which corresponds to 30 years in service with one transport per month and 100 load cycles for each transport.

The average force is calculated by

$$F_{\mathrm{m}} = \frac{F_{\max} + F_{\min}}{2} = 11.6\,\mathrm{kN}$$

Accordingly, the force amplitude is

$$F_{\mathrm{a}} = F_{\max} - F_{\mathrm{m}} = 11.6\,\mathrm{kN}$$

The corresponding stress amplitude and average stress are

$$S_{\mathrm{a,zd}} = \frac{F_{\mathrm{a}}}{A_{\mathrm{AA}}} = 19.8\,\mathrm{MPa}$$

$$S_{\mathrm{m,zd}} = \frac{F_{\mathrm{m}}}{A_{\mathrm{AA}}} = 19.8\,\mathrm{MPa}$$

The fatigue limit for pulsating stress for material no. 1.4301 is

$$\sigma_{\mathrm{W,zd}} = f_{\mathrm{W},\sigma} \cdot R_{\mathrm{m}} = 0.4 \cdot 520\,\mathrm{MPa} = 208\,\mathrm{MPa}$$

The stress slope is

$$\bar{G}_{\sigma} = \frac{2.3}{r} = \frac{2.3}{12.5\,\mathrm{mm}} = 0.184\,\mathrm{mm}^{-1}$$

The derived support number for normal stresses is

$$n_{\sigma} = 1 + \sqrt{\bar{G}_{\sigma} \cdot \mathrm{mm}} \cdot 10^{\left(a_{\mathrm{G}} + \frac{R_{\mathrm{m}}}{b_{\mathrm{G}} \cdot \mathrm{MPa}}\right)}$$

With

$$a_{\mathrm{G}} = 0.4$$

$$b_{\mathrm{G}} = 2400$$

$$n_{\sigma} = 1 + \sqrt{0.184\,\mathrm{mm}^{-1} \cdot \mathrm{mm}} \cdot 10^{\left(0.4 + \frac{520\,\mathrm{MPa}}{2400 \cdot \mathrm{MPa}}\right)} = 1.104$$

The shape factor for flat plates with a hole is

$$K_{\mathrm{t,zd}} = 2.3$$

And finally the fatigue notch factor

$$K_{\mathrm{f,zd}} = \frac{K_{\mathrm{t,zd}}}{n_{\sigma}} = \frac{2.3}{1.104} = 2.1$$

For the fatigue factor considering the surface roughness a value is assumed of

$$K_{\mathrm{R},\sigma} = 0.79$$

is obtained. The total fatigue factor is hence

$$K_{\mathrm{WK,zd}} = K_{\mathrm{f,zd}} + \frac{1}{K_{\mathrm{R},\sigma}} - 1 = 2.35$$

Hence, the fatigue stress limit is

$$S_{\mathrm{WK,zd}} = \frac{\sigma_{\mathrm{W,zd}}}{K_{\mathrm{WK,zd}}} = \frac{208\,\mathrm{MPa}}{2.2} = 88.5\,\mathrm{MPa}$$

Considering the average stress, the factor $K_{\mathrm{AK,zd}}$ is calculated as

$$K_{\mathrm{AK,zd}} = 0.92$$

Hence, the fatigue limit for the stress amplitude is

$$S_{\mathrm{AK,zd}} = K_{\mathrm{AK,zd}} \cdot S_{\mathrm{WK,zd}} = 81.8\,\mathrm{MPa}$$

The safety factor is

$$S_{\mathrm{f}} = \frac{S_{\mathrm{AK,zd}}}{S_{\mathrm{a,zd}}} = \frac{81.8\,\mathrm{MPa}}{19.8\,\mathrm{MPa}} = 4.1 > 1.2$$

The required safety factor is set to 1.2 as the lifting lugs are regularly inspected. Similarly, the fatigue strength against shear is proven for the second cross section. The corresponding shear stress amplitude and average shear stress are

$$T_{\mathrm{a,s}} = \frac{F_{\mathrm{a}}}{A_{\mathrm{BB}}} = 34.4\,\mathrm{MPa}$$

$$T_{\mathrm{m,s}} = \frac{F_{\mathrm{m}}}{A_{\mathrm{BB}}} = 34.4\,\mathrm{MPa}$$

The fatigue limit for pulsating stress for material no. 1.4301 is

$$\tau_{\mathrm{W,s}} = f_{\mathrm{W},\tau} \cdot \sigma_{\mathrm{W,zd}} = 0.58 \cdot 208\,\mathrm{MPa} = 120\,\mathrm{MPa}$$

The derived fatigue notch factor

$$K_{\mathrm{f,s}} = \frac{K_{\mathrm{t,s}}}{n_{\tau}} = \frac{2.3}{1} = 2.3$$

For the fatigue factor considering the surface roughness a value of

$$K_{\mathrm{R},\tau} = 0.88$$

is obtained. The total fatigue factor is hence

$$K_{\mathrm{WK,s}} = K_{\mathrm{f,s}} + \frac{1}{K_{\mathrm{R},\tau}} - 1 = 2.44$$

Hence, the fatigue stress limit is

$$T_{\mathrm{WK,s}} = \frac{\tau_{\mathrm{W,s}}}{K_{\mathrm{WK,s}}} = \frac{120\,\mathrm{MPa}}{2.2} = 49.3\,\mathrm{MPa}$$

Considering the average shear stress, the factor $K_{\mathrm{AK,s}}$ is calculated as

$K_{AK,s} = 0.95$

Hence, the fatigue limit for the stress amplitude is

$T_{AK,s} = K_{AK,s} \cdot T_{WK,s} = 47\text{MPa}$

The safety factor is

$S_f = \frac{T_{AK,s}}{T_{a,s}} = \frac{47\text{MPa}}{34.4\text{MPa}} = 1.4 > 1.2$

The required safety factor is set to 1.2 as the lifting lugs are regularly inspected.

For proof of the fatigue strength of the welding seams between the lifting lug and the DN30 PSP [FKM 2003] is used. The total length of the left welding seam in Figure 15 is

$l = 2 \cdot 53.4\text{mm} + 2 \cdot 15\text{mm} = 137\text{mm}$

The welding thickness is conservatively assumed with minimal

$a = 4\text{mm}$

The corresponding welding cross section is

$A = a \cdot l = 547.2\text{mm}^2$

This results in the following nominal shear stress amplitude and average shear stress

$T_{a,s} = \frac{F_a}{A} = 21.2\text{MPa}$

$T_{m,s} = \frac{F_m}{A} = 21.2\text{MPa}$

For welds the material independent fatigue limit shear stress is taken into account, which is

$\tau_{W,s} = 37\text{MPa}$

The design factor for fillet welds is FAT80 for nominal stresses so that the fatigue notch factor for shear stress is

$K_{WK,s} = \frac{145}{\text{FAT}} = 1.81$

With $M_\tau = 0.17$, the factor for the average stress is calculated as

$K_{AK,s} = \frac{1}{1 + M_\tau \cdot \frac{T_{m,s}}{T_{a,s}}} = 0.85$

The factor for the residual stresses is

$K_{E,\tau} = 1.3$

Overall, the fatigue limit stress for the left weld of the lifting lug is calculated as

$T_{AK,s} = K_{AK,s} \cdot K_{E,\tau} \cdot \frac{\tau_{W,s}}{K_{WK,s}} = 22.6\text{MPa}$

The factor for the endurance limit for 100000 load cycles is with

$N_{\mathrm{D},\tau} = 10^8$

$k_\tau = 5$

$K_{\mathrm{BK,s}} = \left(\frac{N_{\mathrm{D},\tau}}{\bar{N}}\right)^{\frac{1}{k_\tau}} = 3.98$

The endurance limit is then

$T_{\mathrm{BK,s}} = K_{\mathrm{BK,s}} \cdot T_{\mathrm{AK,s}} = 90.1\mathrm{MPa}$

The safety factor is

$S_{\mathrm{f}} = \frac{T_{\mathrm{BK,s}}}{T_{\mathrm{a,s}}} = \frac{90.1\mathrm{MPa}}{21.2\mathrm{MPa}} = 4.3 > 1.2$

The length of the lower welding seam in Figure 15 is

$l = 2 \cdot 63.8\mathrm{mm} + 2 \cdot 15\mathrm{mm} = 157.6\mathrm{mm}$

The welding thickness is minimal

$a = 4\mathrm{mm}$

The corresponding welding cross section is

$A = a \cdot l = 630.2\mathrm{mm}^2$

This results in the following nominal stress amplitude and average stress

$S_{\mathrm{a,zd}} = \frac{F_{\mathrm{a}}}{A} = 18.4\mathrm{MPa}$

$S_{\mathrm{m,zd}} = \frac{F_{\mathrm{m}}}{A} = 18.4\mathrm{MPa}$

For welds the material independent fatigue limit stress is taken into account, which is

$\sigma_{\mathrm{W,zd}} = 92\mathrm{MPa}$

The design factor for fillet welds is FAT80 for nominal stresses so that the fatigue notch factor for stress is

$K_{\mathrm{WK,zd}} = \frac{225}{\mathrm{FAT}} = 2.81$

With $M_\sigma = 0.3$, the factor for the average stress is calculated as

$K_{\mathrm{AK,zd}} = \frac{1}{1 + M_\sigma \cdot \frac{S_{\mathrm{m,zd}}}{S_{\mathrm{a,zd}}}} = 0.77$

The factor for the residual stresses is

$K_{\mathrm{E},\sigma} = 1.54$

Overall, the fatigue limit stress for the left weld of the lifting lug is calculated as

$$S_{\mathrm{AK,zd}} = K_{\mathrm{AK,zd}} \cdot K_{\mathrm{E},\sigma} \cdot \frac{\sigma_{\mathrm{W,zd}}}{K_{\mathrm{WK,zd}}} = 38.8\,\mathrm{MPa}$$

The factor for the endurance limit for 100000 load cycles is with

$$N_{\mathrm{D},\sigma} = 5 \cdot 10^6$$

$$k_\sigma = 3$$

$$K_{\mathrm{BK,zd}} = \left(\frac{N_{\mathrm{D},\sigma}}{\bar{N}}\right)^{\frac{1}{k_\sigma}} = 3.68$$

The endurance limit is then

$$S_{\mathrm{BK,zd}} = K_{\mathrm{BK,zd}} \cdot S_{\mathrm{AK,zd}} = 142.8\,\mathrm{MPa}$$

The safety factor is

$$S_{\mathrm{f}} = \frac{S_{\mathrm{BK,zd}}}{S_{\mathrm{a,zd}}} = \frac{142.8\,\mathrm{MPa}}{18.4\,\mathrm{MPa}} = 7.8 > 1.2$$

The required safety factor is set to 1.2 as the lifting lugs are regularly inspected. Hence, the endurance strength is proven for the welds. This proof is conservative because it is assumed that only one weld carries the entire load for each lifting lug.

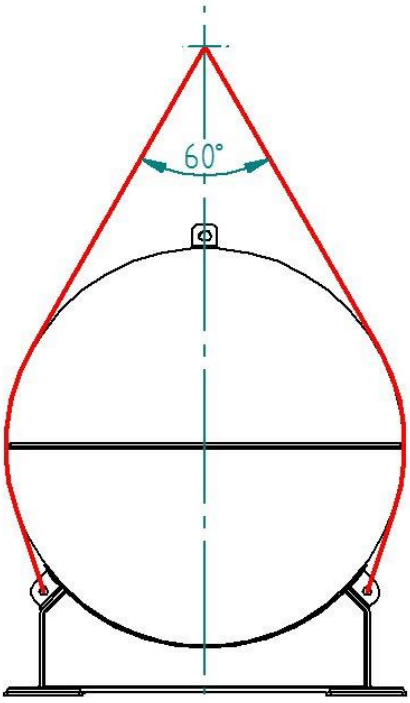

Figure 14: Forces in the handling means of the loaded DN30 package when lifted using the lifting lugs

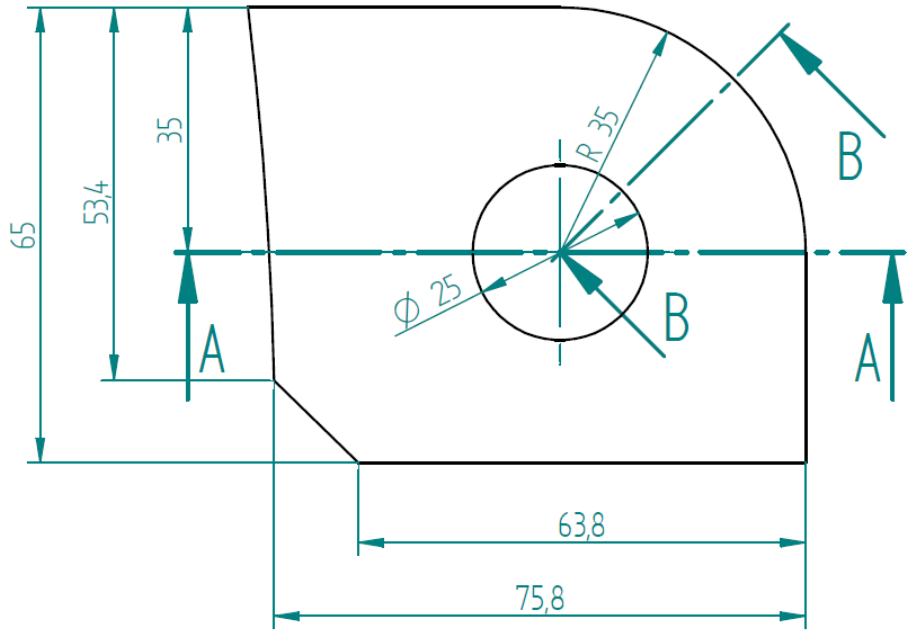

Figure 15: Geometry of the lifting lug for calculation

2.2.1.2.3.2 Fork lifter pockets

Identically to the calculation of the tie-down forces in section 2.2.1.3.1, it is assumed that the forces caused by accelerations are acting in the center of the DN30 package. For simplicity, it is assumed that also the same forces as taken into account for the tie-down analysis are acting when the DN30 package is handled by the fork lifter pockets, i.e. 2g in axial direction and 2g in lateral direction. However, a combination of accelerations in axial and lateral direction is not assumed as this is highly unrealistic. Therefore, the axial and lateral forces are

$$F_{\mathrm{L}} = F_{\mathrm{Q}} = m_{\mathrm{DN30}} \cdot 2\mathrm{g} = 4100\,\mathrm{kg} \cdot 2 \cdot 9.81\,\frac{\mathrm{m}}{\mathrm{s}^2} = 80.4\,\mathrm{kN}$$

The fork lifter pockets consisting of 3mm thick steel plates are welded to the connection profile. With the welding thickness $a = 4\,\mathrm{mm}$, the welding seam area is at each connection point

$$A = a \cdot l = 3\,\mathrm{mm} \cdot 200\,\mathrm{mm} = 600\,\mathrm{mm}^2$$

First, the case of a load in the axial direction of the DN30 package is investigated. Such a load causes a tilting of the DN30 package, which results in tensile stresses in the welding seams. The relevant height of the center of the packaging from the connection point is

$$h = 692\,\mathrm{mm} - 145\,\mathrm{mm} = 547\,\mathrm{mm}$$

The distance between the centers of each fork lifter pocket is

$$d_{\mathrm{FLP}} = 700\ \mathrm{mm}$$

If only one connection point is taking the whole load, the force at one connection point caused by the tilting is

$$F = F_{\mathrm{L}} \cdot \frac{h}{d_{\mathrm{FLP}}} = 80.4\,\mathrm{kN} \cdot \frac{547\,\mathrm{mm}}{700\,\mathrm{mm}} = 62.86\ \mathrm{kN}$$

The tensile stress in the welding seams is

$$\sigma = \frac{F}{2 \cdot A} = \frac{62.86\,\mathrm{kN}}{2 \cdot 600\,\mathrm{mm}^2} = 52.4\,\mathrm{MPa} < R_{\mathrm{p0.2}} = 175\,\mathrm{MPa}\ (\mathrm{at}\ 70°\mathrm{C})$$

Next, tilting in the lateral direction of the DN30 package is investigated. The relevant center distance of the welding seams is

$$d_{\mathrm{WS}} = 500\,\mathrm{mm}$$

Hence the force at one connection point is, if only one connection point is taking the whole load:

$$F = F_{\mathrm{Q}} \cdot \frac{h}{d_{\mathrm{WS}}} = 80.4\,\mathrm{kN} \cdot \frac{547\,\mathrm{mm}}{500\,\mathrm{mm}} = 88\,\mathrm{kN}$$

The tensile stress in the welding seams is

$$\sigma = \frac{F}{2 \cdot A} = \frac{88\,\mathrm{kN}}{2 \cdot 600\,\mathrm{mm}^2} = 73.3\,\mathrm{MPa} < R_{\mathrm{p0.2}} = 175\,\mathrm{MPa}\ (\mathrm{at}\ 70°\mathrm{C})$$

A fatigue analysis is not required as the DN30 package would be resting safely on the forks of the fork lifter even without the fork lifter pockets.

2.2.1.2.3.3 Lifting of the empty DN30 PSP with slings

For the calculation it is assumed that the DN30 package is a beam single supported on both ends. Conservatively, the supports are assumed to be at each end (distance 2435 mm) and the load is concentrated in the center. For the moment of inertia only the outer shell of the bottom half of the DN30 is taken into account.

The force is calculated with a lifting factor of 2:

$$F_{\mathrm{Lift}} = m_{\mathrm{DN30}} \cdot 2\mathrm{g} = 4100\,\mathrm{kg} \cdot 2 \cdot 9.81\,\frac{\mathrm{m}}{\mathrm{s}^2} = 80.4\,\mathrm{kN}$$

The bending moment is hence

$$M_{\mathrm{b}} = 2435\,\mathrm{mm} \cdot \frac{F_{\mathrm{Lift}}}{4} = 4.9 \cdot 10^4\,\mathrm{Nm}$$

The moment of inertia about the vertical axis is according to [YOUNG 1998], Table 1, case 22

$$I = \frac{\pi}{8} \cdot \left(R^4 - R_{\mathrm{i}}^4\right) - \frac{8}{9\pi} \cdot \frac{\left(R^3 - R_{\mathrm{i}}^3\right)^2}{R^2 - R_{\mathrm{i}}^2}$$

And the largest distance of the neutral axis to the outer fiber is

$$y_{1\mathrm{b}} = \frac{4}{3\pi} \cdot \frac{R^3 - R_{\mathrm{i}}^3}{R^2 - R_{\mathrm{i}}^2}$$

With

$$R = 553\,\mathrm{mm}$$

$$R_{\mathrm{i}} = 547\,\mathrm{mm}$$

$$I = 2.97 \cdot 10^8\,\mathrm{mm}^4$$

$y_{1b} = 350\,\mathrm{mm}$

$W_b = 8.48 \cdot 10^5\,\mathrm{mm}^3$

The bending stress is

$$\sigma = \frac{M_b}{W_b} = \frac{4.9 \cdot 10^4\,\mathrm{Nm}}{8.48 \cdot 10^5\,\mathrm{mm}^3} = 59\,\mathrm{MPa} < R_{p0.2} = 175\,\mathrm{MPa}\ (\mathrm{at}\ 70\,°\mathrm{C})$$

Safety factor against $R_{P0.2}$ (70℃)

$$S_f = \frac{175\,\mathrm{MPa}}{59\,\mathrm{MPa}} = 3$$

2.2.1.2.3.4 Lifting lugs at the top half

For the analysis of the stresses in the lifting lugs the model shown in Figure 16 and Figure 17 is used.

The top half of the DN30 PSP is lifted with the two load attaching points. The angle of the load attaching means to the vertical is assumed to be 30°. For the top half of the DN30 PSP a mass of 500 kg is assumed. Hence, the force acting on one lug is

$$F = 2 \cdot \frac{500\,\mathrm{kg} \cdot 9.81\,\frac{\mathrm{m}}{\mathrm{s}^2}}{2 \cdot \cos 30°} = 5.7\,\mathrm{kN}$$

The cross section across the hole is (cross section A-A in Figure 17)

$$A_{AA} = (70\,\mathrm{mm} - 35\,\mathrm{mm}) \cdot 6\,\mathrm{mm} = 210\,\mathrm{mm}^2$$

The nominal stress in the lifting lug is

$$\sigma = \frac{F}{A_{AA}} = \frac{5.7\,\mathrm{kN}}{210\,\mathrm{mm}^2} = 27\,\mathrm{MPa} < R_{p0.2} = 147\,\mathrm{MPa}\ (\mathrm{at}\ 100\,°\mathrm{C})$$

The cross section above the hole is (cross section B-B in Figure 17)

$$A_{BB} = \left(35\,\mathrm{mm} - \frac{35\,\mathrm{mm}}{2}\right) \cdot 6\,\mathrm{mm} = 105\,\mathrm{mm}^2$$

The shear stress is

$$\tau = \frac{F}{A_{BB}} = \frac{5.7\,\mathrm{kN}}{105\,\mathrm{mm}^2} = 53.9\,\mathrm{MPa} < \frac{R_{p0.2}}{\sqrt{3}} = 85\,\mathrm{MPa}\ (\mathrm{at}\ 100\,°\mathrm{C})$$

For proof of the fatigue strength [FKM 2003] is used. The required minimal number of load cycles is assumed to be

$$\overline{N} = 100000$$

This number is higher than the expected number, which corresponds to 30 years in service with one transport per month and 100 load cycles for each transport.

The average force is calculated by

$$F_{\mathrm{m}} = \frac{F_{\max} + F_{\min}}{2} = 2.8\mathrm{kN}$$

Accordingly, the force amplitude is

$$F_{\mathrm{a}} = F_{\max} - F_{\mathrm{m}} = 2.8\mathrm{kN}$$

The corresponding stress amplitude and average stress are

$$S_{\mathrm{a,zd}} = \frac{F_{\mathrm{a}}}{A_{\mathrm{AA}}} = 13.5\mathrm{MPa}$$

$$S_{\mathrm{m,zd}} = \frac{F_{\mathrm{m}}}{A_{\mathrm{AA}}} = 13.5\mathrm{MPa}$$

The fatigue limit for pulsating stress for material no. 1.4301 is

$$\sigma_{\mathrm{W,zd}} = f_{\mathrm{W},\sigma} \cdot R_{\mathrm{m}} = 0.4 \cdot 520\mathrm{MPa} = 208\mathrm{MPa}$$

The stress slope is

$$\bar{G}_{\sigma} = \frac{2.3}{r} = \frac{2.3}{17.5\mathrm{mm}} = 0.131\mathrm{mm}^{-1}$$

The derived support number for normal stresses is

$$n_{\sigma} = 1 + \sqrt{\bar{G}_{\sigma} \cdot \mathrm{mm}} \cdot 10^{\left(a_{\mathrm{G}} + \frac{R_{\mathrm{m}}}{b_{\mathrm{G}} \cdot \mathrm{MPa}}\right)}$$

With

$$a_{\mathrm{G}} = 0.4$$

$$b_{\mathrm{G}} = 2400$$

$$n_{\sigma} = 1 + \sqrt{0.131\mathrm{mm}^{-1} \cdot \mathrm{mm}} \cdot 10^{\left(0.4 + \frac{520\mathrm{MPa}}{2400 \cdot \mathrm{MPa}}\right)} = 1.088$$

The shape factor for flat plates with a hole is

$$K_{\mathrm{t,zd}} = 2.15$$

And finally the fatigue notch factor

$$K_{\mathrm{f,zd}} = \frac{K_{\mathrm{t,zd}}}{n_{\sigma}} = \frac{2.1}{1.104} = 1.98$$

For the fatigue factor considering the surface roughness a value of

$$K_{\mathrm{R},\sigma} = 0.79$$

is obtained. The total fatigue factor is hence

$$K_{\mathrm{WK,zd}} = K_{\mathrm{f,zd}} + \frac{1}{K_{\mathrm{R},\sigma}} - 1 = 2.24$$

Hence, the fatigue stress limit is

$$S_{\mathrm{WK,zd}} = \frac{\sigma_{\mathrm{W,zd}}}{K_{\mathrm{WK,zd}}} = \frac{208\,\mathrm{MPa}}{2.2} = 92.8\,\mathrm{MPa}$$

Considering the average stress, the factor $K_{\mathrm{AK,zd}}$ is calculated as

$$K_{\mathrm{AK,zd}} = 0.92$$

Hence, the fatigue limit for the stress amplitude is

$$S_{\mathrm{AK,zd}} = K_{\mathrm{AK,zd}} \cdot S_{\mathrm{WK,zd}} = 85.7\,\mathrm{MPa}$$

The safety factor is

$$S_{\mathrm{f}} = \frac{S_{\mathrm{AK,zd}}}{S_{\mathrm{a,zd}}} = \frac{85.7\,\mathrm{MPa}}{13.5\,\mathrm{MPa}} = 6.3 > 1.2$$

The required safety factor is set to 1.2 as the lifting lugs are regularly inspected. The corresponding shear stress amplitude and average shear stress are

$$T_{\mathrm{a,s}} = \frac{F_{\mathrm{a}}}{A_{\mathrm{BB}}} = 27\,\mathrm{MPa}$$

$$T_{\mathrm{m,s}} = \frac{F_{\mathrm{m}}}{A_{\mathrm{BB}}} = 27\,\mathrm{MPa}$$

The fatigue limit for pulsating stress for material no. 1.4301 is

$$\tau_{\mathrm{W,s}} = f_{\mathrm{W},\tau} \cdot \sigma_{\mathrm{W,zd}} = 0.58 \cdot 208\,\mathrm{MPa} = 120\,\mathrm{MPa}$$

The derived fatigue notch factor

$$K_{\mathrm{f,s}} = \frac{K_{\mathrm{t,s}}}{n_{\tau}} = \frac{2.15}{1} = 2.15$$

For the fatigue factor considering the surface roughness a value of

$$K_{\mathrm{R},\tau} = 0.88$$

is obtained. The total fatigue factor is hence

$$K_{\mathrm{WK,s}} = K_{\mathrm{f,s}} + \frac{1}{K_{\mathrm{R},\tau}} - 1 = 2.29$$

Hence, the fatigue stress limit is

$$T_{\mathrm{WK,s}} = \frac{\tau_{\mathrm{W,s}}}{K_{\mathrm{WK,s}}} = \frac{120\,\mathrm{MPa}}{2.2} = 52.5\,\mathrm{MPa}$$

Considering the average shear stress, the factor $K_{\mathrm{AK,s}}$ is calculated as

$$K_{\mathrm{AK,s}} = 0.95$$

Hence, the fatigue limit for the stress amplitude is

$$T_{\mathrm{AK,s}} = K_{\mathrm{AK,s}} \cdot T_{\mathrm{WK,s}} = 50.1\,\mathrm{MPa}$$

The safety factor is

$$S_{\mathrm{f}} = \frac{T_{\mathrm{AK,s}}}{T_{\mathrm{a,s}}} = \frac{50.1\,\mathrm{MPa}}{27\,\mathrm{MPa}} = 1.9 > 1.2$$

The required safety factor is set to 1.2 as the lifting lugs are regularly inspected.

For proof of the fatigue strength of the welding seems between the lifting lug and the DN30 PSP [FKM 2003] is used. The welding is subjected to tensile and shear loads. The length of the welding seam in Figure 17 is

$$l = 2 \cdot 70\,\mathrm{mm} + 2 \cdot 6\,\mathrm{mm} = 152\,\mathrm{mm}$$

The welding thickness is minimal

$$a = 2\,\mathrm{mm}$$

The corresponding welding cross section is

$$A = a \cdot l = 304\,\mathrm{mm}^2$$

This results in the following nominal stress amplitude and average stress

$$S_{\mathrm{a,zd}} = \frac{F_{\mathrm{a}} \cdot \cos(30°)}{A} = 8.1\,\mathrm{MPa}$$

$$S_{\mathrm{m,zd}} = \frac{F_{\mathrm{m}} \cdot \cos(30°)}{A} = 8.1\,\mathrm{MPa}$$

For welds the material independent fatigue limit stress is taken into account, which is

$$\sigma_{\mathrm{W,zd}} = 92\,\mathrm{MPa}$$

The design factor for fillet welds is FAT80 for nominal stresses so that the fatigue notch factor for stress is

$$K_{\mathrm{WK,zd}} = \frac{225}{\mathrm{FAT}} = 2.81$$

With $M_{\sigma} = 0.3$, the factor for the average stress is calculated as

$$K_{\mathrm{AK,zd}} = \frac{1}{1 + M_{\sigma} \cdot \frac{S_{\mathrm{m,zd}}}{S_{\mathrm{a,zd}}}} = 0.77$$

The factor for the residual stresses is

$$K_{\mathrm{E},\sigma} = 1.54$$

Overall, the fatigue limit stress for the left weld of the lifting lug is calculated as

$$S_{\mathrm{AK,zd}} = K_{\mathrm{AK,zd}} \cdot K_{\mathrm{E},\sigma} \cdot \frac{\sigma_{\mathrm{W,zd}}}{K_{\mathrm{WK,zd}}} = 38.8\,\mathrm{MPa}$$

The safety factor is

$$S_{\mathrm{f,zd}} = \frac{S_{\mathrm{AK,zd}}}{S_{\mathrm{a,zd}}} = \frac{38.8\,\mathrm{MPa}}{8.1\,\mathrm{MPa}} = 4.8 > 1.2$$

The resulting nominal shear stress amplitude and average shear stress are

$$T_{\mathrm{a,s}} = \frac{F_{\mathrm{a}} \cdot \sin(30°)}{A} = 4.7\,\mathrm{MPa}$$

$$T_{\mathrm{m,s}} = \frac{F_{\mathrm{m}} \cdot \sin(30°)}{A} = 4.7\,\mathrm{MPa}$$

For welds the material independent fatigue limit shear stress is taken into account, which is

$$\tau_{\mathrm{W,s}} = 37\,\mathrm{MPa}$$

The design factor for fillet welds is FAT80 for nominal stresses so that the fatigue notch factor for shear stress is

$$K_{\mathrm{WK,s}} = \frac{145}{\mathrm{FAT}} = 1.81$$

With $M_{\tau} = 0.17$, the factor for the average stress is calculated as

$$K_{\mathrm{AK,s}} = \frac{1}{1 + M_{\tau} \cdot \frac{T_{\mathrm{m,s}}}{T_{\mathrm{a,s}}}} = 0.85$$

The factor for the residual stresses is

$$K_{\mathrm{E},\tau} = 1.3$$

Overall, the fatigue limit stress for the left weld of the lifting lug is calculated as

$$T_{\mathrm{AK,s}} = K_{\mathrm{AK,s}} \cdot K_{\mathrm{E},\tau} \cdot \frac{\tau_{\mathrm{W,s}}}{K_{\mathrm{WK,s}}} = 22.6\,\mathrm{MPa}$$

The safety factor is

$$S_{\mathrm{f,s}} = \frac{T_{\mathrm{BK,s}}}{T_{\mathrm{a,s}}} = \frac{22.6\,\mathrm{MPa}}{4.7\,\mathrm{MPa}} = 4.8 > 1.2$$

Combining the two stress components results in the following total safety factor

$$S_{\mathrm{f}} = \frac{1}{\sqrt{\frac{1}{S_{\mathrm{f,zd}}^2} + \frac{1}{S_{\mathrm{f,s}}^2}}} = 3.4$$

Hence, the fatigue strength of the lifting lugs at the top half is proven for the welding as well.

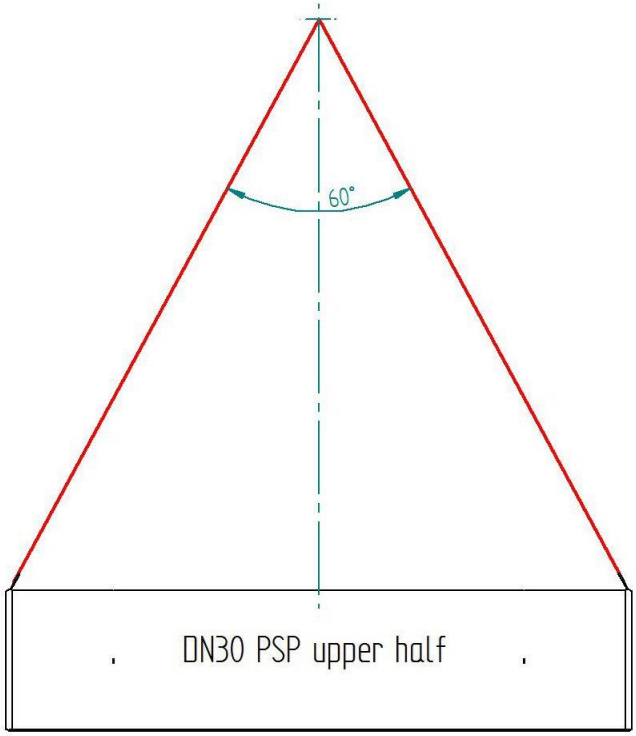

Figure 16: Forces in the handling means when lifting the top half

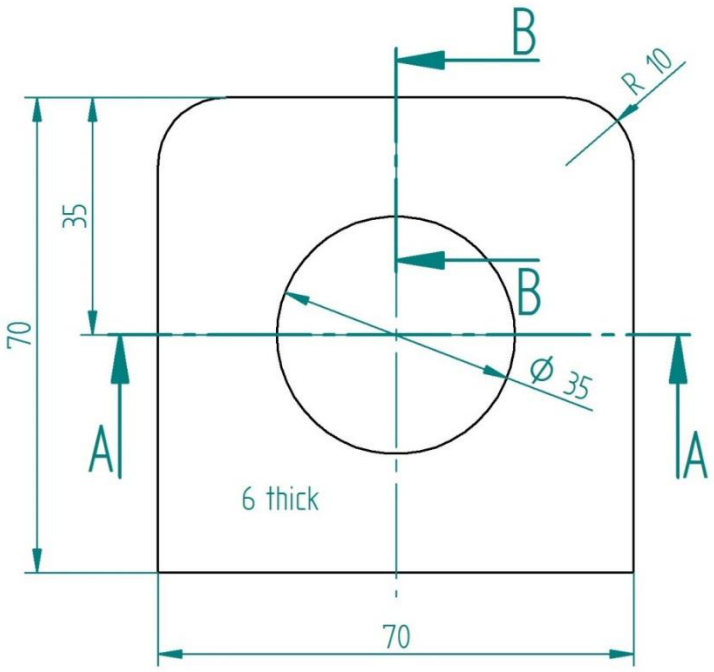

Figure 17: Geometry of the lifting lug for calculation of the handling of the top half

2.2.1.2.4 Stresses caused by temperature influences

There are only minor and negligible stresses caused by temperature influences

- The DN30 PSP consists of a welded structure of austenitic stainless steel with the same thermal expansion coefficients in all parts.
- As there is only a very low thermal load from the content, the temperature differences from the heat produced by the content are negligible.
- The possibly different expansions of the top and bottom half of the DN30 PSP due to temperature differences caused by the different insolating conditions on the top and bottom half are small; the gaps between the flanges of the top and bottom half allow enough relative movement to compensate for the different expansions.
- The gaps between the DN30 PSP and the 30B cylinder are sufficient to compensate the different thermal expansions of the DN30 PSP and the 30B cylinder.

For the conservative proof following is assumed:

- the DN30 PSP has temperature of 100°C (complying with the outer shell of the top half after 12 hours of solar insolation).
- the 30B cylinder has a temperature of 20°C (complying with a 30B stored inside before loading).
- the DN30 PSP cools down to 38°C.
- the 30B cylinder heats up to 64°C.

The length of the 30B cylinder is according to [ISO 7195] and [ANSI N14.1] 2070 +5 -13 mm

The minimal length of the cavity (bottom half) is 2082 +-3 mm

For the 30B cylinder the expansion is

$\Delta l_{cyl} = l \times \alpha \times \Delta\theta = 2070\ mm \times 11.5E\text{-}6\ /°C \times (64°C - 20°C) = 1.1\ mm$

For the DN30 PSP the contraction

$\Delta l_{PSP} = l \times \alpha \times \Delta\theta = 2082\ mm \times 16.0E\text{-}6\ /°C \times (100\ °C - 38\ °C) = 2.1\ mm$

The total expansion difference is

$\Delta l = \Delta l_{cyl} + \Delta l_{PSP} = 1.1\ mm + 2.1\ mm = 3.2\ mm$

The difference between the minimal cavity length and the maximal 30B cylinder length is

$D = 2082\ mm - 3\ mm - 2070\ mm - 5\ mm = 4\ mm$

Hence, the gap is by far wide enough to allow for the dimensional changes due to thermal differences.

2.2.1.3 Ability to withstand RCT

The loaded DN30 packaging is transported by road, rail or sea. For the transport dedicated flat racks are used (see Figure 8). The tie-down is designed such that a relative movement between vehicle and package is excluded. Thus, only the maximum acceleration values defined in Table 18 affect the package during transport.

2.2.1.3.1 Tie-down for maximal accelerations

Mass of the loaded DN30 package assumed for the proof: 4100 kg.

Vertical loads:

Vertical acceleration: 2 g up minus gravity = 1 g up

There are 4 tie-down points securing the DN30 package on the flat rack. Normal force per tie-down point:

$F_{TP\text{-}N,vertical}$ = 4100 kg x 9.81 m/s^2 x 1 / 4 = 10060 N

Axial loads:

Axial acceleration: 2 g

F_{axial} = 4100 kg x 9.81 m/s^2 x 2 = 80500 N

Normal force at two tie-down points at point A in Figure 18

$F_{TP\text{-}N,axial}$ = 80500 N x 692 mm / 1474 mm / 2 = 18896 N

Transversal force at four tie-down points:

$F_{TP\text{-}T,axial}$ = 80500 N / 4 = 20130 N

Lateral loads:

Lateral acceleration: 2 g

$F_{lateral}$ = 4100 N x 9.81 m/s^2 x 2 = 80500 N

Normal force at two tie-down points at point B in Figure 19

$F_{TP\text{-}N,lateral}$ = 80500 N x 692 mm / 1016 mm / 2 = 27414 N

Transversal force at four tie-down points:

$F_{TP\text{-}T,lateral}$ = 80500 N / 4 = 20130 N

Superposition of all loads

Maximal normal force at a tie-down point:

$F_{TP\text{-}N} = F_{TP\text{-}N,vertical} + F_{TP\text{-}N,axial} + F_{TP\text{-}N,lateral}$ = 10060 N + 18896 N + 27414 N = 56370 N

Maximal transversal force in a tie-down point:

$$F_{TP-T} = \sqrt{F_{TP-T,axial}{}^2 + F_{TP-T,lateral}{}^2} = \sqrt{(20130N)^2 + (20130N)^2} = 28470N$$

2.2.1.3.1.1 Welding seams between bottom plate and vertical plate

The welding seam W between bottom plate and vertical plate (see Figure 20) has a thickness of

A = 10 mm

The length is

L = 200 mm

Cross section

A = 2000 mm²

The tension stress in the welding seam is

$\sigma = F_{TP-N} / A = 56370$ N / 2000 mm² = 28.2 MPa

The shear stress is

$\tau = F_{TP-T} / A = 28470$ N / 2000 mm² = 14.3 MPa

Von Mises stress:

$$\sigma_V = \sqrt{28.2^2 + 3*14.3^2} = 37.5\,MPa$$

Safety factor against $R_{P0.2}$ (70°C)

S = 175 MPa / 37.5 MPa = 4.6

2.2.1.3.1.2 Bottom plate

The bottom plate consists of 10 mm steel sheet doubled with another 10 mm steel sheet which are joined by welding (see Figure 20).

It is assumed that at point C there is a support in vertical direction.

Force at the bolts (point B)

$$F_S = \frac{F_{TP} * 2 * (48mm + 47mm)^3}{47mm * \left(3 * (48mm + 47mm)^2 - (47mm)^2\right)} = 1.47 * 56370N = 82864N$$

Force at point C

$F_C = F_S - F_{TP} = 82864$ N – 56370 N = 26494 N

Bending moment at point B

$$M_b = \frac{F_S * 47mm}{2 * (48mm + 47mm)^3} * (48mm)^2 * \left(2 * (48mm + 47mm) + 47mm\right) = 12.967mm * 82864N = 1.24E6\,Nmm$$

The section modulus is

W_b = b h^2 / 6 = (200 mm – 2 x 23 mm) x 20 mm x 20 mm / 6 = 10267 mm^3

The bending stress is

$\sigma = M_b / W_b$ = 1.24E6 Nmm / 10267 mm^3 = 121 MPa < $R_{P0.2}$ = 175 MPa

Bending moment at point A

$$M_b = \frac{F_S * 47mm}{2*(48mm+47mm)^2} * \left((48mm+47mm)^2 - (47mm)^2\right) = 17.75mm * 82864N = 1.47E6\,Nmm$$

The section modulus is

W_b = b h^2 / 6 = 200 mm x 20 mm x 20 mm / 6 = 13333 mm^3

The bending stress is

$\sigma = M_b / W_b$ = 1.47E6 Nmm / 13333 mm^3 = 111 MPa < $R_{P0.2}$ = 175 MPa

The shear stress from normal forces is

A = 200 mm x 20 mm = 4000 mm^2

τ = 56370 N / 4000 mm = 14.1 MPa

The additional stresses from the transversal forces calculated with the model of a cantilever fixed at one end:

$M_b = F_{TP\text{-}T}$ x 48 mm = 28470 N x 48 mm = 1.37E6 Nmm

W_b = b h^2 / 6 = 20 mm x 200 mm x 200 mm / 6 = 133333 mm^3

The bending stress is

$\sigma = M_b / W_b$ = 1.37E6 Nmm / 133333 mm^3 = 10.3 MPa < $R_{P0.2}$ = 175 MPa

The shear stress from transversal forces is

τ= 28470 N/ 4000 mm^2= 7.1 MPa

Superposition:

$$\sigma_V = \sqrt{111^2 + 10.3^2 + 3*(14.1+7.1)^2} = 117.4MPa < R_{P0,2} = 175\,MPa$$

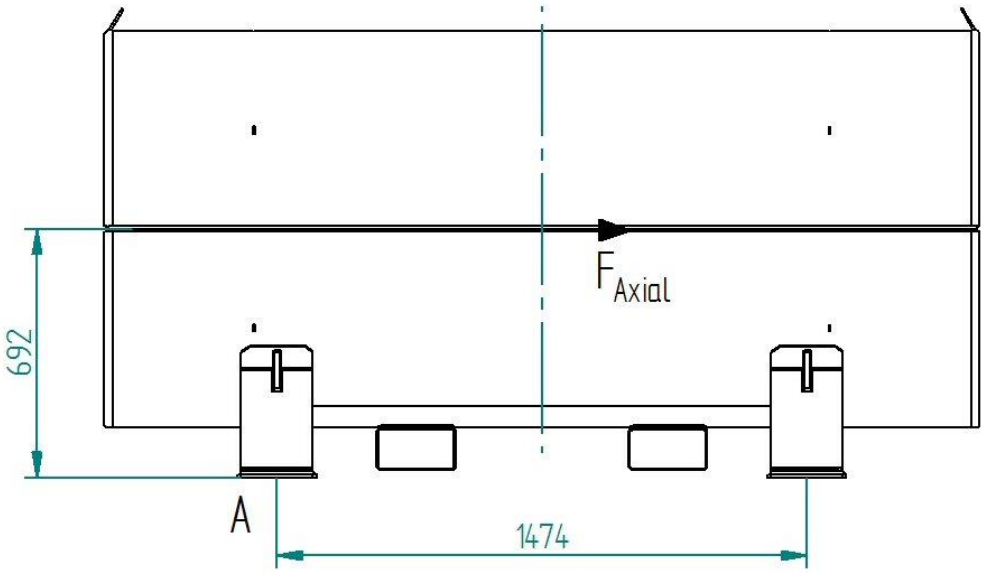

Figure 18: Axial accelerations during RCT

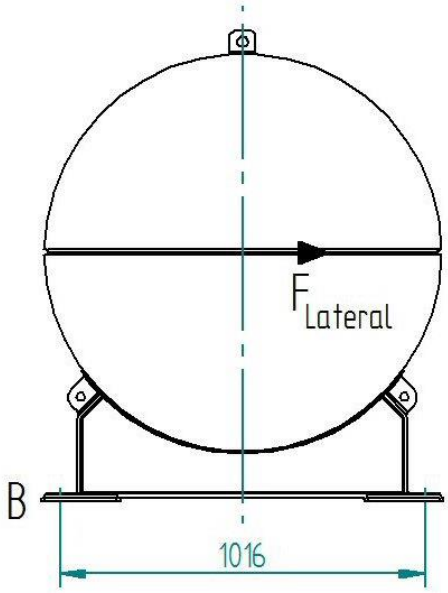

Figure 19: Lateral accelerations during RCT

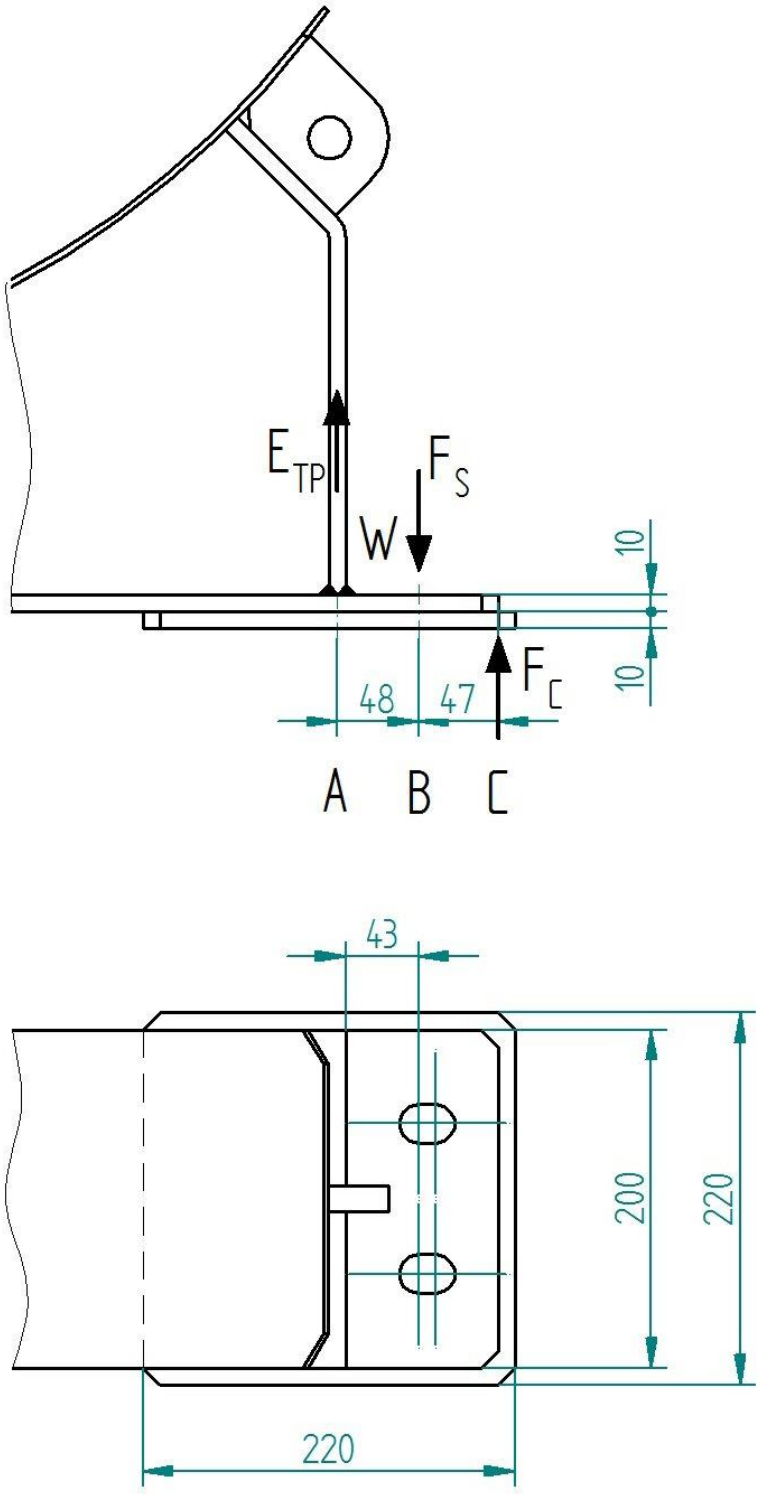

Figure 20: Calculation model of the foot of the DN30 PSP

2.2.1.3.1.3 Bolts

The bolts are not part of the DN30 package. However, to ensure that the tie-down is carried out according to the requirements, an analysis of the stresses in the bolts as well as the determination of the tightening torque is included in this report.

For tie-down bolts M18-8.8 are used. At each tie-down point two bolts are used.

Core cross section M18

A = 175 mm^2

Normal stress:

σ = 82846 N / (2 x 175 mm^2) = 237 MPa

Shear stress:

τ = 28470 N / (2 x 175 mm^2) = 82 MPa

Von Mises stress:

$$\sigma_V = \sqrt{237^2 + 3*82^2} = 277\,MPa$$

The safety factor for the bolts is

S = 640 MPa / 277 MPa= 2.3

Calculation of the bolts according to [VDI 2230] for the normal forces:

Table 24: Parameters for the bolts calculation

Property/calculation parameter	Value	Unit
Nominal diameter	18.00	mm
Thread pitch	2.50	mm
A_0	192.47	mm^2
d_2	16.38	mm
d_0	14.93	mm
F	41285	N
F_Q	0	N
q_F	1	
μ	0	
AD	0	
pi,max	0	
E_s	205000	N/mm^2
l_{Gew}	15	mm
tan φ	0.437467306	

Property/calculation parameter	Value	Unit
w	1	
l_K	30	mm
d_w	27	mm
D_A	50	mm
d_H	20	mm
f_z	0.008	mm
R_{P02}	640	N/mm²
v	0.9	
μ_{Gmin}	0.1	
K_T	0.5	
ρ_G	490	MPa
A_{pmin}	318.09	mm²
F_M	75000	N
R_m	800	N/mm²

Table 25: Results of the bolts calculation

Symbols and notation	Value	Unit
R0: Determining the nominal diameter d		
Selected bolt M	18	
F_{mmin}	67000	N
F_{mmax}	94000	N
R1:Determining the tightening factor α_A		
α_A=	1.4	
R2:Determining the required minimal clamp load F_{Kerf}		
F_{kerf}	14235	N
R3:Force relations and load factors		
δ_G	2.50E-07	mm/N
δ_M	1.13E-07	mm/N
δ_{GM}	3.64E-07	mm/N
δ_{Gew}	2.87E-07	mm/N
δ_{SK}	1.38E-07	mm/N
$D_{A,Gr}$	40.12	mm
δ_S	7.90E-07	
δ_P	2.87E-07	mm/N
Φ_K	0.2667	

Symbols and notation	Value	Unit
R4:Preload changes		
F_z	18804	N
R5: Determining the minimum assembly preload $F_{M\,min}$		
$F_{M,min}$	63413	N
R6: Determining the maximum assembly preload $F_{M\,max}$		
$F_{M,max}$	88968	N
R7:Checking the assembly stress and the bolt size F_{mzul}		
F_{mzul}	100429	N
$F_{mzul} > F_{M,max}$	**satisfied**	
R8: Determining the working stress		
F_{smax}	100017	N
σ_{Zmax}	519	N/mm²
M_G	119539	N/mm²
W_P	871	mm³
τ_{max}	137	N/mm²
$\sigma_{red,B}$	533	N/mm²
$R_{PO2}*A_0$	123182	N
S_F	1.231	
$\sigma_{red,B} < R_{P0.2}$ satisfied	**satisfied**	
$R_{PO2}*A_0=$	**satisfied**	
$S_F \geq 1$	**satisfied**	
R10: Determining the surface pressure		
ρ_{Mmax}	279	MPa
ρ_{Bmax}	314	MPa
$\rho_{Mmax} < p_G$	**satisfied**	
$\rho_{Bmax} < p_G$	**satisfied**	
R11: Determining the minimum length of engagement m_{effmin}		
The standard combination bolt strength grade 8.8 and nut strength grade 8 is used		
$m_{effmin} < m$	**satisfied**	
R12: Determining the shearing stress		
τ_{Qmax}	82	MPa
τ_B / R_m	0.6	
τ_B	480	MPa
$\tau_{Qmax} < \tau_B / R_m$	**satisfied**	
R13: Determining the tightening torque		
M_A	220	Nm

2.2.1.3.2 Tie-down considering vibrations

For the proof of fatigue strength the stresses calculated in section 2.2.1.3.1 are reduced by the factor of the maximal accelerations due to vibrations and the maximal peak acceleration as specified in Table 18.

f_f = 0.3 / 2 = 0.15

For proof of the fatigue strength [FKM 2003] is used.

2.2.1.3.2.1 Welding seams between bottom plate and vertical plate

FAT = 80 (for normal tension and shear stress in fully welded T-connection)

The fatigue notch factor for tension stress is

$K_{WK, N}$ = 225 / FAT = 2.82

The fatigue notch factor for shear stress is

$K_{WK, S}$ = 145 / FAT = 1.82

Hence the fatigue limit tension stress is

$\sigma_{Sch, N}$ / $K_{WK, N}$ = 190 MPa / 2.82 = 67.4 MPa > 0.15 x σ = 0.15 x 28.2 MPa = 4.3 MPa

And the fatigue limit shear stress is

$\tau_{Sch, s}$ / $K_{WK, s}$ = 120 MPa / 1.82 = 65.9 MPa > 0.15 x τ = 0.15 x 14.3 MPa = 2.1 MPa

Von Mises stress:

$$\sigma_V = \sqrt{4.3^2 + 3 * 2.1^2} = 5.6\,MPa$$

The safety factor against von Mises stress is

S = 67.4 MPa / 5.6 MPa = 12 > 1.5

2.2.1.3.2.2 Bottom plate

FAT = 80 (bending stress and shear stress in the bottom plate)

The fatigue notch factor for tension stress is

$K_{WK, N}$ = 225 / FAT = 2.82

The fatigue notch factor for shear stress is

$K_{WK, S}$ = 145 / FAT = 1.82

Hence the fatigue limit tension stress is at point A

$\sigma_{Sch, N}$ / $K_{WK, N}$ = 190 MPa / 2.82 = 67.4 MPa > 0.15 x σ = 0.15 x (111 + 10.3) MPa = 18.2 MPa

And the fatigue limit shear stress is

$\tau_{Sch, s}$ / $K_{WK, s}$ = 120 MPa / 1.82 = 65.9 MPa > 0.15 x τ = 0.15 x (14.1 + 7.1) MPa = 3.2 MPa

Von Mises stress:

$$\sigma_V = \sqrt{18.2^2 + 3 * 3.2^2} = 19.0 MPa$$

The safety factor against von Mises stress is

S = 67.4 MPa / 19.0 MPa = 3.5 > 1.5

2.2.1.3.2.3 Bolts

The bolts are not part of the DN30 package. They are exchanged regularly when the DN30 package is mounted onto the flat racks used for transport. Hence, a fatigue proof is not required.

2.2.1.3.3 Failure-limit for the tie-down features

With respect to the requirement stipulated in [ADR 2015], No. 6.4.7.4 or [IAEA 2012] para. 638 it is shown in the following that the tie-down attachment will fail before the ability of the package to meet the requirements for NCT and ACT is impaired. For this proof the forces are calculated which lead to a failure of the bolts used for tie-down and compared to the forces required to have a failure of the attachment features of the DN30 PSP.

The bolts will fail either when the normal stress in the bolts exceeds the ultimate tensile strength or when the shear stress exceeds the ultimate shear strength.

The stress cross section of a bolt M18 is

A_0 = 192.47 mm^2

Ultimate tensile strength of class 8.8

R_m = 800 MPa

Failure force for normal stress:

$F_{Fail,N}$ = 192.47 mm^2 x 800 MPa = 1.54E05 N

The nominal cross section of a bolt M18 is

A = 254.47 mm^2

Ultimate shear strength of class 8.8

R_m = 800 MPa / √3 = 462 MPa

Failure force for shear stress:

$F_{Fail,S}$ = 254.47 mm^2 x 462 MPa = 1.18E05 N

With these failure forces the stresses in the welding seams between bottom plate and vertical plate as shown in Figure 20 are calculated, taking into account two bolts per attachment point.

The cross section has been calculated in section 2.2.1.3.1.1.

A = 2000 mm^2

The tensile stress is

σ = 2 x $F_{Fail,N}$ / A = 2 x 1.54E5 N / 2000 mm^2 = 154 MPa

The shear stress is

τ = 2 x $F_{Fail,S}$ / A = 2 x 1.18E5 N / 2000 mm^2 = 118 MPa

Von Mises stress:

$$\sigma_V = \sqrt{154^2 + 3*118^2} = 256\,MPa > R_{P0,2}$$

Safety factor against R_m of material no. 1.4301 (see Table 21)

R_m = 520 MPa

S = 520 MPa / 256 MPa = 2

The stress in the welding seam exceeds the yield stress but is well below the ultimate tensile strength when the bolts of the tie-down fail. The plastic deformations to be expected do not result in a rupture of the welding seam and hence the ability of the package to meet NCT and ACT is not impaired. In case of higher loads than to be expected during RCT the bolts will fail and the DN30 package will be separated from the flat rack used for tie-down.

2.2.1.4 Ability to withstand NCT

2.2.1.4.1 Water spray test

The water spray test as defined in [ADR 2015] No. 6.4.15.3 and [IAEA 2012] para. 721 requires the simulation of a heavy rainfall of approximately 5 cm for at least an hour.

The outer shell of the DN30 package consists of stainless steel without any openings except for the flange between top and bottom half of the DN30 PSP. The flange itself is shaped to prevent the ingress of water during the water spray test; additionally, it is equipped with a gasket sealing the top half against the bottom half of the DN30 PSP.

There is no influence of this test on either the loss or dispersal of the radioactive contents or on the dose rate at any external surface of the DN30 package with respect to the requirement stipulated in [ADR 2015], No 6.4.7.14 or [IAEA 2012] para. 648.

2.2.1.4.2 Free drop test

The free drop test from a height of 1.2 m is analyzed in sequence together with the tests simulating ACT, the 9 m drop tests and the 1 m drop test onto the bar. For a better overview and comparison of the deformations after the 1.2 m free drop test and after the 9 m drop test the results of these sequences are described together in section 2.2.1.5.

In section 2.2.1.5 it is shown that the DN30 package is designed to withstand ACT. Hence the proof that the DN30 package is designed to withstand NCT is a direct consequence.

In the following the conditions for proof of [ADR 2015], No 6.4.7.14 or [IAEA 2012] para. 648 are established.

2.2.1.4.2.1 Conditions to prevent loss or dispersal of the radioactive contents

In section 2.2.1.5 it is shown by analysis that there is no contact between valve or plug and any part of the DN30 PSP or any other part of the 30B cylinder other than its initial connection point after the 1.2 m free drop test. Hence, a mechanical damage of valve or plug during the 1.2 m drop test can be excluded.

In section 2.2.1.5.1.5 it is shown in real tests that the results of the analysis comply with the real tests. It is confirmed that there is no contact between valve respectively plug and any part of the DN30 PSP or any other part of the 30B cylinder other than its initial connection point even after the cumulative effects of the 1.2 m free drop test, the 9 m drop and the 1 m drop onto the bar.

Furthermore the leakage rate of the containment system, i.e. the 30B cylinder, was measured and documented after each test sequence. The measurements show that there is no increase of the leakage rate which could lead to a loss or dispersal of the radioactive content.

2.2.1.4.2.2 Conditions to prevent the increase of the maximum external radiation level of more than 20%

In section 2.2.4.6 it is shown that the maximum dose rate at the surface of the DN30 package is to be expected in radial direction in the center of the side of the package. In section 2.2.1.5 the deformations to be expected after the 1.2 m free drop tests are analyzed. For the 1.2 m free drop onto the side of the package, a reduction of the diameter of the package of max. 16 mm was calculated.

2.2.1.4.3 Stacking test

The shape of the DN30 packaging effectively prevents stacking. Hence, according to [ADR 2015] No. 6.4.15.5 and [IAEA 2012] para. 723 the stacking test is not required.

2.2.1.4.4 Penetration test

The DN30 package is designed to withstand ACT (see section 2.2.1.5). The drop of the DN30 package with a mass of approx. 4000 kg onto a steel bar from 1 m height is much more severe than the drop of a 6 kg steel bar from 1 m height onto the DN30 package. Hence the test conditions as defined in [ADR 2015] No. 6.4.15.6 and [IAEA 2012] para. 724 are covered by the test conditions as defined in [ADR 2015] No. 6.4.17.2 b) and [IAEA 2012] para. 727 (b).

There is no influence of this test on the loss or dispersal of the radioactive contents with respect to the requirement stipulated in [ADR 2015], No 6.4.7.14 a) or [IAEA 2012] para. 648 (a).

In comparison to the free drop test from 1.2 m height the influence of this test on the dose rate at any external surface of the DN30 package with respect to the requirement stipulated in [ADR 2015], No 6.4.7.14 b), or [IAEA 2012] para. 648 (b) is negligible.

2.2.1.4.5 Ambient pressure

The 30B cylinder is designed according to [ISO 7195] and [ANSI N14.1] for an external pressure of 172 kPa and an internal pressure of 1.38 MPa. The MNOP during transport is 152 kPa. Hence, a reduction of the ambient pressure to 60 kPa as specified in [ADR 2015] No. 6.4.7.11 and [IAEA 2012] para. 645 will not affect the 30B cylinder and the containment system.

2.2.1.5 Ability to withstand ACT

2.2.1.5.1 Structural analysis of NCT and ACT

The structural analysis of the ability of the package DN30 to withstand ACT is documented in several documents provided as appendices to this PDSR:

- Appendix 2.2.1.1 (Drop Test Program)
- Appendix 2.2.1.2 (Drop Test Reports)
- Appendix 2.2.1.3 (Structural Analysis of the DN30 Package under NCT and ACT)

In this section a summary of these reports describes the main points and results of the analysis and real drop tests.

The analysis

- covers the free drop test of NCT, the 9 m drop test and 1 m drop test onto a bar of ACT,
- is valid for all filling ratios from heels cylinders up to cylinders filled with the maximum amount of UF_6 defined in section 1.3.

The structural analysis of NCT and ACT comprises the analysis of the following tests:

Test 1: Analysis of the free drop test defined in [ADR 2015], No. 6.4.15.4, or [IAEA 2012], para. 722 (1.2 m free drop test)

Test 2: Analysis of the mechanical tests defined in [ADR 2015], No. 6.4.17.2 (a), or [IAEA 2012], para. 727 (a) (drop I, drop height 9 m)

Test 3: Analysis of the mechanical test defined in [ADR 2015], No. 6.4.17.2 (b), or [IAEA 2012], para. 727 (b) (drop II, drop height 1 m onto a bar)

The structural analysis of NCT and ACT was carried out in three major steps:

- Analysis of the behavior of the package by using proven FEM tools and selection of benchmarks.
- Real testing of prototypes by applying the selected benchmark test sequences.
- Comparison and post-analysis of real test results with the calculation results.

2.2.1.5.1.1 Analysis sequences and orientations

In the analysis the following sequences were considered:

- Test 1 – Test 2 – Test 3
- Test 1 – Test 3 – Test 2

The analyses were carried out for all relevant orientations of the package before the tests:

- Flat onto the valve side
- Flat onto the plug side
- Flat onto the closure system

- Flat onto the top side
- Inclined onto the valve side so that the line between center of gravity and point of impact is perpendicular to the target surface
- Inclined onto the plug side so that the line between center of gravity and point of impact is perpendicular to the target surface
- Inclined onto the closure system so that the line between center of gravity and point of impact is perpendicular to the target surface
- Inclined onto the feet (slap-down)

2.2.1.5.1.2 Description of the calculation codes

The results of the drop test simulations in this report are obtained by the numerical solving of differential equations, which are based on the finite element method. Due to the highly dynamic nature of this kind of simulations, the FEM solver LS-DYNA (MPP S R8.0.0) [LS-DYNA 2015] of the software developer LSTC is used, which is integrated in the ANSYS (V17.0) [ANSYS] structural analysis software suite. The results are analyzed in LS-PrePost [LS-PREPOST].

2.2.1.5.1.3 FEM-Model

The FEM-model deviates from the prototype design in the details listed in Table 26

Table 26: Deviations of the FEM model from the design of the DN30 package and their justification

Part	Deviation	Justification
Global		
Steel blocks for sealing	Removed	Not required to be modeled because they have no safety relevant function from the mechanical point of view.
Pads (3mm thick)	Removed	No relevance for the drop test simulations under NCT and ACT because they only cover the interior of the DN30 PSP to protect it against wear and tear due to contact between the 30B cylinder and the inner shell.
Gasket	Removed	The gasket prevents the ingress of water, which is irrelevant for the FEM simulations.
Rounded / beveled edges and boreholes	Removed	Such geometrical details require unreasonably small elements, especially for the evaluation of strains and stresses; they have no significant influence on the results of the FEM analyses.

Part	Deviation	Justification
Welding seams	Replaced by tied contacts / mesh connections	Every welding seam is removed in the FEM model because the investigation of welding seams requires a very fine mesh in those regions. Moreover, the welding seams of the DN30 PSP have no containment function. They serve as a connection between the individual parts of the DN30 PSP and any failure of the welds is investigated in the real drop tests. Therefore, replacing them by tied contacts or simple mesh connections is sufficient for the FEM simulations. Possible failure of welding seams is accounted for by evaluating the strain in the respective parts.
Closure system	Simplified	Each of the closure devices is modeled as two prismatic bodies instead of the complicated design with four teeth on each block connected by a bolt. This simplification allows a coarser mesh in this area leading to acceptable calculation times. The behavior of the real closing system, including local stresses and possible damage in the teeth or the bolt are then calculated separately from the global stresses and forces in the connection between the two bodies. Furthermore, drop tests with prototypes show that no deformations are to be expected at the closing systems which could impair their function.
Bottom half		
Valve protecting device	Hinges removed and foam slightly shrunk	The PIR foam inside the housing of the valve protecting device is slightly scaled down to create a small gap between the foam and the housing. Due to fabrication tolerances, this kind of modeling provides a good representation of the real prototype. The hinges connecting the valve protecting device with the profile of the bottom half of the DN30 PSP are not included in the FEM model but represented by a simple tied contact keeping the valve protecting device in place. The hinges are not meant to withstand the drop tests. Even if they fail, the valve protecting device is pinched between the surrounding elements (30B cylinder, inner shells of the bottom and top half of the DN30 PSP).
Rotation preventing devices	Simplified	The handle has no relevance concerning the mechanical strength of the rotation preventing device. Therefore, it is neglected together with the corresponding slit in the sleeve. Further simplifications concern the bottom part of the flange of the rotation preventing devices. It is removed because the influence on the global deformation behavior is negligible.
Feet	Simplified	Simplifications of the feet mainly concern the replacement of the tongue and groove joints by straight edges.
Top half		
Lifting lugs	Removed	The attachment points are not modeled in the FEM model. These parts are not relevant for the drop tests.

Part	Deviation	Justification
Valve protecting device counterpart	Simplified	Firstly, the bar in the area close to the flange is neglected which allows the whole valve protecting device counterpart to be modeled with shell elements and avoids cumbersome contact modeling between shell and solid elements in this region. Secondly, the roof-like construction is simplified to a single sheet.
Rotation preventing device counterparts	Simplified	Simplified to a square profile.
Content (heavy concrete as surrogate material for UF_6 in the drop tests)	Debris and cracks in the concrete neglected	In reality the content is UF_6. For the drop tests a mixture of steel grid and cement (heavy concrete) is used. This mixture is modeled by a homogeneous material model in the FEM calculation. Furthermore the presence of some loose parts of the UF_6 in the cylinder is not taken into account. The debris was mainly considered in the real drop tests to investigate the leak-tightness of the 30B cylinder due to a secondary impact of the debris. Since the leak-tightness cannot be investigated with FEM simulations, there is no need to consider the debris in the FEM model.

2.2.1.5.1.3.1 Mesh

The mesh of the FEM model consists of shell and solid elements. Solid elements are used for steel, concrete and foam parts. However, most of the steel parts are modeled using shell elements.

In total the model consists of 137571 shell elements and 112432 solid elements. The mesh statistics are listed in Table 27.

Table 27: Mesh statistics

Parameter	Solid elements		Shell elements		Beam elements
	min	max	min	max	
Characteristic length [mm]	3.99	34.45	2.28	28.6	
Aspect ratio [-]	1.01	5.34	1.0	7.64	
Min. Angle [°]	13.04	89.93	31.9	90.0	
Max. Angle [°]	64.9	173.33	90.0	160.0	
Time step [s]	$6.27 \cdot 10^{-7}$		$4.2 \cdot 10^{-7}$		
Number of elements	112432		137571		65
Total number of elements	250068				

The following figures Figure 21 to Figure 25 show the general structure of the mesh. Figure 21 shows the mesh of the outer shell and feet, Figure 22 shows the mesh of the foam parts of the DN30 PSP, Figure 23 shows the mesh of the inner shell of the DN30 PSP, Figure 24 shows the mesh of the 30B cylinder and Figure 25 shows the mesh of the content replacement.

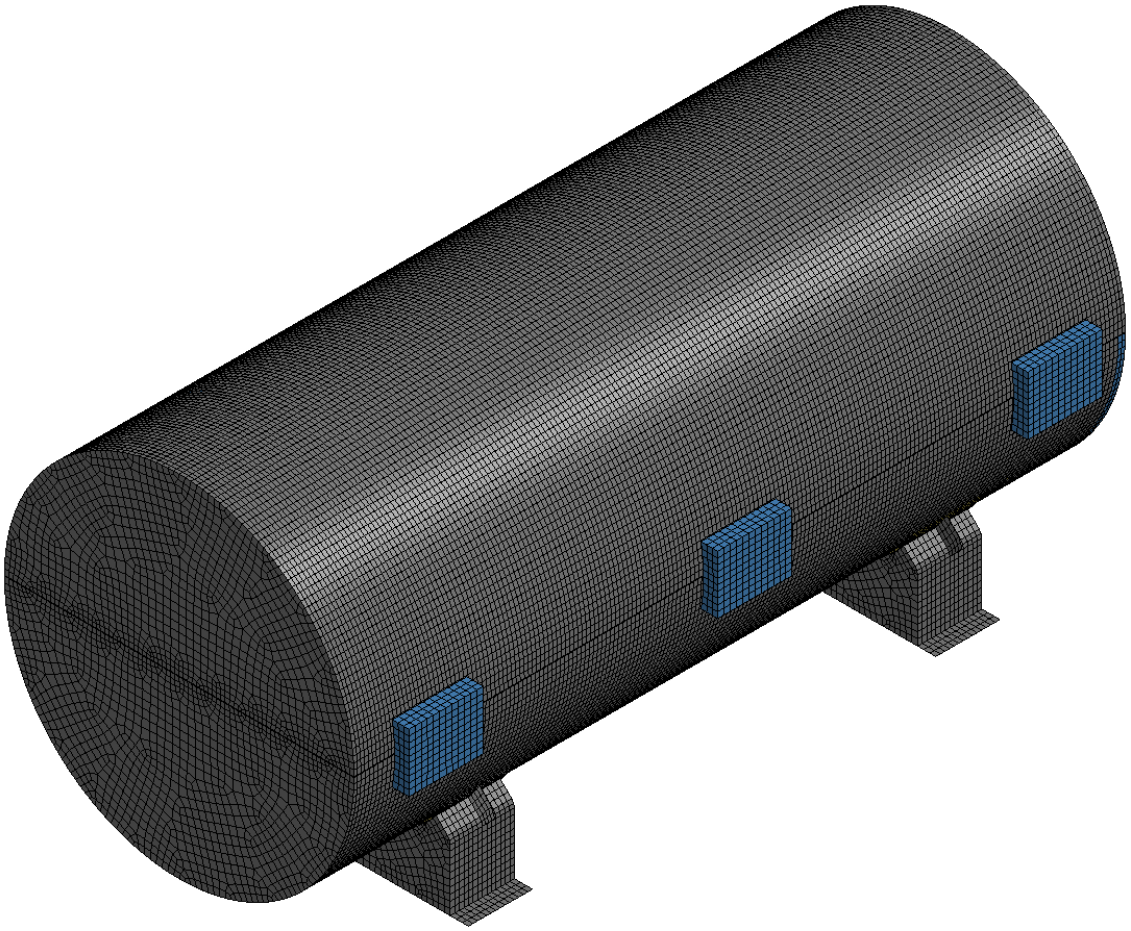

Figure 21: Mesh of the DN30 package, outer shell and feet

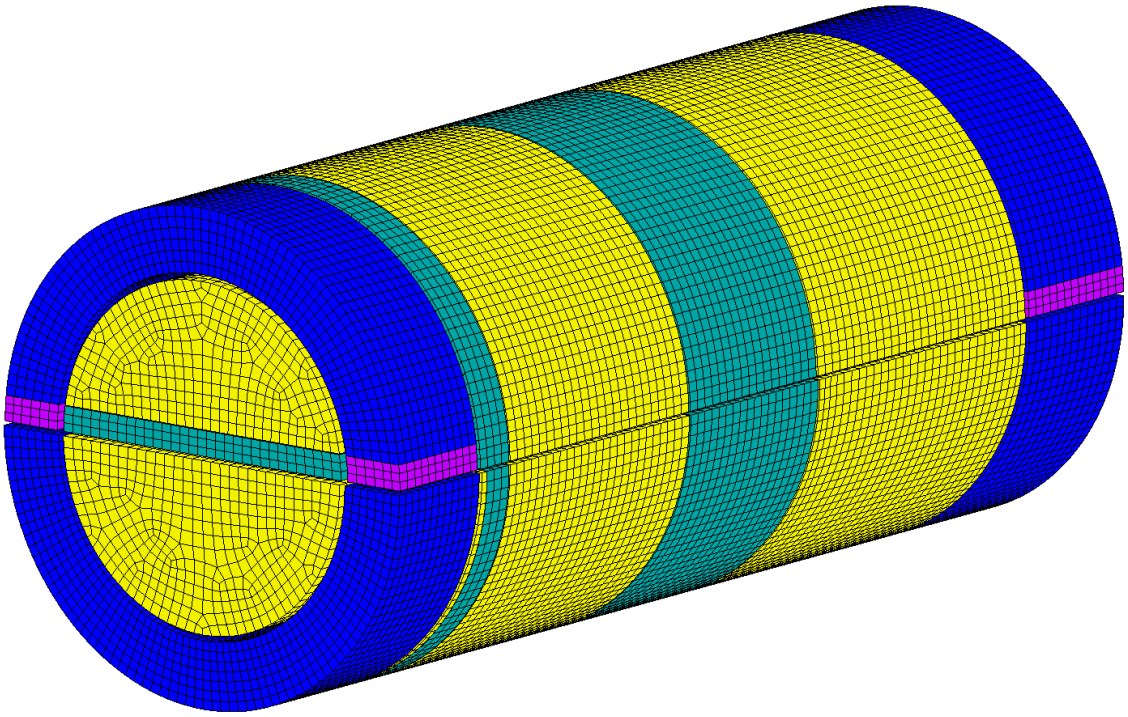

Figure 22: Mesh of the DN30 package, foam parts

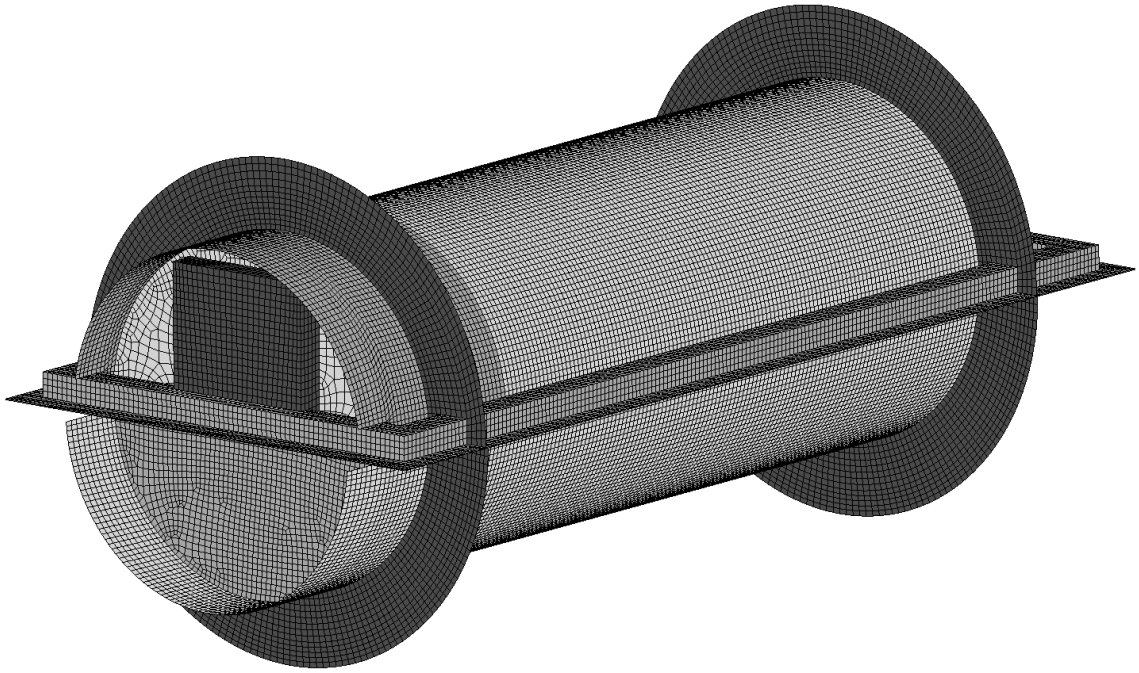

Figure 23: Mesh of the DN30 package, inner shells

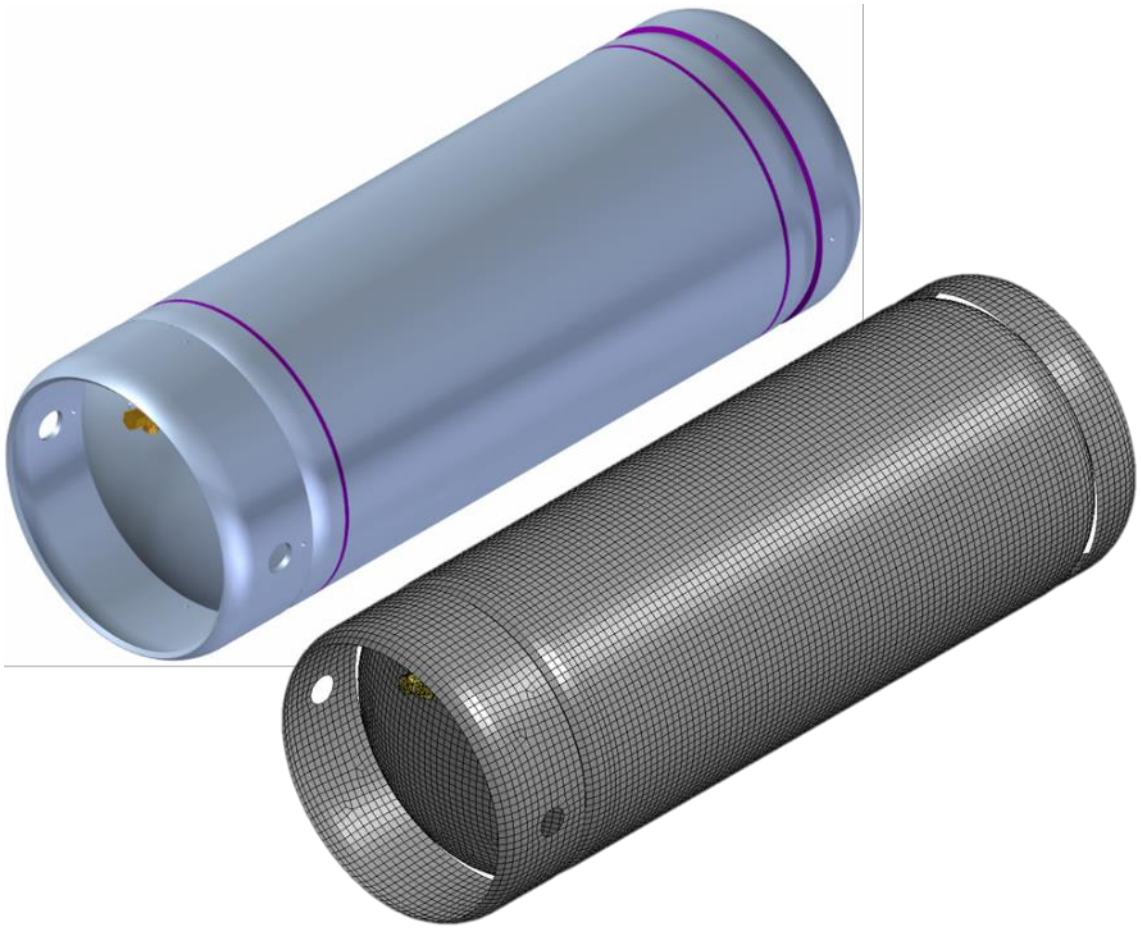

Figure 24: Mesh of the 30B cylinder

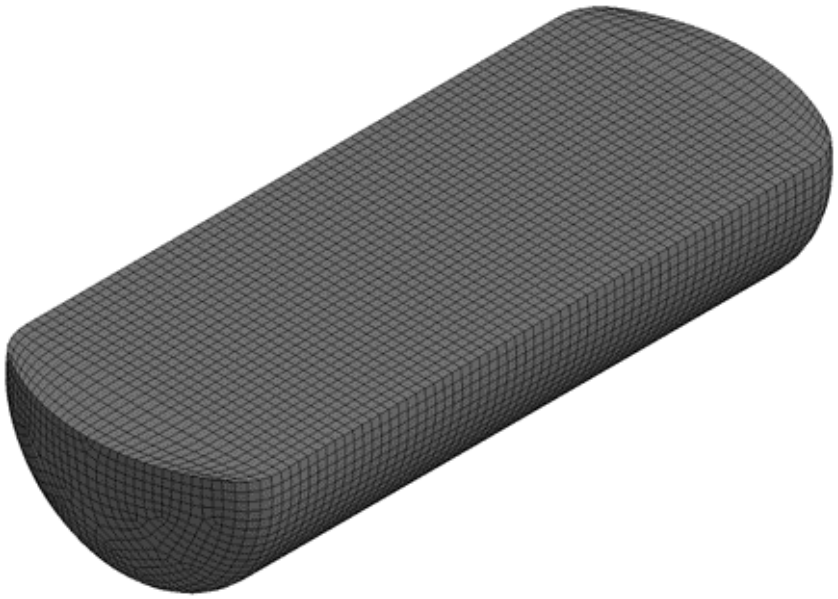

Figure 25: Mesh of the DN30 package, content of the 30B cylinder

2.2.1.5.1.3.2 Boundary conditions

The DN30 package has an initial speed of 4.85 m/s (1.2 m drop), 13.3 m/s (9.0 m drop) and 4.43 m/s (1.0 m drop onto bar), respectively. This velocity is orientated vertical downwards onto the target, a rigid shell element respectively the bar.

The target is fixed in all degrees of freedom.

Gravity is not modeled in this calculation because of its expected small influence.

2.2.1.5.1.3.3 Contacts

Welding seams of metal parts are modeled as mesh connections or tied contacts.

A failure criterion is not modeled for the parts of the DN30 package. Possible cracks in the welding seams are detected “by hand” by gauging the strains and stresses in these areas.

If friction is included in the contact, a static and dynamic coefficient as well as a decay constant is provided because the calculation of the friction coefficient is based on an exponential decay curve. Here, the static and dynamic friction coefficients FS and FD are equally set to 0.15 to avoid additional numerical noise in the contact forces and the decay constant is left at the default value.

2.2.1.5.1.3.4 Foam

The material properties of the two different kinds of foam were investigated in Appendix 1.4.2 (Material Data PIR Foam). The material model which was evaluated in this report is used for the analysis of the drop tests of the DN30 package. The stress-strain relationships are shown in Figure 26 and Figure 26. Best suited for the description of the mechanical behavior of this type of foam is the material model **MAT_CRUSHABLE_FOAM* of LS-DYNA.

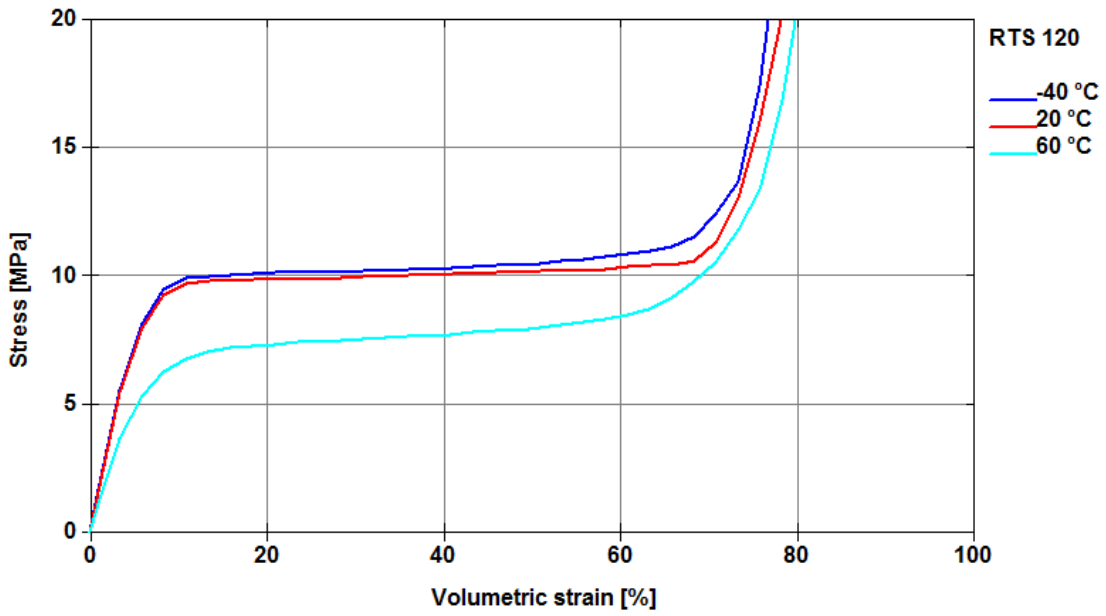

Figure 26: Material properties of PIR foam RTS120 used for the FEM-model

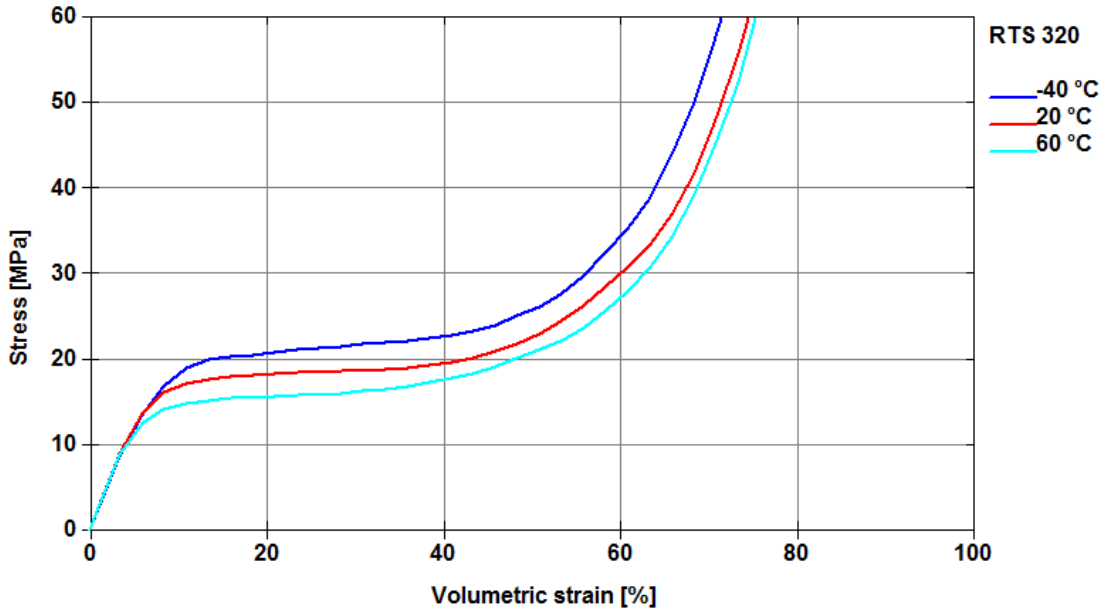

Figure 27: Material properties of PIR foam RTS320 used for the FEM-model

2.2.1.5.1.3.5 Steel

For all kinds of stainless steel the same elastic-plastic material model with isotropic linear hardening is used. It is **MAT_MODIFIED_PIECEWISE_LINEAR_PLASTICITY* with the true stress-strain curve defined in Figure 28.

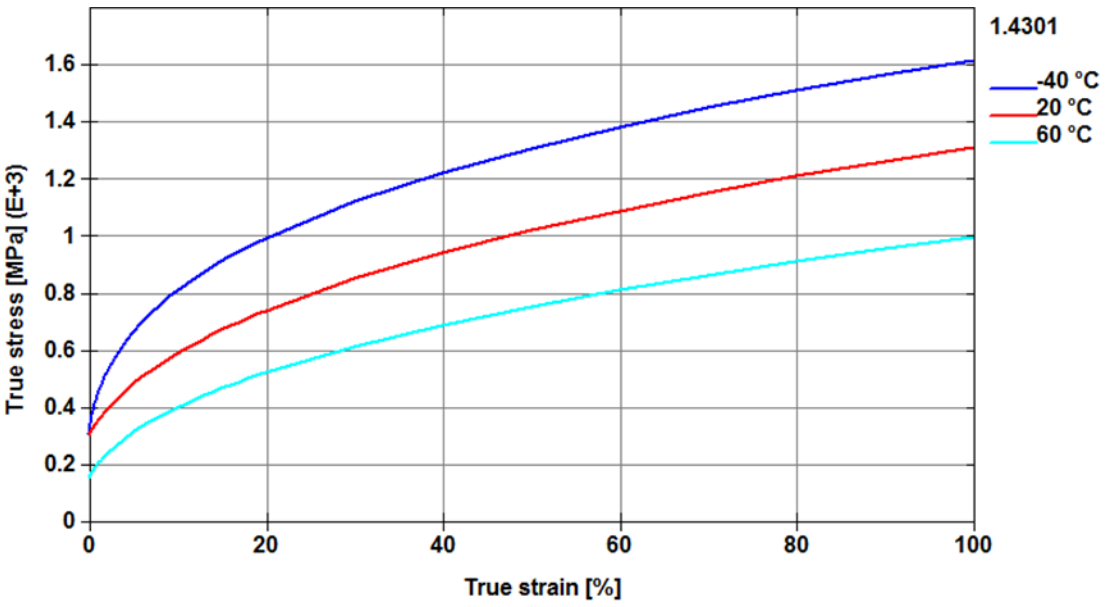

Figure 28: Material properties of stainless steel no. 1.4301 used for the FE-model

The data given in Figure 28 represent common values for stainless steel in contrary to the minimal values defined in the respective standards. The curves are evaluated with the Swift

equation with the input of $R_{p0.2}$, $R_{p1.0}$ and R_m [SWIFT 1952]. Due to the fact that the yield strength and ultimate tensile strength are determined in quasi static conditions, the resulting flow curves are multiplied with a factor taking into account the dynamic stiffening behavior of steel. In the present case, this factor is 1.3. Details are contained in Appendix 2.2.1.3 (Structural Analysis of the DN30 Package under NCT and ACT).

Furthermore, a failure criterion of the steel is not taken into account for the present analysis. So the strain of steel does not end at approximately 50% (common value for the elongation at fracture of austenitic stainless steels) but is extended to higher values to achieve a stable calculation. Possible failures and cracks in the steel parts are evaluated by comparing the calculated strains with the elongation at fracture of the material.

In this calculation, there is only one curve for all kinds of stainless steel. Different kinds of steel are used for the DN30 package, but the differences in the stress-strain curves are insignificant for these steels compared to usual manufacturing tolerances for steel.

2.2.1.5.1.3.6 Content of the 30B cylinder

In the FEM simulation the content of the 30B cylinder (UF_6) is simulated by a block of heavy concrete with a density of 5.1 g/cm³. The simulated mass if 2277 kg.

In the real drop tests the content of the 30B cylinder (UF_6) is simulated by a mixture of steel grit and cement. The density of UF_6 in solid state is 5.1 g/cm³. In order to be close to the real content, the simulated content of steel grit and cement has a similar density to UF_6. The content is modeled as one big block of this mixture positioned at the bottom half of the 30B cylinder and a layer of scraps positioned at the top of this block. The big block as well as the scraps have a density of 5.1 g/cm³. The mass of the block is 1977 kg, the scraps have a total weight of approximately 300 kg. While the scraps can move freely during the drop tests, the block remains a solid body during all drop test simulations.

In the FEM simulation, the content of the 30B cylinder (UF_6) is simulated by a single block of heavy concrete with a density of 5.054 g/cm³. The simulated mass of 2277 kg corresponds to the maximum allowed net weight of the 30B cylinder. An isotropic elastic material model is used for the concrete mixture (E=31480 MPa, equal to the elastic modulus of concrete C25), so nearly no deformation and no energy absorption of the content is to be expected.

2.2.1.5.1.4 Modeling of the drop test sequence

Each drop test sequence (1.2 m drop – 9.0 m drop – drop onto bar) is modeled in the same way. First the 1.2 m drop is calculated, after that a small restart calculation is performed where the velocity of the whole DN30 package model is set to zero and the target is put in the right position for the next drop test. This is required because of possible rotations of the DN30 package model during the previous drop test. In this restart analysis all information about internal stresses and strains are kept.

The short time without any loads on the DN30 package model is also required for relaxation, so internal oscillations can be reduced.

After that the calculation for the 9.0 m drop is carried out followed by another relaxation period and finally the drop onto the bar. The order of the drop tests (9.0 m drop before drop onto the bar or drop onto the bar before 9.0 m drop) is investigated as well. It is demonstrated that the drop order (1.2 m – 9.0 m – bar) is more conservative for the DN30 package.

The drop test program is based on the results of former drop test simulations.

2.2.1.5.1.5 Analysis, results of real drop tests and comparison of analysis and drop tests

2.2.1.5.1.5.1 Corner drop onto the valve side – drop test sequence 1

2.2.1.5.1.5.1.1 General considerations

The valve is the most vulnerable part of the containment system. For the corner drop onto the valve side maximal deformation of the DN30 shell in the valve area is to be expected. The design has to ensure that after the tests simulating ACT:

- There is no contact between valve and any part of the DN30 PSP or any other part of the 30B cylinder except its initial point of contact (the thread).
- The leakage rate of the containment does not exceed the limit specified in section 2.2.3.

In variation calculations, the angle between the longitudinal axis of the DN30 package and the vertical is determined which leads to maximum deformation and thus minimum volume of the foam in the valve area. This angle is then used in real drop tests to validate the results of the analysis.

2.2.1.5.1.5.1.2 FEM Analysis

2.2.1.5.1.5.1.2.1 FEM analysis before the drop tests

In the FEM analysis before the real drop testing, different angles from 12° to 42° between the longitudinal axis of the DN30 package and the vertical line through the center of gravity were analyzed for the 1.2 m drop and the 9 m drop onto the corner onto the valve side. For the drop from 1 m height onto the bar, the angle was in all cases such as that the vertical line from the center of gravity touched the valve and the corner of the bar.

The minimal distance between inner and outer shell above the valve was reached for an angle in the range of 12° to 22° and the minimal remaining foam volume in the valve area after the drop test sequence was reached for an angle in the range of 17° to 27°. For the analysis of accelerations and deformations, the angle of 22° was selected, which was also then used as basis for the real drop tests.

2.2.1.5.1.5.1.2.2 Deformations at -40 °C, RT and +60 °C

In the 1.2 m free drop the corner of the DN30 PSP is deformed as shown in Figure 29. There are no deformations of the inner steel plates, the rotation preventing device and the valve protecting device. Furthermore there are no cracks in the outer shell or the inner shell of the DN30 PSP.

The 9.0 m drop causes larger deformation of the corner of the DN30 PSP as shown in Figure 30. The buckling of the outer shell continues, but still without any cracks in the outer surface. There are also deformations visible at the inner steel parts, especially at the front plate, which is in contact with the skirt of the 30B cylinder. The rotation preventing devices are deformed but their function is still preserved and any rotation of the 30B cylinder is prevented.

Figure 31 shows the deformations during the drop onto the bar. The bar does not penetrate the steel shell of the DN30 PSP. There is a deformation of the outer steel shell and also some deformation of the inner steel shell, but the distance between valve and DN30 PSP is still preserved.

The resulting deformed structure with the smallest distance between inner and outer shell above the valve and minimal remaining foam volume in the valve area is shown in Figure 31.

The deformations and the accelerations are summarized in the Table 28. The measurement points for the values listed are defined in Figure 29.

Table 28: Deformation and remaining dimensions calculated for the drop onto the valve corner

Dimension [mm]	Drop test at temperature								
	-40°C			RT			60°C		
	1.2 m	9.0 m	1 m bar	1.2 m	9.0 m	1 m bar	1.2 m	9.0 m	1 m bar
Largest fold (L1x)	80	178	-	84	195		94	213	-
Largest fold (L1y)	582	561	-	581	557		582	558	-
Weld between head and outer shell (L2x)	62	161	-	67	178		82	205	-
Weld between head and outer shell (L2y)	562	542	-	562	538		558	532	-
Depth of bar penetration (p1)	-	-	7	-	-	34	-	-	44
Depth of bar penetration (p2)	-	-	28	-	-	44	-	-	41

Remark: the values for RT given in Table 28 and Table 29 differ from each other, since different reference nodes of the simulation model were selected for the comparison of the calculated and measured deformations.

The corner drop onto the valve side is the most critical drop orientation concerning the deformations of the DN30 package. Generally, the material response of steel becomes softer with increasing temperature so that even larger deformations are expected at 60 °C. Therefore, sequence 1 is used for the investigation of the deformation behavior of the DN30 package at an ambient temperature of 60 °C. In addition, a simulation at -40 °C is performed to get a general idea of the temperature dependency of the deformation behavior of the DN30 package. In contrast to elevated temperatures, the material response of the austenitic stainless steel becomes stiffer at lower temperatures. Therefore, smaller deformations of the package and higher decelerations in the valve region are expected. Independently of the ambient temperature, the design has to ensure that after the drop tests simulating ACT no contact between the valve and any part of the DN30 PSP or the 30B cylinder occurs, excepting its initial point of contact (the thread).

The deformations at 60°C of the corner of the DN30 PSP are similar to the deformations at RT. The displacements of the inner front plate, where the skirt of the 30B cylinder hits the inner shell, are still small. Additionally, the rotation preventing devices as well as the valve protecting device remain undamaged. Based on the maximum plastic strain of 25% occurring in the simulation at 60 °C, there are neither cracks in the outer shell nor the inner shell of the DN30 PSP to be expected. The valve has no contact to any other part of the DN30 PSP or the 30B cylinder except its initial point of contact.

The deformations at -40°C of the corner of the DN30 PSP are similar to the deformations at RT. Cracks in the outer surface are not to be expected because the observable maximal plastic

strains are below the elongation at fracture of the austenitic stainless steel according to the standards. The inner front plate and the profile of the top half are slightly more deformed in the simulation at -40°C than at RT. According to the simulation, cracks are likely to occur in these regions. The impact of the 30B cylinder skirt causes these deformations. One explanation for this unexpected increase of the deformation of the front plate is related to the 10mm thick inner shell in the valve region. Due to the stiffer material response at -40°C, the plastic deformations of this part of the DN30 PSP are only 16% compared to 22% in the case of the simulation at RT. Consequently, less kinetic energy of the 30B cylinder is transformed into internal energy of this part. The inner front plate and the profile of the top half therefore absorb most of the remaining kinetic energy of the 30B cylinder, which results in larger deformations.

The above mentioned larger deformations of the inner steel parts have no influence on the valve protecting device, so that the valve is still prevented from getting in contact with other parts. In case of the rotation preventing devices, only small deformations at the flange are observed. Hence, their function is still preserved and any rotation of the 30B cylinder is prevented.

Neither at -40°C nor at 60°C is a contact between the valve or the plug and any other part of the DN30 PSP or 30B cylinder other than their initial point of contact (the thread).

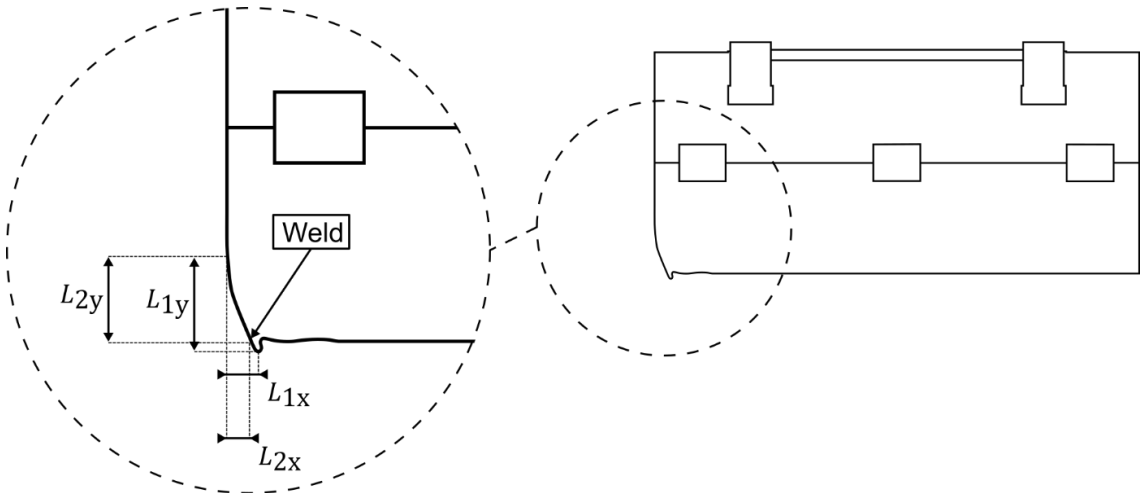

Figure 29: Measured distances in sequence 1

Figure 30: Deformed structure after the 1.2 m free drop onto the valve corner

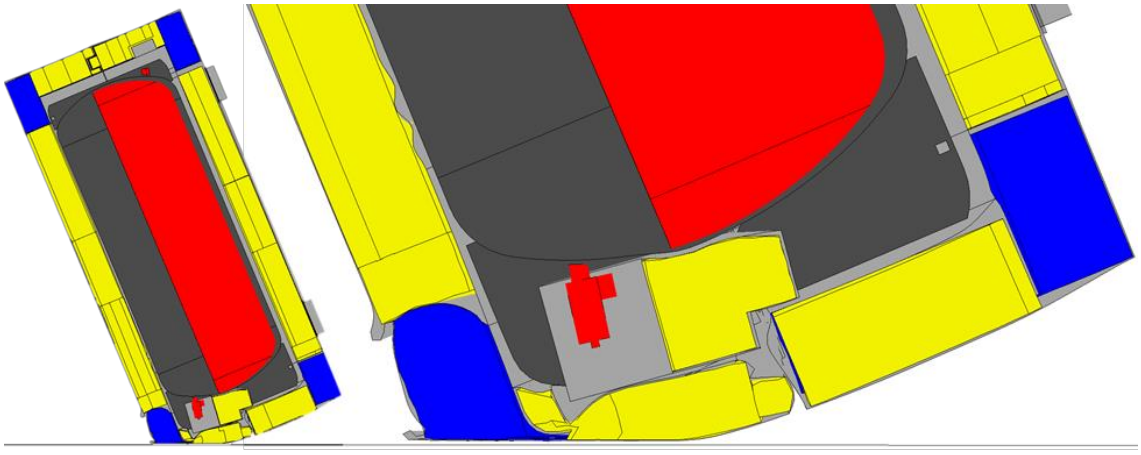

Figure 31: Deformed structure after the 9.0 m drop onto the valve corner

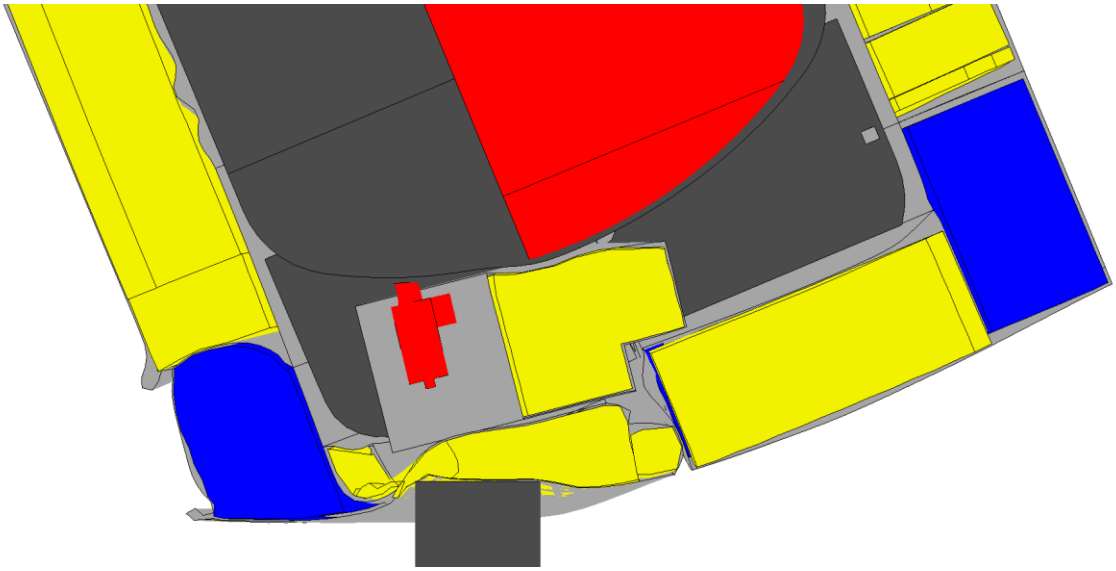

Figure 32: Deformed structure in the valve area after the test sequence onto the valve corner

2.2.1.5.1.5.1.2.3 Decelerations at -40 °C, RT and +60 °C

The deceleration in the valve area is compared in Figure 33 for RT and +60 °C and in Figure 34 for RT and -40 °C. The measured decelerations are filtered with a low-pass Butterworth filter with a cut-off frequency of 584 Hz. The cut-off frequency itself is determined in Appendix 2.2.1.3 (Structural Analysis of the DN30 Package under NCT and ACT).

The smooth increase in Figure 33 for +60 °C in the beginning of the deceleration curve is mainly attributed to the softer material behavior. For the same reasons, the first peak in the simulation at 60 °C is half is large as in the simulation at RT. Consequently, there are fewer oscillations excited in the model, which is clearly visible in the deceleration curve, and the whole drop takes slightly longer.

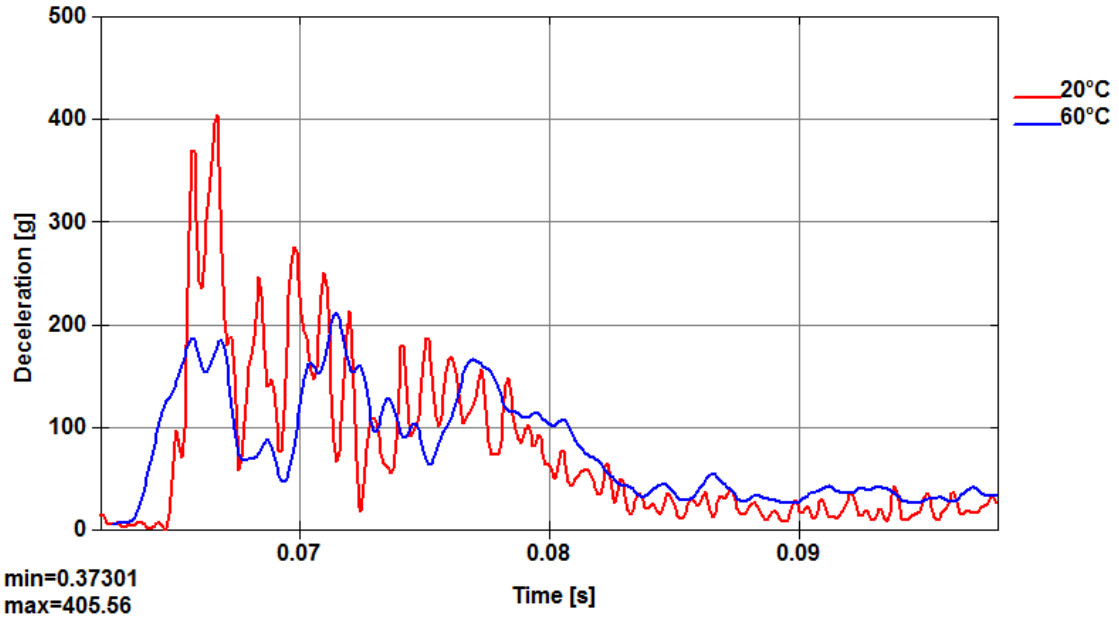

Figure 33: Comparison of the deceleration in the valve area during 9.0 m drop in sequence 1 at 60℃ and 20℃ – low-pass filtered (Butterworth, 584 Hz cut-off)

Each peak amplitude in Figure 33 at -40℃ is smaller than at RT so that the deceleration curve at -40°C is generally smoother, but still similar. This behavior is a consequence of a slightly weaker impact of the 30B cylinder skirt on the inner front plate of the DN30 PSP. However, this is contrary to the expectations that the decelerations increase with increasing material stiffness. Most likely, this discrepancy can be related to a different position of the 30B cylinder after the free drop test at -40°C compared to the simulation at RT.

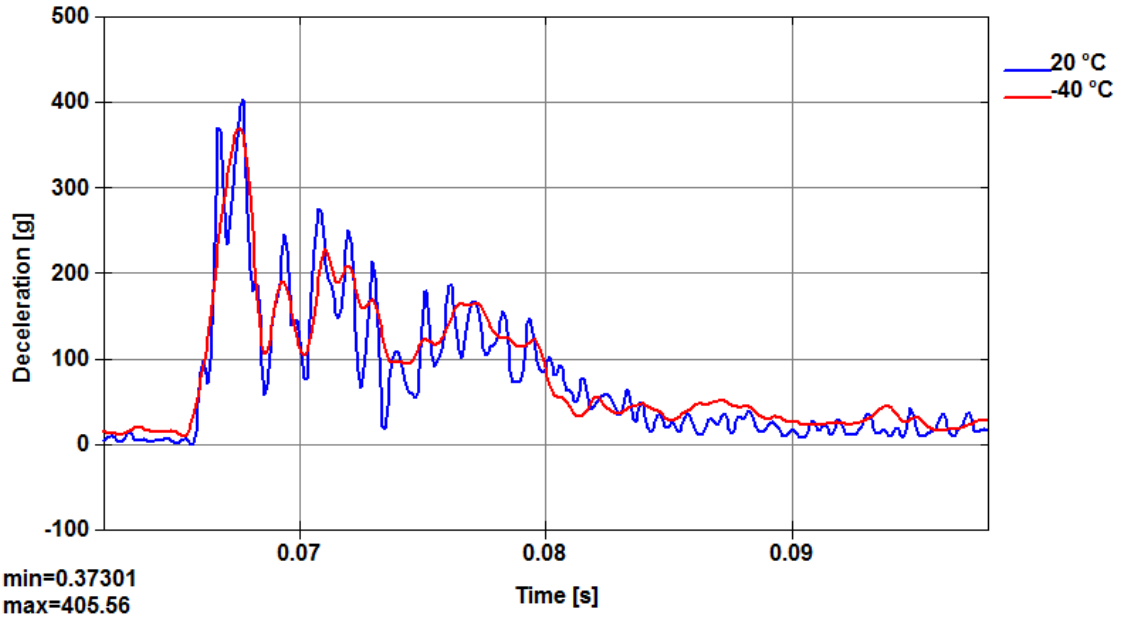

Figure 34: Comparison of the deceleration in the valve area during 9.0 m drop in sequence 1 at -40℃ and 20℃ – low-pass filtered (Butterworth, 584 Hz cut-off)

2.2.1.5.1.5.1.3 Results of the Drop test sequence 1

The drop test sequence onto the corner of the valve side is documented as sequence no. 1 in Appendix 2.2.1.2 (Drop Test Reports).

- Drop No. 1.1 1.2 m corner drop test onto the valve side
- Drop No. 1.2 9 m corner drop test onto the valve side
- Drop No. 1.3 1 m drop onto a bar onto the valve side

2.2.1.5.1.5.1.3.1 Deformations at RT for drop test sequence 1

The 1.2 m drop causes small deformations of the corner of the DN30 package. There is a slight buckling of the outer shell visible (see Figure 35). The 9.0 m drop causes larger deformation of the corner of the DN30 package. The buckling of the outer shell increases but still without any cracks in the outer surface or outer welds (see Figure 35).

The drop onto the bar does not cause a complete penetration of the steel shell of the DN30 package, but a crack of the outer shell is visible at the impact point (see Figure 37).

Figure 35: Sequence 1 - Deformation after the 1.2 m drop

Figure 36: Sequence 1 - Deformation after the 9.0 m drop

Figure 37: Sequence 1 - Deformation after the drop onto a bar from 1.0 m

There are also deformations and cracks visible at the inner steel parts, especially at the front plate which is in contact with the skirt of the 30B cylinder (see Figure 38). The rotation preventing devices are deformed, but their function is still preserved and any rotation of the 30B cylinder is prevented (see Figure 39).

Figure 38: Sequence 1 – Deformation and cracks of the top half, inner shell

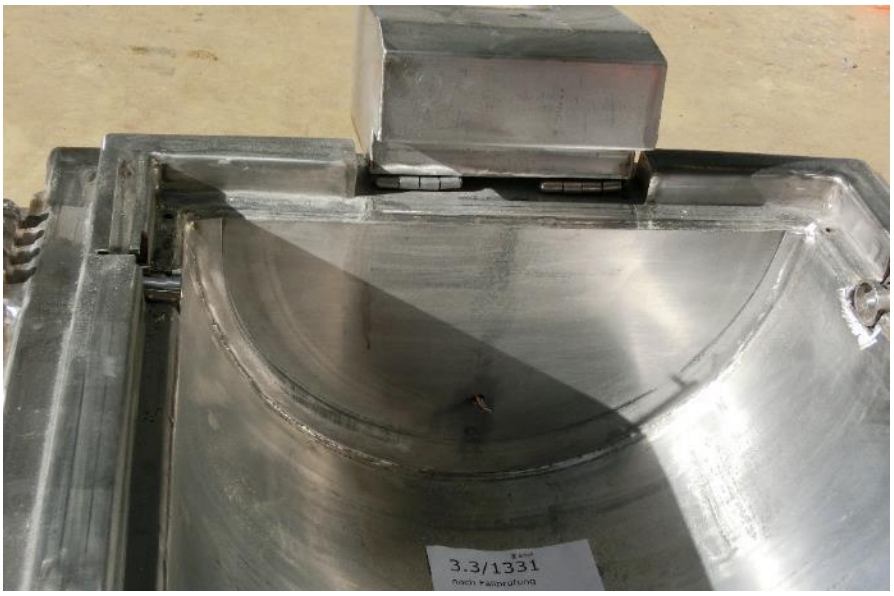

Figure 39: Sequence 1 – Deformation of the bottom half, inner shell

2.2.1.5.1.5.1.3.2 Summary of the drop test results for sequence 1

- The leakage rate after the drop test sequence 1 is Q_{st} = 5.67 E-08 Pa m^3/s.
- All closure systems were intact;
- The DN30 PSP could be opened without any further damage;
- The closure system was still working and the top half could be easily lifted off of the bottom half;
- There was no contact between the valve and any other part of the DN30 PSP or 30B cylinder other than its initial point of contact (the thread);

- There was no contact between the plug and any other part of the DN30 PSP or 30B cylinder other than its initial point of contact (the thread);
- The valve protecting device could still be operated (rotated); the hinges were intact;
- Removal of the 30B cylinder from the bottom half was possible without further damage to the DN30 PSP;
- Loading of a 30B cylinder into the DN30 PSP was still possible.

2.2.1.5.1.5.1.4 Results of the drop test sequence 7

A further drop test sequence onto the valve corner was carried out to prepare a specimen for the subsequent thermal test. This specimen as equipped with the housing and the intumescent material attached to the inner shell These additional features were added to the specimen before the drop test and were part of the prototype during the drop tests. For the specimen the two sequences “drop onto the valve corner” and “drop onto the plug corner” were combined. Furthermore, the 1.2 m free drop test was combined with the 9.0 m drop test to a single 10.2 m drop test, which caused larger deformations than the regulatory sequence.

Drop No. 7.1 10.2 m corner drop tests onto the valve side

Drop No. 7.2 1 m drop onto a bar onto the valve side on top half

Drop No. 7.3 10.2 m corner drop test onto the plug side

Drop No. 7.4 1 m drop onto a bar onto the plug side on bottom half

2.2.1.5.1.5.1.4.1 Deformations at RT for drop test sequence 7

The deformations of the outer shell as well as of the inner shell are identical to the deformations documented in sequence 1 (see Figure 40).). Table 30 shows the comparison of the deformation measured for drop test sequence 1 with the deformations measured for drop test sequence 7. The measurement points for the values listed are defined Figure 29.

Figure 40: Deformations of the DN30 PSP after sequence 7

2.2.1.5.1.5.1.4.2 Summary of the drop test results for sequence 7

For both sequence 7 the results are identical to the results for sequence 1 given in section 2.2.1.5.1.5.1.4. Additionally, following was recorded with respect to the additional features housing and intumescent material:

- The housing in the valve protecting device containing the intumescent material was intact;
- The intumescent material applied to the inner shell of the DN30 PSP as well as the housing and the plug protecting device was undamaged;

- Removal of the 30B cylinder from the bottom half was possible without further damage to the DN30 PSP;
- Loading of a 30B cylinder into the DN30 PSP was still possible.

2.2.1.5.1.5.1.5 Evaluation of the FEM analysis vs. real drop tests

2.2.1.5.1.5.1.5.1 Deformations at RT

The measured deformations and remaining dimensions are compared in Table 29 to the calculated values. The measurement points for the values listed are defined in Figure 29.

Table 29: Deformations and remaining dimensions measured for the drop onto the valve corner (ambient temperature) and comparison with calculated values at RT

Dimension [mm]	Drop								
	1.2 m			9.0 m			1 m bar		
	CV	MV	D %	CV	MV	D %	CV	MV	D %
Largest fold (L1x)	80	90	12	178	170	5	-	-	-
Largest fold (L1y)	237	245	3	452	490	8	-	-	-
Weld between head and outer shell (L2x)	65	-	-	163	-	-	-	-	-
Weld between head and outer shell (L2y)	214	200	7	428	460	7	-	-	-
Depth of bar penetration (p1)	-	-	-	-	-	-	34	32	7
Depth of bar penetration (p2)	-	-		-	-	-	44	50	12

CV = calculated values MV = measured values D % = deviation of measured values from calculated values in %

The measurement error in the experiment is expected to be in the range of approx. 10% due to the applied measurement technique. The resulting error between experiment and calculation does not exceed 12% in all cases and although the calculated deformations indicate that the FEM model has a slightly too stiff response, the simulation reproduces the behavior of the prototype observed in the experiment well.

2.2.1.5.1.5.1.5.2 Decelerations at RT

Figure 41 shows the comparison of the calculated decelerations with the measured decelerations. In contrast to the experiment, the 30B cylinder experiences no deceleration in the simulation until the impact of the skirt on the inner steel plate. In addition, there is a pronounced second peak in the experiment, which is not observed in the simulation. This peak could arise from a secondary impact caused by the debris, which cannot be simulated with the current FEM model.

Nevertheless, the maximal decelerations in the experiment and the simulation occur at the beginning of the drop. The corresponding error is -14% so that the maximal deceleration is only slightly underestimated by the FEM model. Moreover, the decay phase is in very good agreement with the measured decelerations in the experiment.

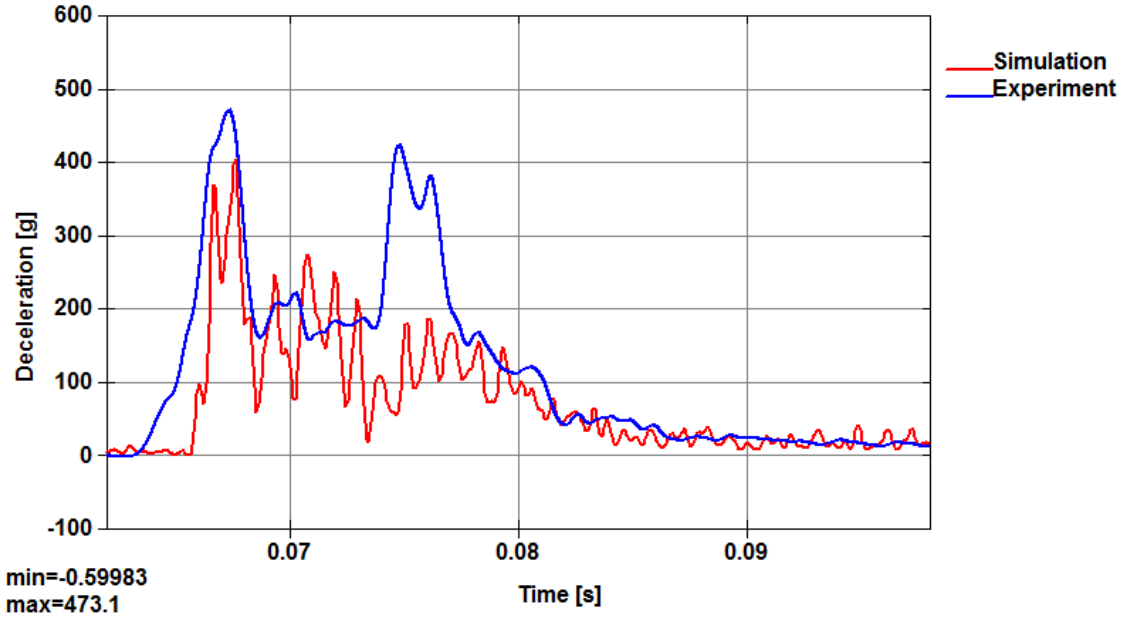

Figure 41: Comparison of simulation and experiment – deceleration in the valve area during 9.0m drop in sequence 1 – low-pass filtered (Butterworth, 584Hz cut-off)

Table 30: Deformations and remaining dimensions measured for the drop onto the valve corner in sequence 1 and sequence 7

Dimension [mm]	Drop					
	1.2 + 9.0 m			1 m bar		
	Seq. 1	Seq. 7	D %	Seq. 1	Seq. 7	D %
Largest fold (L1x)	≈170	≈211	≈24	-	-	-
Largest fold (L1y)	≈490	≈430	≈-12	-	-	-
Weld between head and outer shell (L2x)	-	≈143		-	-	-
Weld between head and outer shell (L2y)	≈460	≈395	≈-14	-	-	-
Depth of bar penetration (p1)	-	-	-	≈32	-	-
Depth of bar penetration (p2)	-	-	-	≈50	≈30	≈-40

2.2.1.5.1.5.2 Corner drop onto the plug side - drop test sequence 2

2.2.1.5.1.5.2.1 General considerations

Apart from the valve, the plug is the only other opening of the containment system. For the corner drop onto the plug side maximal deformation of the DN30 PSP shell in the plug area is to be expected. The design has to ensure that after the tests simulating ACT:

- There is no contact between plug and any part of the DN30 PSP or any other part of the 30B cylinder except its initial point of contact (the thread).
- The leakage rate of the containment does not exceed the limit specified in section 2.2.3.

In variation calculations, the angle between the longitudinal axis of the DN30 and the vertical is determined which leads to maximum deformation and thus minimum volume of the foam in the plug area. This angle is then used in real drop tests to verify the results of the analysis.

2.2.1.5.1.5.2.2 FEM analysis

2.2.1.5.1.5.2.2.1 FEM analysis before the drop tests

In the FEM analysis before the drop tests, different angles from 8° to 38° between the longitudinal axis of the DN30 package and the vertical line through the center of gravity were analyzed for the 1.2 m drop and the 9 m drop onto the corner at the plug side. For the drop from 1 m height onto the bar, the angle was in all cases such as that the vertical line from the center of gravity pointed through the center of the plug protecting device and touched the corner of the bar.

The minimal distance between inner and outer shell above the plug protecting device was reached for an angle in the range of 13° to 23° and the minimal distance between the plug and the plug protecting device was reached for an angle in the range of 8° to 23°. For the analysis of accelerations and deformations, the angle of 23° was selected and used for the real tests as well.

2.2.1.5.1.5.2.2.2 Deformations at RT

In the 1.2 m free drop, the corner of the DN30 PSP is deformed as shown in Figure 42. There are no deformations of the inner steel plates, the rotation preventing device and the plug protecting device. Furthermore, there are no cracks in the outer shell or in the inner shell of the DN30 PSP.

The 9.0 m drop causes larger deformation of the corner of the DN30 PSP. The buckling of the outer shell increases, but still takes place without any cracks in the outer surface. There are also deformations visible at the inner steel parts, especially at the inner front plate, which is in contact with the skirt of the 30B cylinder. The rotation preventing devices are deformed, but their function is still preserved and any rotation of the 30B cylinder is prevented. The foam between outer shell and plug protecting device is compressed, but still present.

The drop onto the bar does not penetrate the steel shell of the DN30 PSP. There is an additional deformation of the outer steel shell, but no further deformation of the inner steel shell. The resulting deformed structure with the smallest distance between inner and outer shell above the plug and minimal remaining foam volume in the plug area is shown in Figure 44 and in detail in Appendix 2.2.1.3 (Structural Analysis of the DN30 Package under NCT and ACT).

The deformations are summarized in Table 31. The measurement points for the values listed are defined in Figure 42.

Table 31: Deformations and remaining dimensions calculated for the drop onto the plug corner

Dimension [mm]	1.2 m drop	9.0 m drop	Drop onto the bar
Largest fold (L1x)	86	203	-
Largest fold (L1y)	580	609	-
Weld between head and outer shell (L2x)	71	161	-
Weld between head and outer shell (L2y)	559	563	-
Depth of bar penetration (p1)	-	-	20
Depth of bar penetration (p2)	-	-	24

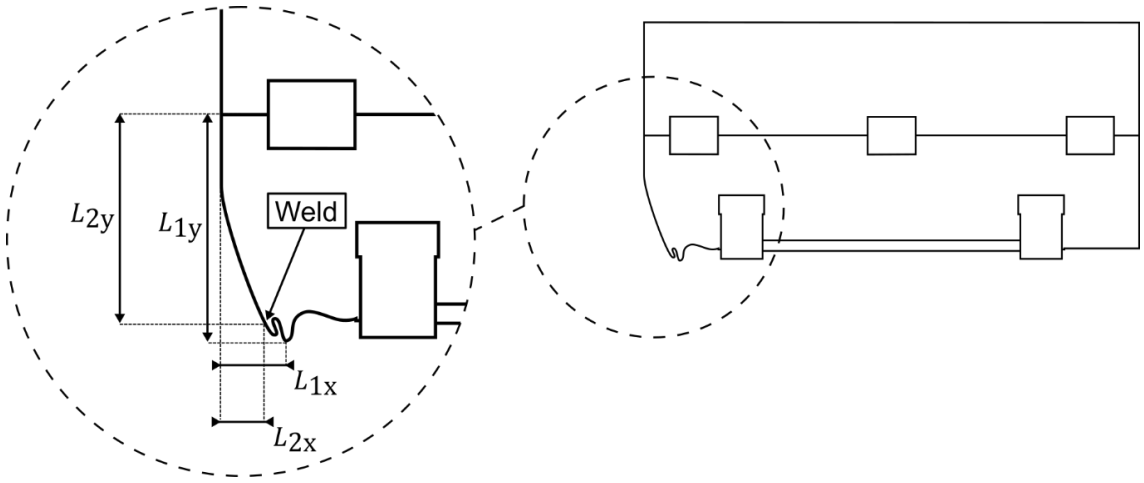

Figure 42: Measured distances in sequence 2

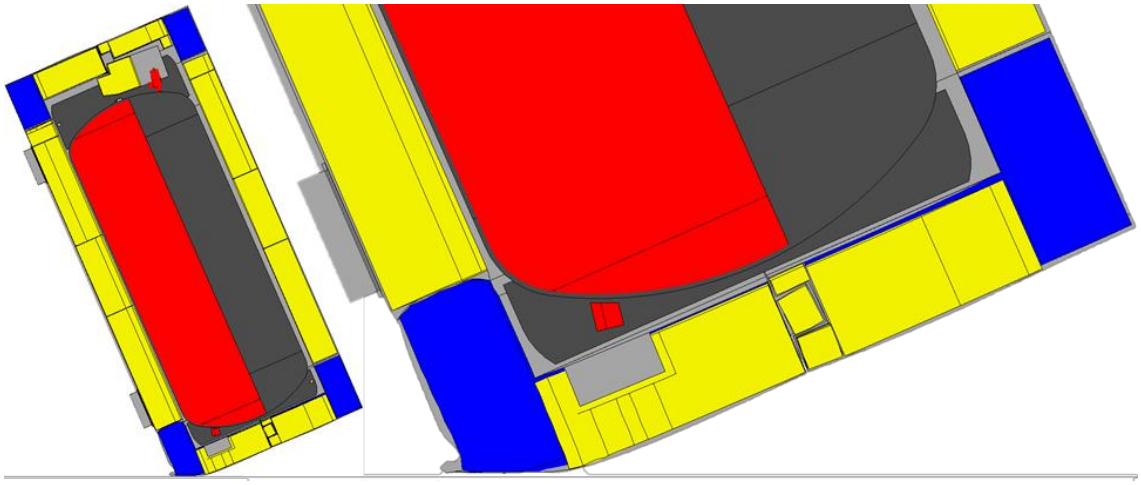

Figure 43: Deformed structure after the 1.2 m free drop onto the plug corner

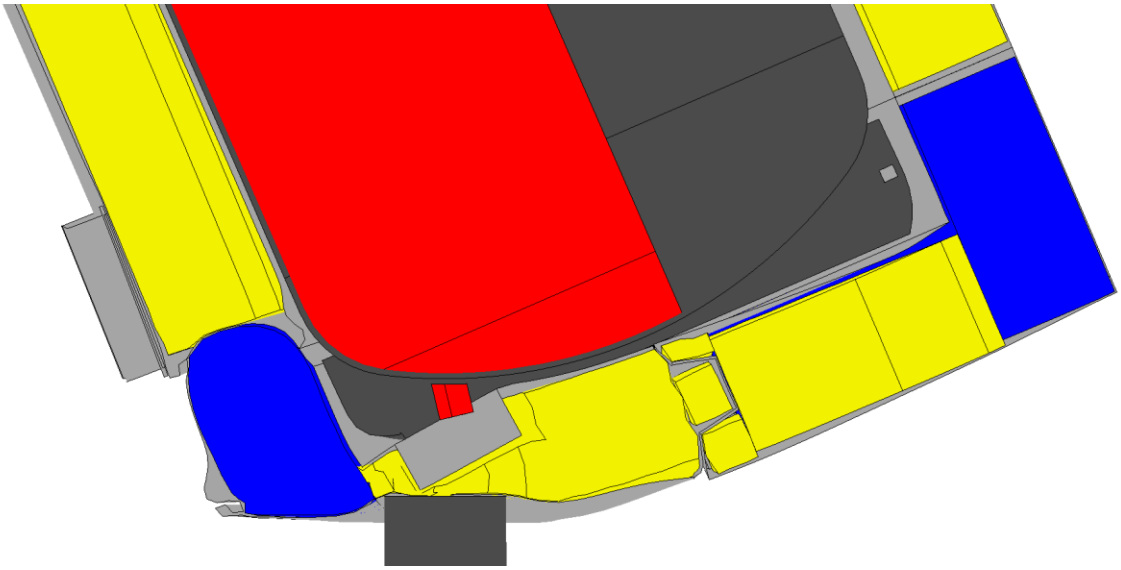

Figure 44: Deformed structure after the test sequence onto the plug corner

2.2.1.5.1.5.2.3 Results of drop tests

The drop test sequence onto the corner of the plug side is documented as sequence no. 2 in Appendix 2.2.1.2 (Drop Test Reports).

- Drop No. 2.1 1.2 m corner drop test onto the plug side
- Drop No. 2.2 9 m corner drop test onto the plug side
- Drop No. 2.3 1 m drop onto a bar onto the plug side

2.2.1.5.1.5.2.3.1 Deformations at RT

The 1.2 m drop causes small deformations of the corner of the DN30 package. A slight buckling is visible (see Figure 45). The 9.0 m drop causes larger deformation of the corner of the DN30 package. The buckling of the outer shell increases, but still without any cracks in the outer surface or outer welds (see Figure 46).

The drop onto the bar does not penetrate the steel shell of the DN30 package (see Figure 47).

Figure 45: Sequence 2 - Deformation after the 1.2 m drop

Figure 46: Sequence 2 - Deformation after the 9.0 m drop

Figure 47: Sequence 2 - Deformation after the drop onto a bar from 1.0 m

There are also deformations and cracks visible at the inner steel parts. The plug protecting device was pushed inside the DN30 PSP due to the impact of the bar (see Figure 48). The rotation preventing devices are deformed, but their function is still preserved and any rotation of the 30B cylinder is prevented.

.

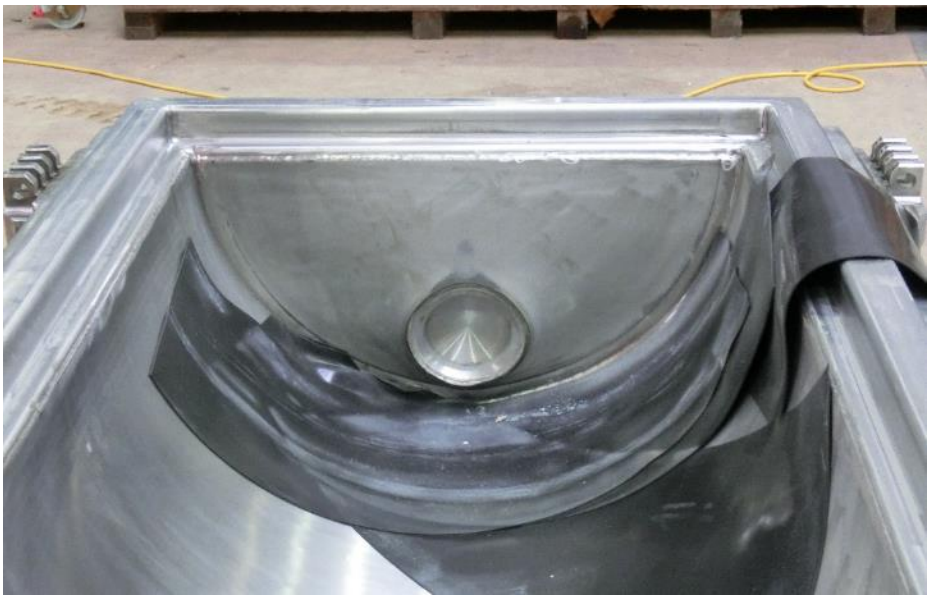

Figure 48: Sequence 2 – Deformation of the bottom half, inner shell

2.2.1.5.1.5.2.3.2 Summary of the drop test results for sequence 2

- The leakage rate after the drop test sequence 2 is Q_{st} = 4.15 E-06 Pa m^3/s.
- All closure systems were intact;
- The DN30 PSP could be opened without any further damage;
- The closure system was still working and the top half could be easily lifted off of the bottom half;
- There was no contact between the valve and any other part of the DN30 PSP or 30B cylinder other than its initial point of contact (the thread);
- There was no contact between the plug and any other part of the DN30 PSP or 30B cylinder other than its initial point of contact (the thread);
- The valve protecting device could still be operated (rotated); the hinges were intact;
- Removal of the 30B cylinder from the bottom half was possible without further damage to the DN30 PSP;
- Loading of a 30B cylinder into the DN30 PSP was still possible.

2.2.1.5.1.5.2.4 Evaluation of the FEM-analysis vs. real drop tests

2.2.1.5.1.5.2.4.1 Deformations at RT

The measured deformations and remaining dimensions are compared in Table 29 with the calculated values.

Table 32: Deformations and remaining dimensions measured for the drop onto the plug corner (ambient temperature) and comparison with calculated values

Dimension [mm]	Drop								
	1.2 m			9.0 m			1 m bar		
	CV	MV	D %	CV	MV	D %	CV	MV	D %
Largest fold (L1x)	86	90	5	203	251	19	-	-	-
Largest fold (L1y)	580	577	1	609	620	2	-	-	-
Weld between head and outer shell (L2x)	71	79	10	161	187	14	-	-	-
Weld between head and outer shell (L2y)	559	560	<1	563	580	3	-	-	-
Depth of bar penetration (p1)	-	-	-	-	-	-	20	24	16
Depth of bar penetration (p2)	-	-		-	-	-	24	34	28

CV = calculated values MV = measured values
D % = deviation of measured values from calculated values in %

The measurement error in the experiment is unknown, but expected to be in the range of about 10% due to the applied measurement technique. Although the calculated errors indicate that the FEM model has a slightly too stiff response, the simulation reproduces behavior observed in the experiment well.

2.2.1.5.1.5.2.4.2 Decelerations at RT

Figure 49 shows the comparison of the calculated decelerations with the measured decelerations. For the 9.0 m drop, it is assumed that the first increase of the deceleration in the experiment is attributed to events prior to the impact of the DN30 package on the drop target that are caused by friction between the 30B cylinder and the inner shell of the DN30 PSP. With this assumption, the duration of the actual drop in the simulation fits well to the experiment.

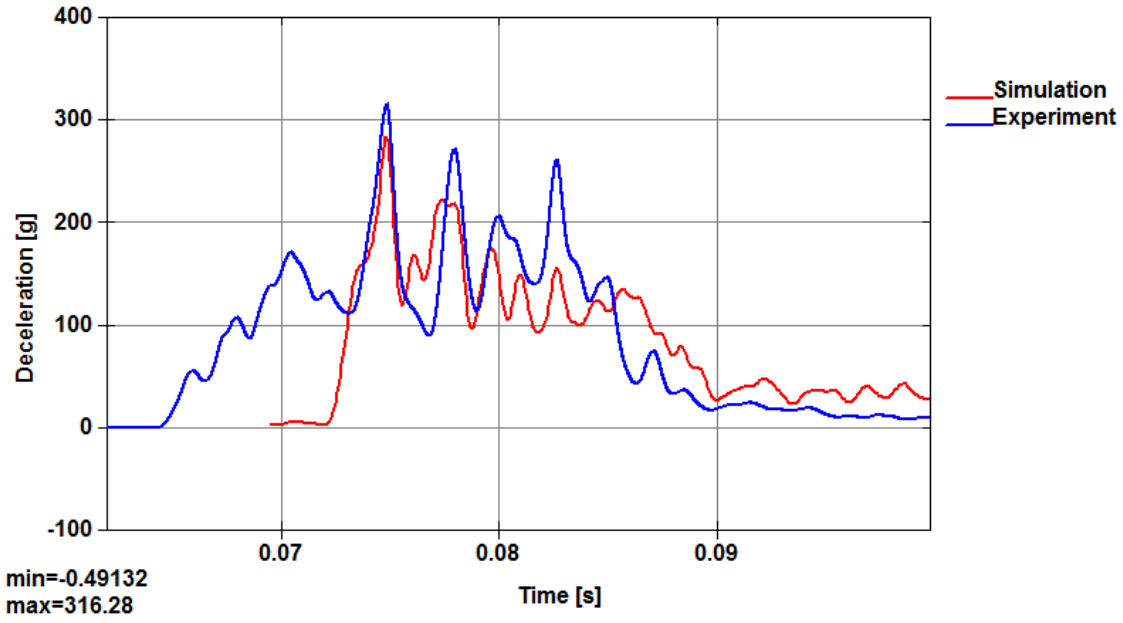

Figure 49: Comparison of simulation and experiment – deceleration in the plug area during 9.0 m drop in sequence 2 – low-pass filtered (Butterworth, 584 Hz cut-off)

2.2.1.5.1.5.3 Flat drop onto the valve side – drop test sequence 3

2.2.1.5.1.5.3.1 General considerations

With the drop onto the valve corner as described in section 2.2.1.5.1.5.1, maximal deformation is reached in the valve area. During the flat drop onto the valve side maximal accelerations and hence maximal forces at the valve are to be expected. The design has to ensure that after the tests simulating ACT:

- There is no contact between valve and any part of the DN30 PSP or any other part of the 30B cylinder except its initial point of contact (the thread).
- The leakage rate of the containment does not exceed the limit specified in section 2.2.3.

2.2.1.5.1.5.3.2 FEM analysis

2.2.1.5.1.5.3.2.1 Deformations at -40°C and RT

The drop orientation is flat onto the valve side for the 1.2 m drop and the 9 m drop. For the drop from 1 m height onto the bar, the angle was in all cases such as that the vertical line from the center of gravity pointed through the center of the valve and the center of the bar.

In the 1.2 m free drop, almost no deformations occur (see Figure 50)

All deformations are in a range of a few millimeters. There are no deformations of the inner steel plates, the rotation preventing device and the valve protecting device. Furthermore there are no cracks in the outer shell or in the inner shell of the DN30 PSP.

The 9.0 m drop causes larger deformations at the outside and inside of the DN30 PSP. There is buckling of the outer shell, but still without any cracks in the outer surface. There are also deformations visible at the inner steel parts, especially at the inner front plate, which is in contact with the skirt of the 30B cylinder. Cracks may occur due to the high stresses and strains in the respective parts. The rotation preventing devices are deformed, but their function is still preserved and any rotation of the 30B cylinder is prevented.

The drop onto the bar does not penetrate the steel shell of the DN30 PSP. There is an additional deformation of the outer steel shell but only small further deformations of the inner steel shell. The distance between valve and DN30 PSP is still preserved.

The resulting deformed structure is shown in Figure 52 and described in detail in Appendix 2.2.1.3 (Structural Analysis of the DN30 Package under NCT and ACT).

The deformations are summarized in Table 33 and the accelerations are shown in Figure 53. The measurement points for the values listed are defined in Figure 50.

As expected, a small increase of the maximal deceleration is observed due to the stiffer material response. However, such small differences are not expected to have any influence on the leak tightness of the 30B cylinder. Apart from the slightly higher decelerations, the curves are very similar.

Table 33: Deformation and remaining dimensions calculated for the flat drop onto the valve side

Dimension [mm]	Drop test at temperature					
	-40 °C			RT		
	1.2 m	9.0 m	1 m bar	1.2 m	9.0 m	1 m bar
Largest fold (L1x)	n.m.	2425	-	n.m.	2422	-
Largest fold (L1y)	n.m.	1144	-	n.m.	1149	-
Gap between top and bottom half (L2x)	n.m.	2425	-	n.m.	2421	-
Depth of bar penetration (p1)	-	-	-	-		-
Depth of bar penetration (p2)	-	-	30	-		32

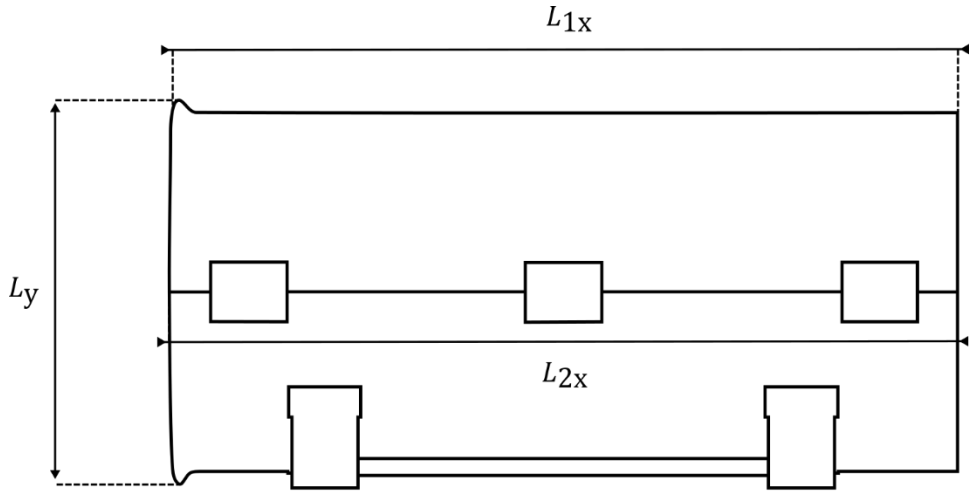

Figure 50: Measured distances in sequence 3

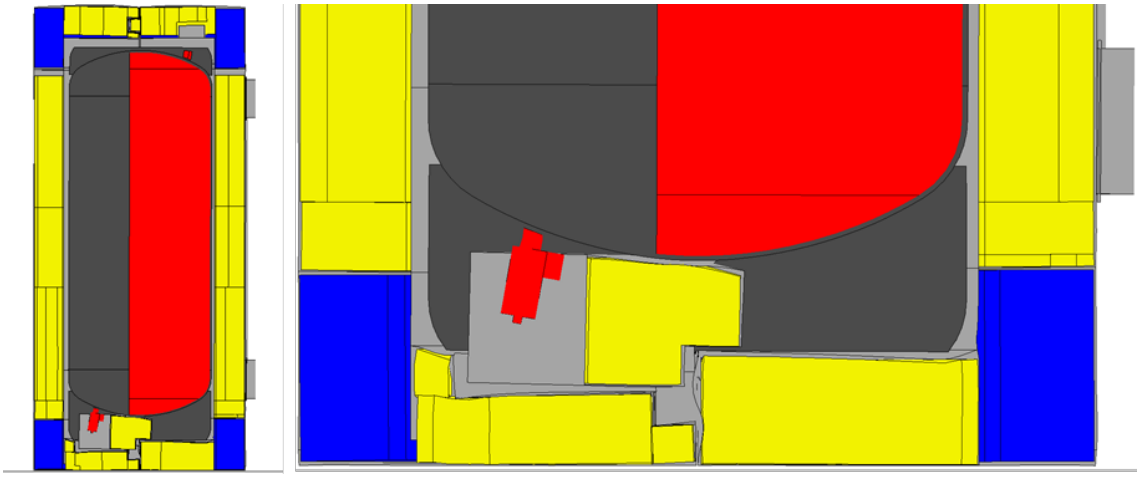

Figure 51: Deformed structure after the 1.2 m free flat drop onto the valve side

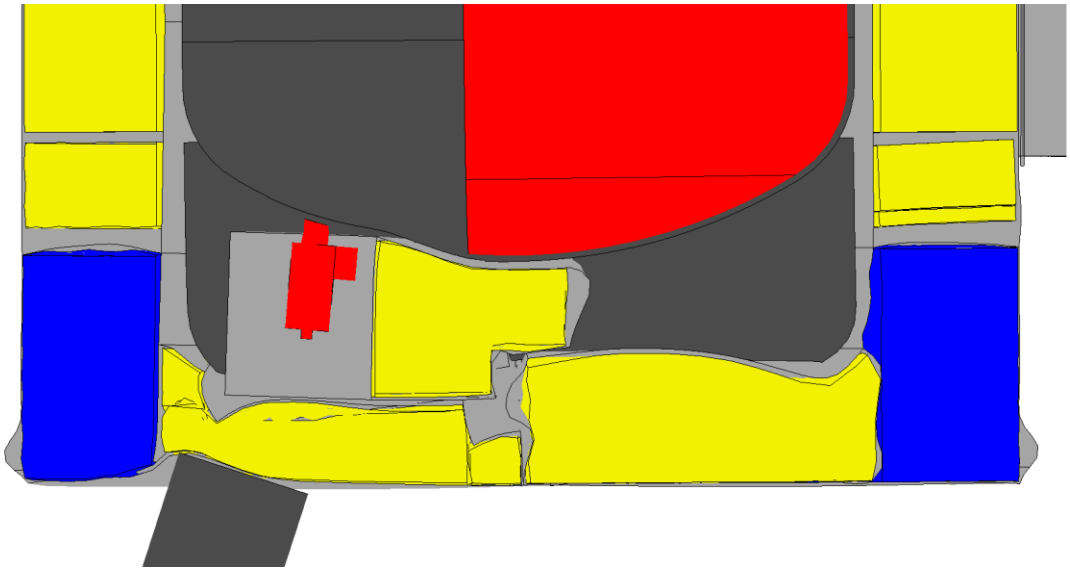

Figure 52: Deformed structure after the test sequence flat onto the valve side

2.2.1.5.1.5.3.2.2 Decelerations at -40°C and RT

Figure 53 shows the comparison of the calculated deceleration at -40°C and at RT. As expected, a small increase of the maximal deceleration is observed due to the stiffer material response at -40°C. Apart from the slightly higher decelerations, the curves are very similar.

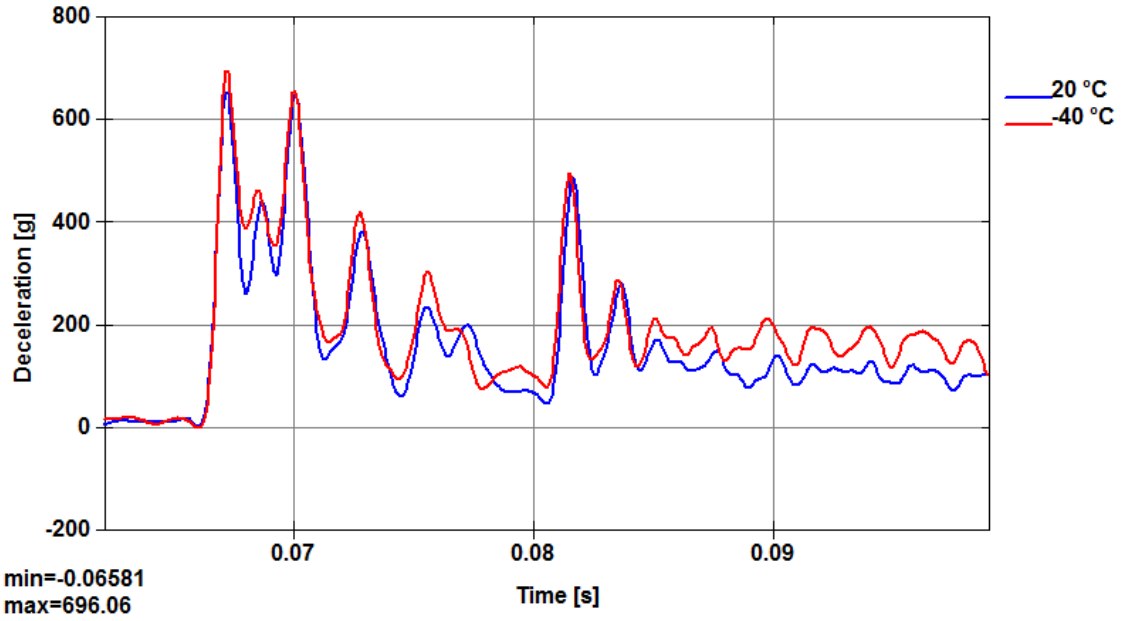

Figure 53: Comparison of deceleration in sequence 3 at -40°c and 20°C – low-pass filtered (Butterworth, 584 Hz cut-off)

2.2.1.5.1.5.3.3 Results of drop tests

The drop test sequence onto the corner of the valve side is documented as sequence no. 3 in Appendix 2.2.1.2 (Drop Test Reports).

- Drop No. 3.1 1.2 m flat drop test onto the valve side
- Drop No. 3.2 9 m flat drop test onto the valve side
- Drop No. 3.3 1 m drop onto a bar onto the valve side

2.2.1.5.1.5.3.3.1 Deformations at RT

The 1.2 m drop causes small deformations of the DN30 package. There is a slight buckling of the outer shell (see Figure 54). The 9.0 m drop causes larger deformation of the DN30 package. The buckling of the outer shell increases, but still without any cracks in the outer surface or outer welds (see Figure 55).

The drop onto the bar does not completely penetrate the steel shell of the DN30 package, but a crack of the outer shell is visible at the impact point (see Figure 56).

Figure 54: Sequence 3 - Deformation after the 1.2 m drop

Figure 55: Sequence 3 - Deformation after the 9.0 m drop

Figure 56: Sequence 3 - Deformation after the drop onto a bar from 1.0 m

There are also deformations and cracks visible at the inner steel parts, especially at the front plate, which is in contact with the skirt of the 30B cylinder. The rotation preventing devices are deformed and heavily damaged but any rotation of the 30B cylinder was prevented (see Figure 57).

Figure 57: Sequence 3 – Deformation of the bottom half, inner shell

2.2.1.5.1.5.3.3.2 Summary of the drop test results for sequence 3

- The leakage rate after the drop test sequence 3 is Q_{st} = 4.91 E-09 Pa m^3/s.
- All closure systems were intact;
- The DN30 PSP could only be opened by cutting the front plate of the DN30 PSP;
- The closure system was still working and the top half could be easily lifted off of the bottom half;
- There was no contact between the valve and any other part of the DN30 PSP or 30B cylinder other than its initial point of contact (the thread);
- There was no contact between the plug and any other part of the DN30 PSP or 30B cylinder other than its initial point of contact (the thread);
- The valve protecting device could still be operated (rotated); the hinges were intact;
- Removal of the 30B cylinder from the bottom half was possible without further damage to the DN30 PSP;
- Loading of a 30B cylinder into the DN30 PSP was still possible.

2.2.1.5.1.5.3.4 Evaluation of the FEM-analysis vs. real drop tests

2.2.1.5.1.5.3.4.1 Deformations at RT

The measured deformations and remaining dimensions are compared in Table 29 to the calculated values. The measurement points for the values listed are defined in Figure 50.

Table 34: Deformations and remaining dimensions measured for the flat drop onto the valve side (ambient temperature) and comparison with calculated values

Dimension [mm]	Drop								
	1.2 m			9.0 m			1 m bar		
	CV	MV	D %	CV	MV	D %	CV	MV	D %
Largest fold (L1x)	-	n.m.	-	2422	2410	1	-	-	-
Largest fold (L1y)	-	n.m.	-	1149	1178	2	-	-	-
Gap between top and bottom half (L2x)	-	n.m.	-	2421	2415	<1	-	-	-
Depth of bar penetration (p1)	-	-	-	-	-	-	-	32	-
Depth of bar penetration (p2)	-	-		-	-	-	32	45	29

CV = calculated values MV = measured values
D % = deviation of measured values from calculated values in %
n.m. = not measurable

The exact measurement error in the experiment is unknown, but expected to be in the range of 10% due to the applied measurement technique. The resulting errors between measurement and simulation does not exceed 2% in all cases. Hence, the simulation reproduces the behavior observed in the experiment well.

The depth of bar penetration p_2 is smaller in the simulation than in the real test, which is probably attributable to the crack that occurred around the valve protecting device. The value for p_1 cannot be measured in the simulation because the bar did not penetrate the outer shell enough. The resulting errors are relatively large because the crack significantly weakens the design in that location and therefore has a significant impact on the resulting penetration depth.

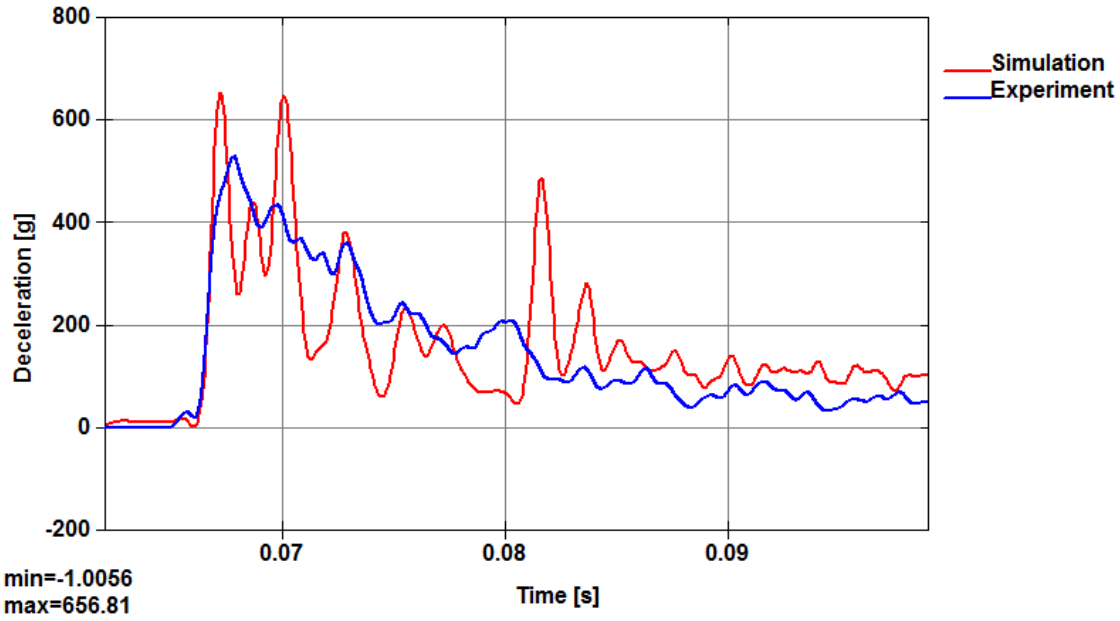

Figure 58: Comparison of simulation and experiment – deceleration in the plug area during 9.0 m drop in sequence 3 – low-pass filtered (Butterworth, 584 Hz cut-off)

2.2.1.5.1.5.3.4.2 Decelerations at RT

Figure 58 shows the comparison of the calculated decelerations with the measured decelerations.The highest peak in the simulation is connected to the impact of the 30B cylinder skirt onto the inner front plate of the DN30 PSP. Taking into account that the deceleration highly depends on the initial position of the 30B cylinder and its content, a very good representation of the behavior of the DN30 package is achieved.

The elastic relaxation of the DN30 PSP causes the 30B cylinder to rebound from the inner steel plate during the free drop test. Without gravity in the FEM model the 30B cylinder remains in that position during the repositioning of the drop target prior to drop I so that there is a large separation between the 30B cylinder skirt and the inner steel plate of the DN30 PSP. Naturally, the resulting decelerations are higher in the simulation than in the experiment, where such a large separation is not expected. Moreover, the formation of cracks at the inner front plate absorbs some energy, which results in lower decelerations as well.

The two peaks around 0.0816 s are attributed to the 30B cylinder skirt that hits the inner shell of the DN30 PSP in the plug area. A reason why these two peaks are not observed in the experiment could be the cracks in the front plate, which cause the rebound of the 30B cylinder to be significantly reduced. Hence, the peaks currently observed in the simulation would be much lower or would not occur at all. In addition, the missing cracks explain the generally higher decelerations in the decay phase compared to the experiment.

2.2.1.5.1.5.4 Flat drop onto the plug side

2.2.1.5.1.5.4.1 General considerations

With the drop onto the plug corner as described in section 2.2.1.5.1.5.2 maximal deformation is reached in the plug area. During the flat drop onto the plug side maximal decelerations and hence maximal forces at the plug are to be expected. The design has to ensure that after the tests simulating ACT:

- There is no contact between plug and any part of the DN30 PSP or any other part of the 30B cylinder except its initial point of contact (the thread).
- The leakage rate of the containment does not exceed the limit specified in section 2.2.3.

2.2.1.5.1.5.4.2 FEM analysis

The drop orientation is flat onto the plug side for the 1.2 m drop and the 9 m drop. For the drop from 1 m height onto the bar, the angle is in all cases such that the vertical line from the center of gravity points through the center of the plug and the center of the bar.

The responses during the drop onto the valve side and the drop onto the plug side are very similar, which is attributed to the construction of the DN30 PSP. The shell thickness on the valve and the plug side of the outer and the inner shell, respectively, is identical. In addition, a similar amount of foam of the same type fills the space between the outer and the inner shell. Naturally, the 30B cylinder experiences comparable decelerations during both drop test sequences. The experimentally measured decelerations during the flat drop onto the valve side did not lead to a failure of the containment system. Therefore, this is expected for the flat drop onto the plug side as well, especially because the mass of the plug is lower compared to the mass of the valve.

For these reasons, further analysis of the flat drop onto the plug side are not carried out with the developed FEM model of the DN30 PSP.

2.2.1.5.1.5.4.3 Drop tests

With respect to the minor differences in the analysis results of the drop test sequence flat onto the valve side (section 2.2.1.5.1.5.3) to the analysis results for the flat drop onto the plug side in this section and the lower mass of the plug compared to the mass of the valve a real drop tests sequence flat onto the plug side was not carried out.

2.2.1.5.1.5.5 Flat drop onto the closure system – drop test sequence 4

2.2.1.5.1.5.5.1 General considerations

During the drop test sequence flat onto the closure system high tensile and transversal loads are to be expected. During the 9 m drop test the closure systems on both sides of the DN30 PSP will experience tensile loads as forces caused by the deceleration of the 30B cylinder act onto the inside of the top and lower shell as inner pressure. During the 1 m drop test onto the bar with the center closure system there are high transversal loads on the closure system.

Furthermore, during the flat drop test sequence onto the closure system maximal forces are to be expected at the rotation preventing device, because in this orientation the moment caused by the eccentric loading of the 30B cylinder is maximal.

Hence, the design has to ensure that after the tests simulating ACT:

- There is no contact between valve and any part of the DN30 PSP or any other part of the 30B cylinder except its initial point of contact (the thread).
- The extent of the rotation of the 30B cylinder relative to the DN30 PSP does not affect the function of the valve protecting device or the plug protecting device.
- The leakage rate of the containment does not exceed the limit specified in section 2.2.3.

2.2.1.5.1.5.5.2 FEM analysis

2.2.1.5.1.5.5.2.1 FEM analysis before the drop tests

The drop orientation is flat onto the closure system for the 1.2 m drop and the 9 m drop. For the drop from 1 m height onto the bar the orientation of the DN30 package is also flat and the center of the lower part of the center closure system is in vertical line above the center of the bar.

For the 1.2 m drop and the 9 m drop two different orientations of the DN30 package are analyzed. In the first orientation, the line across the flange of the DN30 PSP is perpendicular to the target and in a second analysis the line across the flange of the DN30 PSP is inclined by 13.9° so that the impact is onto the top half of the DN30 PSP. This last scenario is selected for the real tests (see Figure 59).

2.2.1.5.1.5.5.2.2 Deformations at RT

After the 1.2 m drop, the three closing systems on the impact side are slightly deformed and pushed into the shell of the DN30 PSP. Inside the DN30 PSP, only little deformations at the rotation preventing devices are visible. Both rotation preventing devices still work properly and are located in the middle of the hole of the cylinder skirt. The damaged DN30 PSP is shown in Figure 59 for the flange line inclined to the target. There are no deformations of the inner steel shell and the valve protecting device. Furthermore there are no cracks in the outer shell or in the inner shell of the DN30 PSP.

After the 9.0 m drop the three closing systems are pushed into the foam parts of the DN30, so that they are nearly in line with the outer steel shell. During this drop, the support structures of the rotation preventing devices are deformed significantly, but both devices are still placed in the holes of the cylinder. There are only small deformations at the cylinder skirt at the hole where the lower rotation preventing device at the impact side is engaged. There are no cracks in the outer shell of the DN30 PSP. Some cracks may be possible at the inner shell as stresses and strains are considerably high at some local points.

The drop onto the bar pushes the center closure system into the shell of the DN30 PSP. Because of this behavior, the inner steel sheet of the DN30 is also bent towards the 30B cylinder shell, but without affecting it. The resulting deformed structure is shown in Figure 59 for the flange line inclined to the target.

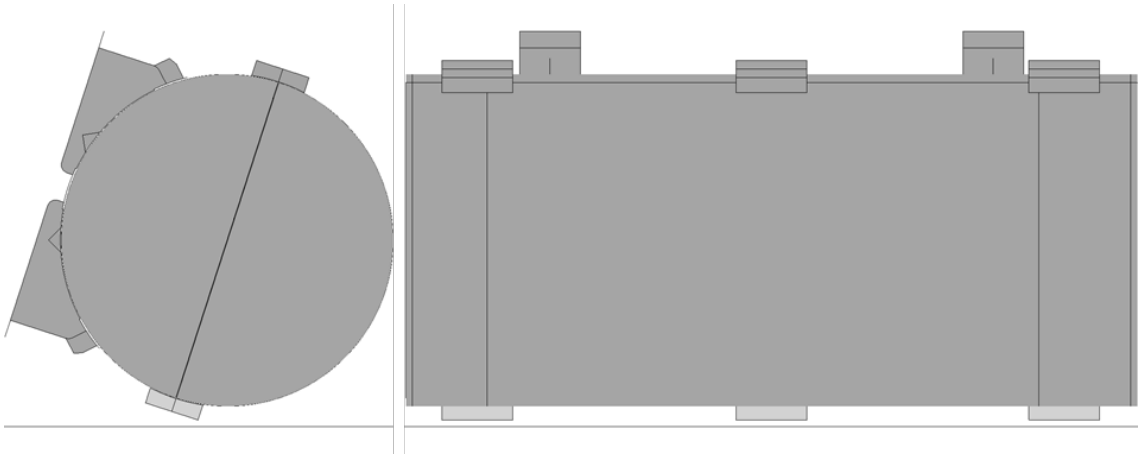

Figure 59: Undeformed initial state of the DN30 package for sequence 4

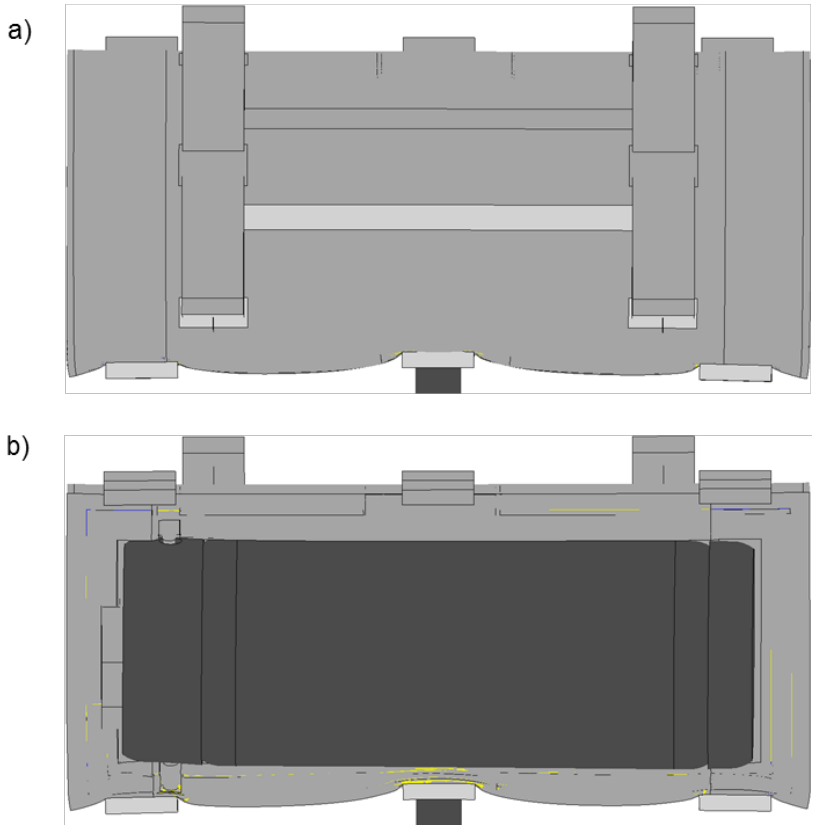

Figure 60: Deformed structure after the test sequence onto the closure system (flange line inclined to the target)

2.2.1.5.1.5.5.3 Drop tests

The drop test sequence onto the corner of the valve side is documented as sequence no. 4 in Appendix 2.2.1.2 (Drop Test Reports).

- Drop No. 4.1 1.2 m flat drop onto the closure system
- Drop No. 4.2 9 m flat drop onto the closure system
- Drop No. 4.3 1 m flat drop onto the closure system

2.2.1.5.1.5.5.3.1 Deformations at RT

The 1.2 m drop causes small deformations; the three closing systems are pushed inside the outer shell of the DN30 PSP so that the foam is noticeably compressed in those regions. The 9.0 m drop causes larger deformations. The penetration of the closing devices in the outer shell continues, but still without any cracks in the outer surface or outer welds.

Figure 61: Sequence 4 - Deformation after the 1.2 m drop

Figure 62: Sequence 4 - Deformation after the 9.0 m drop

The drop onto the bar does not damage the closing device. The bar impact did not push the closure device into the outer shell as a whole. Instead, the closure system buckled due to the rotational degree of freedom about the pin axis.

Figure 63: Sequence 4 - Deformation after the drop onto a bar from 1.0 m

No deformations of the inner shell of the DN30 PSP are visible. The rotation preventing devices are not deformed so that their function is still preserved and any rotation of the 30B cylinder is prevented.

2.2.1.5.1.5.5.3.2 Summary of the drop test results for sequence 4

- The leakage rate after the drop test sequence 4 is Q_{st} = 7.09 E-08 Pa m^3/s.
- All closure systems were intact;
- The DN30 PSP could be opened, by cutting a part of the DN30 PSP;
- The closure system was still working and the top half could be easily lifted off of the bottom half;
- There was no contact between the valve and any other part of the DN30 PSP or 30B cylinder other than its initial point of contact (the thread);
- There was no contact between the plug and any other part of the DN30 PSP or 30B cylinder other than its initial point of contact (the thread);
- The valve protecting device could still be operated (rotated); the hinges were intact;
- Removal of the 30B cylinder from the bottom half was possible without further damage to the DN30 PSP;
- Loading of a 30B cylinder into the DN30 PSP was still possible.

2.2.1.5.1.5.5.4 Evaluation of the FEM-analysis vs. real drop tests

2.2.1.5.1.5.5.4.1 Deformations at RT

The measured deformations and remaining dimensions as numbered in Figure 65 are compared in Table 29 to the calculated values.

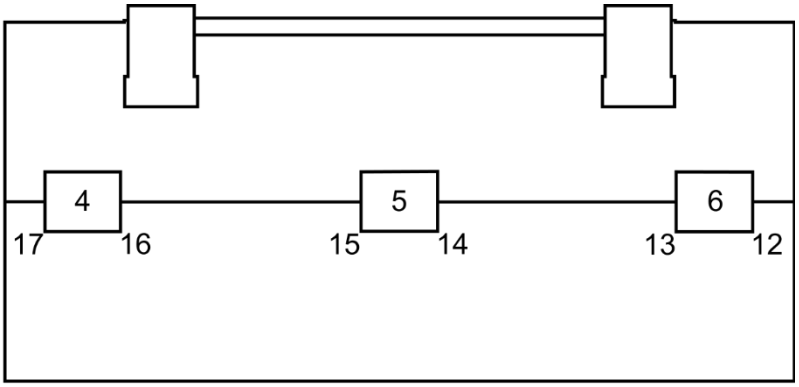

Figure 64: Numbering of the measured depths of impression at the welds of the closure devices for the free drop test and drop I in sequence 4

Table 35: Deformations (depths) measured for the flat drop onto the closure system (ambient temperature) and comparison with calculated values

Dimension [mm]	Drop								
	1.2 m			9.0 m			1 m bar		
	CV	MV	D %	CV	MV	D %	CV	MV	D %
Closing device 4 - 17	22	20	10	46	47	2	45	44	3
Closing device 4 - 16	21	19	10	47	45	4	45	44	3
Closing device 5 - 15	18	19	6	49	42	17	64	46	40
Closing device 5 - 14	18	19	8	49	46	6	64	44	45
Closing device 6 - 13	20	19	5	50	48	4	46	44	4
Closing device 6 - 12	20	18	10	50	46	9	44	42	5

CV = calculated values MV = measured values
D % = deviation of measured values from calculated values in %

The exact measurement error in the experiment is unknown, but expected to be in the range of at least 10% due to the applied measurement technique. Except for measurement point 15, the resulting errors are below the expected measurement error of 10%. Probably, the error of 17% is due to many uncertainties about the correct positioning of the ruler in the experiment. Since such a large error only occurs for one measurement point, it is not weighted much in connection with the validation process. Hence, the negligence of the rotational degree of freedom about the pin axis of the closure devices is an acceptable simplification not only for the 1.2 m drop test but for the 9.0 m drop as well. Overall, the deformation behavior for sequence 4 is accurately reproduced with the developed FEM model.

The depths of impressions at closure device 4 and 6 are similar to the ones after the 9.0 m drop because the impact zone of the bar is too localized to have any noticeable influence at these locations. Consequently, the resulting errors are small. In contrast to that, the depths of impressions at closure device 5 are much smaller in the experiment than in the simulation. The rotational degree of freedom about the pin axis of the closure devices has a significant influence on the results. If the impact zone is localized at one single closure device, the exact deformation behavior cannot be predicted with this FEM model.

2.2.1.5.1.5.5.4.2 Decelerations at RT

Figure 65 shows the deceleration calculated with the FEM model compared to the decelerations measured in drop test sequence 4. A large first deceleration peak of 553 g occurs in the experiment. In contrast to that, a smooth increase of the deceleration is observed in the simulation. Hence, the error of the maximal deceleration in the simulation is about -48% compared to the experiment. Nevertheless, the decelerations are on the same level after the initial peak in the experiment.

The source of the high initial peak in the experiment could be related to a different position of the 30B cylinder and its content relative to the DN30 PSP. As for the free drop test, there is an initial gap between the 30B cylinder and the inner shell of the DN30 PSP.

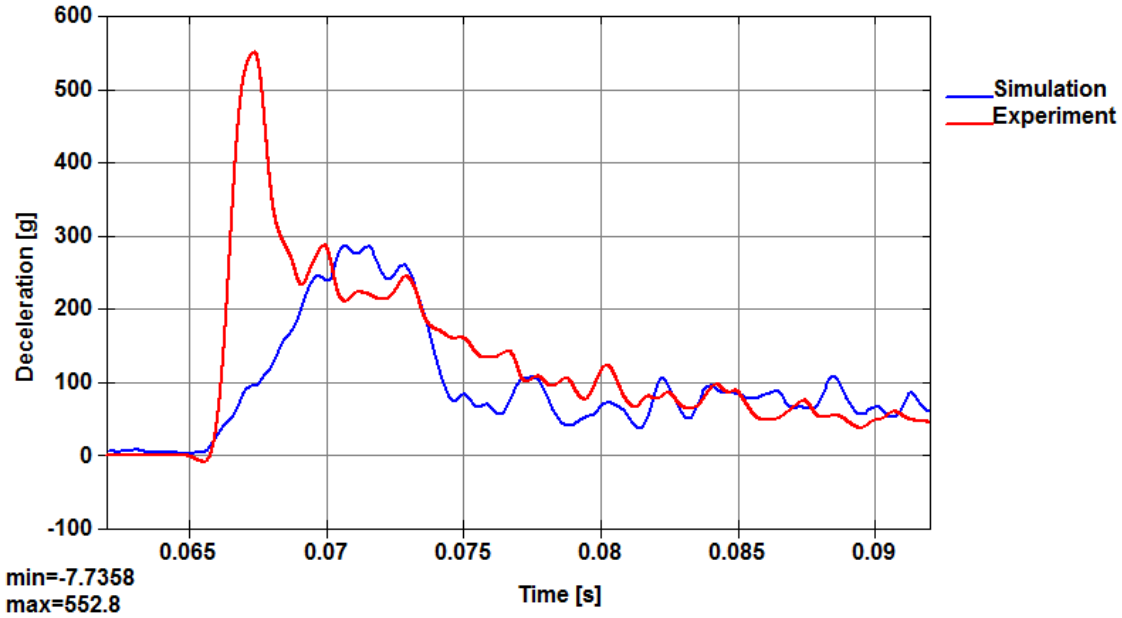

Figure 65: Comparison of simulation and experiment – deceleration in the valve area during drop I in sequence 4 – low-pass filtered (Butterworth, 584 Hz cut-off)

2.2.1.5.1.5.6 Flat drop onto the top

2.2.1.5.1.5.6.1 General considerations

For the drop test sequence flat onto the top of the DN30 PSP, higher radial deformations are expected than for the flat drop onto the closure system. These deformations are relevant for the increase of the maximal dose rate after the tests simulating NCT, as the maximal dose rate is to be expected at the center of the side of the package (see section 2.2.4). These deformations are also relevant for the minimum shell thickness of the specimen before the thermal test. Due to the larger deformations the accelerations acting on the valve and plug are expected to be lower than for the flat drop onto the closure system.

Hence, the design has to ensure that after the tests simulating ACT:

- The extent of the reduction of the thickness of the DN30 PSP after NCT is such that the increase of the dose rate does not exceed the limit specified in section 2.2.4.
- The extent of the reduction of the thickness of the DN30 PSP after ACT is such that the thermal protection properties of the shell DN30 PSP are still sufficient to limit the temperature increase in the thermal tests to the limits specified in section 2.2.2.

2.2.1.5.1.5.6.2 FEM analysis

2.2.1.5.1.5.6.2.1 Deformations at RT

The drop orientation is flat onto the top of the DN30 PSP for the 1.2 m drop and the 9 m drop. For the drop from 1 m height onto the bar, the orientation of the DN30 package is also flat and the impact of the bar is in the center of the top.

After the 1.2 m drop, the top line is slightly deformed (see Figure 67). There are no visible deformations inside the DN30 PSP. Both rotation preventing devices, the valve protecting device and the plug protecting device are not affected by the drop test. There are neither cracks in the outer shell nor in the inner shell of the DN30 PSP.

After the 9.0 m drop, the deformation of the top line is increased and the front faces are bent to the outside (see Figure 67). Both rotation preventing devices, the valve protecting device and the plug protecting device are only slightly affected by the drop test. There are no cracks in the outer or inner shell of the DN30 PSP.

During the drop from 1 m onto the bar, only the impact zone of the bar is further deformed. Even though the kinetic energy is applied locally, the resulting plastic deformations are small. This is due to the soft response of the DN30 PSP in that region so that most of the kinetic energy results only in elastic deformations. Therefore, cracks in the outer shell caused by this kind of bar impact are not to be expected.

Finally, the depth of the bar penetration is measured at the two deepest points with the already deformed outer shell as the baseline for the measurement. For both measurement locations, a depth of bar penetration of 35 mm is obtained due to the drop orientation.

The deformations are summarized in Table 36. The measurement points for the values listed are defined in Figure 66.

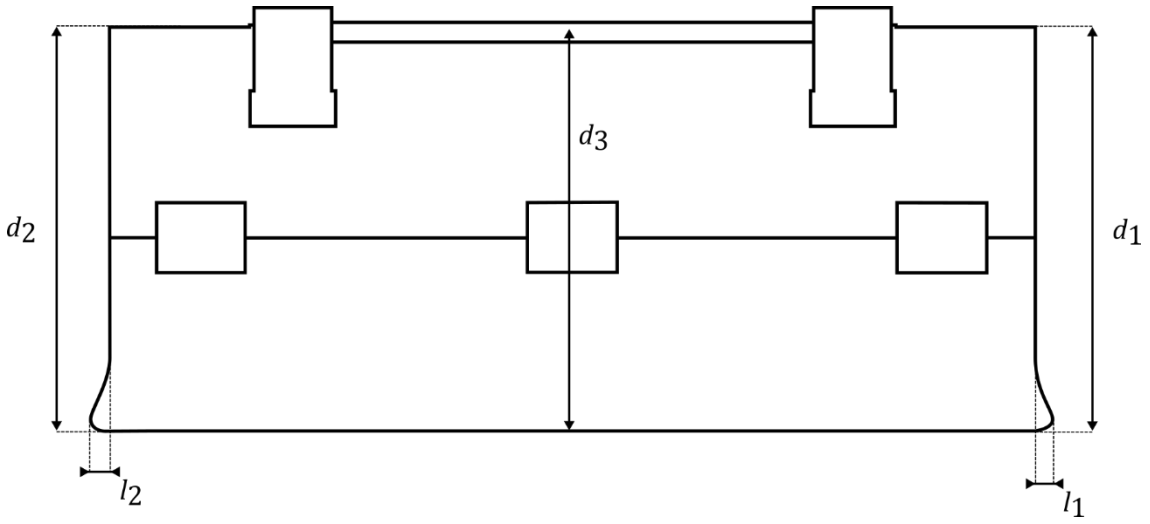

Figure 66: Measured distances for the free drop test and drop I of sequence 8

Table 36: Deformations and remaining dimensions calculated for the flat drop onto the top

Dimension [mm]	1.2 m drop	9.0 m drop	Drop onto the bar
Deformations at the valve corner – l1	15	36	-
Deformations at the valve corner – Ød1	-8	-35	-
Deformations at the plug corner– l2	22	44	-
Deformations at the plug corner – Ød2	-11	-37	-
Deformations at the center (average and maximum) - Ød3	-6	-24	-
Depth	-	-	-35

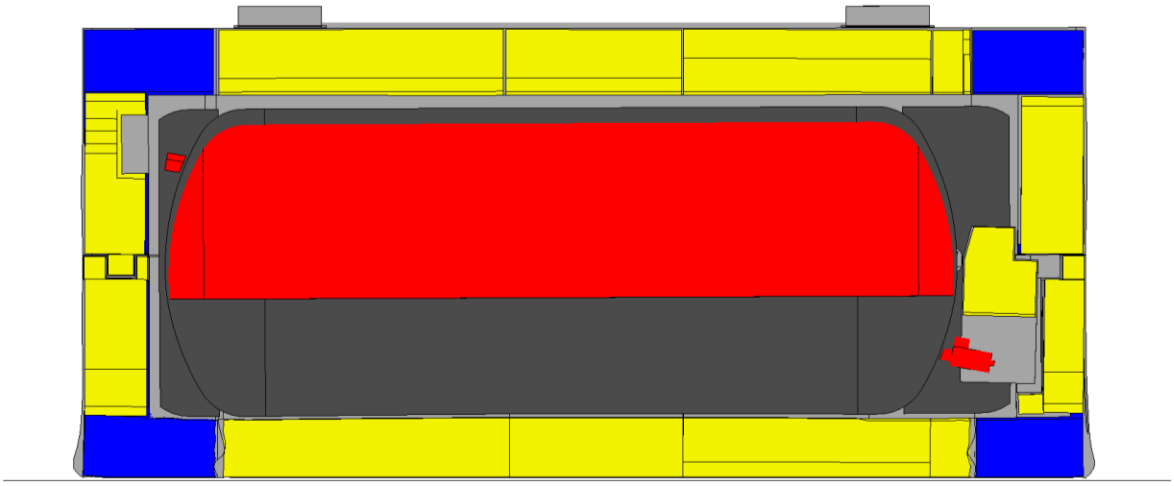

Figure 67: Deformed structure after the 1.2 m free drop flat onto the top

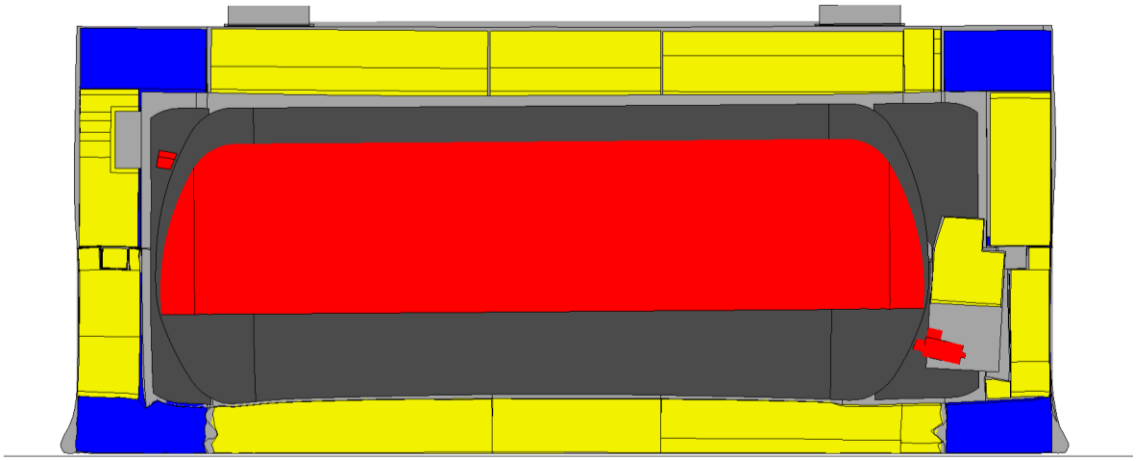

Figure 68: Deformed structure after the test sequence onto the top

2.2.1.5.1.5.6.2.2 Decelerations at RT

Figure 69 shows the deceleration in the valve area of the 30B cylinder in absolute values. The first large peak corresponds to the impact of the 30B cylinder on the inner shell of the top half of the DN30 PSP. After the initial impact, it is accelerated in opposite direction to the drop direction. The second large peak is the impact of the 30B cylinder on the inner shell of the bottom half of the DN30 PSP.

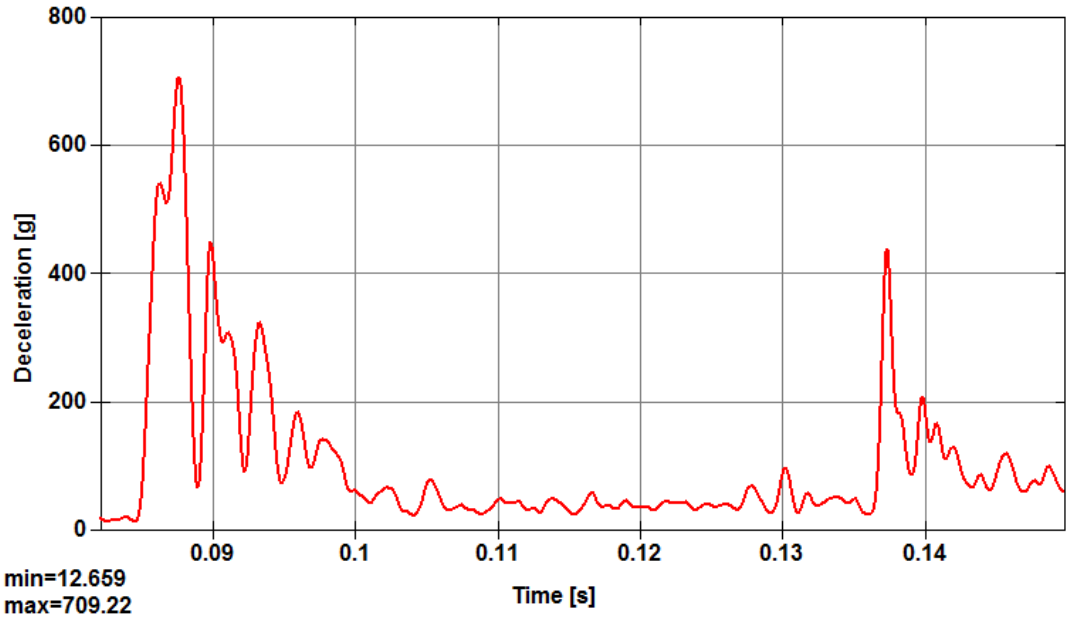

Figure 69: Absolute values of the deceleration in the valve area during the 9.0 m drop test in sequence 8 – low-pass filtered (Butterworth, 584 Hz cut-off)

2.2.1.5.1.5.6.3 Drop tests

The drop tests flat onto the top of the DN30 package are covered by the drop tests onto the closure line:

- The drop tests onto the closure line are similar to the drop test flat onto the top line.
- The FEM analysis of the drop tests onto the closure line provided a good benchmark for the analysis of the flat drop onto the top line.
- The closure line is much more vulnerable to loads from ACT due to the closure system connecting the top and bottom half.
- The deformation of the shell of the DN30 package during NCT is much smaller than permissible for meeting the requirement concerning dose rate increase (see section 2.2.4.8.6); hence a verification of the results of the FEM analysis can be omitted.

Hence, a real drop test flat onto the topline was not performed.

2.2.1.5.1.5.7 Slap-down drop onto the feet – drop test sequence 5

2.2.1.5.1.5.7.1 General considerations

During the slap-down drop test onto the feet of the DN30 PSP there are two impacts:

- The primary impact onto the plug side of the DN30 PSP is expected to cause less deformation at the plug corner as the drop test onto the corner plug as only a part of the drop test energy is absorbed during this impact
- The secondary impact onto the valve side of the DN30 PSP is expected to cause considerably higher deformation at the point of secondary impact as the impact velocity at the point of the secondary impact is higher than the impact velocity of the DN30 PSP in a flat drop.

For the 1 m drop test onto the bar the impact point at the top of the DN30 PSP is selected as there are no reinforcements like the feet and the fork lifter features at the lower side of the DN30 PSP.

The design has to ensure that after the tests simulating ACT:

- There is no contact between the valve and any part of the DN30 PSP or any other part of the 30B cylinder except its initial point of contact (the thread).
- The leakage rate of the containment does not exceed the limit specified in section 2.2.3.

2.2.1.5.1.5.7.2 FEM analysis

2.2.1.5.1.5.7.2.1 FEM analysis before the drop tests

For the slap-down drop onto the feet, different angles from 5° to 30° between the longitudinal axis of the DN30 package and the horizontal line through the center of gravity are analyzed for the 1.2 m drop and the 9 m drop. The impact point for the drop from 1 m height onto the bar is always at the top of the DN30 package (i. e. with respect to the slap-down drop the DN30 package is rotated by 180° around its longitudinal axis). An angle of 25° between the centerline of the bar and the normal of the outer DN30 PSP shell is chosen because this angle is the most critical one with respect to a penetration of the outer shell.

The maximal velocity of the valve for the secondary impact was reached for an angle of 15°. This angle is selected for the analysis of accelerations and deformations, and it was also selected as basis for the real tests.

2.2.1.5.1.5.7.2.2 Deformations at RT

In the 1.2 m free slap-down drop, the corner of the primary impact (plug side) of the DN30 PSP is slightly deformed as shown in Figure 70. There are small deformations at the connection of the feet with the DN30 PSP shell. The corner at the valve side is undamaged. There is no deformation of the inner steel shell, the valve protection device, the rotation preventing device and the plug protecting device. Furthermore, there are no cracks in the inner and outer shell of the DN30 PSP.

The 9.0 m drop causes larger deformation of the corner of the primary impact (plug side) of the DN30 PSP as shown in Figure 71. The corner of the secondary impact (valve side) is damaged as well. The feet show considerable deformations and are pushed into the shell of the DN30 PSP. There is only a slight deformation of the inner steel shell. There is no deformation of the valve protection device, the rotation preventing device and the plug

protecting device. Furthermore, there are no cracks in the inner and outer shell of the DN30 PSP.

The drop onto the bar does not penetrate the steel shell of the DN30 PSP. However, cracks might be possible due to the high stresses and strains in the material. There is a deformation of the outer steel shell, but no deformation of the inner steel shell. The resulting deformed structure with the smallest distance between outer and the inner shell and minimal remaining foam volume at the impact zone of the bar is shown in Figure 71.

The deformations and accelerations are summarized in the tables hereafter.

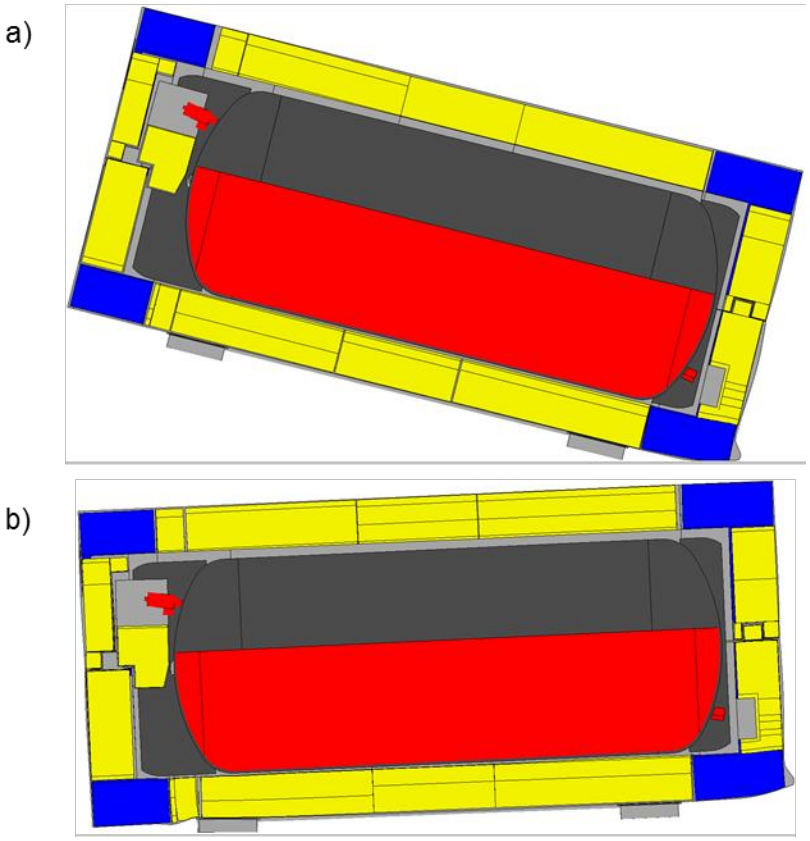

Figure 70: States with maximal deformation of the DN30 package during the free drop test in sequence 5: a) First impact on the plug side b) Secondary impact on the valve side

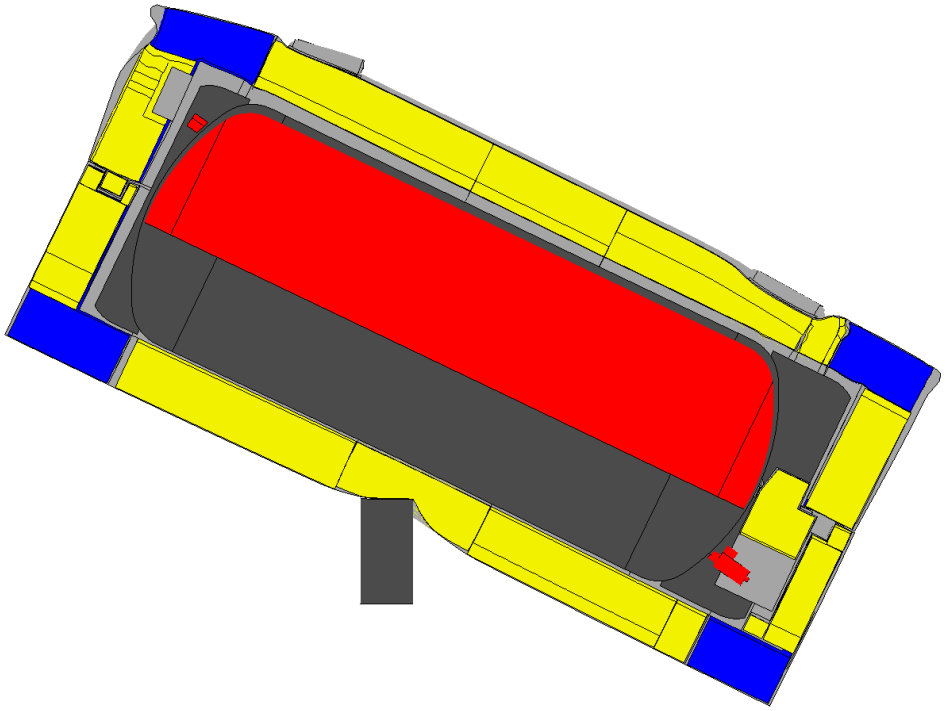

Figure 71: State with the maximal deformation of the DN30 package in sequence 5

2.2.1.5.1.5.7.3 Drop tests

The drop test sequence onto the corner of the valve side is documented as sequence no. 5 in Appendix 2.2.1.2 (Drop Test Reports).

- Drop No. 5.1 1.2 m Slap-down drop onto the feet
- Drop No. 5.2 9 m Slap-down drop onto the feet
- Drop No. 5.3 1 m Slap-down drop onto the top

2.2.1.5.1.5.7.3.1 Deformations at RT

The 1.2 m drop causes small deformations on the feet; the feet are pushed into the outer shell of the DN30 PSP. The 9.0 m drop causes overall larger deformations. The penetration of the feet into the outer shell continues, but still without any cracks in the outer surface or outer welds.

The drop onto the bar does penetrate of the outer steel shell of the DN30 package.

Figure 72: Sequence 5 - Deformation after the 1.2 m drop

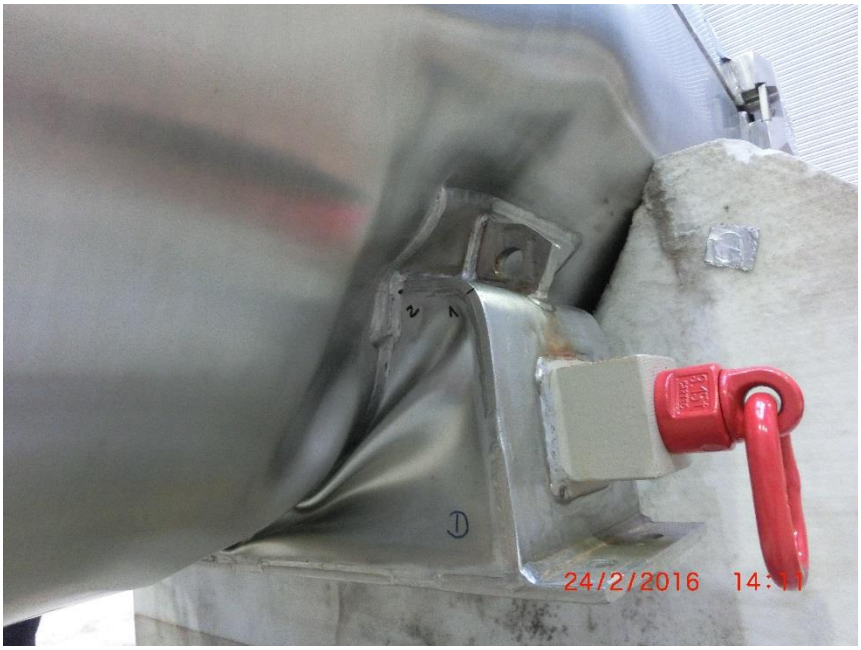

Figure 73: Sequence 5 - Deformation after the 9.0 m drop

Figure 74: Sequence 5 - Deformation after the drop onto a bar from 1.0 m

No deformations of the inner shell of the DN30 PSP are visible. The rotation preventing devices are not deformed, so that their function is still preserved and any rotation of the 30B cylinder is prevented.

2.2.1.5.1.5.7.3.2 Summary of the drop test results for sequence 5

- The leakage rate after the drop test sequence 5 is Q_{st} = 1.37 E-08 Pa m^3/s.
- All closure systems were intact;
- The DN30 PSP could be opened without any further damage;
- The closure system was still working and the top half could be easily lifted off of the bottom half;
- There was no contact between the valve and any other part of the DN30 PSP or 30B cylinder other than its initial point of contact (the thread);
- There was no contact between the plug and any other part of the DN30 PSP or 30B cylinder other than its initial point of contact (the thread);
- The valve protecting device could still be operated (rotated); the hinges were intact;
- Removal of the 30B cylinder from the bottom half was possible without further damage to the DN30 PSP;
- Loading of a 30B cylinder into the DN30 PSP was still possible.

2.2.1.5.1.5.7.4 Evaluation of the FEM-analysis vs. real drop tests

2.2.1.5.1.5.7.4.1 Deformations at RT

The measured deformations and remaining dimensions are compared in Table 29 to the calculated values. The measurement points for the values listed are defined in Figure 75.

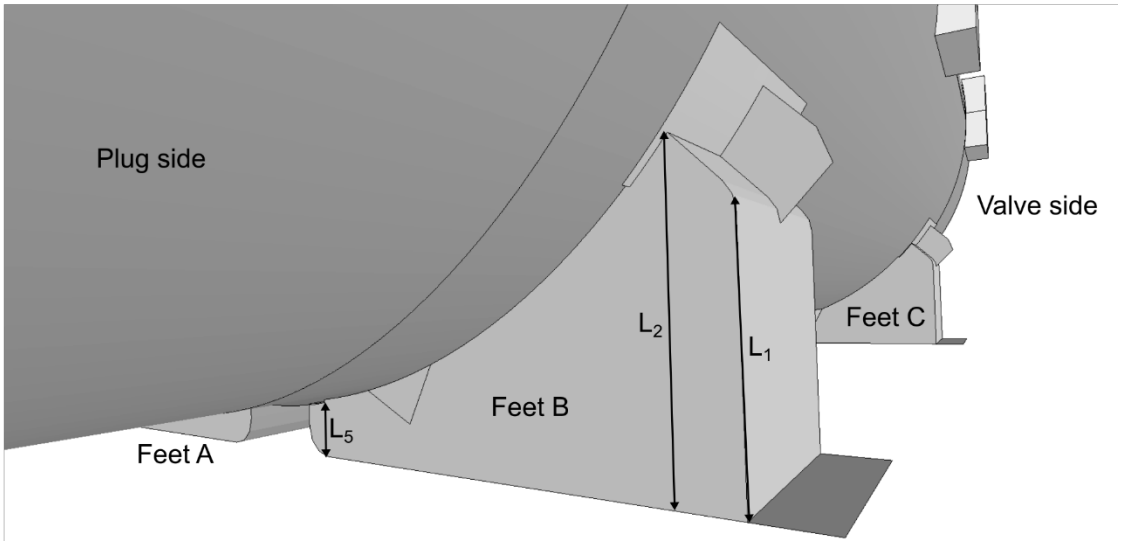

Figure 75: Measurement points in sequence 5

Table 37: Deformations (depths) measured for the slap-down (ambient temperature) and comparison with calculated values

Dimension [mm]	Drop								
	1.2 m			9.0 m			1 m bar		
	CV	MV	D %	CV	MV	D %	CV	MV	D %
A L1/L2/L5	196 /239 /40	195 /240 /42	1/1/5	189 /214 /24	188 /212 /32	1/1/25	-	-	-
B L1/L2/L5	196 /239 /40	195 /241 /41	1/1/2	186 /214 /24	189 /216 /35	2/1/32	-	-	-
C L1/L2/L5	195 /235 /40	195 /236 /40	<1	189 /207 /34	193 /209 /41	2/1/18	-	-	-
D L1/L2/L5	195 /235/ 40	195 /232 /41	<1/1/2	189 /207 /33	194 /206 /41	2/1/18	-	-	-
P1	-	-	-	-	-	-	-	130	-

CV = calculated values MV = measured values
D % = deviation of measured values from calculated values in %

The exact measurement error in the experiment is unknown, but expected to be in the range of at least 10% due to the applied measurement technique. The errors as well as the absolute differences between the measured distances are very low. In the case of the slap-down, the measured deformations mostly depend on the chosen material parameters and flow curves of the applied material model for the austenitic stainless steel 1.4301. For this reason, the slap-down provides a good basis for the validation of this specific part of the FEM model, especially concerning the chosen scale factor of the flow curve. A good agreement shows that the material parameters for the steel are chosen correctly and that the FEM model is capable of reliably reproducing the observed deformation behavior of the slap-down.

The measured depths of bar penetration in the simulation and experiment cannot be compared because of the massive crack in the outer shell at the impact zone.

2.2.1.5.1.5.7.4.2 Decelerations at RT

Figure 76 shows the comparison of the calculated decelerations in the valve area with the decelerations measured during the 9 m drop test. The impact at the corner on the plug side onto the drop target causes the first increase of the deceleration. However, this impact is recorded by the accelerometer near the valve at a later point in the simulation because of an existing separation between the 30B cylinder and the inner shell of the DN30 PSP. In addition, the resulting decelerations are significantly higher than in the experiment. As a result, the deceleration in the simulation is constantly on a higher level than in the experiment, especially due to the impact at the corner of the valve side. Apart from the much higher accelerations, the duration of each impact is perfectly predicted by the FEM model.

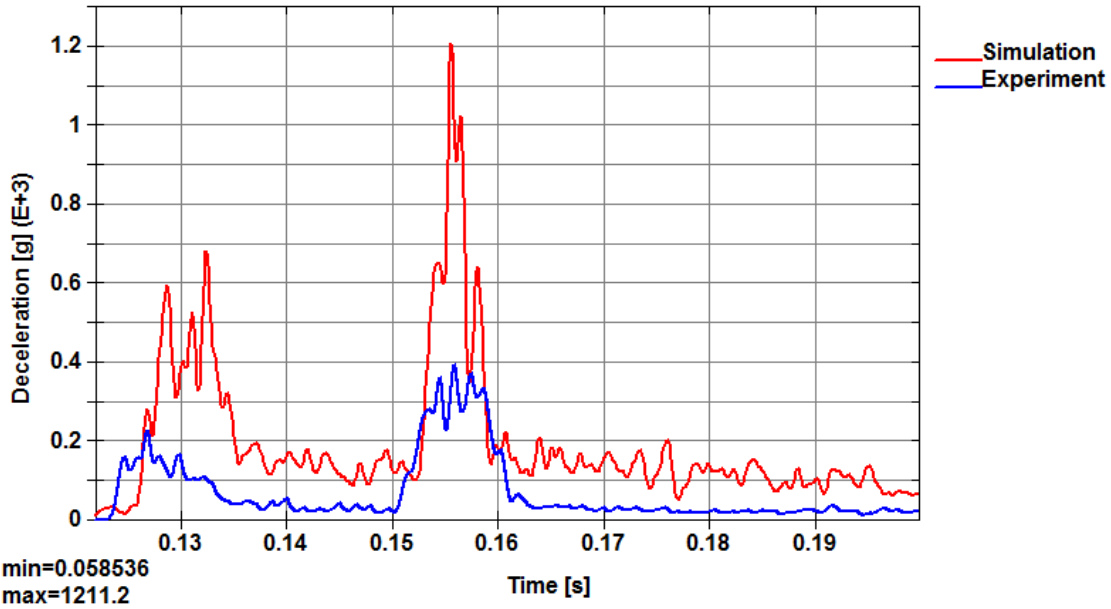

Figure 76: Comparison of simulation and experiment – deceleration in the valve area during drop I in sequence 5 – low-pass filtered (Butterworth, 584 Hz cut-off)

2.2.1.5.1.5.8 Detailed calculation of the closuring system

A detailed model of the closure system is investigated in a static FEM simulation because only a very rough representation of this part of the DN30 PSP is represented in the LS-DYNA model for the dynamic FEM simulations of the drops tests.

The only relevant load is a tensile force normal to the section plane between the two main bodies of each closure device. Such a load is observed during the secondary impact on the feet at the valve side of the DN30 PSP in sequence 5.

2.2.1.5.1.5.8.1 FEM model

Figure 77 a) shows one of the six closure devices in comparison to the corresponding FEM model is shown in Figure 77.

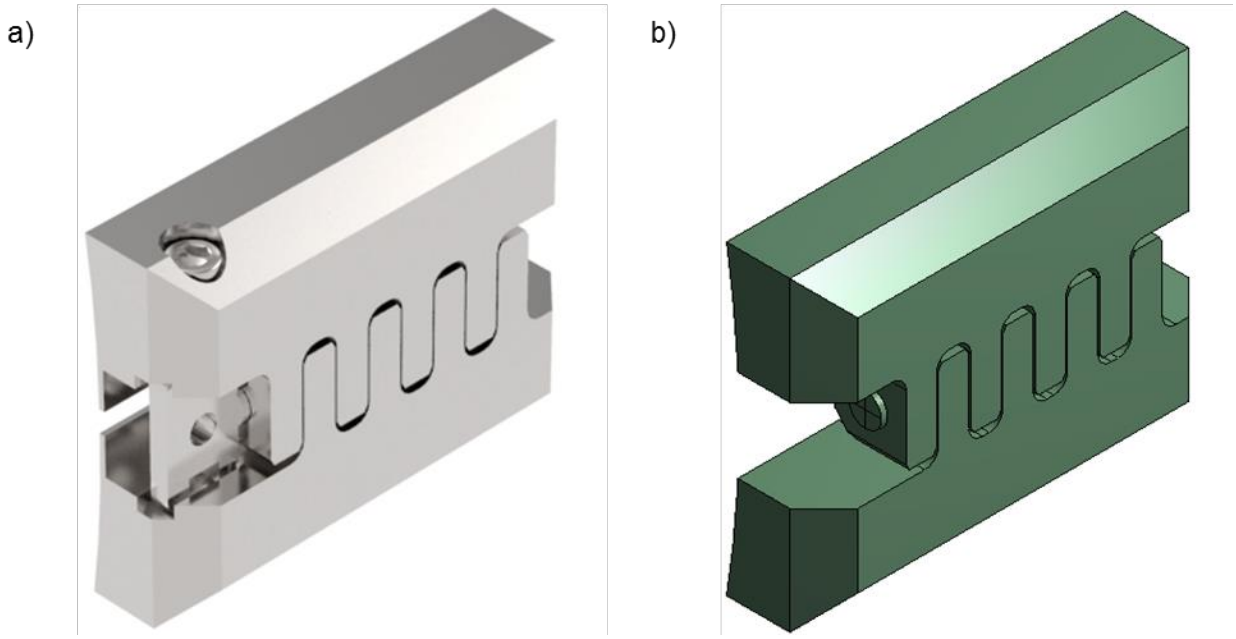

Figure 77: Closure device – comparison between CAD a) and FEM model b)

The design is such that the securing bolt and the pin handle do not experience any significant loads. They keep the pin in place so that a representation as boundary conditions for the pin is an acceptable simplification.

In addition, the boreholes for the securing bolt as well as the notches for the pin handle in the lower and upper part of the closure device are removed. Since these areas are far away from the load transmission zones of the mortise joint, hardly any deformations are expected. This is confirmed by the drop tests of Sequence 5.

2.2.1.5.1.5.8.2 Mesh

The generated mesh for each part is shown in Figure 78. Except for the pin, a mesh of tetrahedral elements is chosen for the lower and the upper part of the closure device. For the pin, a mesh of hexahedral elements is generated.

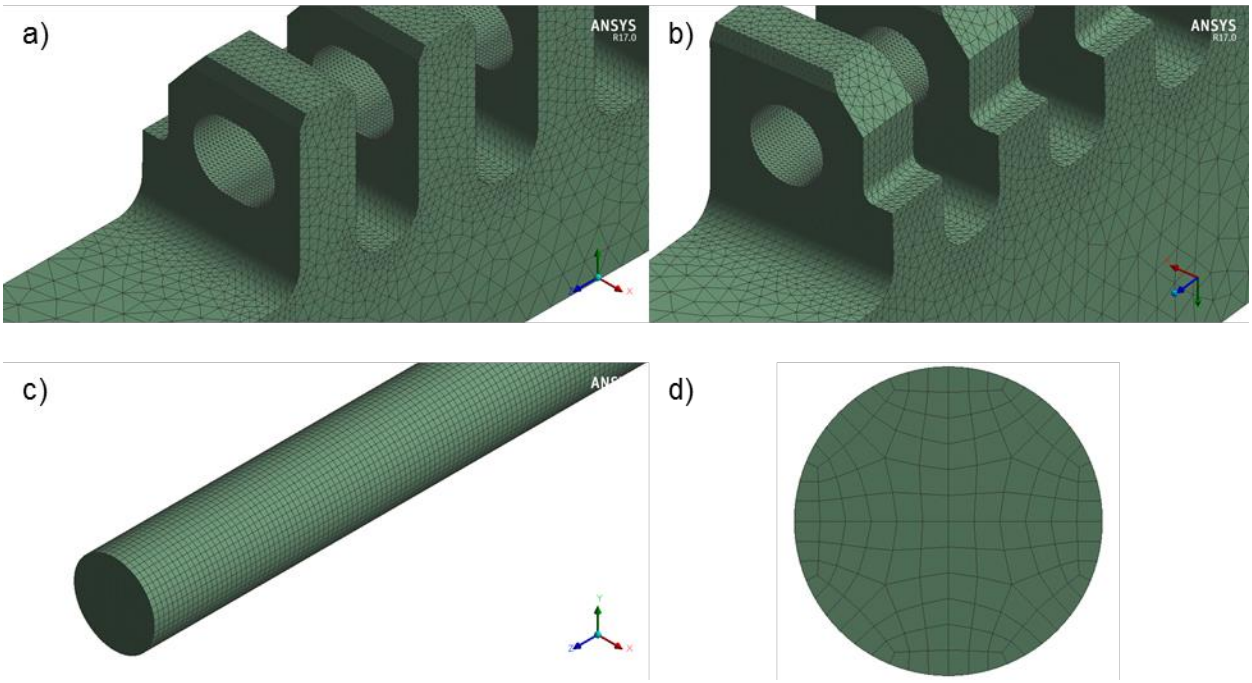

Figure 78: Generated mesh for each part of the closure device: a) Lower part b) Upper part c) Pin d) Pin front view

2.2.1.5.1.5.8.3 Calculation schema

The static simulation is split into two load steps: the first is displacement-controlled, while the second is force-controlled. During the first load step, the structure is preloaded until the gaps between the pin and the mortise and tenon devices are closed to make sure that the defined frictional contacts are closed before the external force is applied in the second load step. The boundary conditions that are applied in the first and second load step are shown in Figure 79 a) and b), respectively.

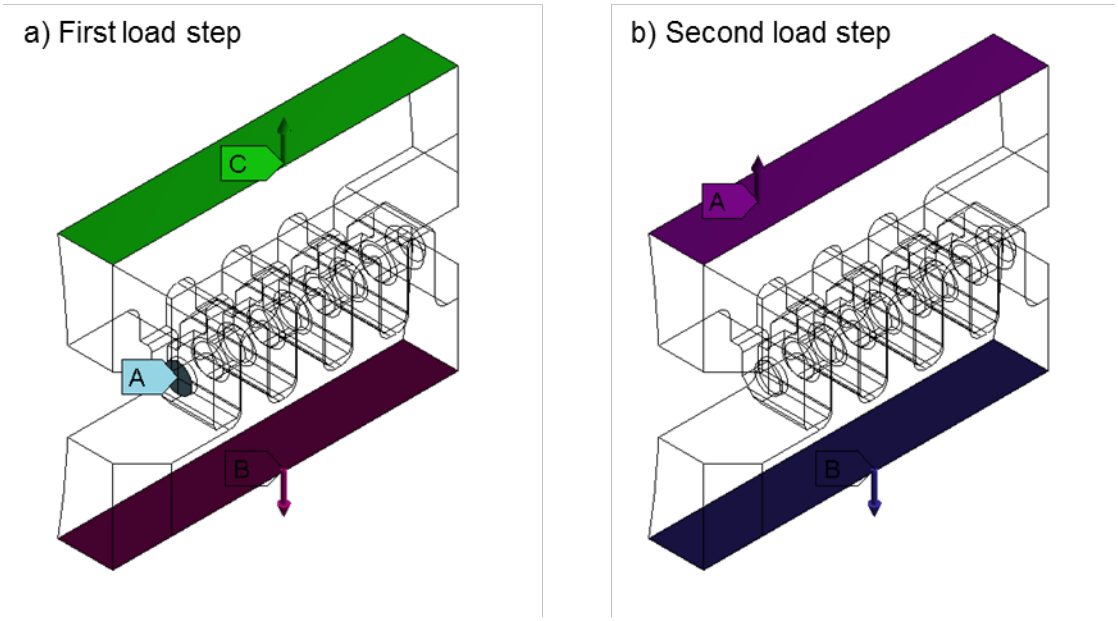

Figure 79: Boundary conditions for the static FEM simulation of the closure device

2.2.1.5.1.5.8.4 Loads

The value for the applied external force is obtained by calculating the maximal normal tensile force acting on the section plane during the 9 m slap-down drop in sequence 5. As explained in Figure 80, a positive value at the corresponding point in time indicates a tensile load. Hence, a maximum of 135 kN occurs during the 9 m slap-down drop. Considering the uncertainties in the dynamic calculations, the force is increased by approximately 10%.

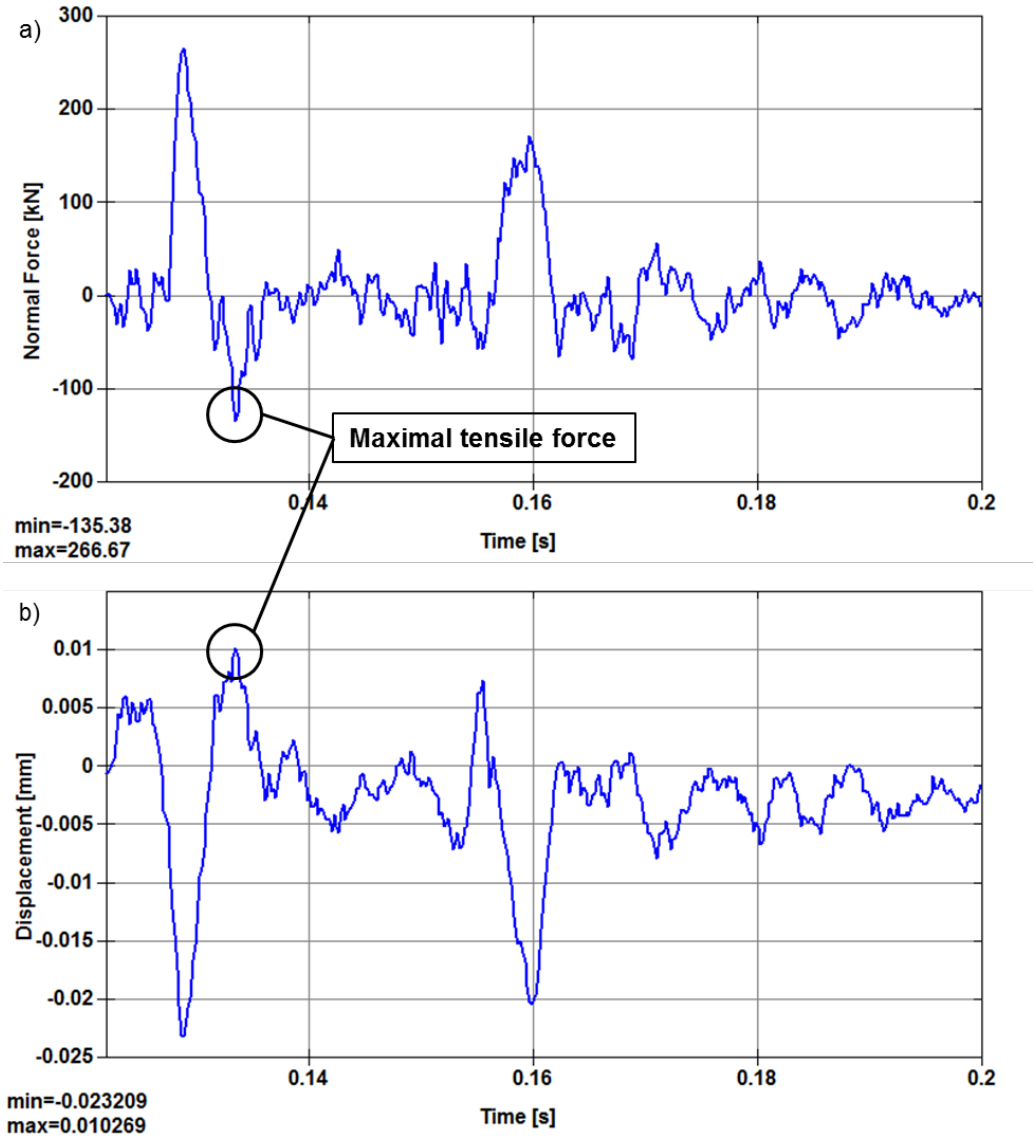

Figure 80: Evaluation of the maximal tensile force at the section plane during the 9 m slap-down drop in Sequence 5

Apart from the boundary condition, two frictional contact interfaces are defined between the pin and each of the mortise and tenon devices. Both contact interfaces are shown in Figure 81.

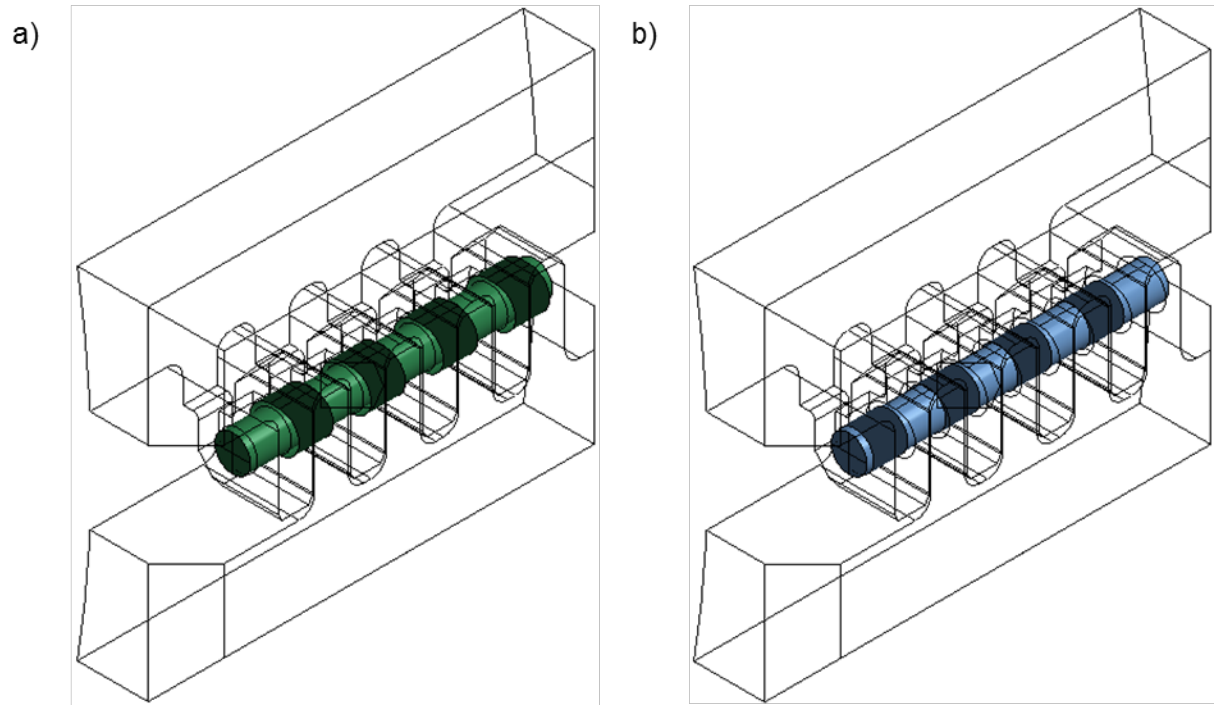

Figure 81: Contact interfaces: a) Between the pin and the lower part b) Between the pin and the upper part

2.2.1.5.1.5.8.5 Materials

Table 38 shows the data for the two different steels used for the closure device.

Table 38: Material specification of the closure device

Item	Material
Lower part of the closure system	1.4541
Upper part of the closure system	1.4541
Pins of the closure system	1.4542 [+P930][4]

2.2.1.5.1.5.8.6 Convergence of calculation results

Table 39 compares the corresponding stresses and strains in the most deformed areas of the lower and upper part of the closure device outside the contact zones as well as the plastic strains in the contact zones for a finer and coarser mesh. The comparison shows that convergence for the finer mesh is reached as the differences in the results for the coarser and finer mesh are negligible.

[4] 1.4542 [+P930] according to DIN EN 10088-3 or ASTM A564 [H1150].

Table 39: Convergence study

Mesh	Part	Variable	Min.	Max.
Coarse	Lower Part	Von Mises stress	1.6974 MPa	292.71 MPa
Fine			1.6936 MPa	292.53 MPa
Coarse	Upper Part	Von Mises stress	1.6065 MPa	248.83 MPa
Fine			1.6182 MPa	249.09 MPa
Coarse	Lower Part	Equivalent plastic strain	0.%	5.1269%
Fine			0.%	5.5318%
Coarse	Upper Part	Equivalent plastic strain	0.%	1.3571%
Fine			0.%	1.5448%

The values in Table 39 prove that the local high stresses in the contact zones have no influence on the areas outside the contact zones.

2.2.1.5.1.5.8.7 Results

The deformed pin is shown in Figure 82 a) and b) at the end of the second load step with the displacements being scaled by a factor of 14. The bending of the pin is attributed to the asymmetrical design of the closure devices, so that the force is not uniformly distributed along the pin. In addition, the pin is exposed to shearing. Nevertheless, only elastic deformations are observed, as shown in Figure 82 a), because of the high strength steel that is used as material for the pin. Consequently, no failure of the pin is expected due to the load occurring in the slap down in sequence 5.

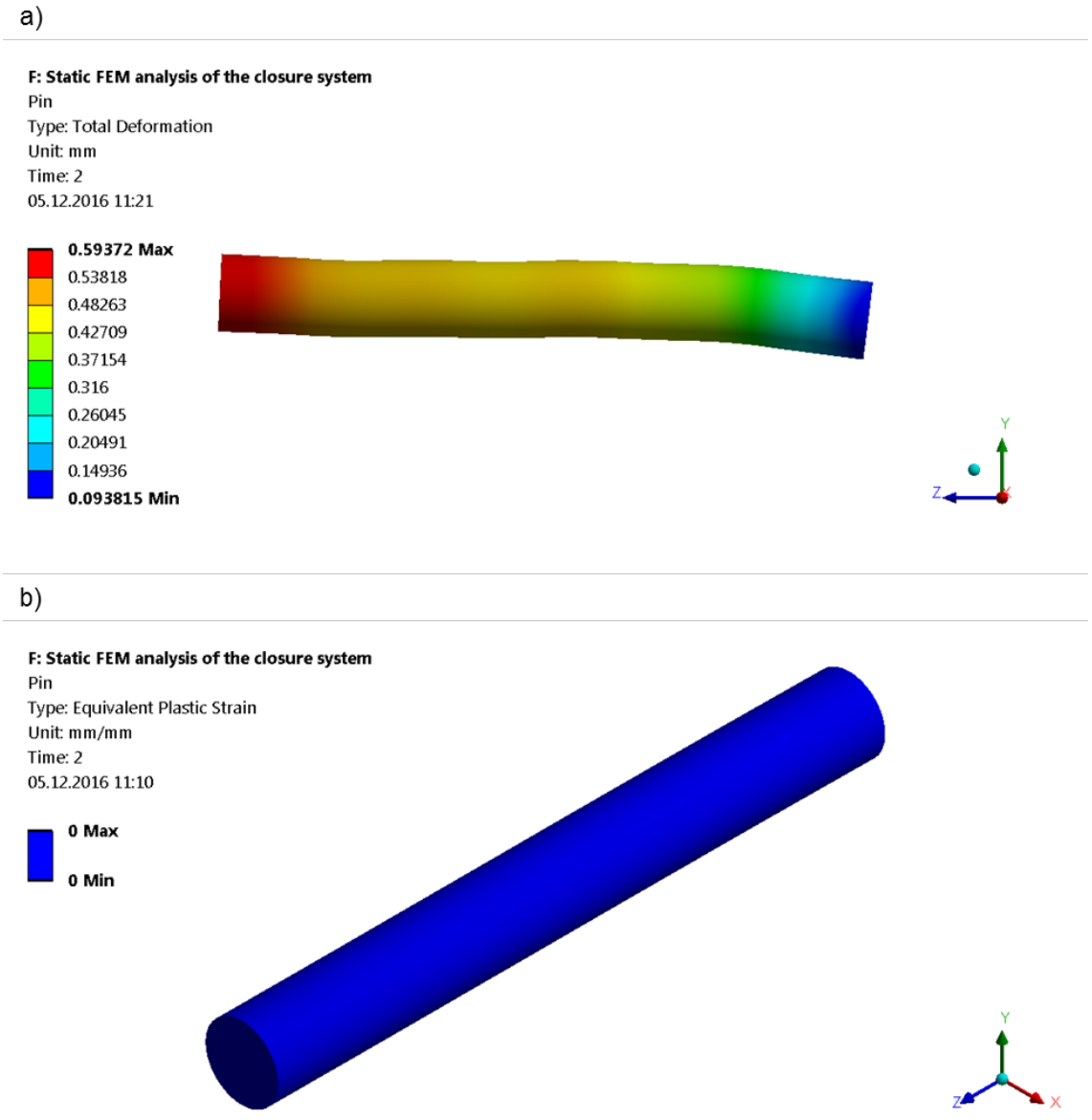

Figure 82: Deformation of the Pin: a) Total deformation (Scale factor 14) b) Equivalent plastic strain

Up to 6% equivalent plastic strains are observed at the lower part and 2% in the upper part of the closure device (see Figure 83). However, the austenitic stainless steel 1.4541 is highly ductile having a minimal elongation at fracture of 35% according to the standards, so that the occurring plastic strains will not lead to any cracks. Moreover, the maximal values occur in the contact zones of the pin. In these areas, the corresponding stresses are of the compressive type. Even with a crack, there is no crack propagation expected. The critical plastic deformations, which are connected to a tensile load, are located on top of each of the teeth.

a)

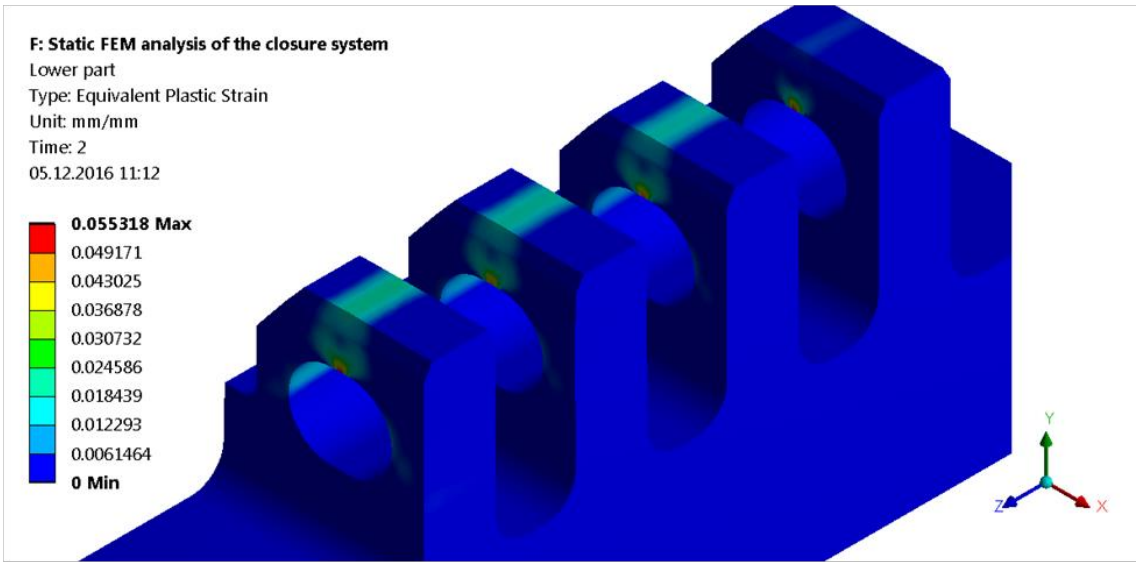

b)

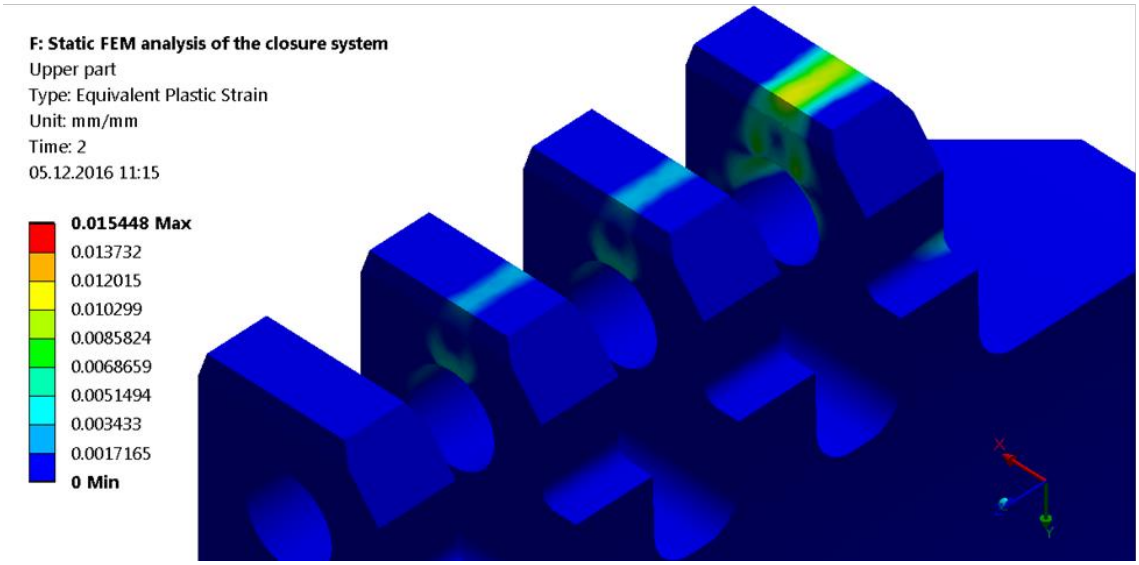

Figure 83: Equivalent plastic strain: a) Lower part b) Upper part

Overall, the closure device is able to withstand the occurring loads during the 9m slap-down drop in sequence 5 and thus all ACT scenarios.

2.2.1.5.1.6 Conclusion

The FEM model is validated based on the 5 drop test sequences with prototypes of the DN30 package. The results of these benchmark analyses are:

- Deformations of the prototype of the DN30 package measured after the real drop test are predicted with sufficient accuracy by the calculation model. The deviations of the calculated deformations from the measured deformations is in general in the range of the measurement error.
- Local effects like rupture of welding seams or puncture of the outer shell of the DN30 PSP can be predicted with sufficient accuracy by evaluating the strains in the respective parts of the DN30 PSP.
- Decelerations of the 30B cylinder are predicted with the calculation model in most cases with sufficient accuracy.
- In some cases the non-deterministic behavior of the 30B cylinder with respect to the DN30 PSP due to an undefined position of the 30B cylinder at the time of impact leads to deceleration peaks which cannot be predicted by the calculation model.
- For the drop test sequences 1 and 3 used for the assessment of the deformations and decelerations at -40°C and at +60°C simulation and experiment are in sufficient agreement to allow the evaluation of the behavior of the DN30 package in the temperature range of -40°C to +60°C.

The analysis of the drop test sequences

- Inclined onto the valve side corner
- Inclined onto the plug side corner
- Flat onto the valve side
- Flat onto the plug side
- Flat onto the closure system with / without rotation of the DN30 prototype around its axis
- Flat onto the top side
- Inclined onto the feet (slap-down)

showed, that

- The leakage rate after each of the drop test sequences is less than 1.0 E-06 Pa m^3/s.
- All closure systems are intact after each drop test sequence.
- There is no contact between the valve and any other part of the DN30 PSP or 30B cylinder other than its initial point of contact (the thread) in any drop test sequence.
- There is no contact between the plug and any other part of the DN30 PSP or 30B cylinder other than its initial point of contact (the thread) in any drop test sequence.
- The valve protecting device fulfills its function after each drop test sequence.
- The rotation preventing device fulfills its function after each drop test sequence.

- The plug protecting device fulfills its function after each drop tests sequence.
- The intumescent material as well as the housing are still present and undamaged after each of the drop tests sequences.

For the analysis of sequence 1 at -40°C and +60°C and sequence 3 at -40°C following applies:

- The deformations at +60°C increase slightly compared to RT.
- The deformations at -40°C are similar to the deformations at RT.
- The decelerations at -40° increase slightly compared to RT.
- There is no contact between the valve and any other part of the DN30 PSP or 30B cylinder other than its initial point of contact (the thread) neither at -40°C nor at +60°C.
- There is no contact between the plug and any other part of the DN30 PSP or 30B cylinder other than its initial point of contact (the thread) neither at -40°C nor at +60°C.
- The valve protecting device fulfills its function after each drop test sequence at the whole temperature range.
- The rotation preventing device fulfills its function after each drop test sequence at the whole temperature range.
- The plug protecting device fulfills its function after each drop tests sequence at the whole temperature range.

It can be concluded that the DN30 PSP provides the required mechanical protection of the 30B cylinder for the temperature range of -40°C to +60°C under RCT; NCT and ACT.

2.2.1.5.2 Water immersion test for packages containing fissile materials

The containment (30B cylinder) is designed according to [ISO 7195] and [ANSI N14.1] for an external pressure of 172 kPa. The water immersion test for packages containing fissile material defined in [ADR 2015] No. 6.4.19 or [IAEA 2015], para. 731 requires the immersion of the specimen under a head of water of at least 0.9 m for a period of not less than 8h. This is equal to a pressure of 9 kPa. Hence, the design pressure is considerably higher than the test pressure. The DN30 package is designed to withstand the water immersion test.

2.2.1.5.3 Influence of the thermal test on the structural safety of the DN30 package under ACT

The containment (30B cylinder) is designed according to [ISO 7195] and [ANSI N14.1] for an internal pressure of 1.38 MPa at a temperature of 121°C. The test pressure is 2.76 MPa at RT.

In section 2.2.2 the maximum temperature of the shell of the 30B cylinder of 1.7 MPa at a temperature of 170°C is calculated. Conservatively, the assessment is based on a steel temperature of 200°C (instead of 175°C).

The mechanical properties of the steel used for the shell of the 30B cylinder (see Table 9, NL certified steels) at elevated temperatures are not specified in the respective standards. For the NH certified steels P275NH and P355NH the yield stress decreases between RT and 200°C by a factor of 0.77. The allowable internal pressure of the 30B cylinder at a temperature of 200°C can hence be estimated:

$p_{200°C}$ = 2.76 MPa x 0.77 = 2.1 MPa > 1.7 MPa

The pressure to be expected during the thermal test is lower than the allowable pressure derived from the test pressure. Damage of the 30B cylinder and hence an influence of the thermal test on the containment system of the DN30 package can be excluded.

2.2.2 THERMAL ANALYSIS

In this chapter, steady state temperatures at the package DN30 which occur under RCT and NCT and transient temperatures which are expected with solar insolation are presented. Furthermore, transient temperatures for the package DN30 expected under ACT (thermal test) are calculated and analyzed.

For the calculated temperatures it is proven that they are lower than the admissible temperatures of the used materials and that the objective of proof as laid out in section 2.2.2.1 is met.

The analyses are valid for all filling ratios from heels cylinders up to cylinders filled with the maximum amount of UF_6 defined in section 1.3.

The thermal analysis is described in detail in Appendix 2.2.2.3 (Thermal Analysis).

2.2.2.1 Objective of verification

2.2.2.1.1 Verification for all types of packages

It is verified that the design of the package takes into account ambient temperatures and pressures that are likely to be encountered in RCT ([ADR 2015], No 6.4.2.10 or [IAEA 2012] para. 616).

2.2.2.1.2 Verification for packages containing uranium hexafluoride

It is verified that the package can withstand, without rupture of the containment system, the thermal test specified in [ADR 2015], No 6.4.17.3 or [IAEA 2012] para. 728.

2.2.2.1.3 Verification for type B(U) packages

It is verified that under ambient conditions specified in [ADR 2015], No 6.4.8.5 or [IAEA 2012] para. 656 (ambient temperature 38°C) and in absence of solar insolation, the temperature of the accessible surfaces of the package is below 50°C ([ADR 2015], No 6.4.8.3 or [IAEA 2012] para. 654).

With this proof it is also verified that the requirements of [ADR 2015], No 6.4.8.4 or [IAEA 2012] para. 655 are met.

Furthermore, the consequences of the thermal test specified in [ADR 2015], No 6.4.17.3 or [IAEA 2012] para. 728 on the package subjected to the mechanical tests specified in [ADR 2015] 6.4.17.1, 6.4.17.2 a), 6.4.17.2 b) und 6.4.17.4 or [IAEA 2012] paras 726, 727 (a), 727 (b) and 729 are analyzed to verify the requirements of [ADR 2015] No. 6.4.8.8 or [IAEA 2012] para. 659:

- Retain sufficient shielding to ensure that the radiation level 1 m from the surface of the package would not exceed 10 mSv/h – verified in section 2.2.4.
- It would restrict the accumulated loss of radioactive material to not more than A_2 per week - verified in section 2.2.3.

2.2.2.1.4 Verification for packages containing fissile material

The consequences of the thermal test specified in [ADR 2015], No 6.4.17.3 or [IAEA 2012] para. 728 on the package subjected to the mechanical tests specified in [ADR 2015] 6.4.17.1, 6.4.17.2 a), 6.4.17.2 b) und 6.4.17.4 or [IAEA 2012] paras 726, 727 (a), 727 (b) and 729 are

analyzed to verify the requirements of [ADR 2015] No. 6.4.11.10 and 6.4.11.13 or [IAEA 2012] para. 682 and 685. The verification is contained in section 2.2.5.

2.2.2.1.5 Admissible component temperatures of the DN30 package

Admissible component temperatures at the package DN30 are specified for RCT, NCT and ACT in Table 40.

Table 40: Admissible component temperatures of the package DN30

Component	Material	Admissible temperature °C		Remark / Reference
		RCT and NCT	ACT	
Outer shell of the DN30 PSP	1.4301	70 / 100[1)]	900[6)]	70 °C for handling and RCT, 100 °C for the lifting lugs at the top half
Inner shell of the DN30 PSP	1.4301	60[1)]	900[6)]	
Foam insulation	PIR-foam	60[2)]	-	
30B cylinder shell	Pressure vessel steel	64[3)]	400[4)]	[DIN EN 10028-3]
Valve and plug thread	Tin	64[3)]	234[5)]	

[1)] calculation temperature

[2)] identical to temperature of shells

[3)] triple point temperature of UF_6

[4)] max. temperature defined in [DIN EN 10028-3] for the similar steel grades P275NH and P355NH

[5)] maximal temperature of the valve during the test with the DN30 prototype

[6)] the hot forming of material 1.4301 is carried out at temperatures of 950 – 1200 °C. At 900 °C a sufficient strength remains, thus a deformation by own weight is not expected. The strength of the outer shell is not relevant for the containment system, shielding nor criticality safety.

2.2.2.2 Results of the thermal tests of specimens and prototypes

In order to support the FEM analyses physical tests with specimens and a prototype of the DN30 package was carried out:

- Thermal tests with specimens of the technical foam used as shock absorbing material and thermal insulation documented in Appendix 1.4.2 (Material Data PIR Foam)
- Thermal tests with specimens of the intumescent material used as thermal insulation documented in Appendix 1.4.3 (Material Data Intumescent Material)
- A thermal test with a prototype of the DN30 package loaded with an empty 30B cylinder. The DN30 prototype was damaged at the valve side and the plug side by two consecutive IAEA drop test sequences (the tests were carried out with a 30B cylinder loaded with 2277 kg surrogate material). The thermal test is documented in Appendix 2.2.2.1 (Thermal Test Program) and Appendix 2.2.2.2 (Thermal Test Report).

2.2.2.2.1 Preparation of the thermal test

2.2.2.2.1.1 Selection and preparation of the prototype for the thermal test

The thermal test prototype was selected according to the following criteria:

- The prototype with the largest deformation (minimal remaining foam thickness) on the valve side.
- The prototype with the largest deformation (minimal remaining foam thickness) on the plug side.

The thermal test is carried out with a prototype which has been tested according to sequence 1 followed by testing according to sequence 2 as described in section 2.2.1.5.1.5.1 as drop test sequence 7 (see Figure 84 and Figure 85). This is a rather conservative approach, as this prototype had therefore to withstand double the drop tests specified in [ADR 2015] or [IAEA 2012] before submitted to the thermal test.

Figure 84: Thermal test prototype after drop test sequence 7

Figure 85: Bottom half of the DN30 PSP before the thermal test

2.2.2.2.1.2 Differences between prototype and series design of the DN30 package

The differences between the prototype and the series design of the DN30 package were:

- The 30B cylinder was empty and did not contain any surrogate material.
- The fixation of the housing in the valve protecting device was provisional and did not comply with the series design (drawer design); however size and position of the housing in the prototype complied with the series design.

- The rails protecting the intumescent material from damage in regular service were not present in the prototype.
- The additional bar and the gasket at the hinge of the valve protecting device preventing water ingress into the cavity of the DN30 PSP was not present.
- Due to deformations of the inner shell of the DN30 prototype (small folds) the top half could not be installed on the bottom half in such a way that the original pins of the closure system could be inserted. Instead bolts with a smaller diameter than the original bolts had to be used.
- As a result of the non-fit of the original pins of the closure system the gap between the top half and bottom half was larger than the measured gap after the double drop test sequence 7 thus leading to a conservative simulation of heat transfer through the flange into the cavity.

2.2.2.2.1.3 Temperature sensors

The DN30 prototype as well as the 30B cylinder were equipped with temperature sensors. These temperature sensors were located:

- On the 30B cylinder body,
- On the valve of the 30B cylinder,
- On the plug of the 30B cylinder,
- On the outer surface of the DN30 PSP,
- At 15 cm from the outer surface of the DN30 PSP,
- At 1 m from the outer surface of the DN30 PSP.

The detailed sensors plan is supplied in Appendix 2.2.2.1 (Thermal Test Program) and in Appendix 2.2.2.2 (Thermal Test Report).

2.2.2.2.1.4 Deviations of the test conditions from the test conditions required by [ADR 2015] or [IAEA 2012]

The performance of a fully complying thermal test as required by [ADR 2015] or [IAEA 2012] was not feasible for the following reasons:

1. The thermal test cannot be performed with a kerosene fire but with a propane gas fire (environmental issues).
2. Several solar insolation cycles to reach a constant temperature pattern with the insolation defined in the Regulations cannot be reached under natural conditions.
3. The ambient temperature of 38°C cannot be reached under natural conditions.

To compensate for the fact that a thermal test cannot be performed as specified in the Regulations, some measures are required:

1. The compliance of a propane gas fire has to be demonstrated.

   The compliance of a propane gas fire with the Regulations was shown in a paper presented at PATRAM 1992 [PATRAM92]. Here it was shown that the thermal flux of both fires is identical and the thermal load is for the propane gas fire the same as for a

kerosene fire.

However, an important difference between a kerosene fire and a propane gas fire is the soot produced by the kerosene fire. This soot increases the surface absorptivity of the specimen considerably. [ADR 2015] or [IAEA 2012] require a coefficient not less than 0.8. Hence the outer surface of the DN30 prototype was painted with a black coating satisfying this requirement (see Figure 86).

Figure 86: DN30 prototype coated for the thermal test

2. Pre-heating of the DN30 prototype before the thermal test to reach NCT conditions.

   The preliminary thermal simulations for NCT show that the temperature inside the DN30 package reaches an average temperature of 60°C. Therefore the DN30 prototype was pre-heated with a heating jacket (see Figure 87). The temperature at the 30B cylinder as well as the temperatures at the valve and plug were approximately 64°C at the beginning of the thermal test.

Figure 87: DN30 prototype in heating jacket

3. Prolongation of the fire phase

   The ambient temperature in the cooling phase is lower than 38°C. Furthermore there could be some wind during the cooling phase increasing the heat transfer from the DN30 prototype to the environment and hence speeding up cooling down. To compensate for these influences on the thermal test, the duration of the fire phase was increased by 7.5% from 30 min. to 32 min.

The comparison of the results shown in Table 46 for the DN30 prototype under test conditions and the calculated values shown in Table 48 for the DN30 package under [ADR 2015] or [IAEA 2012] test conditions proves the adequacy of the compensatory measures.

2.2.2.2.2 Performance of the thermal test

The propane gas fire test was performed at the BAM test facility. Figure 88 shows the fire test and proves that the DN30 prototype is fully engulfed by the flames.

Figure 88: Picture of the fire test showing the full flame engulfment of the DN30 prototype

After the fire, the DN30 PSP was naturally cooled down, no artificial means were used. During the cooling phase there was no rain which could have accelerated cooling-down but wind with a low wind speed accelerating the cool down.

During the cooling phase gases escaped through the openings of the thermal plugs of the DN30.

Figure 89: Gases escaping from the DN30 prototype during the cooling phase

For the fire test and cooling-down phase, the results are in detail:

- A full engulfment of the specimen;
- A flame temperature between 950°C and 1000°C, with a minimal temperature of 794°C and a maximal temperature of 1095°C;
- No use of artificial means (like extinguishers) during the cooling-down phase;
- The thermal plugs behaved as expected, at the beginning of the fire they melt down and were pushed out by the PIR foam decomposition gases. The DN30 prototype showed no signs of overpressure indicating that the thermal plugs fulfilled their function;
- The temperatures reached inside the DN30 at the end of the fire are listed in Table 41.

Table 41: Temperatures at the 30B cylinder at the end of the fire

Location	Min. Temperature (°C)	Max. Temperature (°C)
30B cylinder	75.2	173.3
Plug	104.2	106.8
Valve	91.8	104.2

2.2.2.2.3 Results of the thermal test

The intumescent material behaved as expected. The gaps between the 30B cylinder and the inner shell of the DN30 PSP were sealed with expanded intumescent material (see Figure 90, Figure 91 and Figure 92). The intumescent material in the valve protecting device expanded considerably and enclosed the valve completely. The intumescent material in the plug protecting device expanded as well considerably and enclosed the plug completely.

Figure 90: 30B cylinder inside the DN30 PSP after the thermal test

Figure 91: Expanded intumescent material inside the plug protecting device

Figure 92: Expanded intumescent material inside the bottom half of the DN30 PSP

No deformation of the 30B cylinder, the valve and the plug were documented after the thermal test.

Figure 93: 30B cylinder valve after the thermal test

For the thermal test the results are in detail:

- The leakage rate after the thermal test is Q_{st} = 3.40 E-05 Pa m^3/s.
- The DN30 PSP could be opened without any further damage; the closure system was still working and the top half could be easily lifted off of the bottom half;
- The 30B cylinder can be removed from the DN30 PSP, the expanded intumescent material does not stick to the 30B cylinder;
- The intumescent material expanded and sealed all the gaps and free spaces in the DN30 prototype;
- No deformation of the 30B cylinder, the valve or the plug was documented;
- The maximal temperatures reached inside the DN30 at the end of the fire are listed in Table 42.

Table 42: Maximal temperatures at the 30B cylinder in the thermal test

Location	Temperature (°C) at (time after start of the fire in min)
30B cylinder	283.2 (55)
Plug (close to thread)	204.0 (135)
Plug (tip)	207.2 (123)
Valve (close to thread)	221.1 (119)
Valve (tip)	234.2 (131)

2.2.2.3 Results of the thermal analysis

2.2.2.3.1 Calculation method

The thermal analysis is carried out with the computer code HEATING 7.2 [HEATING 7.2].

HEATING is a general-purpose conduction heat transfer program written in FORTRAN 77. HEATING can solve steady-state and/or transient heat conduction problems in one-, two-, or three-dimensional Cartesian, cylindrical, or spherical coordinates.

The program code HEATING was selected for the analysis of the DN30 package based on the following advantages in important features:

- The formulation of the program allows easy simulation of phase change of the materials; in other codes the formulation of such material behavior is difficult.
- As will be shown later, the insulation material of the DN30 PSP incinerates during and after the fire causing an additional heat source; the simulation of such material behavior is easily implemented in HEATING and difficult to simulate with other codes.
- The shortcomings of HEATING due to its limited modeling capabilities are not relevant for the DN30 package as it can be easily modeled in cylindrical coordinates.

2.2.2.3.2 Calculation model

For the calculation model, cylindrical coordinates are used. The model is two dimensional. The origin of the coordinate system is in the center of the cavity of the 30B cylinder. The longitudinal axis of the DN30 package is the z-axis of the model and the radius is the x-axis.

The outer diameter, the length over the skirts and the wall thickness of the 30B cylinder (green) are identical to the dimensions specified in [ISO 7195]. The ends are modeled with flat heads. The cavity volume is identical to the minimum volume of 0.736 m^3 given in [ISO 7195]. The total mass of the cylinder in the model is 582 kg which is less than the standard mass of 635 kg given in [ISO 7195]. Hence, the calculation model of the cylinder is conservative.

The inner and outer stainless steel shells of the DN30 PSP are modeled with their original thickness of radial 2 mm for the inner shell and 3 mm for the outer shell and axial 10 mm for the inner shell and 4 mm for the outer shell. The radii of inner and outer shell as well as their inner and outer length comply with the original design, too.

The design details flange between top and bottom half, valve and plug protecting device, rotation preventing device and steel structures within the foam are not modeled.

Figure 94 shows the detail of the modeling of the intumescent material (black) attached to the inner shell of the DN30 PSP (dark blue). Between the intumescent material and the 30B cylinder shell there is a gap which is filled in RCT and NCT with air and is closed during ACT by the expanding intumescent material.

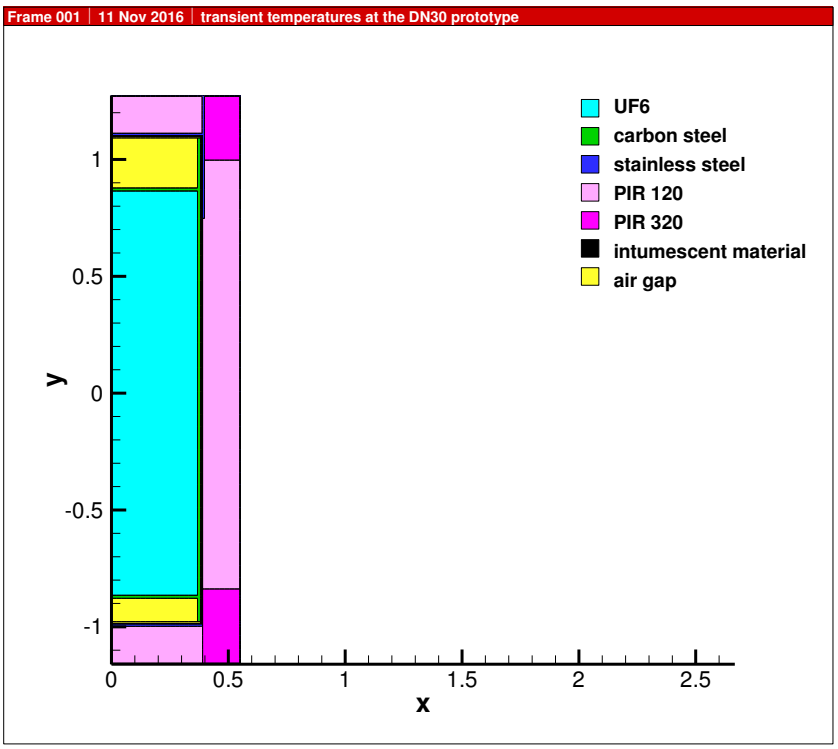

Figure 94: Calculation model for the DN30 package, full view

2.2.2.3.2.1 Initial temperatures

The initial temperatures for the steady state and transient calculations for RCT and NCT are uniformly 38°C.

The initial temperatures for the transient calculations for ACT are:

- For the calculation of the temperatures for the fire: the temperatures calculated with a steady state calculation with solar insolation.
- For the calculation of the temperatures in the cooling phase: the temperatures at the end of the fire phase.

2.2.2.3.2.2 Heat generation

2.2.2.3.2.2.1 Heat generation of the radioactive content

The thermal power of the content is in all cases 3 W.

It is assumed that the UF_6 completely fills the cavity of the 30B cylinder. The volumetric heat source is hence calculated from

V = 0.736 m^3 (minimal certified volume of a 30B cylinder)

Q = 3 W / 0.736 m^3 = 4.1 W/m^3

2.2.2.3.2.2.2 Heat generation due to incineration of the PIR foam

During the thermal test with the DN30 prototype incineration of the foam was recorded. Hence, for ACT heat generation in the PIR foam was assumed in the calculation model. The heat generation rate for the PIR foam is based on the following assumptions which were validated with the results of the thermal test with the DN30 prototype:

- Polyurethane foam with flame-retardant properties has a calorific value of 6.7 kWh/kg [DIN 18230].
- The mass of PIR 120 foam in the DN30 PSP is approx. 117 kg, the mass of PIR 320 foam 86 kg.
- The total incineration energy for the foam types is then for PIR 120 equal to 2.82E9 J and for PIR 320 equal to 2.07E9 J.

As basis for the heat generation of the foam an energy release over a duration of 1800 s is assumed. Hence the volumetric heat generations can be assessed as follows:

PIR foam 120:

$Q_t(120)$ = 2.82E9 J / (117 kg / 120 kg/m^3) / 1800 = 1.51 E6 W/m^3

PIR foam 320:

$Q_t(320)$ = 2.07E9 J / (86 kg / 320 kg/m^3) / 1800 = 4.28 E6 W/m^3

2.2.2.3.2.3 Solar insolation

The solar insolation data are specified in Table 43. They comply with [ADR 2015], No 6.4.8.6 or [IAEA 2012] para. 657. For the calculation of the initial temperatures for ACT a constant solar insolation with the values given in Table 43 was assumed, i. e. 100% over 24 hours / day.

Table 43: Solar insolation data

Surface orientation	RCT + NCT	Fire	Cooling down
	Insolation for 12 h per day W/m^2		
Vertical surfaces (valve and plug end)	200	-	200
All other surfaces (cylindrical surfaces)	400	-	400

2.2.2.3.2.4 Heat transfer to the ambient

2.2.2.3.2.4.1 Ambient temperature

The ambient temperature is defined in Table 44. For RCT, NCT and the cooling phase of ACT the ambient temperature is 38°C according to [ADR 2015], No 6.4.8.5 or [IAEA 2012] para. 656. For the fire phase of ACT the temperature is set to 800°C according to [ADR 2015], No 6.4.17.3 or [IAEA 2012] para. 728.

Table 44: Ambient temperature

RCT + NCT	Fire	Cooling down
Ambient temperature °C		
38	800	38

2.2.2.3.2.4.2 Radiation

The radiation coefficient of the outer surface of the DN30 package is for RCT and NCT 0.44 (stainless steel, rough surface).

During the fire the surface absorptivity is set to 0.8 ([SSG-26] para. 728.29) and the flame emissivity to 0.9 ([SSG-26] para. 728.28). In the cooling phase the emissivity is set to the same value of 0.8 as the absorptivity in the fire.

Table 45: Heat transfer by radiation at the surface of the DN30 package

Temperature °C	RCT + NCT	Fire	Cooling down
	Emissivity/absorptivity		
-	0.44	0.72	0.8

2.2.2.3.2.4.3 Convection

For the convective heat transfer for RCT and NCT as well as the cooling phase of ACT the formula given in [SSG-26] para. 728.31 is used.

$Nu = 0.13 (Pr\ Gr)^{1/3}$

For the convective heat transfer for the fire phase of ACT the formula given in [SSG-26] para. 728.30 is used.

$Nu = 0.036\ Pr^{1/3}\ Re^{0.8}$

The characteristic length is in all cases the diameter of the DN30 package of 1.104 m. The pool fire gas velocity is assumed with 7.5 m/s.

2.2.2.3.3 Benchmark calculations

2.2.2.3.3.1 Benchmark model

For the benchmark calculations the results of a thermal test with a prototype of the DN30 package are compared with the result of the analysis with the program code HEATING used in this report. These calculations are also used to adapt parameters of the model which cannot be derived from standards or literature so that the temperatures at safety relevant parts calculated with the benchmark model comply with measured values. In doing this, also the time-temperature curves of the model are compared with the thermal test results.

The thermal test is described in detail in Appendix 2.2.2.2 of the PDSR.

For the benchmark calculations the ambient conditions of the thermal test are used: the initial temperatures for the benchmark analysis are uniformly 63°C.

In the benchmark the 30B cylinder is empty and contains only air as in the thermal test. The thermal power is hence zero.

2.2.2.3.3.2 Results of the benchmark analysis

The results of the benchmark analysis are shown in Figure 95, Figure 96 and Table 46.

Figure 95 shows an overview of the measured and calculated temperatures at the important temperature positions. The measured data are shown with a dashed line and marked with the initial BM (for benchmark). The calculated values are shown in the same color but with a solid line.

The measured temperature at the surface of the prototype is the average temperature of the 4 sensors placed at the surface of the prototype at 0h, 3h, 6h and 9h position. The measured temperatures are lower than the calculated temperatures during the fire phase. In the cooling phase the measured temperatures at the surface are in good agreement with the calculated values.

The temperatures at the inner stainless steel shell of the DN30 PSP were not measured in the thermal test. They are calculated and shown for information purposes.

Figure 96 shows the comparison of the measured and calculated temperatures at the surface of the 30B cylinder, the valve and plug thread and the center of the DN30 cylinder.

Table 46 shows the maximal temperatures at the important temperature positions as well as the time of their maximum in seconds after start of the thermal test. The maximal temperatures at the surface of the 30B cylinder and the valve and plug thread are identical. The times of their respective maximum are in very good agreement.

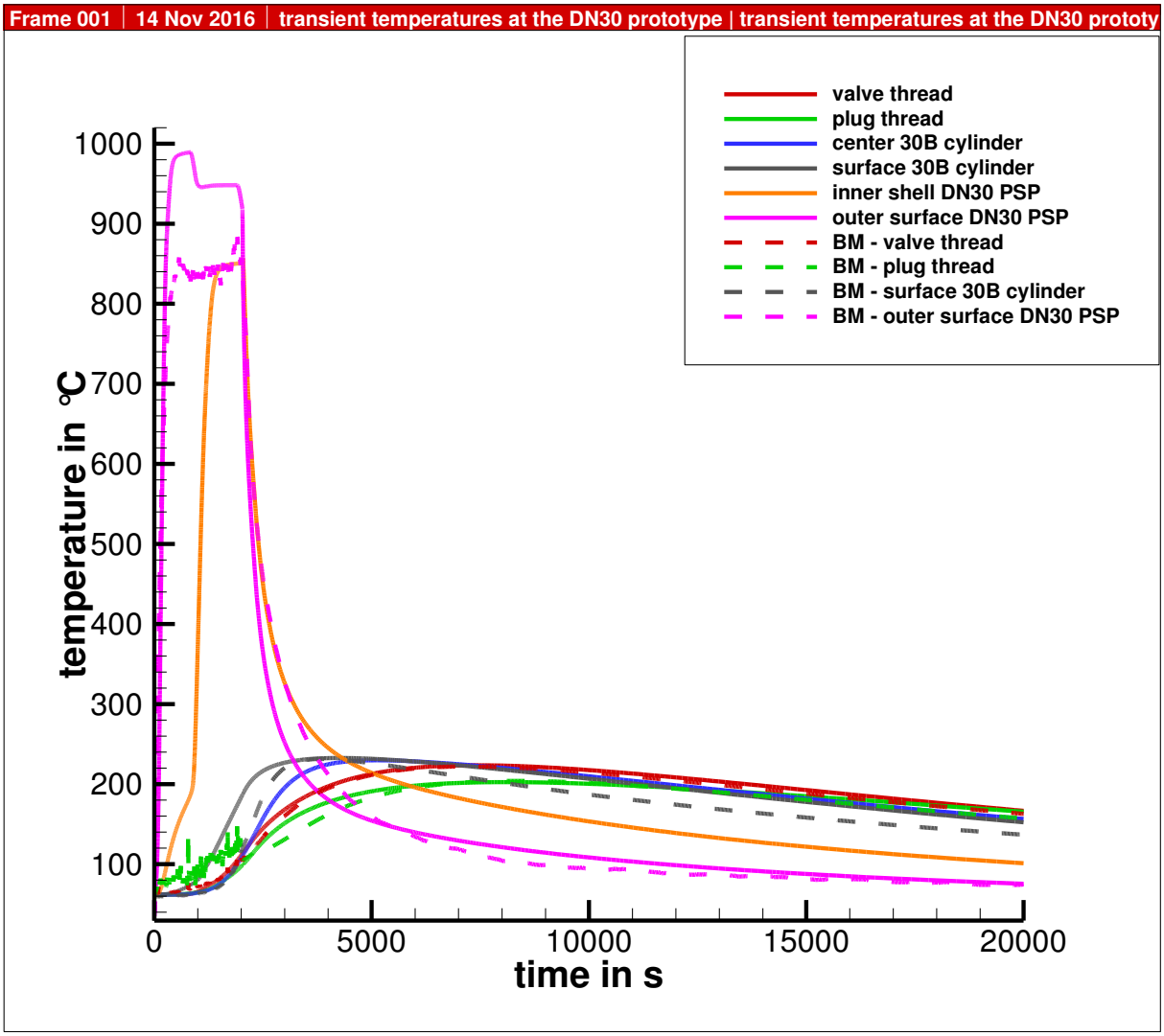

BM = measured values from the thermal test with the DN30 prototype

Figure 95: Measured and calculated temperatures at the prototype of the DN30 package – all temperatures, fire phase and 5 hours cooling time

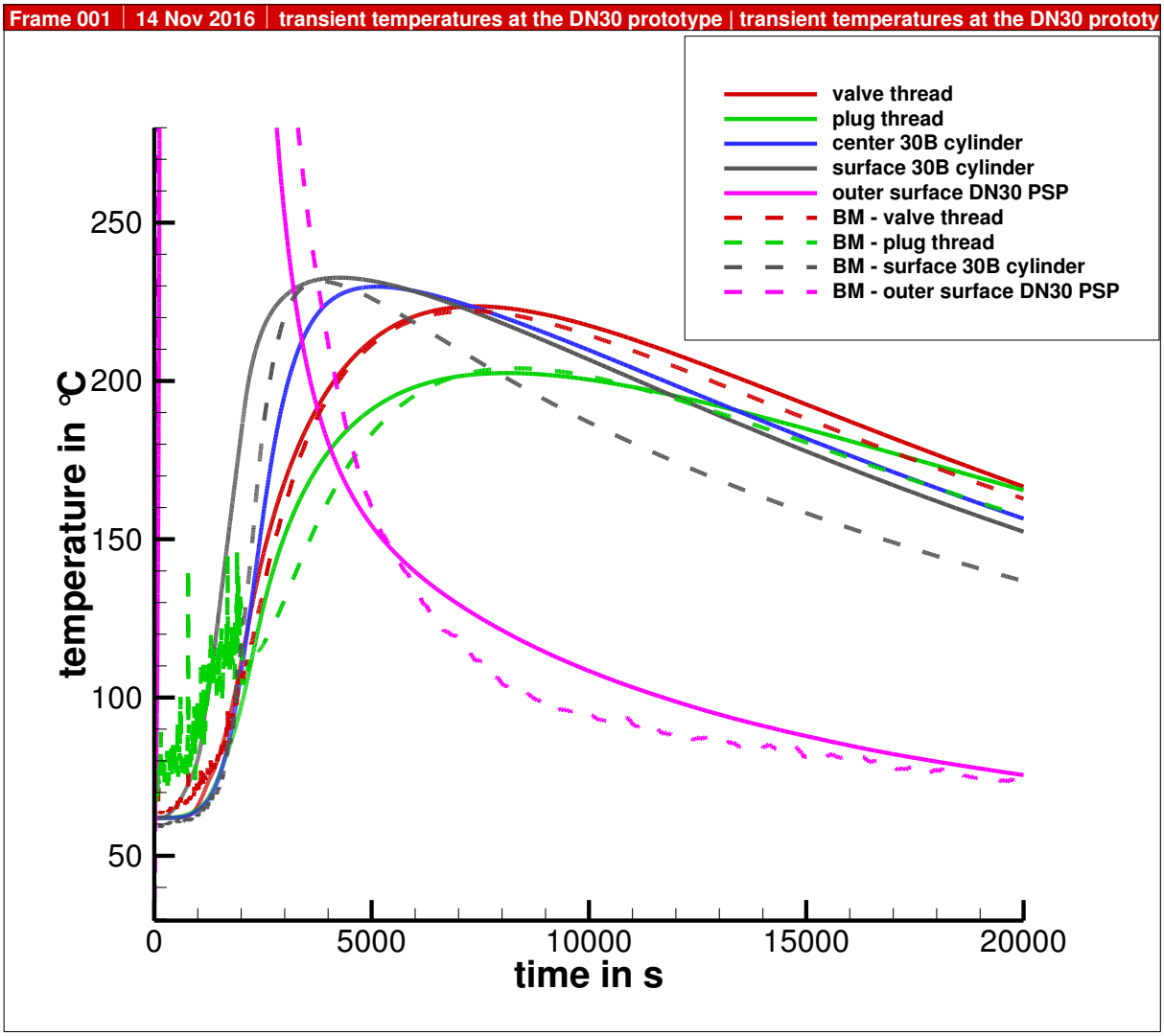

BM = measured values from the thermal test with the DN30 prototype

Figure 96: Measured and calculated temperatures at the prototype of the DN30 package – surface of the 30B cylinder, valve and plug thread, 30 B cylinder center (only calculated); fire phase and 5 hours cooling phase

Table 46: Comparison of measured and calculated maximal temperatures during the thermal test with the prototype of the DN30 package

		Benchmark calculation		Prototype test	
Temperature position	**Coordinates (x; z)**	**Temperature °C**	**Time S**	**Temperature °C**	**Time s**
Valve thread	0.229; 0.878	224	7400	222	7140
Plug thread	0.254; -0.878	203	8100	204	8100
Center 30 B cylinder	0.0; 0.0	230	5100	-	
Surface 30B cylinder	0.381; 0.057	233	4200	232	3800
Inner shell DN30 PSP	0.388; 0.057	857	2040	-	
Outer surface DN30 PSP	0.552; 0.057	990	830	884	1920

2.2.2.3.4 Calculations for RCT and NCT

2.2.2.3.4.1 Results without solar insolation

Due to the very low thermal power of the content the temperatures at the DN30 package are without solar insolation only slightly higher than the ambient temperature. The values are given in Table 47.

2.2.2.3.4.2 Results with solar insolation

The results for the cycle of 12 hours insolation / 12 hours without insolation are shown in Table 47. The maximal temperature of the 30B cylinder and its components is reached after about 20 days. The maximal temperature is 52 °C. Hence, it can be assumed that the UF_6 remains solid under RCT and NCT conditions.

For the case of constant insolation over 24 hours with 100% of the insolation data the maximal temperatures reached are 62 °C for the 30B cylinder and its components. This value complies with the initial conditions of the thermal test.

Table 47: Temperatures at the DN30 package loaded with a filled 30B cylinder under RCT and NCT

		Temperature °C		
Temperature position	**Coordinates (x; z)**	**Without insolation**	**12 hours insolation/no insolation cycles**	**Constant insolation**
Valve thread	0.229; 0.878	39	52	61
Plug thread	0.254; -0.878	39	52	62
Center 30 B cylinder	0.0; 0.0	39	52	62
Surface 30B cylinder	0.381; 0.057	39	52	62
Inner shell DN30 PSP	0.388; 0.057	39	53	62
Outer surface DN30 PSP	0.552; 0.057	38	63	64

2.2.2.3.5 Calculations for ACT

2.2.2.3.5.1 Temperatures at the DN30 package for full and partially filled 30B cylinders

This calculation repeats the benchmark calculation with the ambient temperatures defined in [ADR 2015] and [IAEA 2012]. The deviations from the benchmark calculations are

- The initial temperature is calculated with a steady state calculation taking into account an ambient temperature of 38°C and solar insolation as defined in Table 45.
- The fire temperature is set to 800°C; the duration is 30 min.
- In the cooling phase the ambient temperature is 38°C with solar insolation as defined in Table 45.
- For the heat transfer by convection to the ambient the values defined in section 2.2.2.3.2.4.3 are used.

Table 48: Max. temperatures at the DN30 package loaded with a partially filled 30B cylinder

Temperature position	Coordinates (x; z)	Max. temperatures °C for fill ratio					
		0%	5%	10%	25%	50%	100%
Valve thread	0.229; 0.878	223	205	194	178	163	147
Plug thread	0.254; -0.878	207	188	176	159	144	129
Center 30 B cylinder	0.0; 0.0	225	134	86	64	64	64
Surface 30B cylinder	0.381; 0.057	227	201	192	175	164	149
Inner shell DN30 PSP	0.388; 0.057	847	846	846	846	845	844
Outer surface DN30 PSP	0.552; 0.057	840	840	840	840	840	840

2.2.2.3.5.2 Pressure and temperature in the 30B cylinder

Figure 97 shows the maximal vapor pressure of UF_6 as function of the temperature (green curve) and the maximal possible vapor pressure due to the amount of UF_6 present in the cavity (red curve). The pressure in the cylinder may increase with temperature up to the intersection of the red curve with the green curve. After this point there is no pressure increase possible as there is not enough UF_6 in the cylinder.

Hence, from Figure 97 a maximal pressure in the 30B cylinder of 1.7 MPa at a temperature of 170°C can be derived.

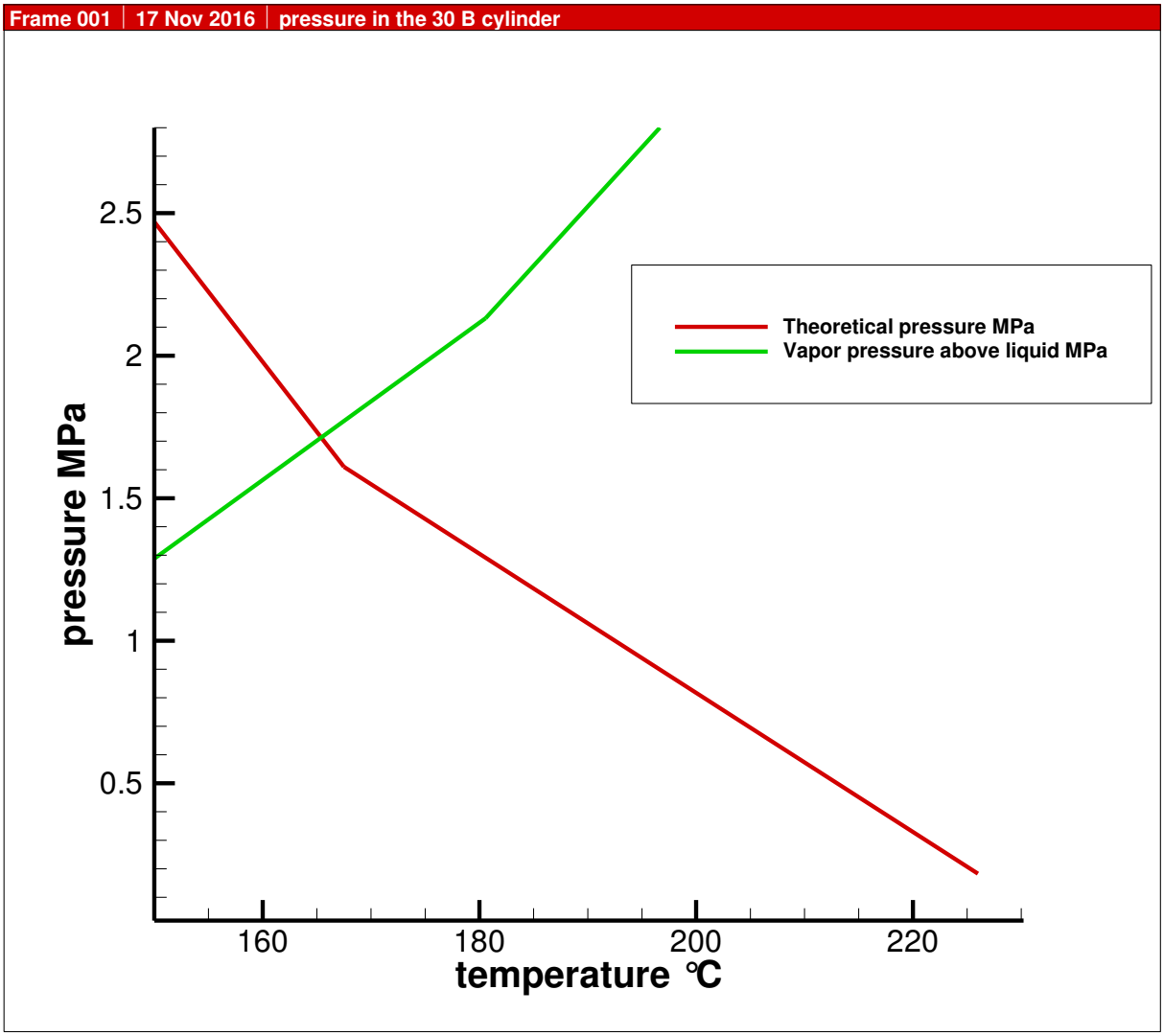

Figure 97: Maximal possible vapor pressure and theoretical maximal pressure in the 30B cylinder during the thermal test

2.2.2.4 Proof for the package DN30 to meet the requirements of [ADR 2015] or [IAEA 2012]

2.2.2.4.1 Ambient temperatures and pressures

For the analysis an ambient temperature of 38°C is taken into account (see section 2.2.2.3.2.4.1). Pressures which are likely to be encountered during RCT and NCT have no effect on the results of the thermal analysis. The requirements of [ADR 2015], No 6.4.2.10 or [IAEA 2012] para. 616 are met.

2.2.2.4.2 Rupture of the containment system

In section 2.2.2.3.5.2 a maximal pressure of 1.7 MPa at a temperature of 170°C is evaluated. In section 2.2.1.5.3 it is shown that the 30B cylinder can withstand without rupture this pressure at that temperature. The requirements of [ADR 2015] No. 6.4.6.2 c) or [IAEA 2012] para. 632 c) are met.

2.2.2.4.3 Temperature of the accessible surface

In section 2.2.2.3.4 the maximal temperature at the surface is calculated with 38°C. This is well below the admissible temperature of 50°C. The requirements of ([ADR 2015], No 6.4.8.3 or [IAEA 2012] para. 654 are met.

With this proof it is also verified that the requirements of [ADR 2015], No 6.4.8.4 or [IAEA 2012] para. 655 are met.

2.2.2.4.4 Influence of the thermal test on the shielding analysis

The analysis in section 2.2.2.3.5 shows that the stainless steel shells of the DN30 PSP as well as the carbon steel shell of the 30B cylinder are not affected by the thermal test in such a way that their shielding properties are reduced. It is verified in section 2.2.4.8.7 that taking into account this result of the thermal analysis the radiation level 1 m from the surface of the package does not exceed 10 mSv/h. In the shielding analysis a complete loss of the PIR foam is taken into account.

The requirements of [ADR 2015] No. 6.4.8.8 or [IAEA 2012] para. 659 with respect to the thermal test are met.

2.2.2.4.5 Influence of the thermal test on the containment analysis

The analysis in section 2.2.2.3.5 shows that the temperature of the valve and plug thread does not exceed the temperatures of these parts of the 30B cylinder measured during the thermal test with the prototype of the DN30 package. Hence it can be assumed that the leakage rate of the DN30 package does not exceed the leakage rate measured for the prototype. The proof of containment in section 2.2.3 takes into account the measured leakage rate for the prototype.

The requirements of [ADR 2015] No. 6.4.8.8 or [IAEA 2012] para. 659 with respect to the thermal test are met.

2.2.2.4.6 Influence of the thermal test on the criticality safety analysis

The analysis in section 2.2.2.3.5 shows that the stainless steel shells of the DN30 PSP as well as the carbon steel shell of the 30B cylinder are not affected by the thermal test in such a way that their thickness and density is reduced. It is verified in section 2.2.5 that taking into account

this result of the thermal analysis criticality safety is ensured. In the criticality safety analysis a complete loss of the PIR foam is taken into account.

The requirements of [ADR 2015] No. 6.4.11.10 and 6.4.11.13 or [IAEA 2012] para. 682 and 685 with respect to the thermal test are met.

2.2.2.4.7 Component temperatures of the DN30 package

The maximal component temperatures during RCT and NCT are with maximal 64°C for the DN30 PSP and 62°C for the 30B cylinder and its contents (see section 2.2.2.3.4) lower than the admissible values specified in Table 40.

The maximal component temperatures of the DN30 PSP during ACT are close to the admissible temperatures defined in Table 40. However, tests with a prototype of the DN30 package showed that these temperatures have no negative effect on the function of the inner and outer shell of the DN30 PSP with respect to shielding or criticality safety.

The maximal temperature of the 30B cylinder shell is well below the admissible temperature defined in Table 40. The temperatures of valve thread and plug thread do not exceed the admissible temperature evaluated in the thermal test with the DN30 prototype.

2.2.2.5 Summary

In this report a calculation model for the DN30 package is developed based on the results of a real fire test with a prototype of the DN30 package. The important parameters in this model are:

- For the PIR foam between inner and outer shell of the DN30 PSP incineration is modelled to achieve a good agreement with the temperatures of the fire test in the benchmark analysis. The energy input into the DN30 by the incineration of the foam is about 70% the total energy input. The fire contributes only with about 30%.
- The thermal conductivity of the PIR foam is adjusted in the fire phase and in the cooling phase to achieve a good agreement of the temperature curves of the fire test in the benchmark analysis.

The temperatures calculated with the benchmark model and their curves over time are in rather good agreement with the results of the fire test as shown in section 2.2.2.3.3.2.

With this model the temperatures at the DN30 package are calculated with the ambient conditions specified in [ADR 2015] and [IAEA 2012].

The maximal temperatures at important points of the DN30 package loaded with an empty 30B cylinder are in good agreement with the maximal temperatures measured at the prototype. For the DN30 package loaded with a filled or partially filled cylinder the temperatures are below the temperatures calculated for the empty 30B cylinder.

In chapter 2.2.2.4 it is shown that the DN30 package fulfills the requirements of [ADR 2015] and [IAEA 2012] towards the thermal conditions under RCT, NCT and ACT loaded with a 30B cylinder containing any mass of UF_6 between zero and 2277 kg.

2.2.3 CONTAINMENT DESIGN ANALYSIS

The containment design analysis is documented in Appendix 2.2.3.1 (Containment Analysis).

In this section a summary of this report describes the main points and results of the analysis.

The analysis

- covers RCT, NCT and ACT,
- is valid for enriched uranium from uranium with natural isotopic composition or from reprocessed uranium,
- is valid for all filling ratios from heels cylinders up to cylinders filled with the maximum amount of UF_6 defined in section 1.3.

2.2.3.1 Objective of verification

2.2.3.1.1 Verification for type IP-2 and IF packages

It is verified that the package complies under NCT with the requirements according to [ADR 2015], No 6.4.5.2 a) or [IAEA 2012] para. 624 (a) when submitted to the tests according to [ADR 2015], No. 6.4.15.4 and 6.4.14.5 or [IAEA 2012] para. 722 and 723:

Prevent loss or dispersal of the radioactive content

It is precised in the Advisory Material for the IAEA Regulations for the Transport of Radioactive Material [SSG-26] para. 624.1, which refers to para. 648.2, that a maximum allowable leakage rate for normal transport conditions has never been defined quantitatively. In para. 646.3 it is specified that the intention of para. 622 (a) “is to ensure that under normal conditions of transport the radioactive contents of the package cannot escape in quantities that may create a radiological hazard”.

For type B packages a quantitative maximum allowable leakage rate is defined for normal conditions of transport in [ADR 2015], No. 6.4.8.8 a) or [IAEA 2012] para. 659 (a). This criterion is used in this report also for type IP-2 and IF packages. Hence the condition for the activity leakage rate is

$$\mathbf{LA_{NCT} \leq 10^{-6}\ A_2/h}$$

2.2.3.1.2 Verification for type A and AF packages

It is verified that the package complies under NCT with the requirements according to [ADR 2015], No 6.4.7.14 a) or [IAEA 2012] para. 648 (a) when submitted to the tests according to [ADR 2015], No. 6.4.15.4 and 6.4.15.5 or [IAEA 2012] para. 722 and 723:

Prevent loss or dispersal of the radioactive content

For type A packages the same discussion as in section 2.2.3.1.1 applies. Hence the condition for the activity leakage rate is

$$\mathbf{LA_{NCT} \leq 10^{-6}\ A_2/h}$$

2.2.3.1.3 Verification for type B(U) and B(U)F packages

It is verified that the admissible limit values are not exceeded under NCT according to [ADR 2015] No. 6.4.8.8 a) or [IAEA 2012], para. 659 (a):

$$\mathbf{LA_{NCT} \leq 10^{-6}\ A_2/h}$$

It is verified that the admissible limit values are not exceeded under ACT according to [ADR 2015] No. 6.4.8.8 b) (ii) or [IAEA 2009], para. 659 (b) (ii):

$$\mathbf{LA_{ACT} \leq 1\ A_2/week}$$

The provisions for Kr-85 do not apply because Kr-85 is not present in the nuclide inventory.

2.2.3.2 Calculation method

The containment design analysis is carried out according to [ISO 12807] in following steps:

Step 1:	Determination of the radioactive inventory (see Appendix 1.3 (Radioactivity))
Step 2:	Determination of the activity releasable rate
Step 3:	Specification of the permissible activity release rate
Step 4:	Determination of the permissible activity release rate due to leakage
Step 5:	Determination of the activity concentration
Step 6:	Determination of the maximal volume leakage rate
Step 7:	Determination of the equivalent capillary diameter
Step 8:	Evaluation of the permissible standard leakage rate

The package has no elastomeric gaskets; hence there is no permeation activity release rate to be considered.

2.2.3.3 Package data used for the analysis

The package data used for the analysis are listed in Table 49.

Table 49: Package data used for the containment design analysis

Item	Condition of transport	Condition of cylinder	Value
Temperature	NCT	filled	64 °C
	ACT		121 °C
Free volume of cavity	NCT	filled	0.269 m^3
	ACT		0.0368 m^3
	NCT/ACT	heels	0.736 m^3
Design standard leakage rate	NCT	filled/heels	1.0E-4 Pa m^3 s^{-1}
	ACT		1.0E-4 Pa m^3 s^{-1}

2.2.3.4 Radioactive inventory, releasable radioactive inventory and activity concentration in the cavity atmosphere

The radioactive inventory, the derived releasable inventory and the respective activity concentration in the cavity atmosphere are listed in Table 50.

Table 50: Radioactive inventory, releasable radioactive inventory and activity concentration in the cavity atmosphere

Item	Package type	Condition of transport	Condition of cylinder	Value
Radioactive inventory	IP-2	NCT	filled	227 A_2
	A			1 A_2
	B(U)			227 A_2
	B(U)	ACT		227 A_2
	A	NCT	heels	1 A_2
	B(U)			64.2 A_2
	B(U)	ACT		64.2 A_2
Releasable activity	IP-2	NCT	filled	0.54 A_2
	A			0.0024 A_2
	B(U)			0.54 A_2
	B(U)	ACT		227 A_2
	A	NCT	heels	1 A_2
	B(U)			3.21 A_2
	B(U)	ACT		3.21 A_2
Activity concentration	IP-2	NCT	filled	2.0 A_2/m^3
	A			0.0088 A_2/m^3
	B(U)			2.0 A_2/m^3
	B(U)	ACT		309 A_2/m^3
	A	NCT	heels	1.36 A_2/m^3
	B(U)			4.36 A_2/m^3
	B(U)	ACT		4.36 A_2/m^3

2.2.3.5 Permissible standard Helium leakage rates

The permissible standard Helium leakage rates are listed in Table 51.

Table 51: Permissible standard Helium leakage rates

Item	Package type	Condition of transport	Condition of cylinder	Permissible leakage rate
Required standard Helium leakage rate	IP-2	NCT	filled	4.0E-4 Pa m^3 s^{-1}
	A			1.6E-1 Pa m^3 s^{-1}
	B(U)			4.0E-4 Pa m^3 s^{-1}
	B(U)	ACT		7.0E-3 Pa m^3 s^{-1}
	A	NCT	heels	7.6E-4 Pa m^3 s^{-1}
	B(U)			1.9E-4 Pa m^3 s^{-1}
	B(U)	ACT		2.7E+0 Pa m^3 s^{-1}

2.2.3.6 Summary and evaluation of results

2.2.3.6.1 Loss of radioactive content under NCT

The containment design analysis presented in this section shows that the permissible activity release limits for NCT as defined in [ADR 2015] resp. [IAEA 2012] and listed in chapter 2.2.3.1 are met for all contents specified in section 1.3 if the leakage rate of 1.0 x 10^{-4} Pa m^3 s^{-1} as specified in [ISO 7195] is not exceeded.

The loss of radioactive content under NCT of the DN30 package having a leakage rate of 1.0 x 10^{-4} Pa m^3 s^{-1} is for the DN30 type B(U) package design:

LA_{NCT} = 1.0E-4 / 1.7E-4 x 1E-6 A_2/h = 6E-7 A_2/h

2.2.3.6.2 Accumulated loss of radioactive content under NCT

For ACT conditions the standard Helium leakage rate can be 7.0 E-3 Pa m^3 s^{-1} and hence by a factor of 70 higher than for NCT.

Under the assumption that the leakage rate of the DN30 package after the tests simulating ACT is 10 times higher than under NCT and that there is a continuous and uniform release of radioactivity during a period of one week, the accumulated loss of radioactive content under ACT of the DN30 package having a leakage rate of 1.0 xE-3 Pa m^3 s^{-1} is for the DN30 type B(U) package design:

LA_{NCT} = 1.0E-3 / 7E-3 x A_2/week = 0.15 A_2/week

2.2.4 EXTERNAL DOSE RATES ANALYSIS

The external dose rate analysis is documented in the full report contained in Appendix 2.2.4 (Dose Rate Analysis). In this section a summary of this report describes the main points of the analysis.

The external dose rate analysis covers the DN30 package loaded with filled cylinders as well as cylinders containing heels under RCT, NCT and ACT. The analysis is valid for uranium with an enrichment of max. 5 wt%, commercial grade and reprocessed. It covers all contents specified in section 1.3.

2.2.4.1 Objective of verification

2.2.4.1.1 Verification for all types of packages containing LSA-II material

It has to be verified that the limit value for LSA-II material specified in [ADR 2015], no. 4.1.9.2.1, or in [IAEA 2012], para. 517 is not exceeded:

DL ≤ 10 mSv/h at a distance of 3 m from the unshielded material

2.2.4.1.2 Verification for all types of packages

For DN30 packages loaded with 30B cylinders filled with UF_6 compositions complying with Table 1 or Table 6 or loaded with 30B cylinders containing heels of UF_6 complying with Table 1 or Table 6 it has to be verified that the limit value for RCT specified in [ADR 2015], no. 4.1.9.1.10, or in [IAEA 2012], para. 526 is not exceeded:

TI ≤ 10

which is equivalent to

DL ≤ 0.1 mSv/h at a distance of 1 m from the external surface of the package

For DN30 packages loaded with 30B cylinders filled with UF_6 compositions complying with Table 2 or Table 4 the condition of a TI ≤ 10 cannot be verified in all cases. The TI must be determined by measurements by taking into account the possible increase of the dose rates due to the decay of U-232 to Th-228.

For DN30 packages loaded with 30B cylinders containing heels of UF_6 complying with Table 2 or Table 4 and exceeding the criterion TI ≤ 10, a certain time period between emptying and transport is required to reach TI ≤ 10. Hence, in these cases the transportability of the cylinders must be assured by dose rate measurements at the bare cylinder (see section 1.3.2.4), and if transportability is ensured the transport index (TI) must be determined by dose rate measurements.

It has to be verified that the limit value for RCT specified in [ADR 2015], no. 4.1.9.1.11, or in [IAEA 2012], para. 527 is not exceeded:

DL ≤ 2 mSv/h at cask surface

It has to be verified that the limit values for RCT specified in [ADR 2015], no. 7.5.11, CV 33, No 3.3 b), or in [IAEA 2012], para. 566 (b) are not exceeded:

DL ≤ 2 mSv/h at any point on the external surface of the vehicle,

DL ≤ 0.1 mSv/h at any point 2 m from the vertical planes represented by the outer lateral surfaces of the vehicle, or, if the load is transported in an open vehicle, at any point 2 m from the vertical planes projected from the outer edges of the vehicle.

Whenever calculations are performed for the vehicle, it is assumed that the external surface of the package coincides with the external surface of the vehicle. The package might be oriented with its longitudinal axis parallel or perpendicular to the longitudinal axis of the vehicle. In case of parallel orientation, two adjacent packages positioned face to face along their symmetry axis are considered. In case of perpendicular orientation four adjacent packages positioned side by side are considered.

2.2.4.1.3 Verification for type AF and B(U)F packages

It has to be verified that the package complies under NCT with the requirements according to [ADR 2015], No 6.4.7.14 b), or [IAEA 2012] para. 648 (b), when submitted to tests according to [ADR 2015], No. 6.4.15 or [IAEA 2012] para. 719 – 724:

ΔDL ≤ 20%,

where **ΔDL** is the increase in the maximal radiation level at any external surface of the package.

2.2.4.1.4 Verification for type B(U)F packages

It has to be verified that the admissible limit values are not exceeded under ACT according to [ADR 2015] No. 6.4.8.8 (b) (ii) first bullet point or [IAEA 2012], para. 659 (b) (i):

DL ≤ 10 mSv/h at a distance of 1 m from the cask surface

2.2.4.2 Assumptions for the calculations

The calculations of dose rates at the DN30 package and at the vehicle are based on the following assumptions:

2.2.4.2.1 Assumptions valid for all calculations

The following assumptions are valid for all calculations carried out throughout this report:

- The treated contents comply with the content description given in chapter 1.3.
- Based on [ISO 7195], maximal dimensions are assumed for the modeled 30B cylinders. A conservative wall thickness of 1.1 cm is considered.

- Axial and radial dimensions of the 30B cylinder are identical under RCT, NCT and ACT.
- The skirts of the considered 30B cylinders, on the valve and the plug side respectively, are neglected. All 30B cylinders are assumed to have flat axial faces.
- The DN30 PSP is taken into account in the calculations, unless unshielded material is analyzed. In this case, neither the DN30 PSP nor the 30B cylinder is considered.

2.2.4.2.2 Assumptions for routine conditions of transport (RCT)

- For the polyisocyanurate rigid foam (PIC foam) a conservative density of 0.1 g/cm^3 is assumed for all calculations. In fact, the PIC foam fitted in all parts of the DN30 PSP has a density higher than 0.1 g/cm^3.

2.2.4.2.3 Assumptions for normal conditions of transport (NCT)

For NCT, taking into account the tests mentioned in [ADR 2015], No. 6.4.15 or [IAEA 2012] para. 719 – 724, the following assumptions are made:

- Neither the shape of UF_6 inside the 30B cylinder nor the dimensions of the 30B cylinder are affected by the tests.
- A maximum admissible deformation is assessed for the PSP, up to which the dose rate increase remains within the admissible limit value.

2.2.4.2.4 Assumptions for accident conditions of transport (ACT)

The following assumptions are made for ACT taking into account the tests mentioned in [ADR 2015] No. 6.4.8.8 (b) (ii) or [IAEA 2012], para. 659 (b) (second item):

- The shape of the UF_6 inside the 30B cylinder may change arbitrarily.
- The dimensions of the 30B cylinder are not affected by the tests.
- The thickness of the inner and outer steel shells of the DN30 PSP remain unchanged. However, the PIC foam is completely neglected and the inner and outer shells are pressed together to a single sheet modeled to be in direct contact with the outer surface of the 30B cylinder.

2.2.4.3 Calculation method, its verification and validation

The calculation of dose rates at the DN30 package is carried out by means of the program system SCALE 6.1 [SCALE 2011]. The gamma and neutron source terms are determined by means of the depletion analysis sequence ORIGEN-ARP in the v7-27n-19g energy-group structure [SCALE 2011]. The dose rates are calculated by means of the analysis sequence MAVRIC.

Statistical errors, verification and validation are described in Appendix 2.2.4 (Dose Rate Analysis).

2.2.4.4 Gamma and neutron source terms

The gamma and neutron source terms needed for subsequent dose rate calculations are determined over a period of up to 10 years. This specific period is considered due to the source intensity of U-232 and its decay products reaching their maximum over this period of time. This way, arbitrary time periods are covered by the analysis.

Table 52 provides a list of the considered nuclides, as well as the contribution of their daughter nuclides.

2.2.4.4.1 Gamma source

The performed decay calculations of the nuclides of interest specified in Table 52 result in the gamma source terms needed for subsequent dose rate calculations. The gamma source intensities and the gamma energy release rates, given as a function of time, as well as the gamma spectra, are included in Appendix 2.2.4 (Dose Rate Analysis).

The fission product Tc-99 and the actinides Pu-239, Pu-240 and U-236 practically have a constant total gamma energy release rates over a period of 10 years. The total gamma energy release rates of almost all of the fission products and light elements decrease over the considered period of time. Only for the nuclide Zr-95 the total gamma energy release rate increases over the first month due to the build-up of Nb-95 and then decreases.

The total gamma energy release rate of U-235 increases slightly over the first 10 days before keeping a constant level over the rest of the considered time period. A similar behavior is observed for Np-237 and U-238. Their total gamma energy release rates increase over the first 6 months approx. by a factor of 6 and 23, respectively, and then keep a constant level. For U-232 an increase by a factor of approx. 620 is observed over the first 10 years. After this period of time the total gamma energy release rate decreases slowly. The total gamma energy release rate of Pu-238 decreases as well over the first 10 years. The total energy release rate of U-234 is constant over the considered time of 10 years. However, the contribution of the energy groups differs as time elapses and influences the dose rate of this nuclide.

Figure 98 and Figure 99 show the double logarithmic plot of the total gamma energy release rates as a function of the decay time for fission products / light elements and actinides respectively over a period of 10 years.

Table 52: Nuclides and associated daughter nuclides considered for the determination of the source intensities

Nuclide	Daughter nuclides
Uranium nuclides	
U-232	Th-228 Ra-224 Rn-220 Po-216 Pb-212 Bi-212 Po-212 Pb-208 Tl-208
U-234	Th-230 Ra-226 Rn-222 Po-218 At-218 Rn-218 Pb-214 Bi-214 Po-214 Bi-210 Pb-210 Tl-210 Po-210 Pb-209 Bi-209 Pb-206 Tl-206 Hg-206
U-235	Pa-231 Th-231 Ac-227 Th-227 Ra-223 Fr-223 Rn-219 Po-215 Pb-211 Bi-211 Po-211 Pb-207 Tl-207
U-236	Th-232 Ra-228 Th-228 Ac-228 Ra-224 Rn-220 Po-216 Pb-212 Po-212 Bi-212 Tl-208 Pb-208
U-238	U-234 Th-234 Pa-234m Pa-234 Th-230 Ra-226 Rn-222 At-218 Po-218 Po-214 Pb-214 Bi-214 Pb-210 Po-210 Bi-210 Pb-206 Tl-210 Bi-209
Actinides	
Np-237	U-233 Pa-233 Th-229 Ra-225 Ac-225 Fr-221 At-217 Rn-217 Po-213 Bi-213 Tl-209 Pb-209 Bi-209
Pu-238	U-234 Th-230 Ra-226 Rn-222 Po-218 Rn-218 At-218 Pb-214 Po-214 Bi-214 Pb-210 Po-210 Bi-210 Tl-210 Pb-209 Bi-209 Tl-206 Hg-206 Pb-206
Pu-239	U-235 Pa-231 Th-231 Ac-227 Th-227 Fr-223 Ra-223 Rn-219 Po-215 Po-211 Pb-211 Bi-211 Tl-207 Pb-207
Pu-240	U-236 Th-232 Ra-228 Th-228 Ac-228 Ra-224 Rn-220 Po-216 Po-212 Pb-212 Bi-212 Pb-208 Tl-208
Fission products and light elements	
Ag-110m	Cd-110 Ag-110 Pd-110
Ce-144	Nd-144 Ce-144 Pr-144 Pr-144m
Co-60	Ni-60
Cs-134	Ba-134 Xe-134
Cs-137	Ba-137 Ba-137m
Nb-95	Mo-95
Ru-103	Rh-103m Ru-103
Ru-106	Pd-106 Ru-106
Sb125	Te-125 Te-125m
Tc-99	Ru-99
Zr-95	Mo-95 Nb-95 Nb-95m

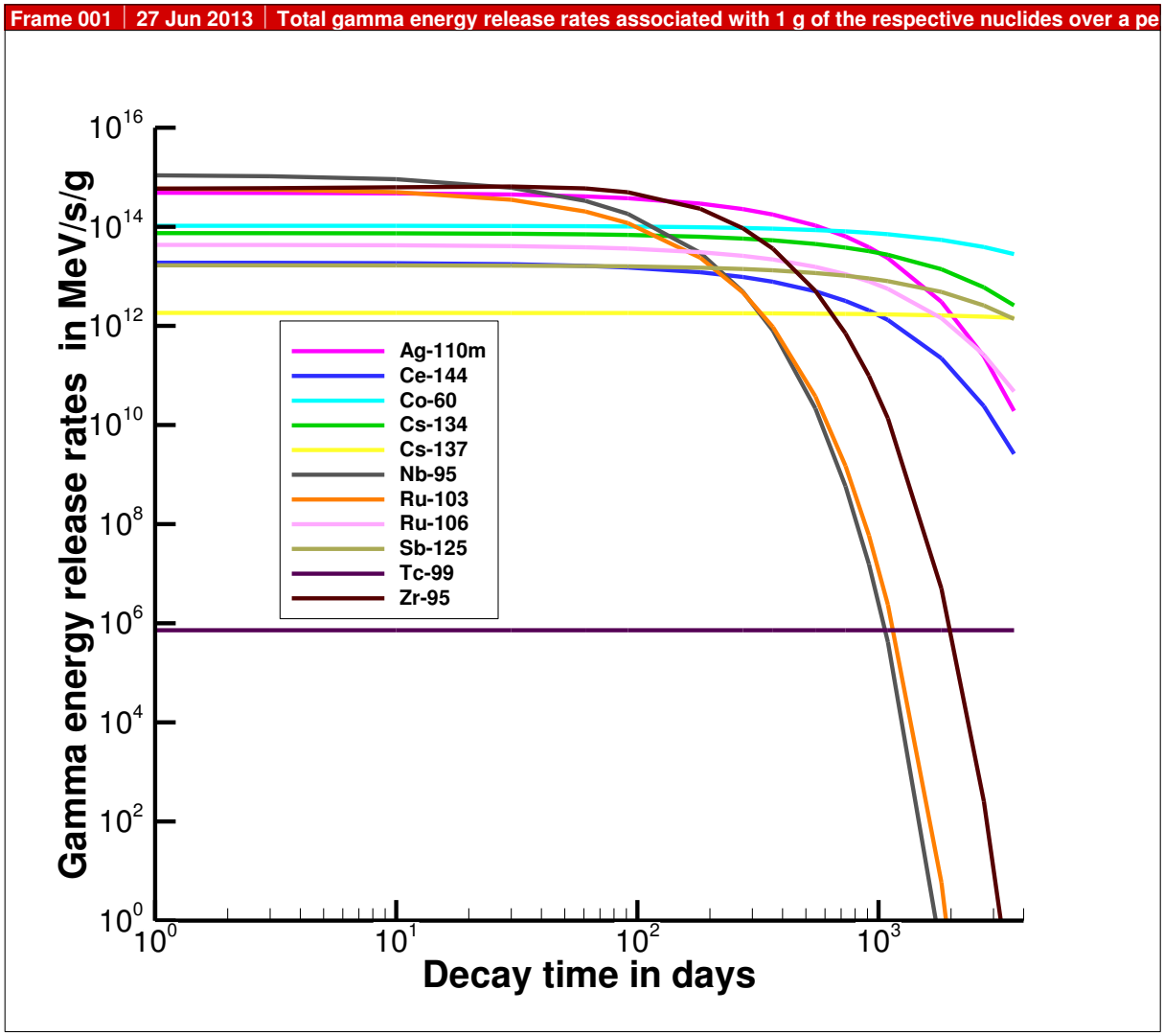

Figure 98: Total gamma energy release rates for initially 1 g of the fission products / light elements Ag-110m, Ce-144, Co-60, Cs-134, Cs-137, Nb-95, Ru-103, Ru-106, Sb-125, Tc-99, Zr-95 in MeV/s over a period of 10 years

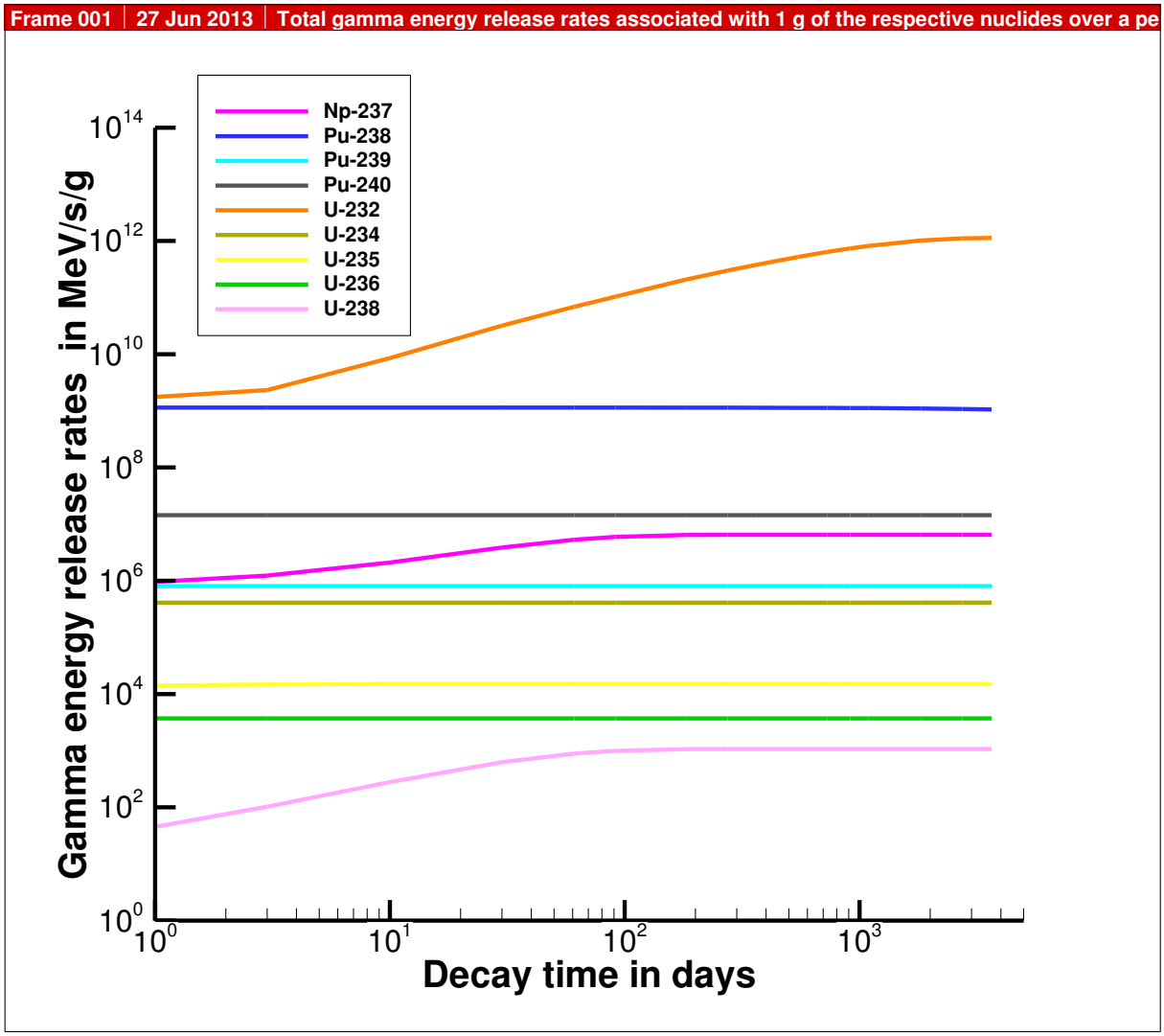

Figure 99: Total gamma energy release rates for initially 1 g of the actinides Np-237, Pu-238, Pu-239, Pu-240, U-232, U-234, U-235, U-236, U-238 in n/s over a period of 10 years

2.2.4.4.2 Neutron source

The actinides Np-237, Pu-239, Pu-240, U-234, U-236 and U-238 have practically constant neutron source intensities over a period of 10 years. The neutron source intensity of the actinide Pu-238 decreases slightly, for U-235 it increases slightly and for U-232 it increases constantly.

All other nuclides specified in Table 52 and not mentioned in this section do not have decays involving neutron production or release.

Figure 100 shows the double logarithmic plot of the total neutron intensities as a function of the decay time for the actinides over a period of 10 years.

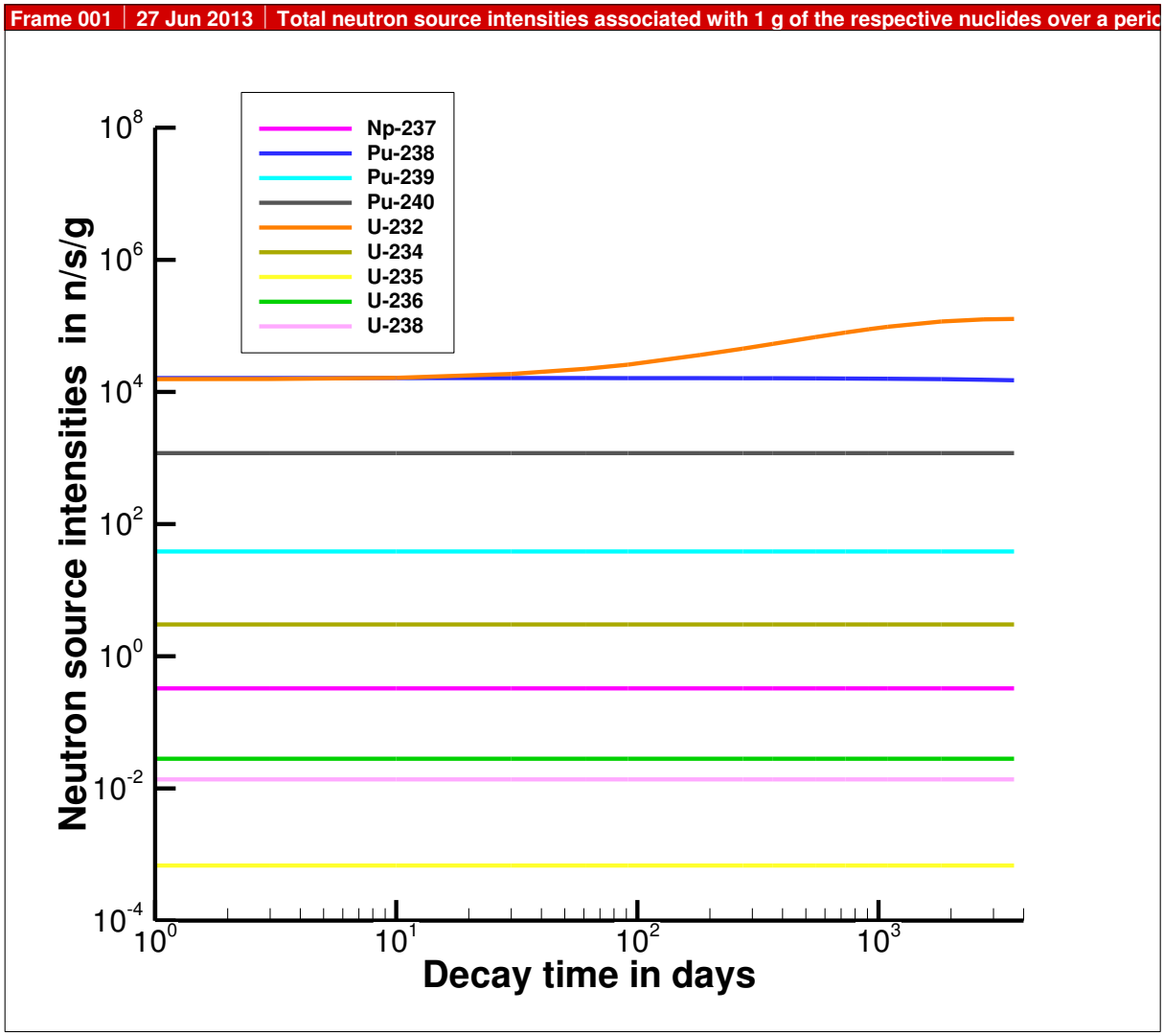

Figure 100: Total neutron source intensities for initially 1 g of the actinides Np-237, Pu-238, Pu-239, Pu-240, U-232, U-234, U-235, U-236, U-238 in MeV/s over a period of 10 years

2.2.4.5 Model Specification

2.2.4.5.1 Geometrical models for the DN30 packaging

2.2.4.5.1.1 30B cylinder

Based on the dimensions of the 30B cylinder as specified in [ISO 7195], a conservative 30B cylinder has been considered throughout the external dose rate analysis of the DN30 package. The 30B cylinder is simplified to a cylinder with flat heads. The modeled 30B cylinder is in compliance with the maximal dimensions specified in [ISO 7195]. The skirts, valve, plug and nameplate are completely neglected.

2.2.4.5.1.2 DN30 PSP

The DN30 PSP has been modeled as simplified as possible. For this reason, neither the feet nor the six closure devices have been modeled even though they are made up of stainless steel and contribute to the attenuation of gamma radiation. Based on the condition of transport to be modeled, three types of DN30 PSPs have been considered throughout the external dose rate analysis of the DN30 package:

- RCT: In this case, the DN30 PSP is composed of two cylindrical shells of stainless steel with the full thickness of the foam insulation in between.
- NCT: Similar to for RCT; however, a reduction of the thickness of foam insulation by 5 cm is assumed so that the outer diameter is also reduced by 5 cm. The density of the foam is conservatively kept unchanged.
- ACT: The shells of the DN30 PSP are assumed to be compressed in such a way that no more foam is present and that the inner and outer stainless steel shell of the DN30 PSP are pressed together to a single shell in radial and axial directions modeled in direct contact with the 30B cylinder. The outer surface is hence moved close to the cylinder surface.

2.2.4.5.2 Geometrical models for the content

2.2.4.5.2.1 Dose rate at unshielded material

For the calculation of the dose rate at the unshielded material, a cylindrical shape of the UF_6 is considered. The source is homogeneously distributed within the UF_6.

2.2.4.5.2.2 Filled cylinder under RCT, NCT and ACT

The calculation model used for the filled cylinder under RCT, NCT and ACT is a completely filled 30B cylinder without any void at the top of the UF_6. The source is homogeneously distributed within the UF_6.

2.2.4.5.2.3 Cylinder containing heels under RCT, NCT and ACT

For heels, three models were investigated:

1) The heels material distributed over the whole inner surface of the cylinder as a thin layer.
2) The heels material accumulated in the form of a 0.1 cm thick puddle at the bottom of the cylinder.
3) The heels material distributed over the inner surface of a front side of the cylinder.

2.2.4.6 Dose rate profiles

In order to assess the maximum dose rates at the DN30 package, dose rate profiles were calculated showing the levels of dose rate around the package.

Figure 101 shows the dose rate profile for a single DN30 package. This profile shows that the maximum radiation level is to be expected at the center of the side of the package. The axial dose rate is about a factor of 3 lower than the radial dose rate.

Figure 102 shows the dose rate profile of a possible transport configuration with two packages arranged face to face, and Figure 103 shows the dose rate profile for the standard transport configuration four packages on a flat-rack side by side. From the profile it can be seen that the dose rate at the surface of the vehicle (equivalent to the surface of the DN30 packages) is not affected by the adjacent packages and hence identical to the dose rate at the surface of a single package.

However, the dose rate in 2 m distance from the vehicle is higher than the dose rate in 2 m distance from the single package. The maximal dose rate in 2 m distance from the vehicle is for the face to face configuration about the factor 1.5 higher than for the single package. For the configuration of four packages side by side, the factor is about 3.1. However, it must be noted that the radial dose rate for the face to face configuration of two packages is still higher than the axial dose rate for the side by side configuration of four packages.

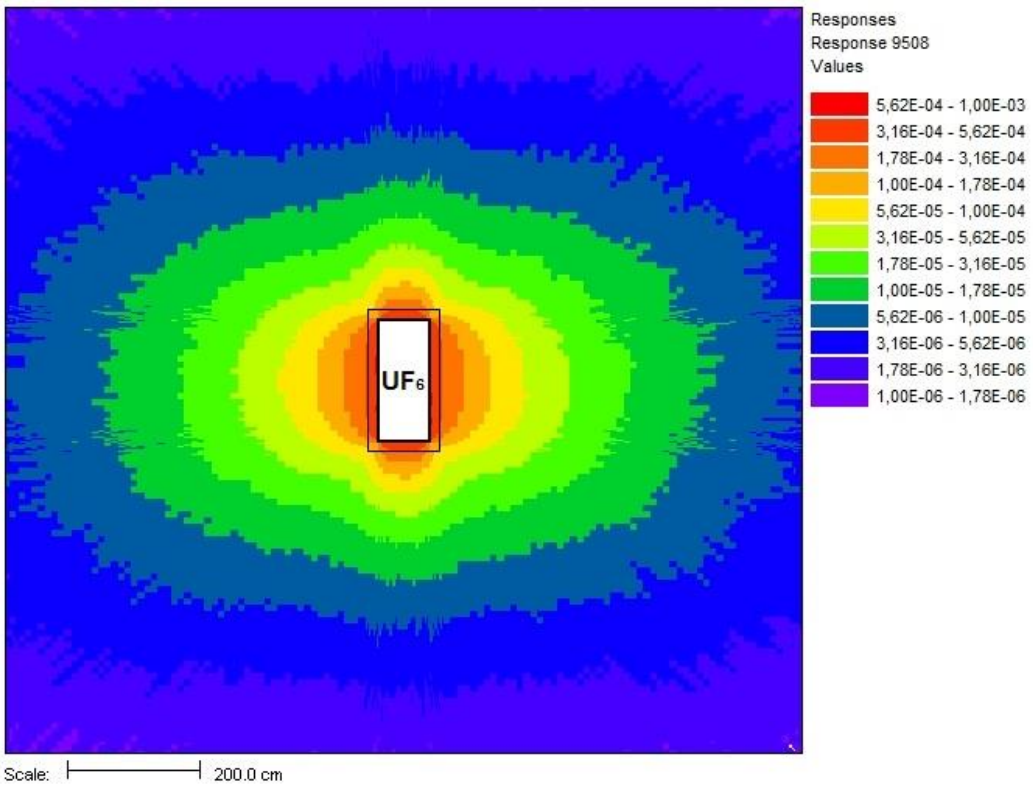

Figure 101: Gamma dose rate profile for the package DN30 loaded with a 30B cylinder completely filled with UF6 (values are given in Sv/h)

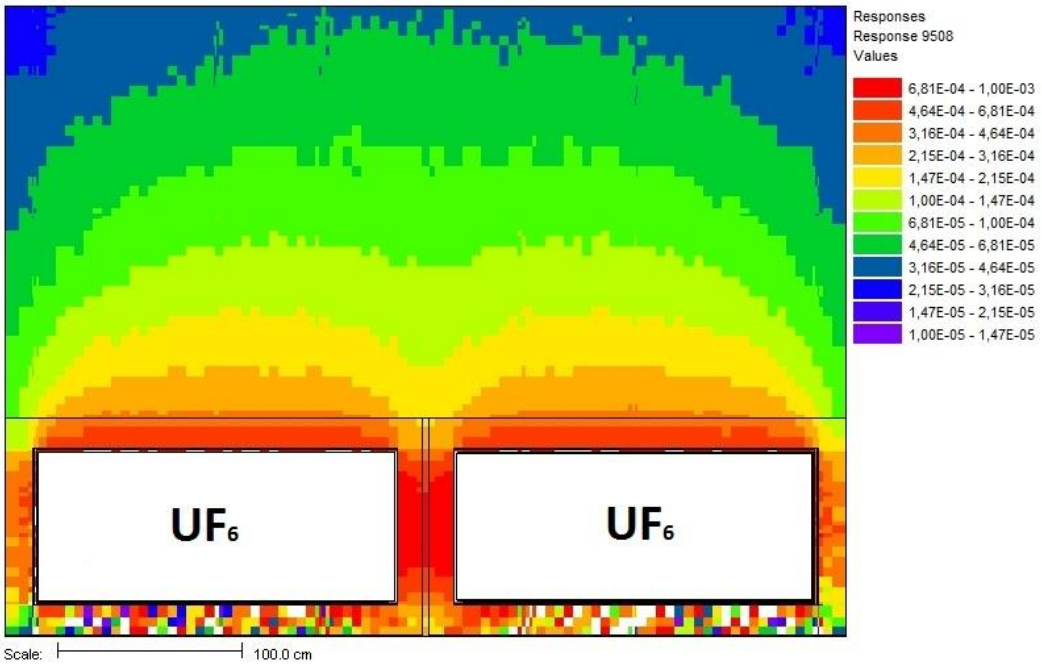

Figure 102: Axial gamma dose rates for two packages DN30 positioned face to face (values are given in Sv/h) – possible transport configuration

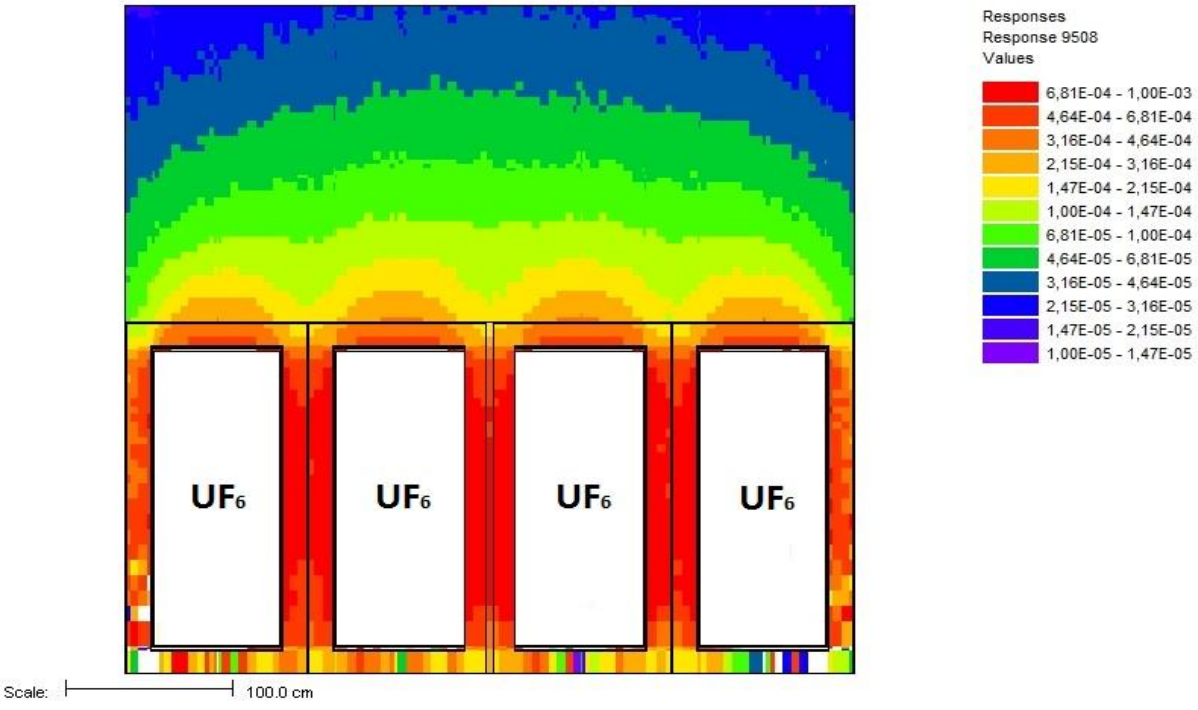

Figure 103: Axial gamma dose rates for four packages DN30 positioned side by side (values are given in Sv/h) – standard transport configuration

2.2.4.7 Dose rate criterion for cylinders containing reprocessed UF_6

In case measurements at the surface of a 30B cylinder result in a maximum measured dose rate of not more than 5000 µSv/h, the dose rates listed in Table 53 can be expected which would allow the transport under exclusive use.

In case measurements at the surface of a 30B cylinder result in a maximum measured dose rate of not more than 2000 µSv/h, it can be expected that the dose rate at 1 m distance from the DN30 is below 100 µSv/h for all calculation models (see Table 54) and hence non-exclusive use would be allowed.

Table 53: External dose rates at the DN30 package loaded with a cylinder with a maximal dose rate at the surface of the cylinder of 5000 µSv/h

Detector	Model 1	Model 2	Model 3
Surface	1860	1140	1730
1 m distance	250	120	150
2 m distance	94	41	45

Table 54: External dose rates at the DN30 package loaded with a cylinder with a maximal dose rate at the surface of the cylinder of 2000 µSv/h

Detector	Model 1	Model 2	Model 3
Surface	750	460	700
1 m distance	100	48	60
2 m distance	38	17	18

2.2.4.8 Verification of compliance with the dose rate limits according to ADR [ADR 2015] or [IAEA 2012]

2.2.4.8.1 General results of the dose rate calculations

- The neutron dose rates are in all cases negligible in comparison to the gamma dose rates.
- The calculations have shown that the contribution of U-232 daughter nuclides as the most significant gamma radiation emitters reaches its maximum after a decay time of ten years. Therefore, the evolution of dose rate is assessed over a period of 10 years.

2.2.4.8.2 Verification of the dose rates according to ADR [ADR 2015], no. 4.1.9.2.1 or [IAEA 2012], para. 517

The maximal dose rates at a distance of 3 m from unshielded UF_6 complying with Table 1, Table 2 and Table 4 are summarized in Table 55. The calculated values are well below the limit value. The objective of verification is met.

Table 55: Maximal dose rates at a distance of 3 m from unshielded UF_6 complying with Table 1, Table 2 and Table 4

Content	Maximal total dose rate at a distance of 3 m from unshielded material µSv/h
UF_6 complying with Table 1	1.3
UF_6 complying with Table 2	144
UF_6 complying with Table 4	200
Limit value	**10000**

2.2.4.8.3 Verification of the dose rates according to ADR [ADR 2015], no. 4.1.9.1.10 or [IAEA 2012], para. 526

The maximal total dose rates at a distance of 1 m from the surface of the DN30 package loaded with a 30B cylinder filled with UF_6 complying with Table 1, Table 2, Table 4 and Table 6 or heels of UF_6 complying with Table 1, Table 2, Table 4 and Table 6 are listed in Table 56.

For the DN30 package loaded with a filled 30B cylinder the following applies:

- Contents complying with Table 1: The maximal total dose rate at a distance of 1 m from the surface of the DN30 package loaded with a 30B cylinder containing UF_6 complying with Table 1 is listed in Table 56. The transport index is equal to 0.3 and the transport of the DN30 package loaded with a 30B cylinder containing UF_6 complying with Table 1 may be carried out under non-exclusive use.
- Contents complying with Table 2: The maximal dose rate at a distance of 1 m from the surface of the DN30 package loaded with a 30B cylinder containing UF_6 complying with Table 2 is listed in Table 56. The transport index is maximal 15.2 and the transport of

the DN30 package loaded with a 30B cylinder containing heels of UF_6 complying with Table 2 must be carried out under exclusive use, unless measurement of the dose rate before transport shows that the TI is less or equal to 10.

Attention: increase of the dose rate between the time of measurement and the arrival of the transport at the destination due to the decay of U-232 and build-up of Th-228 must be taken into account when determining the TI.

- Contents complying with Table 4: The transport at a distance of 1 m from the surface of the DN30 package loaded with a 30B cylinder containing UF_6 complying with Table 4 is listed in Table 56. The transport index is equal to 16.3 and the transport of the DN30 package loaded with a 30B cylinder containing UF_6 complying with Table 4 must be carried out under exclusive use, unless measurement of the dose rate before transport shows that the TI is less or equal to 10.

  Attention: increase of the dose rate between the time of measurement and the arrival of the transport at the destination due to the decay of U-232 and build-up of Th-228 must be taken into account when determining the TI.

- Contents complying with Table 6: The maximal dose rate at a distance of 1 m from the surface of the DN30 package loaded with a 30B cylinder containing UF_6 complying with Table 6 is given in Table 56. The transport index is equal to 1 and the transport of the DN30 package loaded with a 30B cylinder containing UF_6 complying with Table 6 may be carried out under non-exclusive use.

For the DN30 package loaded with a 30B cylinder containing heels the following applies:

- Heels of contents complying with Table 1: The maximal total dose rate at a distance of 1 m from the surface of the DN30 package loaded with a 30B cylinder containing heels of contents complying with Table 1 is listed in Table 56. The transport index is equal to 3.6 and the transport of the DN30 package loaded with a 30B cylinder containing heels of UF_6 complying with Table 1 may be carried out under non-exclusive use.

- Heels of contents complying with Table 2: The maximal dose rate at a distance of 1 m from the surface of the DN30 package loaded with a 30B cylinder containing heels of contents complying with Table 2 is listed in Table 56. The transport index is maximal 18.3 and the transport of the DN30 package loaded with a 30B cylinder containing heels of UF_6 complying with Table 2 must be carried out under exclusive use, unless measurement of the dose rate before transport shows that the TI is less or equal to 10.

- Heels of contents complying with Table 4: The maximal tdose rate at a distance of 1 m from the surface of the DN30 package loaded with a 30B cylinder containing heels of contents complying with Table 4 is listed in Table 56. The transport index is equal to 17.40 and the transport of the DN30 package loaded with a 30B cylinder containing heels of UF_6 complying with Table 4 must be carried out under exclusive use, unless measurement of the dose rate before transport shows that the TI is less or equal to 10.

- Heels of contents complying with Table 6: The maximal dose rate at a distance of 1 m from the surface of the DN30 package loaded with a 30B cylinder containing heels of contents complying with Table 6 is given in Table 56. The transport index is equal to 10.0 and the transport of the DN30 package loaded with a 30B cylinder containing heels of UF_6 complying with Table 6 may be carried out under non-exclusive use.

Table 56: Maximal dose rates at 1 m distance from the external surface of the DN30 package under RCT loaded with a 30B cylinder containing UF_6 complying with Table 1, Table 2 and Table 4 and Table 6 or heels of UF_6 complying with Table 1, Table 2 and Table 4 and Table 6

UF_6 Composition	Total dose rate µSv/h
Table 1	2.9
Table 2	152
Table 4	163
Table 6	9.5
Heels of compositions Table 1	36
Heels of compositions Table 2	183
Heels of compositions Table 4	174
Heels of compositions Table 6	100
Limit value (for non-exclusive use)	**100**

2.2.4.8.4 Verification of the dose rates according to ADR [ADR 2015], no. 4.1.9.1.11 or [IAEA 2012], para. 527

The maximal total dose rates at the surface of the DN30 package loaded with a 30B cylinder filled with UF_6 complying with Table 1, Table 2 and Table 4 and Table 6 or heels of UF_6 complying with Table 1, Table 2 and Table 4 and Table 6 are listed in Table 57.

The calculated dose rates for contents complying with Table 1, Table 2 and Table 4 and Table 6 or heels of contents complying with Table 1 and Table 6 are below the limit value. The objective of verification is met.

For the DN30 package loaded with a 30B cylinder containing heels of UF_6 complying with Table 2 and Table 4 the dose rates at the surface are expected to be below the limit value after a certain storage period. However, the assessment of the required storage period is based on conservative assumptions. The required storage period would be affected by such parameters as:

- the concentration of U-232 in the filled cylinder,
- the time period since the cylinder has been filled with UF_6,
- the time period the cylinder has been empty before transport,
- the amount of residual heels in the cylinder,
- the evaporation rate of the decay products of U-232 during evaporation of UF_6,
- the internal arrangement of the heels containing the decay products (concentrated in one spot, distributed as inner surface layer).

As it can be expected that not all of the parameters will not have their most conservative value at the same time, use of the actual dose rate measurement and its evaluation (see section 1.3.2.4) is preferable for the specification of storage time requirements.

Table 57: Maximal total dose rates at the surface of the DN30 package loaded with a 30B cylinder containing UF_6 complying with Table 1, Table 2 and Table 4 and Table 6 or heels of UF_6 complying with Table 1, Table 2 and Table 4 and Table 6

UF_6 Composition	Total dose rate µSv/h
Table 1	12.4
Table 2	670
Table 4	717
Table 6	43
Heels of compositions Table 1	311
Heels of compositions Table 2 after 9 years between emptying and transport	1720
Heels of compositions Table 4 after 25 years between emptying and transport	1522
Heels of compositions Table 6	916
Limit value (for non-exclusive use)	**2000**

2.2.4.8.5 Verification of the dose rates according to ADR [ADR 2015], no. 7.5.11, CV 33, No 3.3 b) or [IAEA 2012], para. 566 (b)

Maximal total dose rates at the external surface of the vehicle (equivalent to the external surface of the DN30 package loaded with a 30B cylinder filled with contents complying with Table 1, Table 2 and Table 4 and Table 6 or loaded with a 30B cylinder containing heels of the respective contents) are summarized in Table 58.

The dose rates are below the limit of 2000 µSv/h; the objective of verification is met.

Table 58: Maximal total dose rates at the external surface of a vehicle loaded with DN30 packages loaded each with 30B cylinders filled with contents complying with Table 1, Table 2 and Table 4 and Table 6 or each loaded with 30B cylinders containing heels of contents complying with the respective contents

UF_6 Composition	Total dose rate µSv/h
Table 1	12.4
Table 2	670
Table 4	717
Table 6	43
Heels of compositions Table 1	311
Heels of compositions Table 2 after 9 years between emptying and transport	1720
Heels of compositions Table 4 after 25 years between emptying and transport	1522
Heels of compositions Table 6	916
Limit value	**2000**

Maximal total dose rates at 2 m distance from the external surface of the vehicle loaded with four DN30 packages loaded each with a 30B cylinder filled with contents complying with Table 1, Table 2 and Table 4 and Table 6 or each loaded with a 30B cylinder containing heels of the respective contents are summarized in Table 59.

The dose rates are below the limit of 100 µSv/h. The objective of verification is met.

Table 59: Maximal total dose rates at 2 m distance from the external surface of a vehicle loaded with DN30 packages loaded each with 30B cylinders filled with contents complying with Table 1, Table 2 and Table 4 and Table 6 or each loaded with 30B cylinders containing heels of contents complying with the respective contents

UF_6 Composition	Total dose rate µSv/h
Table 1	1.3
Table 2	91
Table 4	98
Table 6	5.8
Heels of compositions Table 1	19
Heels of compositions Table 2 after 9 years between emptying and transport	94
Heels of compositions Table 4 after 25 years between emptying and transport	93
Heels of compositions Table 6	52
Limit value	**100**

2.2.4.8.6 Verification according to ADR [ADR 2015], No. 6.4.7.14 b) or [IAEA 2012], para. 648 (b)

The increase of the dose rate after the tests simulating normal conditions of transport has been evaluated under the conservative assumption of a deformation of 50 mm. The calculated increase of the total dose rate is in this case 16.7%.

The maximal deformation in the center of the DN30 package calculated in section 2.2.1.5.1.5.6 is 6 mm. Hence, the increase of the maximal dose rate is expected to be much less than the admissible limit of 20%.

2.2.4.8.7 Verification according to ADR [ADR 2015], No. 6.4.8.8 b) (ii) or [IAEA 2012], para. 659 (b) (i)

Table 60 shows the conservative total dose rates at a distance of 1 m from the surface of the DN30 package under ACT. The table shows that the dose rate for all contents is well below the limit value. The objective of verification is met with a very large safety margin.

Table 60: Dose rates in 1 m distance from the surface of the package DN30 under accidental conditions of transport

UF_6 Composition	Total dose rate µSv/h
Table 1	12
Table 2	605
Table 4	650
Table 6	38
Heels of compositions Table 1	141
Heels of compositions Table 2 after 9 years between emptying and transport	729
Heels of compositions Table 4 after 25 years between emptying and transport	692
Heels of compositions Table 6	397
Limit value	**10 000**

2.2.4.9 Summary and evaluation of results

The analysis performed in this section shows that the dose rate limits as defined in [ADR 2015] resp. [IAEA 2012] and listed in section 2.2.4.1 are complied with for all contents specified in chapter 1.3.

For contents complying with Table 1 (enriched commercial grade UF_6 complying with the requirements for type A packages), the calculated dose rates at the DN30 package containing full cylinders or cylinders containing heels the dose rate limits are always met. The assessment covers also multiple refilling of cylinders containing heels with new product.

For contents complying with Table 6 (enriched reprocessed UF_6 complying with the requirements for type A packages), the calculated dose rates at the DN30 package containing full cylinders or cylinders containing heels are higher than for contents complying with Table 1 but still meet the dose rate limits.

For contents complying with Table 2 and Table 4 (enriched reprocessed UF_6 complying with the requirements for type IF packages), the calculated dose rates at the DN30 package containing full cylinders meet the dose rate limits except for the limit for non-exclusive use (TI=10). For the envelope of the composition defined in Table 2 and Table 4, the dose rates in 1 m distance from the surface are higher than 100 µSv/h. Depending on the actual composition of the material, measurements carried out to determine the transport index might result in a lower TI allowing transport under non-exclusive use. However, the increase of the dose rate due to the build-up of Th-228 from the decay of U-232 must be taken into account when the TI is determined by measurement.

For heels of contents complying with Table 2 and Table 4, the dose rates are expected to be too high for immediate transport after emptying. The calculations show that in any case transport is possible after a certain storage time, even under non-exclusive use.

As the calculated storage times are rather long, a criterion is developed to assess the dose rates to be expected at a DN30 package loaded with a cylinder containing heels by measuring the dose rate at a bare 30B cylinder.

Unlike for DN30 packages loaded with filled cylinders, the TI decreases over time for a DN30 package loaded with cylinders containing heels. The TI determined before shipment by means of measurements is therefore valid for the whole journey and might be used to determine whether a transport under exclusive use conditions is required.

2.2.5 CRITICALITY SAFETY ANALYSIS

The criticality safety analysis is documented in the full report in Appendix 2.2.5 (Criticality Safety Analysis). In this section a summary of this report describes the main points and results of the analysis.

The analysis

- covers RCT, NCT and ACT taking into account a maximal enrichment of 5 wt. % U-235 in uranium,
- is valid for enriched uranium from uranium with natural isotopic composition or from reprocessed uranium,
- is valid for UF_6 containing up to 0.5 wt.% volatile impurities (HF) and additional hydrogenated uranium residues from the reaction of humidity with UF_6 accumulated during the time period between recertifications,
- is valid for all filling ratios from heels cylinders up to cylinders filled with the maximum amount of UF_6 defined in section 1.3.

2.2.5.1 Objective of verification

The criticality safety of the package DN30 is proved according to [ADR 2015], no. 6.4.11.1, or [IAEA 2012], para. 673. For RCT, NCT and ACT following criticality safety criterion is complied with:

$$\mathbf{k_{eff} + 3\,\sigma + \Delta k \leq 0.95}$$

For the proof of criticality safety, systematical deviations Δk of the calculation method have to be considered [DIN 25478]. These systematical deviations are determined in Appendix 2.2.5 (Criticality Safety Analysis) in detail. For the calculation method used for the proof (see 2.2.5.3) the systematical deviations Δk are zero.

It is shown that taking into account credible and hypothetical conditions of the arrangement of the UF_6 in the cylinder, the composition and density of UF_6 and the distribution of hydrogenated uranium residues:

- The DN30 package fulfills the criticality safety criterion for a 30B cylinder with a wall thickness down to a minimal value of 7.94 mm.
- The bare 30B cylinder with a wall thickness of at least 11 mm fulfills the criticality safety criterion.

2.2.5.2 Assumptions for the proof of criticality safety

The proof of criticality safety for the DN30 package is based on following assumptions:

2.2.5.2.1 Assumptions valid for all calculations

The following assumptions are valid for all calculations carried out in the following chapters:

- The admissible number is N = infinite.
- The content is enriched UF_6 with an enrichment of maximal 5 wt.% U-235 in Uranium.

- Volatile impurities in the UF_6 are defined in [ASTM C996] with maximal 0.5 wt.%; these impurities are considered to consist only of HF.
- Other impurities created during the filing and extracting operations, i. e. hydrogenated uranium residues (HUR) are also determined and considered.
- The 30B cylinder might be completely or partially filled with UF_6. For the partially filled 30B cylinder, there might be a void on top of the UF_6. A cylindrical void at the center of UF_6 is also considered.
- The density is varied between 3.1 g/cm^3 (equivalent to a cylinder having a certified minimal volume of 0.736 m^3 completely filled with 2277 kg UF_6) and a theoretical density of 5.5 g/cm^3 extrapolated from given data at different temperatures to -40°C.
- Axial and radial dimensions of the 30B cylinder are the same under RCT, NCT and ACT.
- The skirts of the cylinder on the valve and plug side are neglected for the simplified calculation model. In this model the cylinder is assumed to have flat axial faces.
- For heterogeneous distributions of impurities, the shape of the cylinder heads is modeled closer to reality and the skirts are modeled.
- The valve and plug as well as the name plate are neglected in all calculation models.
- In case the DN30 PSP is taken into account, water might penetrate freely into the gap between the cylinder and the PSP or into the foam of the PSP.

2.2.5.2.2 Assumptions for the analysis of the single package under RCT, NCT and ACT

The proof for the package under RCT, NCT and ACT is carried out for the dry, fully reflected package.

The following assumptions are valid for the single package in isolation:

- The 30B cylinder or DN30 package is surrounded by a 20 cm water reflector.
- There is no water ingress into the 30B cylinder under RCT and NCT.
- Ingress of water in larger volumes into the cavity of the 30B cylinder is not assumed as the mechanical analysis shows that [ADR 2015], no. 6.4.11.8 b), resp. [IAEA 2012] para. 680 (b) (i) is met. The very small amount of water ingress possible through leakage is calculated, however the very small amount is covered by the conservative assumptions with respect to HF and HUR.

2.2.5.2.3 Assumptions for 5 x N packages under NCT

The proof is carried out for an infinite number of packages under ACT according to section 2.2.5.2.4. The proof for 5 x N = infinite number of packages under NCT is covered by the proof for 2 x N = infinite number of packages under ACT.

2.2.5.2.4 Assumptions for 2 x N packages under ACT

The proof is carried out for 2 x N = infinite number of packages under ACT. The proof is based on the conditions of the packages after the tests required to demonstrate their ability to withstand ACT.

The following assumptions are made for ACT, taking into account the tests mentioned in [ADR 2015] No. 6.4.11.13 (b) or [IAEA 2012], para. 685 (b):

- The shape of the UF_6 inside the 30B cylinder may change arbitrarily.

- The dimensions of the 30B cylinder are not affected by the tests.
- The thickness of the inner and outer steel shells of the DN30 PSP remain unchanged, however the PIC foam is completely neglected and the inner and outer shell are collapsed to a single shell. The position of this collapsed shell is varied (contact to the surface of the 30B cylinder or gap between surface and shell).
- Water ingress due to the immersion under a head of 15 m water for 8 hours according to [ADR 2015] no. 6.4.17.4, [IAEA 2012] para. 729 (covering [ADR 2015] no. 6.4.19, [IAEA 2012] para. 733).

2.2.5.3 Calculation method, verification and validation

All criticality safety calculations are performed by means of the sequence CSAS6 of the criticality safety code KENO VI which are both part of the SCALE software package. Both versions SCALE 6.0 [SCALE 2009] and SCALE 6.1.1 [SCALE 2011] are used for the analyses.

The most recent libraries based on ENDB/BVII data are used for the criticality safety calculations for the DN30 package. This includes the library v7-238 being used for energy multi-group cross sections.

2.2.5.3.1 Verification

The verification consists of the installation verification and of functional verification of the used modules of the SCALE 6 / SCALE 6.1.1 program systems. The functional verification is carried out by the editor of program systems on the basis of the appropriate verification plan. For the individual user the verification of program system SCALE 6 / SCALE 6.1.1 consists of the installation verification on the basis of case studies delivered by the editor. The case studies were calculated successfully and compared with the likewise delivered reference output files. There were no differences in the output files which exceeded the range of admissible deviations mentioned in the installation guide accompanying the code package. Thus, successful installation verification is given.

2.2.5.3.2 Validation

The calculation method (code and cross-section data) used to establish criticality safety must be validated against measured data (e.g. criticality benchmark experiments) that can be applicable to the package design characteristics. The validation process provides a basis for the reliability of the calculation method and should justify that the calculated k_{eff} plus Bias and uncertainties (if necessary) for the actual package conditions will ensure the compliance with the criticality safety criterion.

[NEA 2008] contains a large number of evaluated criticality safety benchmark experiments which can be used for validation purposes. The most suitable criticality safety benchmark experiments for UF_6 arrangements available in [NEA 2008] are described in NEA/NSC/DOC/(95)03/IV LEU-COMP-THERM-033. In Appendix 2.2.5, the 52 cases associated with the benchmark experiment LEU-COMP-THERM-033, involving cases of reflected and unreflected assemblies of 2 and 3 %-enriched Uranium fluoride in paraffin, are modeled for computational verification purposes by means of both codes SCALE 6.0 and SCALE 6.1.1. The two SCALE versions are used in association with the multi-group libraries v7-238 to prove criticality safety. Their calculation abilities are validated for the actual package criticality characteristics using the same libraries.

The validation of the calculation method by means of modeled benchmark experiments shows a positive Bias for all models (see Appendix 2.2.5 (Criticality Safety Analysis)). The sequence CSAS6 of the software KENO VI of both program system versions SCALE 6.0 and SCALE

6.1.1 overestimates the reactivity in arrangements similar to those of LEU-COMP-THERM-033 for multigroup energy libraries. In particular, an overestimation of k_{eff} is expected for the criticality analysis of the package DN30. Conservatively, the Bias is hence assumed to be zero.

$\Delta k = 0$

2.2.5.4 Model Specification

2.2.5.4.1.1 Geometrical properties

2.2.5.4.1.2 30B cylinder

Two models of the 30B cylinder are considered for the criticality safety analysis of the DN30 package:

- **A simplified 30B cylinder model:** The 30B cylinder is simplified to a cylinder with flat ends. The outer diameter is varied between 75.6 cm and 76.8 cm and the outer length is varied between 191.7 cm and 193.5 cm. The wall thickness is varied between 1.3 cm and 0.794 cm (minimum wall thickness according to [ISO 7195], Table 3). The skirts, the valve, plug and nameplate are neglected. The maximal possible UF_6 volume of the model is hence between 0.791 m^3 and 0.853 m^3.

- **Detailed 30B cylinder model:** The ends of the 30B cylinder are of a spherical shape similar to the original cylinder heads, and both skirts are taken into consideration. Maximal dimensions specified in [ISO 7195] are used for the 30B cylinder; the outer diameter is 76.8 cm and the outer length 207.5 cm over the skirts and 193.5 cm over the ends. Each cylinder end is modeled as part of a spherical shell with an outer radius of 62.3 cm. The centers of the two spherical shells of both 30B cylinder ends are at a distance of 68.9 cm to each other and are located on the symmetry axis. In deviation to the dimensions given in [ISO 7195] the plug end is modeled in such a way that the outer surface of the bended end is in line with the end of the skirt, i. e. moved 1.3 cm to the end of the cylinder. The valve, plug and nameplate are neglected. The wall thickness is varied between 1.3 cm and 0.794 cm (minimum wall thickness according to [ISO 7195], Table 3). The maximal possible UF_6 volume of the model is between 0.773 m^3 and 0.7907 m^3.

2.2.5.4.1.3 DN30 PSP

Two models of the DN30 PSP are considered for the criticality safety analysis of the DN30 package.

- **DN30 PSP model as designed:** The PSP is composed of two concentric shells of stainless steel in the form of a cylinder enclosing the insulating foam. In radial direction from inside to outside there is 0.2 cm stainless steel, 15 cm insulation and 0.3 cm stainless steel modeled. In axial direction from inside to outside 1.0 cm stainless steel, 15 cm insulation and 0.4 cm stainless steel is modeled.

- **Damaged DN30 PSP model:** The shells of the DN30 PSP are compressed to a single shell; the thickness of the shells is kept. The insulating foam is completely neglected. This compressed shell has a thickness of 0.5 cm in radial and of 1.4 cm in axial direction.

2.2.5.4.2 Material compositions

2.2.5.4.2.1 UF_6

For the UF_6 the following compositions are considered:

- Pure UF_6 with a density between 3.1 g/cm^3 and 5.5 g/cm^3.
- UF_6 with a purity of 99.5 wt. % UF_6 containing 0.5 wt. % HF at a density of 5.5 g/cm^3.
- UF_6 with a purity of 99.5 wt. % UF_6 with 0.5 wt.% HF and additional HUR.
- The enrichment is in all cases 5.0 wt. % U-235 in uranium. For the criticality assessment it is considered that apart from U-235 only U-238 is present with 95 wt. %. The very small amounts of the nuclides U-232, U-234 and U-236 have no significant influence on reactivity. They are therefore neglected.
- The small traces of Pu-239 and Pu-241 in reprocessed uranium are as well neglected as they have no influence on reactivity.

2.2.5.4.2.2 HF

For pure HF acid, the standard material „hfacid“ of the SCALE library with a theoretical density of 1.15 g/cm^3 is used. For UF_6 containing impurities in form of HF (homogeneously mixed), the density of UF_6 is used for the mixture.

2.2.5.4.2.3 Hydrogenated uranium residues

In Appendix 2.2.5 (Criticality Safety Analysis) the credible accumulation of hydrogenated uranium residues is evaluated. This evaluation is based on recent work to assess the composition and amount of HUR.

The creation of hydrogenated uranium residues has been investigated in [MILIN 2016], [CONNOR 2013], [BEGUE 2013] and [REZGUI 2013].

In [MILIN 2016] it is shown that the envelope composition of HUR is UO_2F_2-2H_2O-2HF with a H/U ratio of 6. The mass of HUR is assumed to be equivalent to the maximal allowable mass of heels in the 30B cylinder of 11.4 kg.

In [CONNOR 2013] and [REZGUI 2013] the composition of HUR was assumed to be UO_2F_2-5.5H_2O with a H/U ratio of 11. [CONNOR 2013] assumed a mass of 12 kg and [REZGUI 2013] a mass of 3.91 kg HUR.

[BEGUE 2013] showed the influence of the mass of HUR and the H/U ratio on reactivity.

For the proof of criticality safety for the DN30 package in this report two approaches are considered.

In a first approach based on a usage period of 5 years under the assumption that the 30B cylinder is filled each year four times, an amount of 3.9083 kg of UO_2F_2*5.5H_2O is calculated at the end of the 5 year period between recertifications. This amount of HUR can be mixed homogeneously in the total amount or a small portion of the UF_6.

In a second approach it is assumed that a maximum of 11.4 kg of HUR in the form of UO_2F_2*3H_2O is present as lump in the UF_6.

2.2.5.4.2.4 Carbon steel (30B cylinder)

For the carbon steel of the 30B cylinder, the standard material „carbonsteel“ of the SCALE library at a density of 7.8212 g/cm^3 is used.

2.2.5.4.2.5 Stainless steel (DN30 PSP)

For stainless steel the standard material „ss304“ of the SCALE library with a density of 7.94 g/cm^3 is used.

2.2.5.4.2.6 Polyisocyanurate rigid foam (DN30 PSP)

Polyisocyanurate rigid foam is used for the DN30 PSP. For the variation calculations different densities with the same composition were used. The results of the variation calculations show that maximal reactivity does not depend on the foam density, so that foam densities of less than 0.2 g/cm^3 and more than 0.375 g/cm^3 as well as any intermediate value are covered by the calculations as well. The chemical composition of the foam is given in Table 61.

Table 61: Composition of the polyisocyanurate rigid foam

Element	Weight %
H	5.41
C	68.27
N	7.42
O	18.9

2.2.5.5 Proof of criticality safety

2.2.5.5.1 Proof according to ADR [ADR 2015], No. 6.4.11.10 and [IAEA 2012], para. 682 for the single package in isolation under RCT, NCT and ACT

2.2.5.5.1.1 Performed calculations

The maximum effective neutron multiplication factor k_{eff} for the single package in isolation is determined for RCT, NCT and ACT. Variation calculations are performed to determine the most reactive arrangements. This includes:

- the variation of geometrical parameters of the 30B cylinder and the DN30 PSP such as the variation of the outer dimensions and the wall thickness of a 30B cylinder according to the tolerances specified in [ISO 7195],
- the consideration or neglecting of the DN30 PSP,
- the variation of the foam density of the DN30 PSP,
- the consideration of an intact or damaged DN30 PSP for ACT (steel shells compressed together to a single layer),
- variation of the thickness of a water layer between the 30B cylinder and the DN30 PSP.

Parameters related to the fissile material are varied:

- density of the modeled UF_6,
- composition of the modeled UF_6 (impurities),
- different arrangements of the UF_6 like a central hole and partial fill conditions.

2.2.5.5.1.2 Results of the calculations

The results of the calculations are:

- The 30B cylinder with maximal outer dimensions and hence maximal mass of UF_6 results in maximal k_{eff}.
- The 30B cylinder with minimal wall thickness results in maximal k_{eff}.
- Reactivity increases with increasing UF_6 density. Maximal k_{eff} is reached for a theoretical density of 5.5 g/cm³ (value for -40°C).
- Homogeneous UF_6 with 0.5 wt. % HF impurity results in maximal k_{eff}.
- A completely filled cylinder results in maximal k_{eff}.
- The bare cylinder has a higher reactivity than the DN30 package (30B cylinder in the DN30 PSP).

2.2.5.5.1.3 Proof according to ADR [ADR 2015], No. 6.4.11.10 and [IAEA 2012], para. 682 for RCT and NCT

For the single package under RCT and NCT maximal reactivity is reached for the calculation model shown in Figure 104 and Figure 105:

$$\mathbf{k_{eff} + 3\,\sigma = 0.5734}$$

This value is reached by taking into account the following conservative assumptions:

1. Minimal wall thickness of the 30B cylinder of 0.794 cm
2. Maximal UF_6 density of 5.5 g/cm³
3. Maximal cylinder dimensions
4. Completely filled cylinder
5. 0.5 wt.% impurities as HF

The criticality safety criterion is complied with.

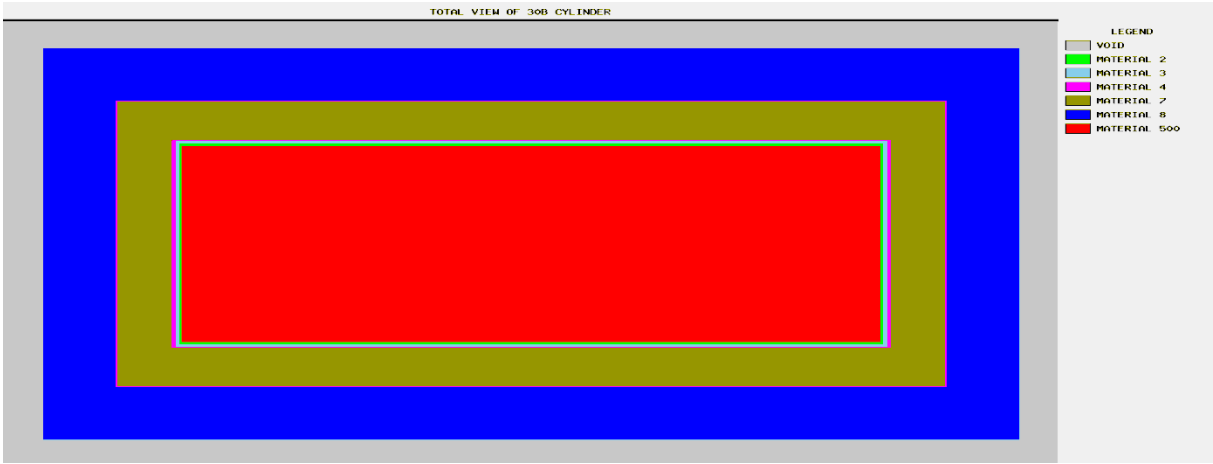

red = UF_6, green = carbon steel, magenta = stainless steel, dark blue = water layer, brown = foam

Figure 104: Longitudinal section of the calculation model used for RCT and NCT

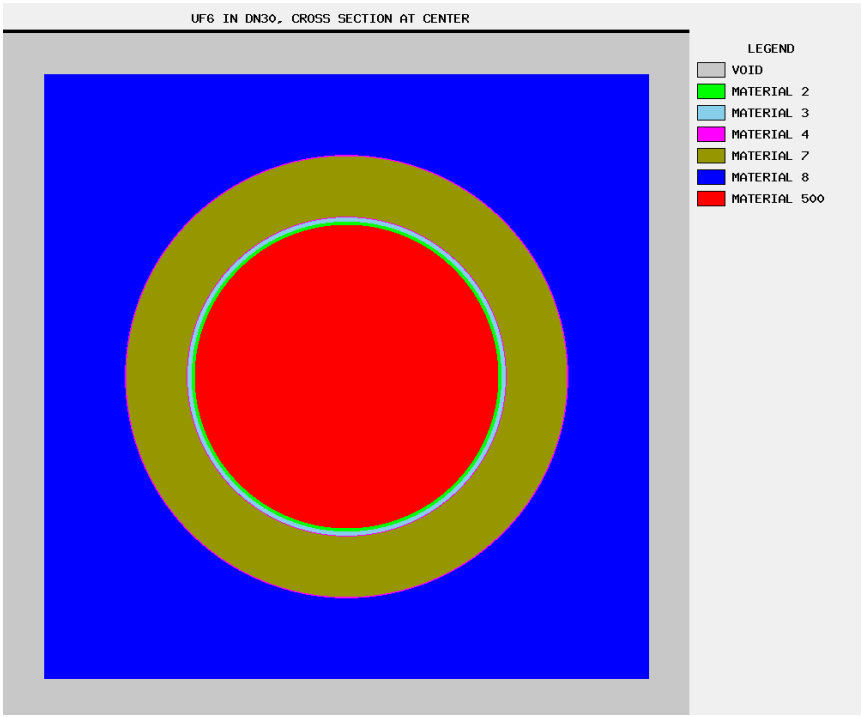

red = UF_6, green = carbon steel, magenta = stainless steel, dark blue = water layer, brown = foam)

Figure 105: Cross section of the calculation model used for RCT and NCT

2.2.5.5.1.4 Proof according to ADR [ADR 2015], No. 6.4.11.10 and [IAEA 2012], para. 682 for ACT

For the single package under ACT maximal reactivity is reached for the calculation model shown in Figure 106:

k_{eff} + 3 σ = 0.6101

This value is reached by taking into account following conservative assumptions:

1. Minimal wall thickness of the 30B cylinder 0.794 cm
2. Maximal UF_6 density of 5.5 g/cm^3
3. Maximal cylinder dimensions
4. Completely filled cylinder
5. 0.5 wt.% impurities as HF
6. The DN30 PSP is completely neglected.

The criticality safety criterion is complied with.

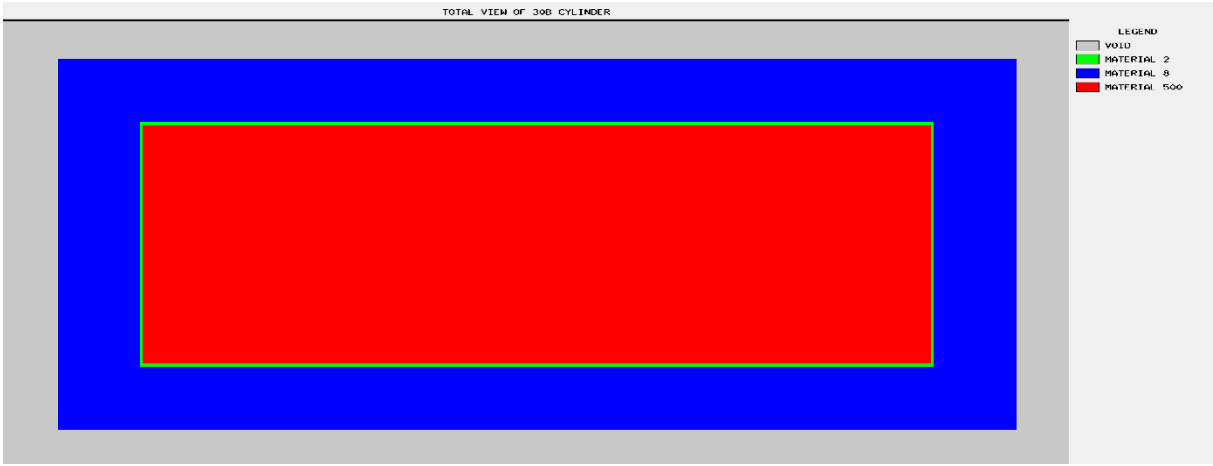

red = UF_6, green = carbon steel, dark blue = water layer

Figure 106: Longitudinal section of the calculation model used for ACT

2.2.5.5.2 Proof according to ADR [ADR 2015], No. 6.4.11.12 and [IAEA 2012], para. 684 for an array of packages under NCT

The criticality safety index for the package DN30 is CSI = 0. Thus, an infinite number of packages under NCT and under ACT have to be analyzed. Calculation assumptions for the proof of the array of packages under ACT are more restrictive than assumptions for NCT. Thus, proof for the array of packages under NCT is covered by the proof in the following section 2.2.5.5.3.

2.2.5.5.3 Proof according to ADR [ADR 2015], No. 6.4.11.13 and [IAEA 2012], para. 685 for an array of packages under ACT

2.2.5.5.3.1 Performed calculations

For the array of packages the condition of the packages under ACT is assumed. The conservative assumptions are:

Complete loss of the thermal insulation: Conservatively, for all calculations a complete loss of the thermal insulation (PIC foam) is assumed.

Neglect of the steel shells of the DN30 PSP: For most of the analyses the steel shells of the DN30 PSP are completely neglected and only the bare cylinder is assumed to be present. When required for the proof the influence of the steel shells on reactivity is assessed.

Compaction of the steel shells to a single layer of steel: In all cases where the steel shells of the DN30 PSP are considered a compaction of these steel shells to a single stainless steel layer is assumed. The gap between this single steel shell, the 30B cylinder and adjacent DN30 packages is varied. Hence, rather compact arrangements of packages are taken into account for the proof.

For the array of DN30 packages following variation calculations are performed

- Consideration of quadratic and hexagonal arrays.
- Variation of the gap size between adjacent cylinders for the cylinder completely filled with UF_6 for the different array models.
- Variation of the water density and the gap size between adjacent cylinders for the cylinder completely filled with UF_6 for the different array models.
- Variation of the water density in the gap and gussets between adjacent cylinders for the cylinder completely filled with UF_6 for the hexagonal array model.
- Variation of the UF_6 composition (impurities) for the hexagonal array model.
- Variation of the fill level and the size of a central void for the hexagonal array model.
- Variation of the wall thickness of the 30B cylinder for the hexagonal array model.
- Consideration of the stainless steel shells of the DN30 PSP and variation of the gap between shells and cylinder.
- Consideration of possible and realistic inhomogeneous distributions of the impurities.
    - The assumption of a grain structure consisting of UF_6 cubes surrounded by an impurity layer and the variation of the cube dimensions.
    - The assumption of a grain structure consisting of UF_6 cubes surrounded by an impurity layer, a central void in the UF_6 and variation of the dimensions of this central void.
- Consideration of possible but unrealistic inhomogeneous distributions of the impurities.

- The assumption of a central void in the UF_6, concentration of the impurities in a layer at the inside of the UF_6 layer and the variation of the dimensions of the central void.
- Concentration of the impurities in an impurity sphere and the variation of its size, composition and position in the 30B cylinder.

- Consideration of hypothetical and unrealistic inhomogeneous distributions of the impurities.
  - Arrangement of the impurities concentrated in a spherical impurity shell and the variation of its size, composition and position in the 30B cylinder.
  - Arrangement of one composition of impurities in a sphere, surrounded by a shell of UF_6 and further surrounded by a spherical shell of another composition of impurities and variation of the size, composition and position of this arrangement in the 30B cylinder.

Water ingress due to the water immersion test [ADR 2015], no.6.4.17.4, 6.4.19, [IAEA 2012], para. 729, 733 is not considered as it was shown in Appendix 2.2.5 (Criticality Safety Analysis) that the amount of water to be expected to leak into the cylinder is negligible compared to the assumed amount of volatile hydrogenous material and HUR.

2.2.5.5.3.2 Results of the calculations

The general results of the calculations are:

- Hexagonal infinite arrays lead to a higher k_{eff} than quadratic arrays. Highest reactivity is reached for an infinite hexagonal array composed of hexagonal prisms, in which the package (depending on the scenario, only a 30B cylinder or a 30B cylinder accommodated in the compressed steel shells of the DN30 PSP) is surrounded by a water layer. The apothem of the hexagonal prism is equal to the outer radius of the cylinder resp. package plus the thickness of the surrounding water layer. Highest reactivity is reached if the gussets between hexagon and water layer are void (see Figure 107).

- Calculation models with homogeneously modeled impurities are less reactive than those with inhomogeneous concentrations of impurities.

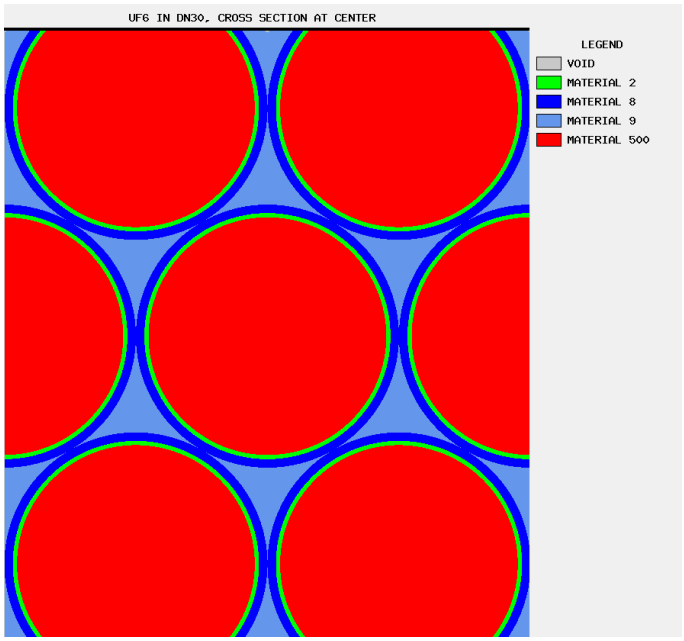

red = UF_6, green = carbon steel, dark blue = water layer, light blue = gussets

Figure 107: Cross section of calculation model for the hexagonal array for ACT

2.2.5.5.3.3 Proof according to ADR [ADR 2015], No. 6.4.11.13 and [IAEA 2012], para. 685 for an array of DN30 packages

For the array of packages under ACT maximal reactivity is reached for the calculation model shown in Figure 108 and Figure 109:

$k_{eff} + 3\,\sigma = 0.9228$

This value is reached by taking into account following conservative assumptions:

1. Minimal wall thickness of 7.94 mm
2. Maximal UF_6 density of 5.5 g/cm^3
3. Maximal cylinder dimensions
4. Completely filled cylinder
5. Hypothetical impurity arrangement consisting of a central impurity sphere consisting of HUR and UF_6 surrounded by a shell of UF_6 surrounded by a shell of HF

The criticality safety criterion is complied with.

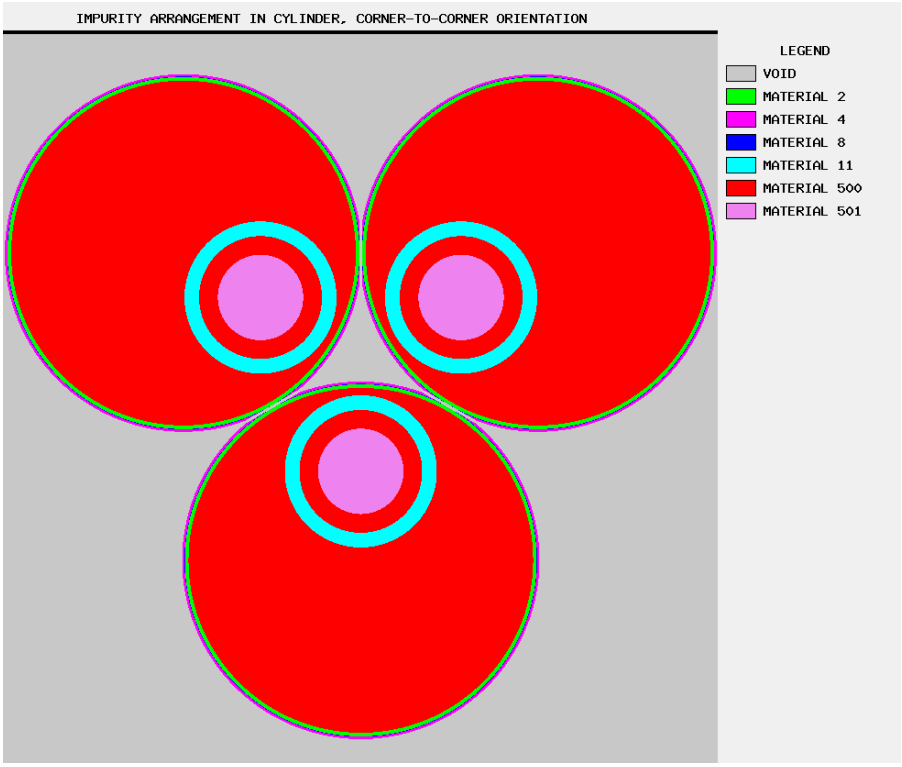

red = UF_6, pink = HUR, light blue = HF, green = carbon steel, dark blue = water layer, magenta = stainless steel

Figure 108: Cross section of the arrangement of two cylinders with impurity sphere for corner-to-corner orientation (plane through center of spherical arrangements)

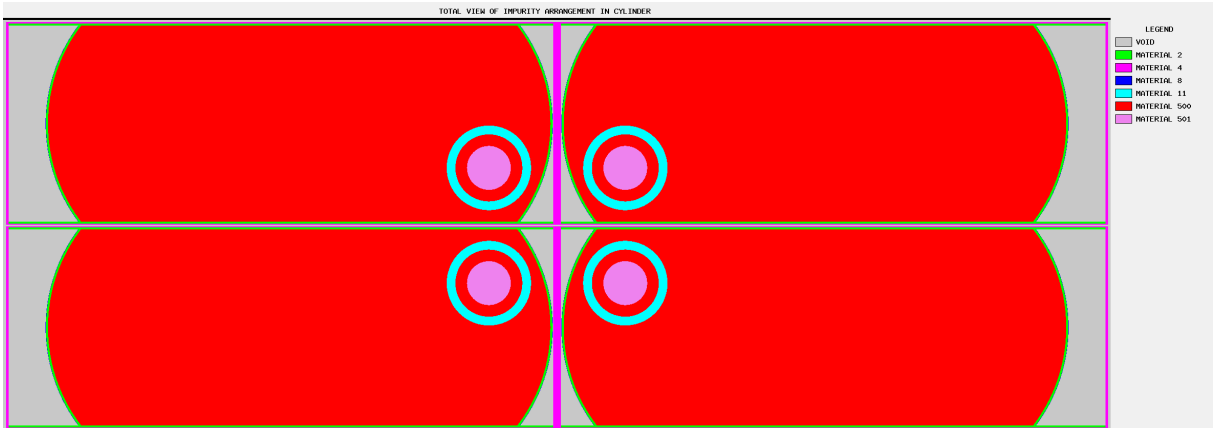

red = UF_6, pink = HUR, light blue = HF, green = carbon steel, dark blue = water layer, magenta = stainless steel

Figure 109: Longitudinal section of the arrangement of two cylinders with impurity sphere for corner-to-corner orientation (plane through center of spherical arrangements)

2.2.5.5.3.4 Proof according to ADR [ADR 2015], No. 6.4.11.13 and [IAEA 2012], para. 685 for an array of bare 30B cylinder

For an array of bare 30B cylinders under ACT maximal reactivity is reached for the calculation model shown in Figure 110:

k_{eff} + 3 σ = 0.9420

This value is reached by taking into account following conservative assumptions:

1. Minimal wall thickness of 1.1 cm
2. Maximal UF_6 density of 5.5 g/cm^3
3. Maximal cylinder dimensions
4. Arrangement of the UF_6 in a layer attached to the inner side of the cylinder, thus leaving a central void in the UF_6
5. Volatile impurities (HF) and HUR concentrated in a layer at the inside of the UF_6 layer

The criticality safety criterion is complied with.

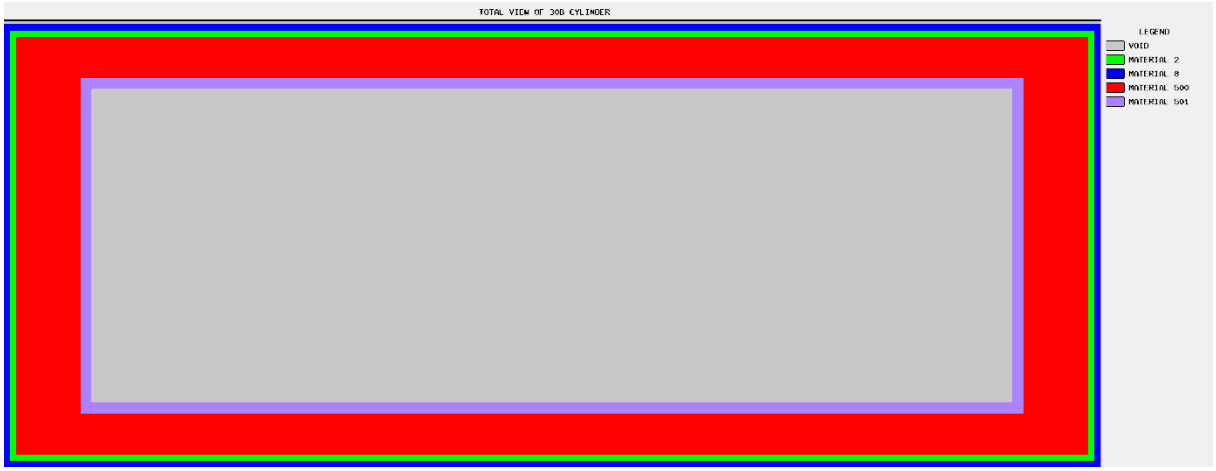

red = UF_6, violet = HF and HUR, green = carbon steel, dark blue = water layer

Figure 110: Longitudinal section of the calculation model with highest k_{eff} for an array of bare cylinders

APPENDIX 1.1 (LIST OF APPLICABLE DOCUMENTS)

Applicable documents, list ref. 0023-LST-2016-001

APPENDIX 1.3 (RADIOACTIVITY)

Analysis of the total radioactivity of the contents specified for the packaging DN30

APPENDIX 1.4.1 (DRAWINGS)

Drawing parts list no 0023-STL-1000-000

Proprietary Information

Not to be published

APPENDIX 1.4.2 (MATERIAL DATA PIR FOAM)

Material Report, PIR Foam of DUNA CORRADINI

Proprietary Information

Not to be published

APPENDIX 1.4.3 (MATERIAL DATA INTUMESCENT MATERIAL)

Material Report, Intumescent material PROMASEAL-PL® of PROMAT

Proprietary Information

Not to be published

APPENDIX 1.7.1 (HANDLING INSTRUCTION)

Handling instructions for the DN30 packaging, Handling Instruction No. 0023-HA-2015-001

APPENDIX 1.7.2 (CONTAMINATION AND DOSE RATE MEASUREMENTS)

Test Instruction No. 0023-PA-2017-016

APPENDIX 1.7.3 (DOSE RATE MEASUREMENTS AT 30B CYLINDERS CONTAINING REPU HEELS)

Test Instruction No. 0023-PA-2015-019

APPENDIX 1.8.1 (PERIODICAL INSPECTIONS)

Periodical inspections of packaging DN30, Test Instruction No. 0023-PA-2015-015

APPENDIX 1.8.2 (INSPECTION CRITERIA)

Inspections at the packaging DN30 and measures in case of non-conformances and deviations, Test Instruction No. 0023-PA-2015-016

APPENDIX 1.9.1 (IMS)

1) Quality Management Handbook of company DAHER Nuclear Technology GmbH
2) DIN EN ISO 9001
3) Confirmation on quality assurance according to nuclear standard KTA 1401
4) Confirmation of the Qualification for the development, manufacturing and operation of packagings of packages requiring approval for the transport of radioactive material

APPENDIX 1.9.2 (MANUFACTURING SPECIFICATION)

Specification no. 0023-SPZ-2016-001: Manufacturing of the DN30 PSP

Manufacturing Test Sequence Plan no. 0023BPP-2016-001

Proprietary Information

Not to be published

APPENDIX 2.2.1.1 (DROP TEST PROGRAM)

Drop test Specification No. 0023-BDI-2015-002-Rev1

Proprietary Information

Not to be published

APPENDIX 2.2.1.2 (DROP TEST REPORTS)

Drop Test report no. BAM/11627

Proprietary Information

Not to be published

APPENDIX 2.2.1.3 (STRUCTURAL ANALYSIS OF THE DN30 PACKAGE UNDER NCT AND ACT)

Structural Analysis of the DN30 package under NCT and ACT

Proprietary Information

Not to be published

APPENDIX 2.2.2.1 (THERMAL TEST PROGRAM)

DN30 thermal test No. 0023-BDI-2014-001-Rev4

Proprietary Information

Not to be published

APPENDIX 2.2.2.2 (THERMAL TEST REPORT)

Drop Test report no. BAM/16010

Proprietary Information

Not to be published

APPENDIX 2.2.2.3 (THERMAL ANALYSIS)

Thermal Analysis of the DN30 Package for the Transport of Uranium Hexafluoride

Proprietary Information

Not to be published

APPENDIX 2.2.3.1 (CONTAINMENT ANALYSIS)

Containment Design Analysis for the DN30 Package for the Transport of Uranium Hexafluoride

Proprietary Information

Not to be published

APPENDIX 2.2.3.2 (URANIUM HEXAFLUORIDE DEWITT 1960)

APPENDIX 2.2.4 (DOSE RATE ANALYSIS)

Dose Rate calculations for the DN30 Package for the Transport of Uranium Hexafluoride

Proprietary Information

Not to be published

APPENDIX 2.2.5 (CRITICALITY SAFETY ANALYSIS)

Criticality Analysis of the DN30 Package for the Transport of Uranium Hexafluoride

Proprietary Information

Not to be published